Reconstructing the Character of the Eastern Sector of the Scandinavian Ice Sheet Using Remote Sensing

J. E. H. Perry

Thesis submitted in fulfillment of
the requirements for the degree of
Doctor of Philosophy
to the
University of Edinburgh – 1998

This thesis has been composed by myself and it has not been submitted in any previous application for a degree. The work reported within was executed by myself, unless otherwise stated.

Jonathan Eric Hayward Perry
Edinburgh, November 1998.

ABSTRACT

The extensive glacial landforms in the Baltic States and neighbouring countries have been used to infer the dynamic behaviour of the Scandinavian ice sheet.

Landsat TM imagery was acquired of the Baltic States and neighbouring regions south of the Gulf of Finland (the Eastern Baltic region) in digital form. Computer image processing techniques were used to enhance the glacial geomorphology without enhancing the pattern of agricultural land usage. Mapping of glacial landforms was done (on-screen) using computer software. Using computers allowed the interpretations to be manipulated, analysed and compared with further information from digital elevation models, land cover maps and published literature/maps. This allowed the limit of Weichselian ice to be delineated using four different methods.

Streamlined glacial lineations, including megaflutes, drumlins, megadrumlins and elongated hills have been mapped using this technique. Coherent groups of lineations were identified as flow sets, which were considered to have been formed by the same phase of ice flow. Where the lineations of different flow sets intersect, the temporal relationship between the flow sets, and therefore between the ice flows, was determined.

While pre-Weichselian phases of ice flow were identified, it was concluded that the majority of lineations within the Eastern Baltic formed during the Late Weichselian. Long (up to 21 km), well-defined lineations were found to have formed during the Late Weichselian maximum when the ice velocities were greatest. These form flow sets with a north-south trend. Lineations from the final deglaciation are shorter in length and form flow sets orientated at 170°. During the final deglaciation ice streams developed. Interstream areas generally coincide with regions of elevated bed rock.

The interpretations resulting from these observations were combined with similar data from Finland to create a data set covering the area from the ice divide to beyond the limit of Weichselian ice. The spatial distribution of lineation size was examined using this data set and compared to output from a glaciological model. It was concluded that flow-parallel lineations were most likely formed by a single mechanism. The most likely mechanism was concluded to be subglacial deformation with the most active zone of lineation formation occurring within 100 km of the ice sheet margin.

Variations in the frequency distribution of lineation length between Finland and the Eastern Baltic regions point to differences in the controls on lineation formation. Differences in the character of deglaciation between Finland and the Eastern Baltic were identified. Ice streams in Finland appear to have been more stable in location and about twice the width of those observed in the Eastern Baltic region. These differences may be explained by the interaction between the ice sheet and its substratum.

ACKNOWLEDGEMENTS

This project was funded by a NERC scholarship, for which I am grateful. I wish to thank my supervisor Professor G. S. Boulton for providing the opportunity to study in the beautiful city of Edinburgh, and from whom I have learnt a lot. Many others have, at various times, also acted as supervisor. I am indebted to: Mikko Punkari for his advice during the early stages of this study; Richard Holme for his mathematical know-how and patient explanations during the final stages; Marianne Broadgate for her encouragement and useful discussions at the start and end; and Nick Hulton who has provided guidance throughout.

This study would not have been possible without the help of the support staff in the Department of Geology and Geophysics. The kindness of all my friends has also been greatly appreciated. In particular I would like to thank: Al, Dave, Mark, Roger and especially Rachel for their constructive comments on earlier drafts of this thesis; Sally for a pint when I wasn't expecting it; Pentti and Katri Laaksonen for their kind hospitality whilst I was in Finland; Susie and Al for looking after a ghost flatmate; Patience Cowie for giving time freely to discuss my work; and the Computer Officers, Chis, Shane, Justin and Chris Place for their willingness to assist beyond their job descriptions. I am also grateful to Fiona for facilitating the arrangement of meetings and always providing a welcome to room 333.

I especially thank my family, Nick, Chris, Sarah and in particular Mum and Dad, who have consistently provided love and support throughout all my endeavours. Finally, special thanks to Andy for her understanding and being there through to the end - another name for a new beginning.

'... left over from the time when the Creator hadn't really decided what He wanted to make and was, as it were, just idly messing around with the Pleistocene.'

Terry Pratchett, *Equal Rites*, 1987.

Contents

List of Tables

List of Figures

Acronyms

A description of all the acronyms used in this thesis are given here.

ACRONYM	DESCRIPTION
AVHRR	Advanced Very High Resolution Radiometer (sensor)
BDBP	Baltic Drainage Basin Project
BP	Before Present
CAD	Computer Aided Design
DCW	Digital Chart of the World (vector coverage)
DEM	Digital Elevation Model
DTED	Digital Terrain Elevation Data
ELA	Equilibrium Line Altitude
ERTS	Earth Resources Technology Satellite
EU	European Union
GIS	Geographical Information System
GRID	Global Resource Information Database
GTOPO30	Global Topography at 30 arc seconds (DEM)
HSI	HyperSpectral Imager (sensor)
IFOV	Instantaneous Field of View
IWA	Instantaneous Working Area
LCC	Lambert Conformal Conic (map projection)
LU	Leningrad University
MO	Moscow
MSS	Multi-Spectral Scanner (sensor)
NMP/EO-1	New Millennium Program Earth Orbiting 1 (spacecraft)
RI	Riga
RGB	Red, Green and Blue
TA	Tallinn Academy
TL	Thermoluminescence
TM	Thematic Mapper (sensor)
TU	Tartu
UNEP	United Nations Environmental Program
WDBII	World Data Bank II (vector coverage)
UK	United Kingdom
m.s.l	mean sea level

Chapter 1

Introduction

During the past 2 Ma, the surface environment of the earth has been shaped by the interaction of the atmosphere, oceans and ice sheets. During this period ice sheets have built up and decayed during cycles lasting approximately 40-100 ka. There is a strong coupling between climate and ice sheets (Boulton and Payne, 1992). Global climate drives the growth and decay of ice sheets which in turn interact with the oceans and atmosphere to influence climate change. Understanding ice sheet dynamics makes an important contribution to understanding the mechanisms of global climate change and therefore improving our ability to predict the effects of future glaciations. For example, the facilities built to store long-lived nuclear waste may have to survive beneath a future ice sheet. Since radioactivity can take hundreds of thousand years to decay, the impact of a future ice sheet on the pattern of erosion, deposition and groundwater flow must be considered (Boulton and Payne, 1992). Understanding the pattern of glacial deposition can also have present day economic benefits. Crimes *et al.* (1992) used maps of glacial landforms to identify areas in which sand and gravel could occur, so reducing the surveying time to find these materials which are used in the production of concrete, ballast and road stone. A knowledge of the spatial distribution of glacial sediments also allows structures such as gas and oil pipe lines to be positioned on sediments suitable for supporting them (Knight, 1996).

Glacier ice covers approximately 10 per cent of the earth's land surface at the present time, with 99 per cent of this ice within the present day ice sheets of Greenland and Antarctica (Paterson, 1994). There are, however, important differences between present day ice sheets and the mid-latitude Eurasian and North American ice sheets which existed during past ice ages. Previous ice sheets have occupied regions three times the area of todays glacier ice (Paterson, 1994). Middle latitude ice sheets during the last glacial cycle underwent large fluctuations in size, in contrast to modern ice sheets (Table 1.1). Whereas, ice calving into the sea is a significant mechanism by which ice is removed from the present day ice sheets (Paterson, 1994), land surface ablation is thought to have been a more important factor in controlling the size of past mid-latitude ice sheets, large proportions of whose

margins extended over internal areas of the continents. Finally, both the Greenland and Antarctica ice sheets are underlain by crystalline basement rock, while large regions of the area formerly occupied by the Eurasian and North American ice sheets are covered by fine-grained sediment. These fine-grained sediments are more susceptible to deformation than coarse crystalline sediments. Sediment deformation is an important mechanism of ice motion which may account for the rapid ice movement during the final stages of the Weichselian (Ehlers, 1990).

Ice Sheet	Volume $10^6 km^3$	
	Present Day	Weichselian Maximum
North American	0	34.8
Eurasian	0	13.3
Greenland	2.4	3.5
Antarctic	30.0	34.0

Table 1.1: Volumetric changes between present day and past maxima volumes of the major ice sheets during the last glaciation: (Andrews, 1989; Orelemans and Van der Veen, 1984; Reeh, 1989).

It has not been possible to monitor the complete life cycle of an ice sheet. The best way of predicting the future dynamics of existing ice sheets is to improve our understanding of the ways in which past ice sheets behaved through time. A better knowledge of the behaviour and dynamics of former ice sheets can lead to an increased understanding of landform organisation in formerly glaciated areas. A greater understanding provides better constraints for theoretical models with which to predict the size and dynamics of future ice sheets.

Many studies have been undertaken to reconstruct the flow dynamics of former mid-latitude ice sheets (e.g., Ljunger 1949, Sugden 1978, Hughes *et al.* 1981, Boulton *et al.* 1985, Holmlund and Fastook 1995). Studies of the Eurasian ice sheet initially concentrated on the behaviour of the glacial ice over Fenno-Scandinavia. However, until the early 1980's, only local studies of ice movement direction were available (Ehlers, 1990). Punkari (1982) achieved a larger regional overview of ice flow direction during the retreat of the Fenno-Scandinavian ice sheet in Finland by using interpretations and maps of glacial landforms produced from Landsat MSS satellite imagery. The overall ice movement patterns in northern Germany were reconstructed using till fabric data (Ehlers and Stephan, 1983). Further ice movement information was added from neighbouring countries, such as Denmark and the Netherlands (Lundqvist, 1986; Ehlers, 1990) to refine the reconstructions of the Eurasian ice sheet. However, little attempt has been made to include information from the areas to the south of Finland and east of Poland. This area, which shall be referred to as the Eastern Baltic region, comprises the Baltic States (Estonia, Latvia and Lithuania) and neighbouring areas of Russia, Belarus and Poland (Figure 1.1). The present study uses the extensive terrestrial record of glacigenic landforms in the Baltic States and neighbouring countries to analyse and reconstruct the overall setting and internal organisation of the Fenno-Scandinavian ice sheet in the Eastern Baltic region.

The interaction between the mid-latitude ice sheets and the underlying terrain during the cycles of ice advance and decay substantially reshaped the surface of the land. Glacigenic

Figure 1.1: Location map of northwest Europe

deposits and landforms dominated the surface topography of formerly glaciated areas. Of the wide variety of glacigenic landforms that occur in these areas, subglacially streamlined landforms are of most interest in this study and are referred to herein as *lineations*. These streamlined landforms exhibit a wide variety of shapes, sizes and internal composition. However, most authors agree that the lineation long axes are parallel to ice movement, and that they formed subglacially (Boulton *et al.*, 1985; Clark, 1990; Dongelmans, 1996). Neighbouring lineations with similar orientations or with a smooth, gradual, continuous change of orientation across a region may be grouped together to form *flow sets*. In addition, lineations within flow sets generally display similar lengths, are similarly well-formed and have relatively uniform spacing (Clark, 1990). These flow sets represent coherent groups of glacial features which are assumed to relate to one phase of ice flow (Punkari, 1980). Using the techniques developed across Finland, Punkari (1984) mapped glacial streamlined landforms within Soviet Karelia. For most of the areas a single flow pattern existed, regarded as the deglacial pattern, but other orientations of flow were also found which could be demonstrated, by superimposition, to be older. The superimposition of lineations and the remoulding of older lineations by younger ice flows has since been used extensively to determine the relative ages of lineation flow sets (Punkari, 1984; Boulton *et al.*, 1985; Clark, 1990; Punkari, 1985; Dongelmans, 1996; Knight, 1996).

Satellite imagery probably provides the best data source to study the regional ice flow patterns across the Eastern Baltic region. Mapping lineations from satellite imagery has several benefits over more traditional fieldwork mapping. Many landforms can be detected more easily and mapped more quickly (Clark, 1997). Satellite imagery also provides a standard data set from which a homogeneous result can be produced rather than the mosaic of results collected by many workers using differing methods which makes correlations between countries of the Eastern Baltic region difficult (Guobyte and Pavlovskaya, 1998). Satellite imagery used for mapping geomorphology has been predominantly in the form of photographic prints. Boulton and Clark (1990) used mostly Landsat MSS mosaics to map former flow sets over regions glaciated by the Laurentide ice sheet, with the relative ages of flow sets determined using aerial photographs and selected regions of digital Landsat TM images. Dongelmans (1996) and Punkari (1996) used photographic copies of Landsat MSS and Landsat TM imagery to reconstruct the glacial dynamics over Fenno-Scandinavia and Soviet Karelia, while Knight (1996) used Synthetic Aperture Radar imagery to study regions of the Laurentide ice sheet. This study uses Landsat TM imagery to interpret and map the glacial landforms across the Eastern Baltic region. This is thought to represent a new data source for the region. In contrast to previous studies, the satellite imagery and interpretations made from the imagery are retained in digital format throughout the study. Using digital data allows interpretations to be made more quickly and at many scales from 1:45,000 to 1:1,000,000. In addition, by using digital data, the interpretations can be easily manipulated, analysed, or compared with other digital data sets, for example topography or geology.

The shape and pattern of glacial landforms are widely thought to reflect the glacial conditions and the processes that occur within an ice sheet (Clark and Wilson, 1994). The interpretations

made in this study were integrated with the digital glacial landform data interpretations of satellite imagery from Fenno-Scandinavia, made by Dongelmans (1996). A data set of lineations extending from the ice divide in the Scandinavian mountains, to beyond the limit of Weichselian ice was thus formed. This data set allows the spatial distribution of lineation morphology to be studied across the Eurasian ice sheet using a single set of techniques.

1.1 Structure of Thesis

The following Chapter gives a description of the bedrock geology and present day topography of the East European Platform. An account of the various Weichselian stratigraphies used across the Eastern Baltic region and how they are thought to relate to each other is also provided. In Chapter 3 the advantages of using remotely sensed data, such as satellite imagery, for palaeo-ice sheet reconstruction are listed. In addition, the characteristics of Landsat TM satellite imagery are given and a description of the image-processing methods used to enhance the geomorphology observed from the images. The other raw data used within this study are also described. The prerequisites for the development of glacigenic landforms, and especially stream-lined landforms are outlined in Chapter 4 together with an account of how the images were interpreted to form flow sets. Chapter 5 contains descriptions of the imagery, the lineations interpreted and the flow sets formed.

Using the flow sets described in Chapter 5 the dynamics of the ice across the region are reconstructed to form a palaeo-glaciological reconstruction discussed in Chapter 6. Storing the interpretations in digital form allows the data to be further analysed. Chapter 7 describes techniques used to present the data sets to show the limit of Weichselian ice; to compare interpretations with underlying topography; and to analyse the spatial distribution in the variance of lineation orientations and the distribution of lineation lengths. Chapter 8 explores the use of digital data to permit a numerical comparison of the interpretations of satellite imagery with the output from a glaciological model. Conclusions concerning the ice sheet dynamics and the possible influence of underlying geology are discussed in Chapter 9. A perspective on future work is also presented.

Chapter 2

Geology, Topography and Weichselian Stratigraphy of the Baltic Region

The first two Sections of this Chapter provide an introduction to the geology and topography of the study area, which are both considered in this study to be important variables controlling the evolution of the internal dynamics of the ice sheet. Section 2.1 describes the geology of the study region. Variations in the rheology of material beneath an ice sheet are considered to influence the stability of the ice (Boulton and Jones, 1979) and consequently may explain the organisation of ice sheet dynamics and the formation of ice streaming and Heinrich events (Clark and Wilson, 1994; Blankenship *et al.*, 1987; Ehlers, 1990; Andrews and Tedescoo, 1992). The type of substrate material has also been proposed as one of the variables controlling the formation of geomorphological features such as drumlins and eskers (Walder and Fowler, 1994). The role substrate material may have had on the formation of lineations and on ice sheet dynamics is explored further in Chapters 4, 6 and 7.

Section 2.2, briefly describes the topography of the study area. It has been suggested that local topography may be an important factor in the formation of geomorphological features such as drumlins (Menzies, 1979). The influence of topography on regional ice sheet dynamics is considered in Section 6.3 and the relationship between topography and lineations observed in this study is analysed in Section 7.2.

The final Section of this Chapter, Section 2.3, provides an overview of the Weichselian stratigraphy of the study area. Understanding the extent of previous glaciations can help place features observed in this study within a wider stratigraphical and temporal framework. Work by Lagerbäck (1988) suggests that Early Weichselian moraines may be preserved, even after being over ridden by later glaciations. While many attempts have been made to unify

the separate stratigraphic schemes of the Baltic States and their neighbours (Velichko, 1984; Raukas *et al.*, 1995; Ehlers *et al.*, 1995) a regional overview of the lithostratigraphy and its relation to the morphostratigraphy could not be found. An overview for the whole of the Weichselian is therefore presented here.

2.1 Geology

Northwest Europe can be divided into two geologically distinct regions. Fenno-Scandinavia comprises the Baltic Shield and the Scandinavian Caledonides which consist mainly of metamorphic and plutonic rocks (Figure 2.1). The areas surrounding Fenno-Scandinavia to the south and east are characterised by undisturbed sedimentary sequences which overlie the basement rock. Good general summaries of the structure and setting of the geology in this area are given in Ager (1980) and Donner (1995).

The Baltic Shield, which consists mainly of exposed Precambrian crust, dips towards the south and east under the sediments of the East European Platform. To the west and the north, the shield area is bordered by the Paleozoic Caledonides mountain chain. The Scandinavian Caledonides were formed mainly during the Silurian and Devonian as the result of folding and metamorphism of Cambro-Silurian sediments and older Precambrian rocks at the edge of the continent of which the Fenno-Scandinavian Shield was a part. Large nappes formed which were thrust from west to east.

In combination with uplift, the Baltic Shield has undergone a long period of erosion which has led to the removal of the majority of the Paleozoic platform cover over Fenno-Scandinavia. Erosion of the exposed Precambrian crystalline rock would form discontinuous, coarse-grained sediment with high-permeability. As a result of the Pleistocene glaciations, most of the loose material was removed from the mountains and the bedrock became striated and polished (Donner, 1995).

Tills and morainic and fluvial-glacial deposits are widespread in Fenno-Scandinavia and form the most important source of unconsolidated material. Upon deglaciation most of Finland, large areas of Sweden and and all of Norway was depressed isostatically by the ice mass and subsequently became submerged by the rise in sea-level caused by ice melting. Therefore, marine and lacustrine deposits are widespread in these formerly submerged areas.

The Baltic Shield is bordered to the south and east by the East European Platform (Figure 2.1). After the Late Precambrian, the East European Platform was no longer subject to orogenic activity and, in comparison with the Baltic Shield, is relatively undeformed. Subsidence of the platform has led to sedimentary rocks dipping gently to the south in sublatitudinal belts. Vendian and Cambrian rocks in north Estonia are overlain up sequence and southwards by Mesozoic and Neogene rocks in south Lithuania and Poland (Figure 2.2). Southwest of the Baltic Shield lies the Baltic Plain, also an area of subsidence and sedimentation. It is separated

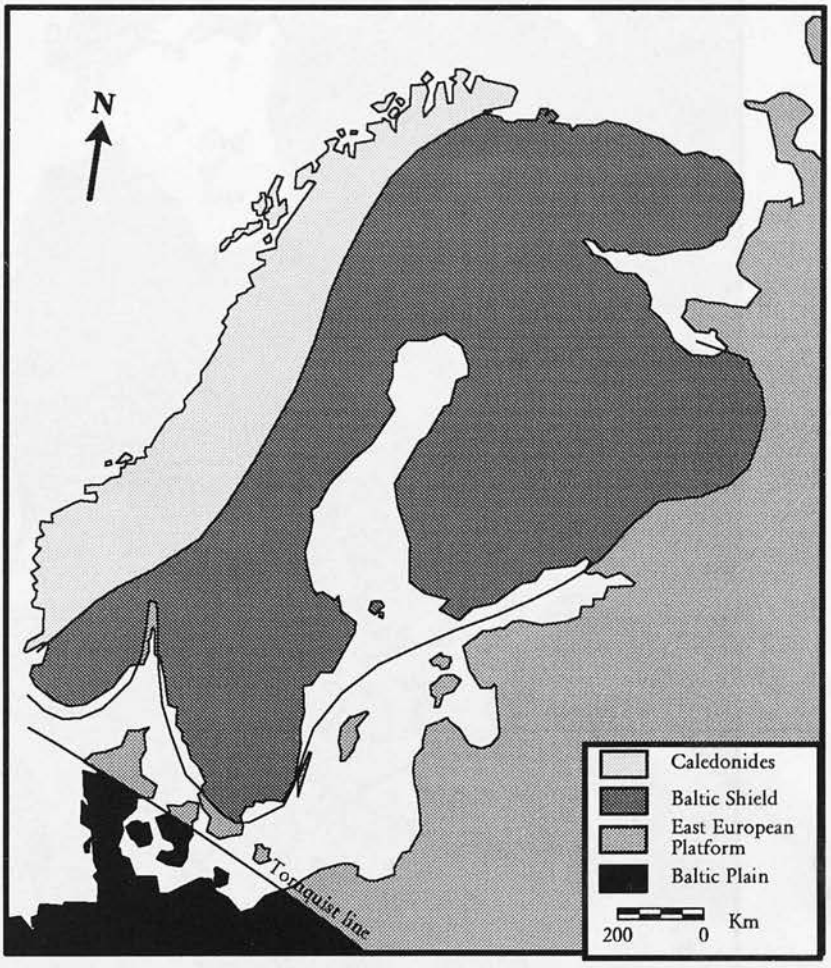

Figure 2.1: Simplified physiography map of northwest Europe

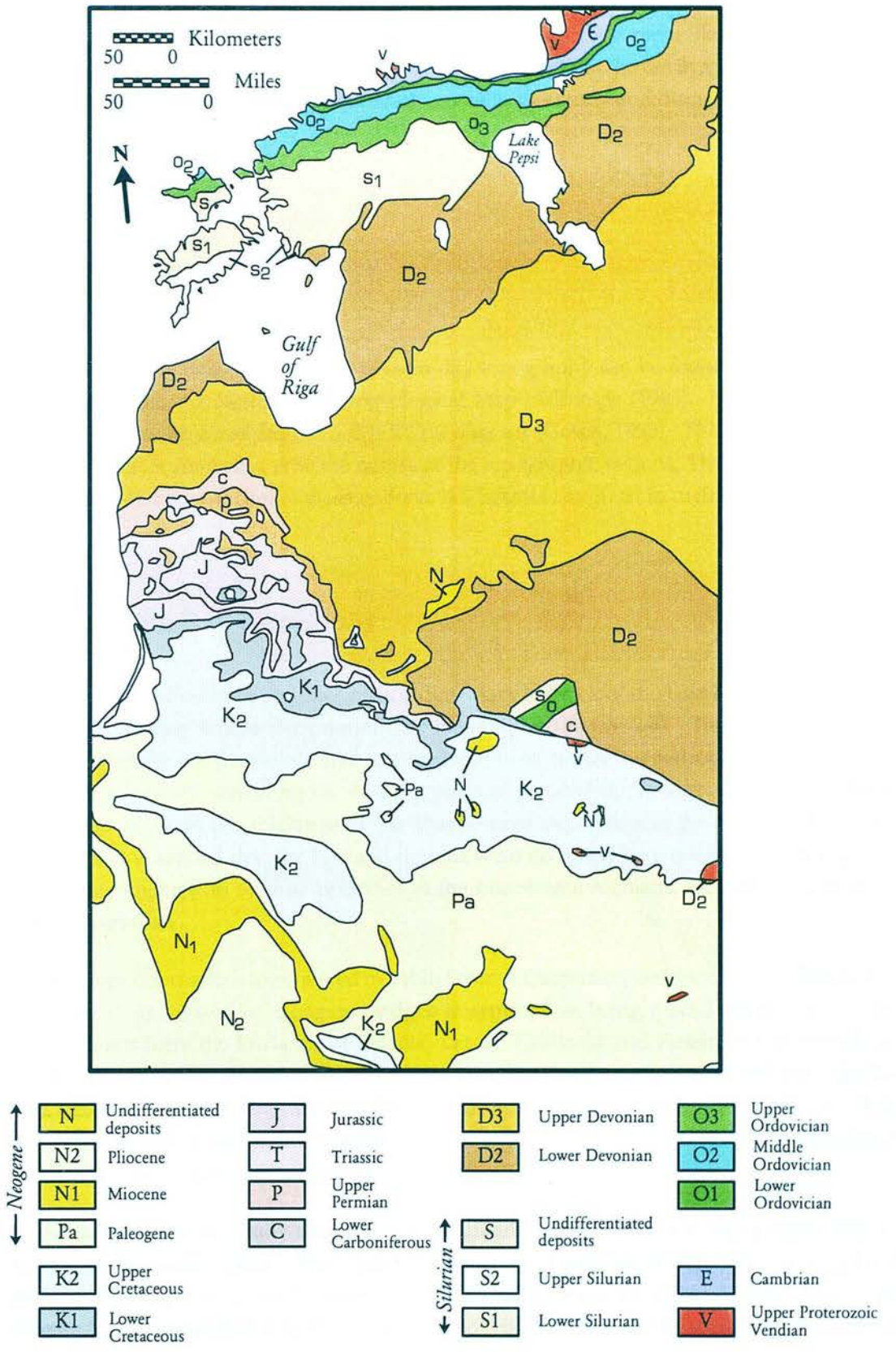

Figure 2.2: Geological map of the East European Platform, after Leningrad (1982)

from the East European Platform by the Tornquist line, south of which a Precambrian basement is not proven. The erosion of these Paleozoic sediments would form a fine-grained till of low-permeability. It is thought that this fine-grained till is more likely to deform than the coarse till formed from the crystalline Precambrian rocks in the north and may explain the variation in the distribution of lineations observed in this study and discussed in Chapter 7.

2.2 Topography

2.2.1 Introduction

A comprehensive description of the present day topography can be found in the guides accompanying the International Hydrogeological Map of Europe (1985). Present day topography data was acquired from the GTOPO30 data set (Gesch, 1996). This data is shown in Figure 2.3 and is annotated with the names of the topographic regions. The following Section provides a brief description of these regions. All heights are given in metres above mean sea level.

2.2.2 Present Day Topography

The relief of the Paleozoic and Mesozoic sedimentary bedrock of the East European Platform is clearly reflected within the present day topography (Figure 2.4). The bedrock relief is characterized by small absolute and relative heights such that the bedrock could not contol the dynamics of an overriding ice sheet by physical constraint. Nevertheless, there is some correlation between the thickness of the Quarternary deposits and the bedrock relief. In Chapter 6 it is argued that the lowland regions were occupied by ice streams with high ice velocities compared to the low velocities in the interstream highland areas where sediment could accumulate.

The bedrock depressions are covered in a thin layer of Quaternary sediments, up to 50m thick. They are characterised by elongated ridges interpreted as being glacial lineations. Today these regions form the lowlands of Estonia, Latvia, Lithuania and Russia and surround the insular highlands (*sensu* Raukas *et al.* 1995). These highlands are formed from thick glacial and lacustrine deposits and are usually centred on a bedrock elevation (Figure 2.4). They are characterised by the occurrence of numerous hills and by a very complex distribution of terminal moraines and kames (Geer *et al.*, 1985).

In the southeast of the study area a chain of highlands form part of the topographic feature known as the Baltic Ridge. The ridge extends to the southwest of the Bežanicy Highland through the regions of the Latgale and Augšzeme Highlands, Baltic Uplands (Gr'iada, Neman-Vilia), Lithuanian and Mazury (Mazuren) Highlands. It can be seen from the satellite

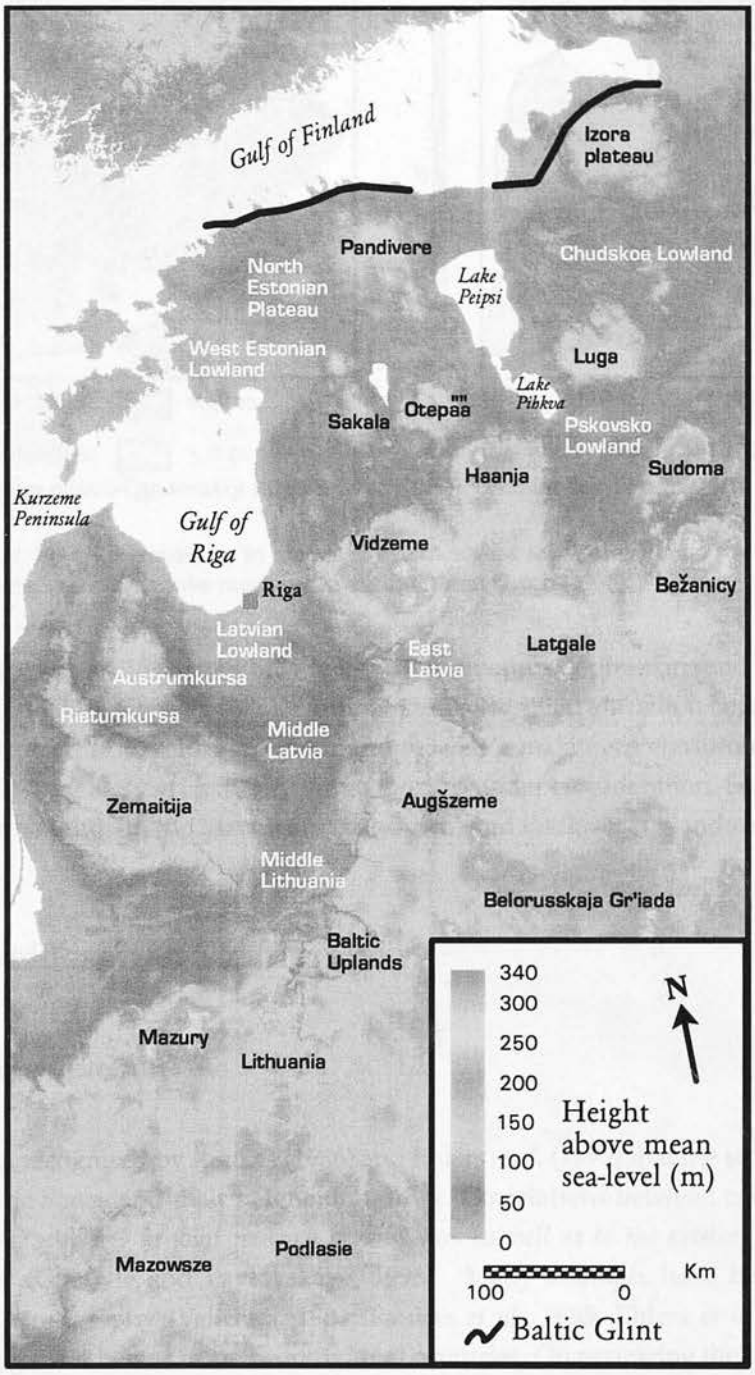

Figure 2.3: Topographic map of the East European Platform

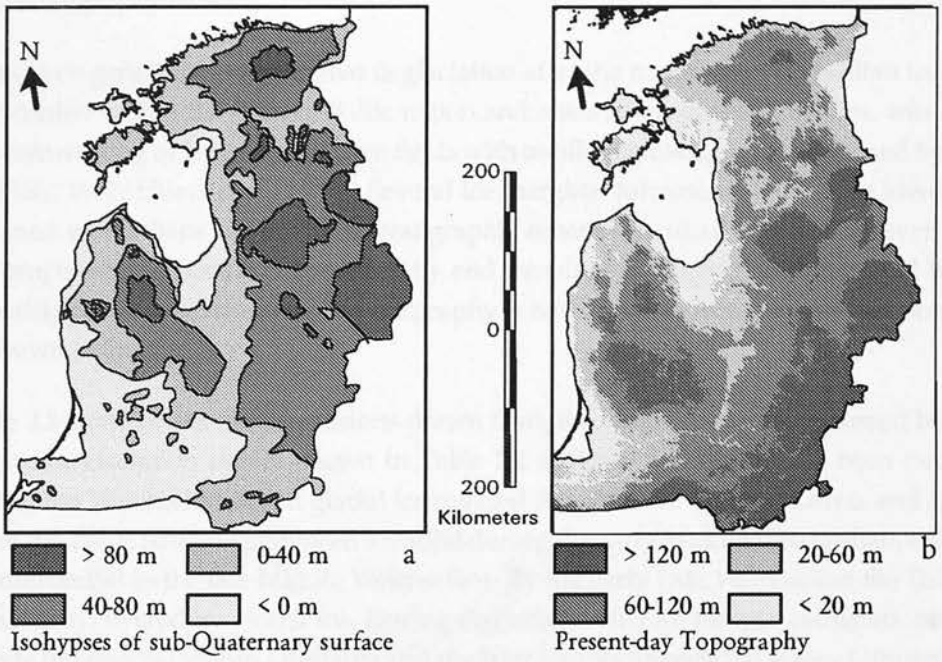

Figure 2.4: a: Bedrock elevations in metres above mean sea level, after Raukas *et al.* (1995). b: Present day elevations in metres above mean sea level, data from Gesch (1996).

data that the Baltic Ridge has a hilly relief with numerous depressions and basins occupied by swamps and lakes (Chapter 5). The limit of the Weichselian glaciation occurs along the ridge, which is formed of terminal moraines and reaches a maximum elevation of 333 m (Kolago, 1985). This is the highest elevation within the area under consideration. South of the ridge the land lowers slightly to the Mazowsze (Masovien) and Podlasie lowlands of Poland.

2.3 Weichselian Stratigraphy

2.3.1 Introduction

It has been recognised by Raukas (1986) and Ehlers *et al.* (1995) that the stratigraphic schemes of the Baltic States and their neighbours differ. Correlations between countries are difficult due to the *'problems in joint research organisation as well as to the existing different methodical approaches'* (Guobyte and Pavlovskaya, 1998). Many attempts have been made to create a unified stratigraphy (Velichko, 1984; Raukas *et al.*, 1995; Ehlers *et al.*, 1995) usually by simplifying the schemes from the individual countries. On reviewing the literature, a regional overview of the lithostratigraphy and its relation to the morphostratigraphy was found to be lacking. Table 2.1 is a proposed correlation of the most common stratigraphic terms used within the countries of this study. For the following discussion, the Weichselian has been divided into Early, Middle and Late phases. Table 2.2 shows how these phases relate to the

local stratigraphic units.

It has been generally accepted that deglaciation after the maximum Weichselian ice advance, as recorded within the Eastern Baltic region and areas south of the Baltic Sea, was a process of downwasting of large stagnant ice fields with oscillating margins characterised by ice lobes (Raukas, 1977; Ehlers *et al.*, 1995). Several ice marginal formations have been identified and are used as the basis of a morphostratigraphic scheme (Raukas, 1986). However, many of the proposed stadials are not marked by end moraines or other glacial marginal landforms (Karukäpp, 1997) and the morphostratigraphy is not always reflected by the lithostratigraphy as shown in Table 2.2.

Table 2.2 summarises the conclusions drawn from the various sources discussed below. The schematic glaciation curves shown in Table 2.2 indicate that there have been two periods during the Weichselian when glacial ice covered the whole of Estonia, Latvia and Lithuania. All of the Baltic States experienced a stadial during the early Middle Weichselian, followed by an interstadial in the late Middle Weichselian. By the early Late Weichselian the Baltic States were again covered by glacial ice. During deglaciation the ice margin oscillated, causing the Pavyte interstadial within Lithuania and the later Raunis interstadial across Lithuania, Latvia and the southern regions of Estonia. By 11,000 B.P., towards the end of the Late Weichselian, the ice finally retreated from the Eastern Baltic region.

2.3.2 The Early Weichselian

During the Early Weichselian, cooling led to the renewed build-up of ice sheets in the circumpolar region and to a lowering of sea level (Mangerud, 1983). Deposits of Early Weichselian glaciations have been found in Norway, Finland and northern and central Sweden (Ehlers *et al.*, 1995). However, the exact extent of the Early Weichselian glaciations are unknown. It is thought unlikely that they reached the most southerly parts of Finland or the Eastern Baltic region (Ehlers *et al.*, 1995; Donner, 1995).

In the Eastern Baltic region, the transition from the Eemian to the Weichselian is identified from pollen and spore spectra. Interglacial forests disappeared and were replaced by a tundra forest vegetation (Liivrand, 1992). For example, Meirons (1986) identified deposits of glaciolacustrine silts at Rogaļi, Latvia. As well as redeposited pollen derived from the preceding Eemian interglacial, these sediments contain vegetation indicative of a colder climate (*Betula nana* L., *Dryas* sp and others). Further Early Weichselian stratigraphic sites are shown in Figure 2.5. Some of the thermoluminescence (TL) dates obtained from these sites are shown in Table 2.3. Throughout the Early Weichselian, periglacial conditions prevailed in Estonia and Latvia (Liivrand, 1992; Dreimanis and Zelcs, 1995) with two interstadial warmings being traced in Estonia (Liivrand, 1992). The periglacial conditions were followed by the first Weichselian glacial advance into the Eastern Baltic region.

Finland	Estonia	Latvia	Lithuania	Belarus	Russia	Poland	Germany
Holocene	Holocene	Holocene	Holocene	Holocene	Holocene	Holocene	Holocene
Weichselian	Vortsjärve Järva Savaia Valgjärve Kelnase	Latvian Baltija Lejasciems Lower Baltija	Nemunas Baltija Aukštaitija Grūda Rokai Varduva	Poozerje Upper Middle Lower	Valdai Upper Middle Lower	Vistulian	Weichselian
Eemian	Prangli	Felicianovo	Merkinė	Murava	Mikulino	Eemian	Eemian
Saalian	Ugandi Upper Middle Lower	Kurzeme	Zeimena Medininkai Snaigupėlė Zemaitija	Sazh Shklov Dnieper	Moscow Odintsovo Dneiper	Odranian Wartanian Odranian	Saalian Warthe Drenthe
Holsteinian	Karuküla	Pulvernieki	Butėnai	Alexandriya	Likhvin	Mazovian	Holsteinian

Table 2.1: Correlation of the most common stratigraphic terms used within the countries referred to in this study, adapted from Raukas *et al.* (1995) and Ehlers *et al.* (1995)

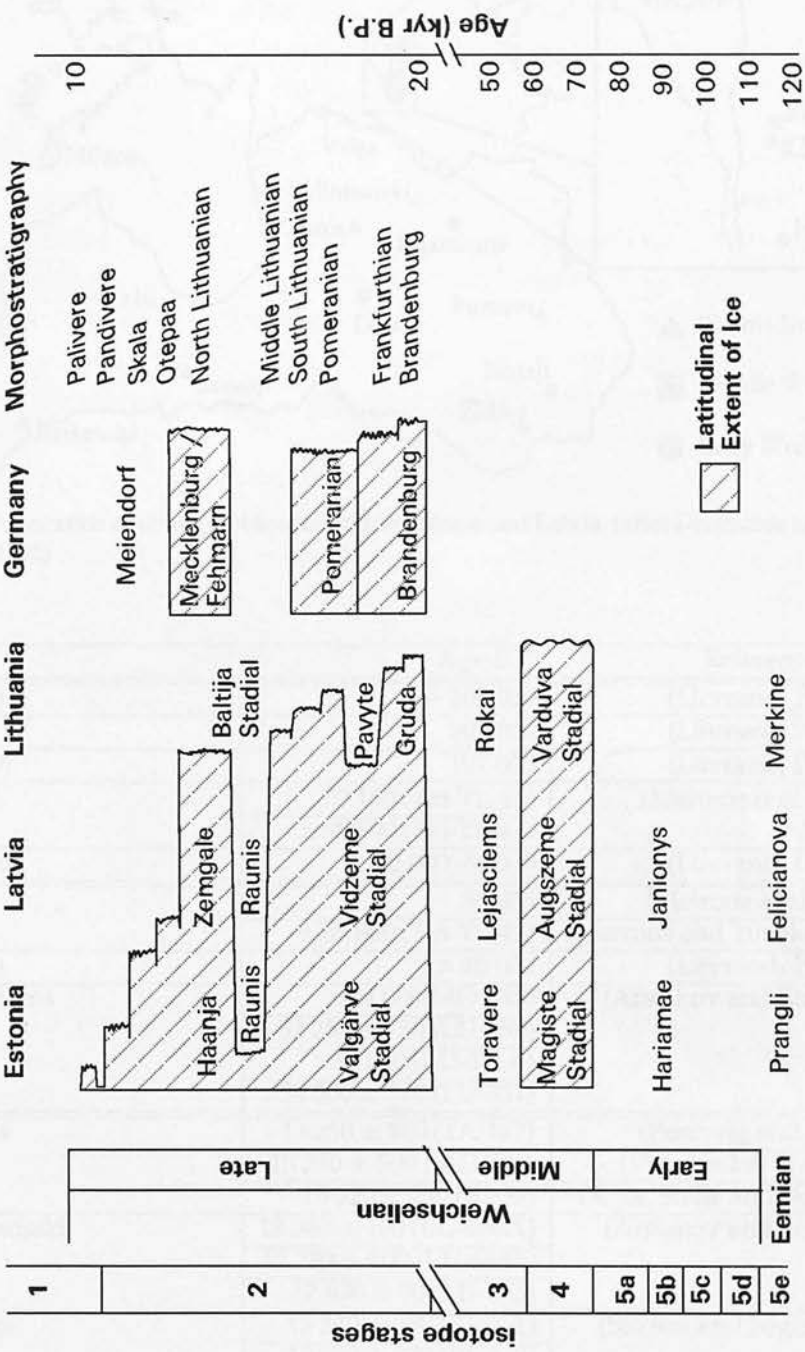

Table 2.2: Schematic glaciation curves for the Weichselian in the Eastern Baltic region compared with stratigraphic units and deep-sea isotope stages. (Adapted from Donner 1995; Liivrand 1992 and Raukas *et al.* 1995)

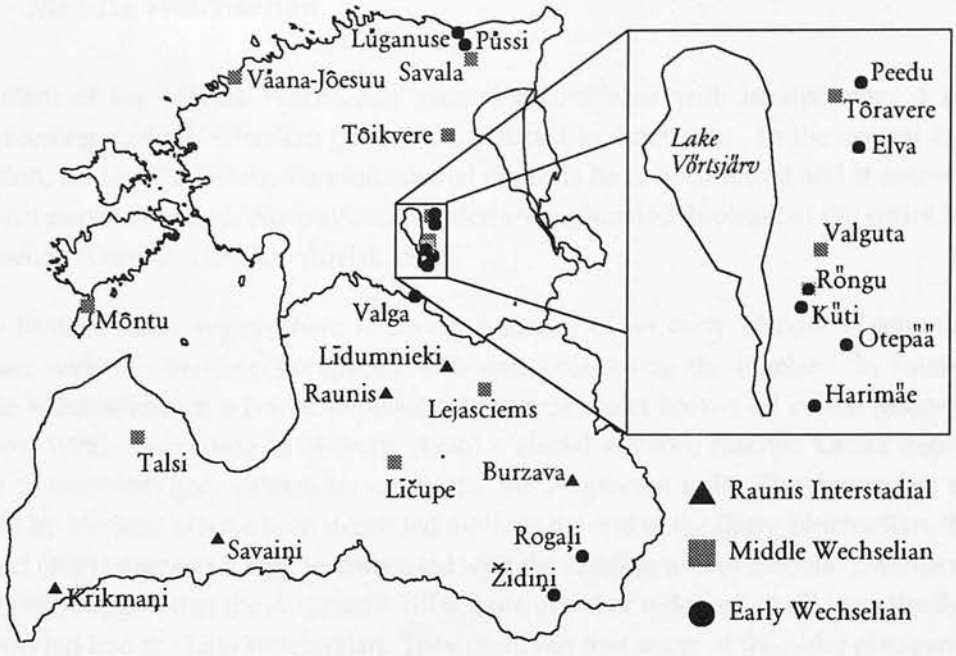

Figure 2.5: Location of stratigraphic sites within Estonia and Latvia, (after Dreimanis and Zelcs 1995 and Liivrand 1992)

Site	Age B.P.	Reference
Röngu	> 108 000	(Liivrand, 1992)
Valga	101 000	(Liivrand, 1992)
Otepää	101 000	(Liivrand, 1992)
Židiņi	79 150 (Tln-TL-45)	(Meirons *et al.*, 1981)
	> 68 800 (Tln-TL-42)	
Valguta	62 000, 66 000	(Liivrand, 1992)
Talsi	56 056	(Meirons et al 1984)
	> 68 800 (Tln-TL-42)	(Meirons and Yushkevichs, 1984)
Röngu	> 40 000	(Liivrand, 1992)
Lejasciems	>34 000(MO-318)	(Arslanov and Stelle, 1975)
	>32 250 ± 730 (LU-159)	
	>33 000 (LU-311A)	
	>34 500 ± 790 (LU-311)	
Raunis	13 250 ± 160 (TA-177)	(Punning *et al.*, 1968)
	13 390 ± 500 (MO-296)	(Vinogradov *et al.*, 1966)
	13 320 ± 250 (RI-39)	(V. Ya. Stelle and Veksler, 1975)
Līdumnieki	13 080 ± 160 (LU-668A)	(Arslanov and Stelle, 1975)
	12 780 ± 100 (LU-668B)	
	12 830 ± 90 (LU-695)	
Savaiņi	13 840 ± 350 (RI-A-1)	(Sakson and Seglinsh, 1990)
	13 970 ± 370 (RI-A-2)	
Kurenurme (S.E. Estonia)	12 650 ± 520 TU	(Raukas, 1986)
	12 420 ± 100 TU	

Table 2.3: Dating of intermorainic deposits from Weichselian sites in Estonia and Latvia

2.3.3 Middle Weichselian

The extent of the Middle Weichselian glaciation correlated with isotope stage 4 is, like the preceding Early Weichselian glaciations, difficult to determine. In the central areas of glaciation, no Middle Weichselian interstadial deposits have been found and it seems likely that most parts of Finland, Norway and Sweden were glaciated throughout the entire Middle Weichselian (Donner, 1995; Lundqvist, 1986).

In the Eastern Baltic region there is strong evidence of an early Middle Weichselian ice advance, with tills between periglacial sediments post-dating the Eemian. In Estonia the Middle Weichselian ice advance deposited the single violet brown till of the Mägiste unit (Donner, 1995). According to Meirons (1986) a glacial advance reached Latvia depositing a grey to brownish grey calcareous sandy till, the Augszeme unit. The Augszeme unit is thought by Merions to have been deposited towards the end of the Early Weichselian, though Liivrand (1991) suggests it may be correlated with the Mägiste unit of Estonia. Dreimanis and Zelcs (1995) suggest that the Augszeme Till is a reworked or redeposited till from the Saalian, incorporated into the Late Weichselian. They point out that many of the older glacigenic and non-glacial deposits have been glaciotectonically deformed and that the Augszeme Till closely resembles the underlying Kurzeme Till, which has been placed stratigraphically within the Saalian.

However, the similarity in appearance of tills does not necessarily imply a similar time of deposition. Furthermore, to the south of the Augszeme unit borehole evidence from northern Lithuania shows a till (Varduva unit) younger than the Eemian and older than the Lejasciems Interstadial, stratigraphically placing it in the Middle Weichselian (Raukas and Gaigalas, 1993). Therefore it follows that there was an ice advance during the Middle Weichselian covering Estonia, Latvia and northern parts of Lithuania. In the more southerly areas including Belarus, the Early and Middle Weichselian are represented by periglacial conditions, with no evidence of glacial advance (Liivrand, 1991).

An early Middle Weichselian ice advance is also recorded in regions outside of the Eastern Baltic region. At Holmstrup in Denmark (Figure 2.6), Middle Weichselian marine sediments rest on a till bed younger than the Eemian and which could thus be correlated with isotope stage 4 (Andersen and Mangerud, 1990; Houmark-Nielsen, 1990). In northern Poland, an early Middle Weichselian ice advance has also been proposed (Bowen *et al.*, 1986). Drozdowski (1986) has dated glacial deposits and related facies in the lower Vistula region to 50 - 70 ka, correlating with the Middle Weichselian. On the western shore of Lake Onega at the Petrozavodsk site (Figure 2.6), borings show that Eemian marine clays are overlain by a Middle Weichselian till (Lukashov, 1982).

Many regions experienced an ice free period after the Middle Weichselian glacial and before the first ice advance of the Late Weichselian. At the Petrozavodsk site, Middle Weichselian till is covered by freshwater sediments (Lukashov, 1982). An ice free interval is also proposed to have followed the early Middle Weichselian ice advance in northern Poland (Bowen *et al.*,

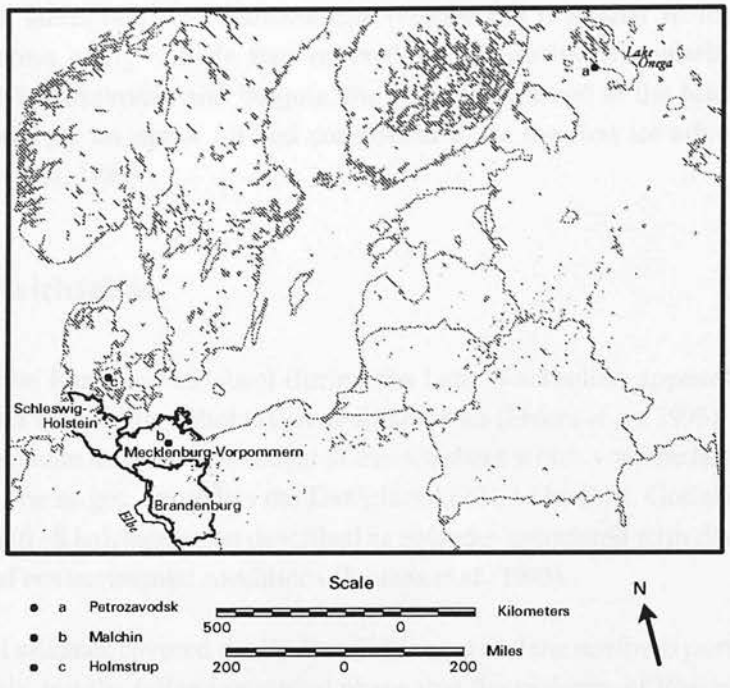

Figure 2.6: Location of Weichselian stratigraphic sites and regions mentioned within the text and not shown in Figure 2.5

1986). Sediments indicative of an interstadial overlie the Mägiste and Augszeme till units in the Baltic States.

At Volguta, Estonia (Figure 2.5), a pollen diagram of till-covered silts and clays has, if the re-bedded Eemian pollen is excluded, an assemblage dominated by *Artemisia* plus other non arboreal pollen and with some *Betula*, which is a composition typical for a periglacial environment (Liivrand, 1991). This non-glacial interval in Estonia was named Tôravere, after a site similar to Volguta, where silty clays can be found overlying a lower till bed.

In Latvia periglacial vegetation appears to dominate within silts found overlying the Augszeme unit. These sediments contain plant remains and are extremely rich in non-arboreal pollen and spores. A mammoth tooth (*Mammus primigenius* Blum) was also found at Tiltalejas, near Lejasciems (Danilāns 1973 in Dreimanis and Zelcs 1995). Radiocarbon dates from these sediments range from 32 ka to 36 ka and >34 ka (Table 2.3). Thermoluminescence dates (obtained by A. Raukas and reported by Dreimanis and Zelcs 1995) suggest the sediments to be older and possibly already accumulating during the Early Weichselian. This interpretation, however, should be treated with caution since the thermoluminescence method tends to over estimate the age of glacial sediments. This is because glacial sediments were often not exposed to sunlight long enough before burial to empty all the electron traps which fill with time and upon which thermoluminescence dating depends. A review of thermoluminescence dating is provided by Wintle (1990).

The Weichselian stratigraphy at Petrozavodsk (Figure 2.6) is similar to that at Volguta in Estonia, both areas being outside that covered by ice during the whole of the Middle Weichselian. At Petrozavodsk and Volguta, the silty clays placed in the Middle Weichselian are partly covered by an upper till bed considered to be the first ice advance of the Late Weichselian (Donner, 1995).

2.3.4 Late Weichselian

The growth of the European ice sheet during the Late Weichselian appears to have begun around 21 ka and reached its culmination at about 18 ka (Ehlers *et al.*, 1995). De Geer (1940) established three main stages in the retreat of this ice sheet which was the last deglaciation of the Baltic area. The stages, known as the Daniglacial (20 - 13 ka B.P.), Gotiglacial (13 - 10 ka) and Finiglacial (10 - 8 ka), have been described as episodes associated with distinctly different glaciological and environmental conditions (Raukas *et al.*, 1995).

The main glacial advance covered the Eastern Baltic area and the northern part of Belarus, and it was during this and the following retreat phase that the majority of Weichselian tills were deposited (Liivrand, 1992; Dreimanis and Zelcs, 1995). The Valgjärve unit was formed at this time and consists of a violet-grey till together with a restricted grey till in south east Estonia and most of the grey tills in northern Estonia (Liivrand, 1992).

The classic subdivision of the Late Weichselian glaciation has been based on morphostratigraphy. By mapping the different ice marginal positions in Mecklenburg-Vorpommern and Brandenburg in east Germany (Figure 2.6), Woldstedt (1925) distinguishes Brandenburg, Frankfurt and Pomeranian Stages, each of which comprised several belts of end moraines. This morphostratigraphy, however, is not reflected in the lithostratigraphy. According to clast lithological investigations by Cepek (1962) the Eemian deposits are covered by till units, which are correlated with the Brandenburg and Pomeranian phases. The end moraines of the so-called 'Frankfurt Stage' are thought to represent landforms created by a minor oscillation during the ice retreat from the maximum Brandenburg ice marginal position (Ehlers, 1996).

In eastern Germany the ice advanced more than 200 kilometres inland. In western Germany, the Late Weichselian ice only covered a small margin of the coastal zone south of the Baltic Sea (Ehlers, 1996). Gripp (1924) mapped the maximum extent of the Weichselian ice margin in Schleswig-Holstein, Germany on the basis of morphological criteria (Ehlers, 1996). He concluded that the Weichselian ice had not crossed the Elbe River. According to Gripp (1964) three major end moraine belts can be distinguished, these he termed A (outermost), M (Middle) and I (innermost) ice marginal positions. It is, however, not possible to identify these belts beyond Schleswig-Holstein and correlations with the Weichselian tills of Mecklenburg-Vorpommern are difficult (Stephan, 1983).

In Lithuania, the morphostratigraphy (Figure 2.7) is similar to that in eastern Germany. The maximum extent of the Weichselian ice is marked by three series of end moraines:

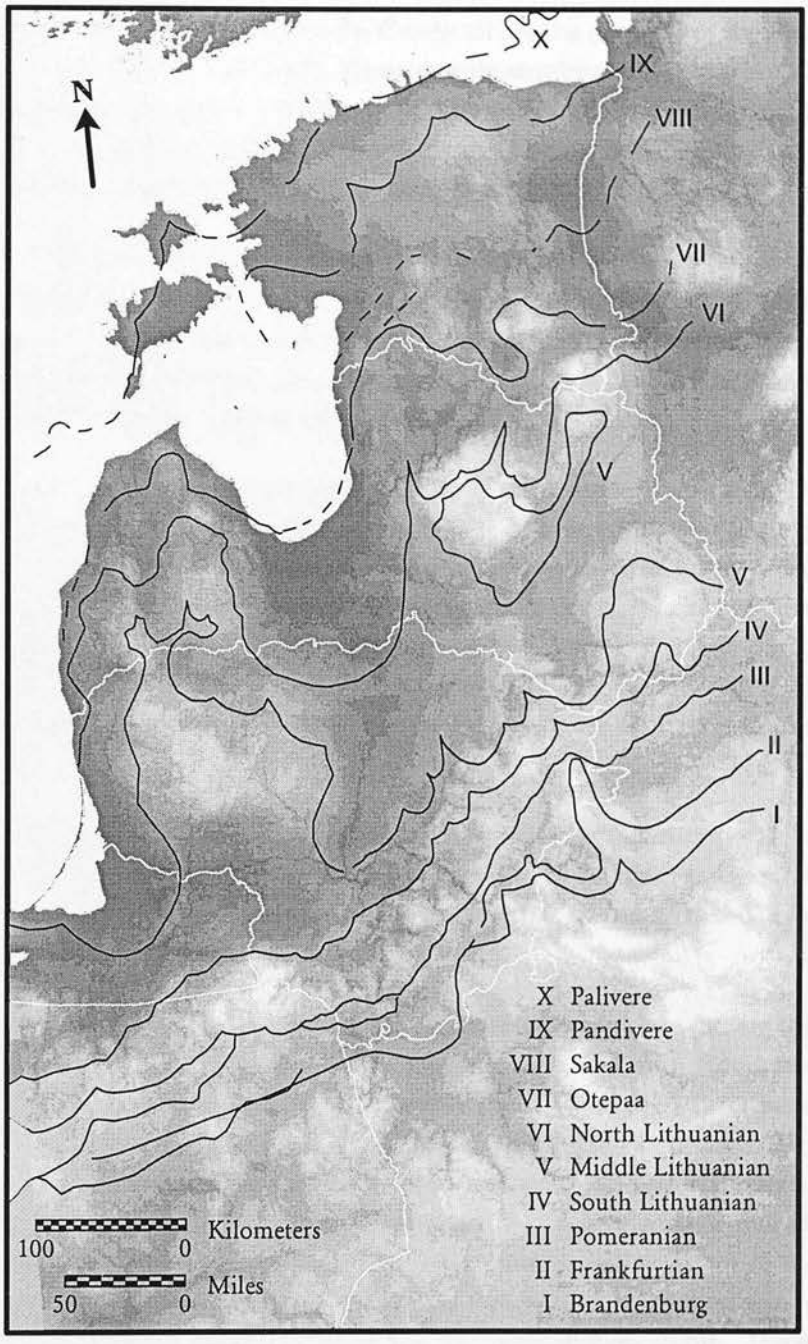

Figure 2.7: Palaeo-ice marginal positions within the Baltic States, after Raukas *et al.* (1995)

the Aukštaičiai (Pomeranian), Ziogeliai (Frankfurt) and Gruda (Brandenburg) (Raukas *et al.*, 1995). During these stages one till unit, the Gruda till, has been identified in Lithuania. The till is enriched with Mesozoic marl clasts and is rich in crystalline rocks from Central Sweden, the Åland Islands and the Baltic Sea Floor (Gaigalas, 1995).

According to Gaigalas (1995), above the Gruda till are the deposits of the Pavyte Interstadial and then another till, the Baltija till. Three morphostratigraphic stages are identified during deposition of the Baltija till: the Southern, Middle and Northern Lithuanian Stages. The latter is identified as a major re-advance throughout the Eastern Baltic region, preceded in Latvia and Estonia by interstadial sediments as described below.

The Weichselian ice only extended into the north of Belarus in the Orsha substage (Figure 2.7). Morainic deposits from the Weichselian are represented by red-brown, sometimes crimson clast rich, sandy clayey silts and clays with lenses of gravel and sorted sands. Far-travelled erratics are rarely found within the sediments and are small in size. The thickness of deposits generally varies between 10-40 m up to 60-80 m.

Two glacigenic beds have been distinguished within Weichselian deposits in Latvia, separated by the Raunis interstadial beds (Meirons, 1986). The lower Vidzeme till, like the overlying Zemgale till are both reddish brown, the colour being derived from the incorporated Devonian sandstones. Palaeozoic carbonates and Precambrian crystalline rocks dominate the clast assemblage (Knoshin 1965 reported in Dreimanis and Zelcs 1995). The dominant highlands of eastern Latvia, were formed mainly during the early Late Weichselian deglaciation phase. Tills and associated meltwater sediments in the highlands are up to 90 m thick (Dreimanis and Zelcs, 1995).

In the southern Baltic area, the conditions during the Brandenburg and Frankfurt stages proved unfavourable for the development of large proglacial basins. Due to the unimpeded drainage of glaciofluvial streams, out-wash plains and ice marginal valleys (urstromtaler) formed frequently (Ehlers, 1996).

The most pronounced warming during the deglaciation took place during the Raunis phase. It has been dated using the radiocarbon method at several sites throughout Estonia and Latvia to be approximately 13 250 B.P (Table 2.3 and Figure 2.5). The peat bed at Raunis sampled for the radiocarbon dating is, however, thoroughly penetrated by recent rootlets and therefore the dates determined may not be accurate. Moreover, the Raunis organic bed is glaciotectonically deformed, possibly being a raft of interglacial or interstadial sediment of uncertain age, glacially thrust from the buried Raunis valley. Most of the other organic deposits interbedded in the till strata of the Late Weichselian Formation also occur in areas of abundant glaciotectonic deformations and at relatively shallow depth. The organic remains may therefore have been contaminated either by recent rootlets or by secondary carbonates produced by pedogenic processes (Dreimanis and Zelcs, 1995)

The Raunis interstadial was followed by the North Lithuanian (Luga, Haanja) advance

which deposited a reddish brown till in Estonia (Liivrand, 1992). In the Kurenurme section, south eastern Estonia, remains of *Salix* wood were taken from sandy loam overlying North Lithuanian till. Radiocarbon dating of the wood and organic detritus indicates that these were deposited at the beginning of the Bölling interstadial , 12 650 B.P. (Table 2.3). The North Lithuanian stadial preceded the Bölling interstadial and belongs to the Oldest Dryas (Raukas, 1986).

Heerdt (1965) demonstrated the existence of a thin, third till unit within Germany. It lies above the tills correlated with the Brandenburg and Pomeranian and was deposited during an ice advance which is equivalent of the Fehmarn Advance in Schleswig Holstein and the Baelthav Advance in Denmark (Ehlers, 1996). The advance has been assigned to the period 13,200 - 13,000 B.P. and thus coincides with the Oldest Dryas (Ehlers, 1996). This Weichselian till is a sandy till with a high limestone content. Where this till directly overlies older tills, differences in colour help to distinguish them (Ehlers, 1996). The till sheet largely forms a cover over pre-existing landforms, hardly altering the relief and with little disturbance of the subsurface. The greatest thicknesses of till are observed in depressions (Rühberg, 1987). It is interpreted that the ice in many cases has over-ridden dead ice of the Pomeranian phase. Only in cases where the ice sheet encountered steep slopes, were major push moraines formed. Geological mapping has shown that this ice advanced south to Malchin (Ehlers, 1996). Most eskers in Mecklenburg-Vorpommern were formed during this advance. No major sandurs formed beyond the glacier during this phase. (Rühberg, 1987).

It is likely that between deposition of the second and third Weichselian tills in Germany, the ice margin had melted back into the Baltic Sea depression. The tills are separated by glaciofluvial and glaciolacustrine deposits (Ehlers, 1996). The distinctive clast inventory of the youngest Weichselian till in Germany is interpreted by Rühberg (1987) as indicative of a change in the ice movement direction to a more east-westerly course.

In Estonia, in places to the north of the Palivere advance (for example on the island of Prangli, Figure 2.5), Eemian deposits are overlain by up to four Weichselian till beds of thickness 8.15, 9.50, 11.35 and 6.50 metres in ascending order. The tills are separated from each other by thin layers of water-laid sediments (Raukas, 1992). Indicator boulders occurring in the tills support the existence of at least four stages during the Weichselian glaciation (Raukas, 1986), the distinctive combination of boulders from identifiable sources, suggesting changing direction of ice flow. The Haanja, Otepää and Sakala stages are characterised by a prevalent south easterly direction of continental ice flow, the Pandivere stage by a southerly or even southwesterly direction (west of the Pandivere elevation) and the Palivere stage again by a south easterly direction (Raukas, 1986).

While dating of the older end moraines is largely hypothetical (Ehlers, 1996), Raukas (1986) proposed that the Haanja heights first emerged from beneath the ice about 13,000 B.P., with ice marginal formations in the region of the Otepää heights being formed at about 12,600 B.P.. The Sakala belt emerged at approximately 12,250 B.P. and about 12,050 B.P. the Pandivere zone was formed. These dates are based on the ^{14}C age of buried organic deposits in till and assume

a new readvance of the glacier to the organic deposits. However, according to Karukäpp *et al.* (1992) the organic material dated in South Estonia is mostly redeposited in glaciolacustrine sediments and probably results from glaciokarst of stagnant ice. It cannot therefore date a new readvance of the active glacier.

The later Palivere ice marginal formation in Estonia resembles the Finnish Salpausselkä ridges. Apart from end moraines on the island of Saaremaa (Figure 2.5), it largely consists of ice marginal meltwater formations, accumulated in the Nômme Lake, an early development phase of the Baltic Ice Lake (Ehlers, 1996). Varved clays containing interstadial plant remains separate the upper two tills in Estonia. The correlation of this varve series with those in the Luga basin in the St. Petersburg district is based on varves which mark the connection of the Luga and Neva basins about 12,000 years ago, when the ice margin receded. This event, which occurred twice (in the 79th and 111th years of the existence of the Luga basin), was used as a fixed point for dating the ice retreat from the Pandivere Upland (Raukas, 1992), and the ice advance of the Palivere 11,200 B.P. (Raukas, 1986). Karukäpp *et al.* (1992) established about 600 annual layers on the bottom of the Gulf of Finland which cannot be connected to a general time-scale.

Connecting the Finnish varve chronology established by Sauramo (1923) with the Swedish chronology as suggested by Strömberg (1990) revises the date of the ice marginal position at the Finnish coast to 12,123 B.P. and the beginning of the formation of the moraine of Salpausselkä I to 11,303 B.P. (Donner, 1995). This is not in agreement with the dates proposed for the formations in Estonia. The age of the Palivere and Pandivere marginal zones appear to be too young in comparison with the Salpausselkä moraines. An attempt to explain the difference in dates has been made by assuming that the central parts of the Gulf of Finland were occupied by huge blocks of dead ice with the deglaciation in Finland starting before the ice blocks melted (Raukas, 1986). This seems unlikely, since those parts of the Gulf of Finland sea-floor which have been observed show strong drumlinization and no evidence of stagnant ice features such as hummocky moraine (Karukäpp *et al.*, 1992). The use of varved clays, radiocarbon dating and biostratigraphy have not reconciled the different dates (Raukas, 1992). The varve chronology appears to be considered the more accurate method of dating, and it has been proposed that 430 years be added to the Haanja, Otepää, Sakala and Pandivere ^{14}C dates given above (Raukas, 1996).

2.4 Late Weichselian and Holocene Land/Sea-Level Changes

With the withdrawal of the ice margin from the Pandivere moraine in northern Estonia, the ice-dammed lakes east of the Pandivere uplands joined with the ice-dammed waters in the southern parts of the Baltic to form a large lake which Donner and Raukas (1989) suggested represented the beginning of the formation of the Baltic Ice Lake about 12.2 ka to 12 ka B.P.

The extent of the Baltic Ice Lake (Figure 2.8) is based on a number of morphological observations of raised beaches around the coasts of the Baltic. Using the marginal deltas of the Fenno-Scandinavian moraines that formed just before the drainage of the Baltic Ice Lake as a starting point, the corresponding contemporaneous raised beaches have been traced west along the coasts of Lake Ladoga and the St Petersburg area in the east and further along the coasts of Estonia, Latvia and Lithuania. Further south, the former coastline of the Baltic Ice Lake is submerged, but on the Swedish east coast it is again above the present sea level. The final drainage of the Baltic Ice Lake, resulting in a drop of the water level by 27-28 m, is believed to have taken place at Billingen in Central Sweden at about 10.6 ka B.P. according to the varve chronology. Radiocarbon dating of this event yields approximately the same age (Donner, 1995).

The final drainage of the Baltic Ice Lake at Billingen marked the beginning of the Yoldia Sea stage. With the opening of the Närke Strait, the connection between the Baltic and the sea widened allowing sea water to enter the Baltic, changing its salinity from fresh water to brackish water (Figure 2.9.) However, the connection between the Baltic basin and the sea that had opened through the Närke Strait soon became narrower and shallower as a result of isostatic uplift. The Yoldia Sea stage was thus followed by the Ancylus Lake (Figure 2.10), so called after the freshwater gastropod *Ancylus fluviatilis* found in the littoral deposits of the island of Gotland, the island of Öland and in Estonia.

The decreasing rate of isostatic uplift coupled with a relatively rapid eustatic rise of the ocean level resulted in widening of the connection between the Baltic and the North Sea. Salt water could penetrate into the Baltic basin between Denmark and Sweden and the water within the Baltic became brackish. As the straits widened further, the Baltic water became marine and formed the Litorina Sea stage, named after the gastropod *Littorina littorea* which requires a water salinity of at least 8.1ppm. The transition to marine conditions occurred in a time transgressive manner. Even by 7 ka (Figure 2.11) the Gulf of Finland had a salinity below 8ppm, while the rest of the Baltic ranged from 8ppm to 20ppm.

Today, the uplift of the earth's crust induced by the unloading of the Late Weichselian ice sheet is still occurring in Scandinavia, with the centre of uplift in the northern part of the Gulf of Bothnia.

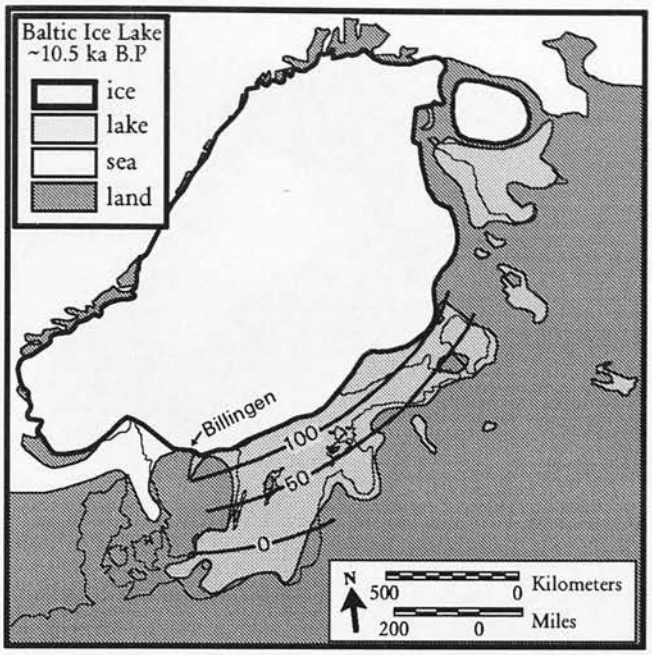

Figure 2.8. Baltic Ice Lake about 10.5 ka B.P. before its drainage at Billingen. With isobases (*sensu* Flint 1971), after Donner (1995)

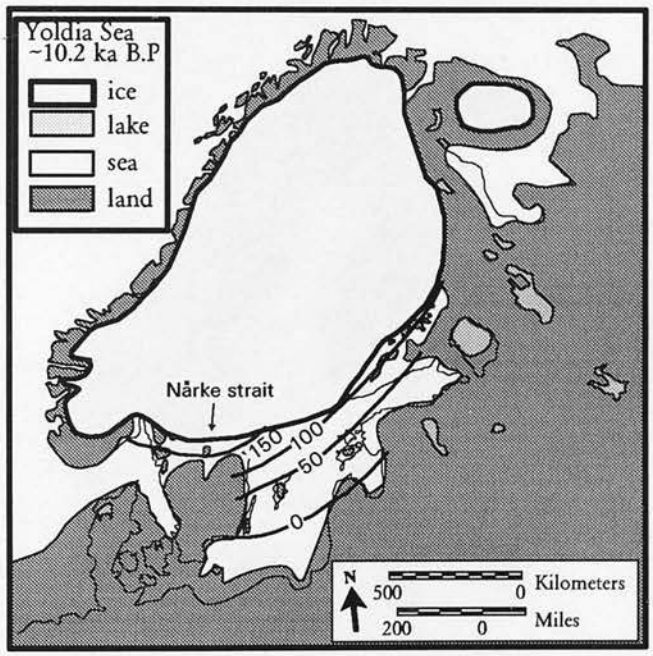

Figure 2.9. Yoldia Sea about 10.2 ka B.P. with isobases, after Donner (1995)

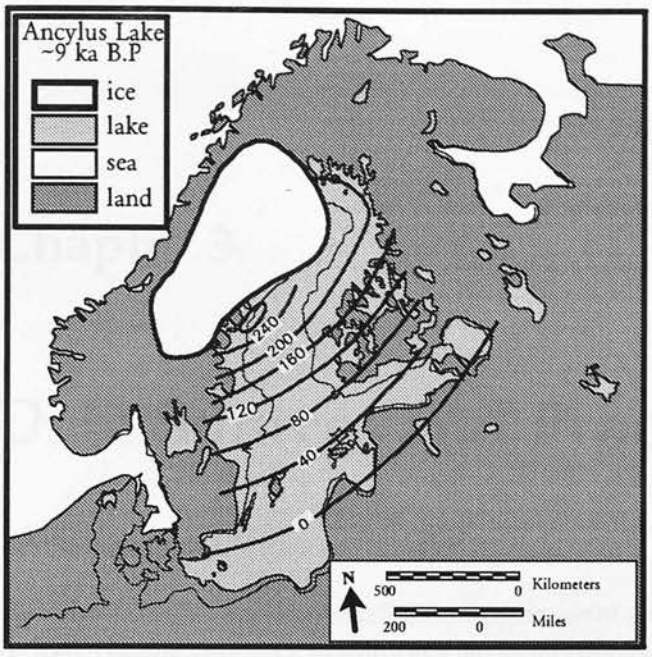

Figure 2.10. Ancylus Lake about 9 ka B.P. with isobases, after Donner (1995)

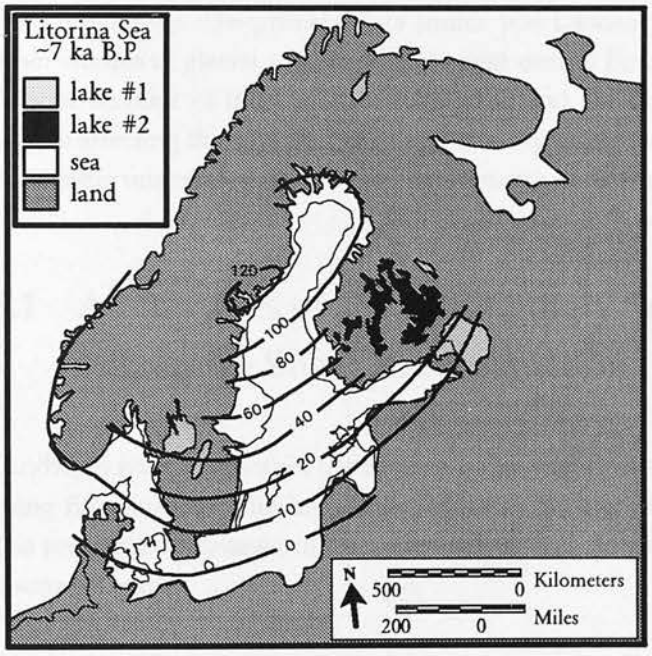

Figure 2.11. Litorina Sea about 7.5 ka B.P. with isobases. Lakes #1 formed during the Ancylus Lake stage, Lakes #2 formed after Ancylus Lake stage. After Donner (1995)

Chapter 3

Data Sources and Processing

The aim of this Chapter is to describe the advantages of using remote sensing, and in particular the use of satellite imagery, to study glacial geomorphology. Examples of previous work using satellite imagery for studying large scale glacial geomorphology are given, and an account of the advantages of working with digital data, as used in this study, over photographic data used previously. The primary data source was Landsat TM imagery. To our knowledge no other studies of glacial geomorphology over central Europe have used Landsat TM imagery. A brief account of the Landsat programme and the system specifications are given. The factors affecting the selection of images are explained along with a description of the image processing undertaken. Additional data sources used within this study are also documented.

3.1 Advantages of Using Remotely Sensed Imagery in Palaeo-Ice Sheet Reconstruction

Landform mapping within the Eastern Baltic region has been, for the most part, conducted using field-surveys with limited use of aerial photography, for example by Guobyte (1995). The principle advantages of using remotely sensed data for landform mapping are listed and discussed below.

3.1.1 The Study of a Large Working Area

To map the area in this study (≈275,000 km^2) using fieldwork would be both expensive and time-consuming. Remote sensing, in particular the use of satellite imagery, provides a practical alternative.

Using aerial photographs alone over the area would be very time-consuming. Table 3.1 shows

the spatial resolution and maximum Instantaneous Working Area (IWA) of different remote sensing systems. It can be seen from Table 3.1 that to study the area of one Landsat TM image would require at least 36 aerial photographs, assuming zero-overlap. While there is a reduction in spatial resolution, medium scale data like Landsat TM can be advantageous in studying overall ice flow direction, filtering out small variations in direction due to local anomalies. The use of a computers allows the co-ordination of additional data sets, such as published maps, fieldwork, digital elevation models and so on, within a single spatial framework. Combined with satellite imagery, such a data-base provides a cost- and time-effective method of studying large scale glacial dynamics.

System Type	Resolution (m)	Instantaneous Working Area (Km)
Air-photography	5	30x30
Synthetic Aperture Radar	25	100 x 100
Landsat TM	30	185 x 185
Landsat MSS	80	185 x 185
AVHRR	1100	3000 x 3000

Table 3.1: Areal Coverage and spatial resolution of several remote-sensing systems

3.1.2 Consistency of Technique and Data

Over the last few decades Quaternary science has evolved differently within the countries covered in this study (Ehlers *et al.*, 1995). The consequences of this are the emergence of terminological as well as linguistic barriers. Remotely sensed data and in particular satellite data provides a standard data set over a large area which may be studied by a single operator using a standard technique. This produces a homogeneous result rather than a mosaic of results derived from many workers using varying techniques.

3.1.3 Confidence in Distinguishing Lineations

By studying an area in subsections, an overall picture can be built up of the glacial lineation pattern. Satellite imagery shows evidence of palimpsets of lineations. These lineations are often sparsely distributed with, on the small scale, a discontinuous appearance. Their continuity, however, may be traced over the large area which contiguous satellite images provide. When lying beneath the dominant lineation pattern, these palimpsets have been used to provide evidence of earlier lineation patterns in Canada (Boulton and Clark, 1990; Knight, 1996) and Fenno-Scandinavia (Dongelmans, 1996).

3.1.4 The Study of Large Scale Glacial Dynamics

Table 3.2 shows the dimensions of different glacial streamlined landforms. Comparing Table 3.2 and Table 3.1 it appears that aerial photography may be used to map mega-lineations. In reality, however, it is very difficult to see features that are of the same order of magnitude as the Instantaneous Working Area (Lillesand and Kiefer, 1987), and larger features will be ignored. The inability to observe patterns on a scale greater than the sample area is a recurring problem in many sciences. Within glacial geomorphology it is important to consider the scale of sample area when considering features such as glacial ice lobes which may have a width of up to 300 km. Such features may be observed using satellite images and therefore the use of satellite imagery facilitates an investigation of large scale glacial dynamics.

Lineation Type	Length (m)	Height (m)
Flute	< 100	< 3
Megaflute	> 100	< 5
Drumlin	> 200	> 5
Megadrumlin	> 1000	>10
Streamlined Hill	> 1500	>50

Table 3.2: Dimensions of glacially streamlined landforms, After Rose (1987)

3.2 Previous Work Using Remote Sensing to Map Geomorphology

Areal photography has been used for many years in geological and glaciological studies (for example Thwaites 1947). The first unmanned image gathering satellite was launched in 1960. However, it was not until the launch of Landsat-1 in 1972 that images which were practical for geological investigations were obtained. The potential for many earth science applications and studies was quickly recognised (Short and Blair, 1976). The development of Landsat-4 in 1982 gave greater resolution and the limitations as well as the advantages of Landsat have become much better understood. With the release of old data at a moderately low price, Landsat and other similar systems are now being used more often.

Patterns of large end moraines, hummocky moraine, Rogen moraine, drumlins, eskers and other glacial features, have been studied using Landsat data by several workers (Short and Blair, 1976; Punkari, 1982; Williams, 1986; Boulton and Clark, 1990; Skoye and Eyton, 1992). The first studies using Landsat over Fenno-Scandinavia were carried out by Punkari (1978) who continued this work using data collected from the Landsat series of satellites (Punkari, 1980, 1984, 1992). More recently, Dongelmans (1996) used Landsat data to provide information on the direction and strength of glacial flow and the relationship between glacial dynamics, morphology and topography in Fenno-Scandinavia. All these studies used images in a

hardcopy format, and were therefore limited not only by the resolution of the satellite sensor, but by the scale of reproduction to hardcopy. A hardcopy does not permit further image enhancing. Any image processing may only be applied before reproduction.

3.3 Advantages of Using Digital Data

The hardcopy images previously used, in some cases, have been digitised to form a single data set (Punkari, 1980; Boulton and Clark, 1990; Dongelmans, 1996; Knight, 1996). However, there are many advantages in acquiring the image in a digital format, and using computer software for display and processing.

Computer software packages, such as the ERDAS IMAGINE software used within this study, allow interpretations to be made 'on screen', combining the stages of interpretation and digitising in a single step. The software also allows data to be displayed and interpreted at various scales, with the resolution limits being those of the satellite sensor. This allows the operator to work almost simultaneously on multiple scales using multiple views, studying closely areas of ambiguity as well as maintaining an overview. Any Instantaneous Working Area can be chosen since images may be combined together. The scale at which an Instantaneous Working Area can be viewed is limited by the size of the computer monitor. Having all the spectral bands provided by the satellite sensor in digital format allows the operator to experiment with different band combinations so that a combination which best enhances the geomorphological features can be chosen. Image processing (Section 3.5.3) may be used to enhance an image further. For example, by changing the intensity histograms, or by using spatial or spectral filters. The consistency and accuracy of interpretations from satellite imagery can be ensured by using small areas where features observed from the satellite imagery can be compared to interpretations from aerial photography or field work.

3.4 Landsat TM Data

Landsat TM imagery was chosen for this study because it produces images with better spectral and spatial resolution than many other sensors, for example the Advanced Very High Resolution Radiometer (AVHRR) or the Landsat Multi-spectral Scanner (MSS), and a large Instantaneous Working Area. Processing the imagery is relatively simple compared with systems such as Synthetic Aperture Radar (Clark, 1997). The quality of the TM data, although designed to provide high resolution multi-spectral data on world agriculture, permits its application to geological and geomorphological studies.

3.4.1 Brief History of Landsat TM

The first satellite in the Earth Resources Technology Satellite (ERTS) programme was launched on 23 July 1972. In 1975 the programme was re-designated as the Landsat programme to complement the Seasat programme and to emphasise its primary area of interest which was land resources. The initial Landsat satellites carried a multi-spectral scanner and produced data with a spatial resolution of 80 m^2. Landsat-4, launched in July 1982, carried a thematic mapper and combined with other additions and innovations improved the spatial resolution to $(30\ m)^2$. Landsat TM data is now provided by Landsat-5. It should be noted that features such as roads and railways with a width less than 30 m, can still be seen with Landsat TM due to their length continuity. This can be seen in Figure 3.2.

3.4.2 Data Characteristics of Landsat TM Imagery

Landsat TM covers an area between 82° N and 82° S Latitude except for an area over India and Thailand between 50° N 67° E by 50° S and 82° E. Landsat-4 was designed to provide higher image resolution, sharper spectral separation, improved geometric fidelity and greater radiometric accuracy and resolution than the previous Landsat series satellites. The data is gathered in seven spectral bands simultaneously for wavelengths as shown in Table 3.3. The Instantaneous Field of View (IFOV) on the ground of a TM image is 30 m^2 in bands 1-5 and 7, and 120 m^2 for band 6 (infrared sensor, not used in this study).

Landsats 4-5	Wavelength (micrometers)
Band 1 (Visible - blue)	0.45-0.52
Band 2 (Visible - green)	0.52-0.60
Band 3 (Visible - red)	0.63-0.69
Band 4 (Near-Infra Red)	0.76-0.90
Band 5 (Mid-Infra Red)	1.55-1.75
Band 6 (Thermal-Infra Red)	10.40-12.50
Band 7 (Mid-Infra Red)	2.08-2.35

Table 3.3: Spectral range of Landsat TM sensors

The data is stored in raster form. The raster format refers to storing spatial data within grids which are used to depict continuous surfaces (Goodchild, 1988). A grid comprises a series of cells, often referred to as pixels. In the case of satellite imagery each pixel relates to an area on the Earth's surface. Landsat TM bands are stored within separate grids where each pixel value records the intensity of light measured for a particular range of wavelengths as shown in Table 3.3.

The Landsat Satellites have a sun-synchronous, near polar orbit at a nominal altitude of 705.3 km at the equator. Being sun-synchronous, Landsat TM acquires images of a particular

area at the same time of day, so the only way of obtaining different solar elevation data is by choosing the appropriate season. The descending orbital node time is 9:45 ± 15 minutes at the equator with an orbital period of 98.9 minutes, completing 14 $\frac{9}{16}$ orbits per day and imaging the same 185 km ground swath every 16 days. TM data is received directly by a network of 15 world-wide ground stations, and also via a Tracking and Delay Relay Satellite system.

3.5 Image Selection and Processing

3.5.1 Time of Year of Imagery

Geomorphological features can be observed on images due to their composition and/or shape. In all cases cloud cover must be restricted to 10% or less for satisfactory results. The time of year of data acquisition is significant in highlighting different characteristics of landforms and hence influencing the information available.

In spring vegetation phenology and soil moisture conditions can be used to reflect subtle differences in soil texture, organic content, land slope and aspect, in land cover and in agricultural practices. Landforms consisting of certain material and having a particular shape may be covered by characteristic vegetation which can be distinguished by its spectral reflectance properties. This geobotanical interpretation has been particularly successful in sub-artic locations where there is a distinct difference in the vegetation between waterlogged interdrumlin areas and drier drumlin ridges (Punkari, 1982; Boulton and Clark, 1990). Punkari (1985), mapping Finland, was able to distinguish areas of till, sand, clay, peat and bedrock with eskers (discussed in section 4.1.2) being particularly distinctive. In summer, vegetation dominates the image, obscuring geomorphic information.

Winter imagery is best for highlighting topographic variations. There are two reasons for this. First, there is little or no active vegetation to obscure topographic features. It has been argued by Eyton (1989) that snow can further smooth the landscape forming a homogeneous background, with a uniform spectral characteristic which allows the topography to be most clearly expressed. Snow cover if too deep, however, can obliterate topographic information and the advantage of a homogeneous background has the disadvantage of removing the possibility of using the multi-spectral attributes of Landsat data.

The second reason, and perhaps the most important factor in using winter imagery is the low angle of solar illumination which creates shadows that most sharply express relief. Figure 3.1 shows two Landsat TM images of the same region. Figure 3.1a represents a winter image while Figure 3.1b was taken in the spring. The geomorphology is much more clearly displayed in the former. With winter imagery the sun intensity becomes an important factor, with shadows being less distinct at low sun intensity. Marsh *et al.* (1995), on the basis of studying TM images of Northern Ireland, Scotland and northern England suggest that November, December and

February, are the best months for depicting geomorphology from the imagery in these areas, provided there is no snow cover. Drury (1986a) also recommends February for satellite imagery due to the low vegetation heterogeneity. In January the sun intensity is found to be too low for satisfactory reflection values (Marsh *et al.*, 1995).

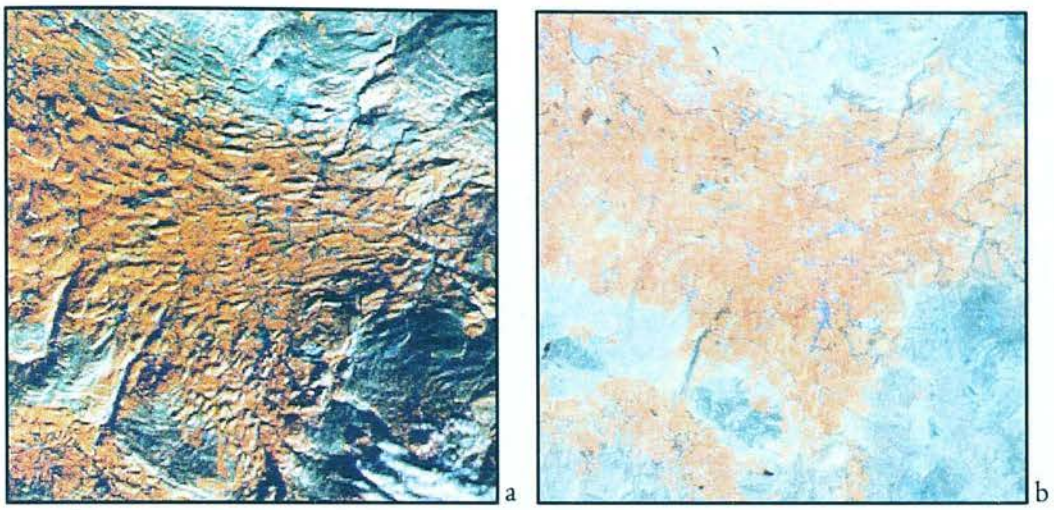

Figure 3.1: Landsat TM images; bands 4, 5 and 7 for red, green and blue respectively: Figure 3.1a shows the scene with winter illumination, Figure 3.1b shows the same scene in the spring

The solar illumination for each image was from the SSE. Linear features normal to this azimuth are selectively enhanced. While spatial-frequency filters may be used to overcome the directional bias of solar shadowing, Drury (1986b) concludes that directional filtering is probably unsuitable for agricultural terrains, such as the study region, where subtle remnants of agricultural boundaries may be exagerrated. However, comparing the satellite interpretations with published geomorphological maps of local areas gives confidence that nearly all linear features can be recorded without using directional filters.

It was intended to replicate the quality and high definition of geomorphological features achieved by Marsh *et al.* (1995) for the U.K. Since the Eastern Baltic region lies at roughly the same Latitude as the U.K. an attempt was made to acquire images from February when the sun angle is similar. However, due to the large amount of snow covering the Eastern Baltic region during winter, the nearest snow-free images to November/December were acquired in mid-October. The resultant images were usable with geomorphological features visible, but not of the same quality as achieved for the U.K. In an attempt to improve on these images, further images were acquired in early May making more use of the variation in vegetation at this time, but less use of a low sun-angle.

Landsat TM Image Path/Row	Acquisition Date
188/019	14 Oct 1991
187/020	12 Oct 1987
187/021	12 Oct 1987
187/022	12 Oct 1987
187/023	14 Oct 1988
185/020	10 May 1994
185/021	10 May 1994
185/022	10 May 1994

Table 3.4: Acquisition dates of Landsat TM images used in this study

3.5.2 Choice of Bands

Figure 3.2 shows a 'true colour' image (TM bands 3, 2, 1 for red, green and blue respectively). A true colour image does not highlight glacial geomorphology well. The subtle variations in vegetation and topography are enhanced by producing a false colour composite image, made by assigning the primary colours red, green and blue to selected bands of the satellite system. For geological interpretations, Marsh *et al.* (1995) found it best to use TM bands 4, 5 and 7 for the primary colours red, green and blue respectively. It can be seen from Figure 3.3 that the bands 4, 5 and 7 cover the peaks in the reflectance spectra of vegetation. This is particularly true of green vegetation.

Figure 3.4 shows the same region as in Figure 3.2, with bands 4, 5 and 7 for red, green and blue as described above. Already the geomorphology is better depicted than in the true colour composite. Band 4 is recommended by Aber *et al.* (1993) and Dongelmans (1996) for the study of geomorphic features and is the approximate equivalent of AVHRR band 2 and Landsat MSS band 7 used by Johnston (1987) and Punkari (1985) respectively for glacial geomorphological studies. Band 5 was recommended by Drury (1986b) for its low vegetation heterogeneity. An alternative selection of bands was recommended by Punkari (personal communication) who suggested the combination of bands 2, 3 and 5 for the primary colours red, green and blue respectively. This combination has proved successful in mapping geomorphology within Fenno-Scandinavia. Both of these combinations were used in this study. Attempts to use other combinations including bands 4, 3 and 2 for red, green and blue respectively were less successful.

3.5.3 Image Processing

Figure 3.4 also shows the histogram intensity profiles for the corresponding image. The raw data intensity values will only occupy a small section of the available range of values. To increase the contrast in the image the raw data values are normalised. Marsh *et al.* (1995) adopted a method of normalising each band to a mean and standard deviation found by

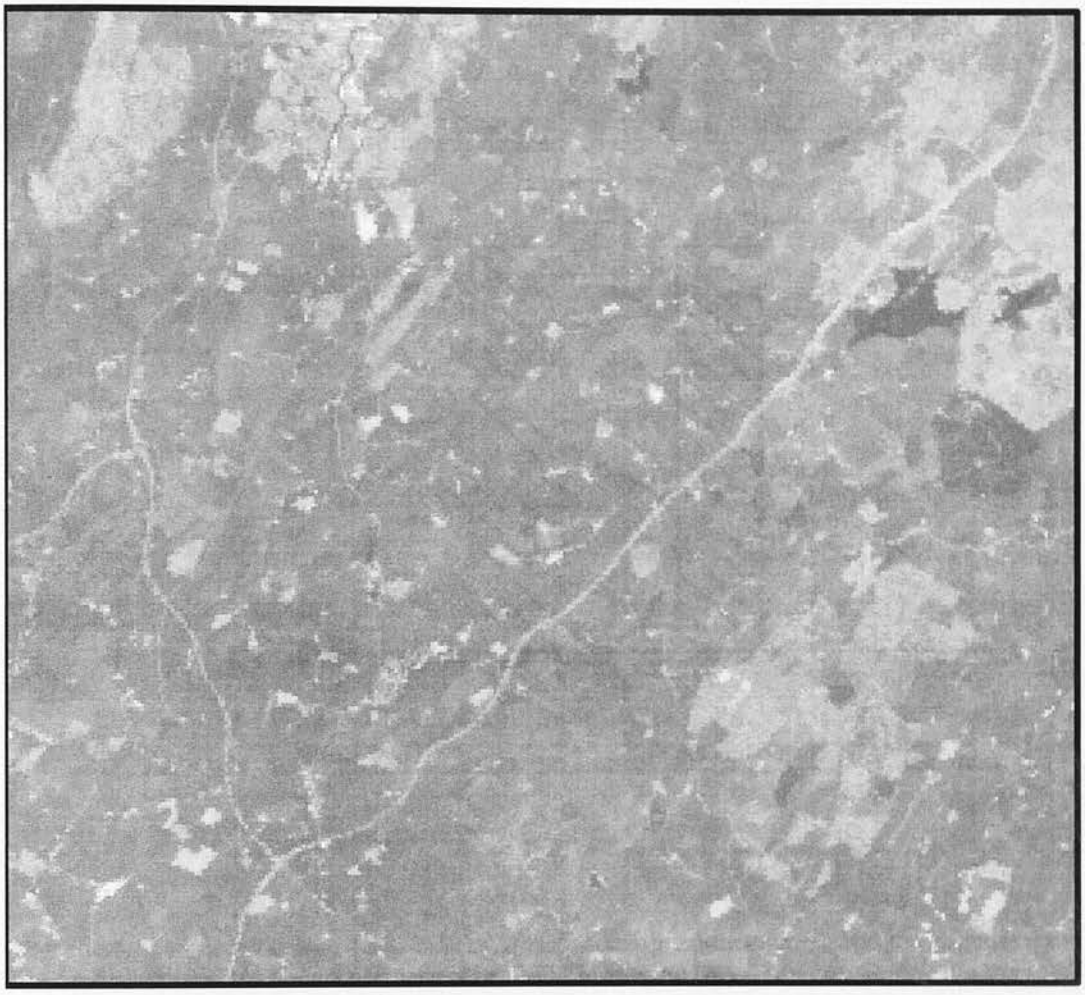

Figure 3.2: Landsat TM true colour composite, bands 3, 2, 1 for red, green and blue respectively: scale 1:100,000. Geomorphology is not shown well by this band combination

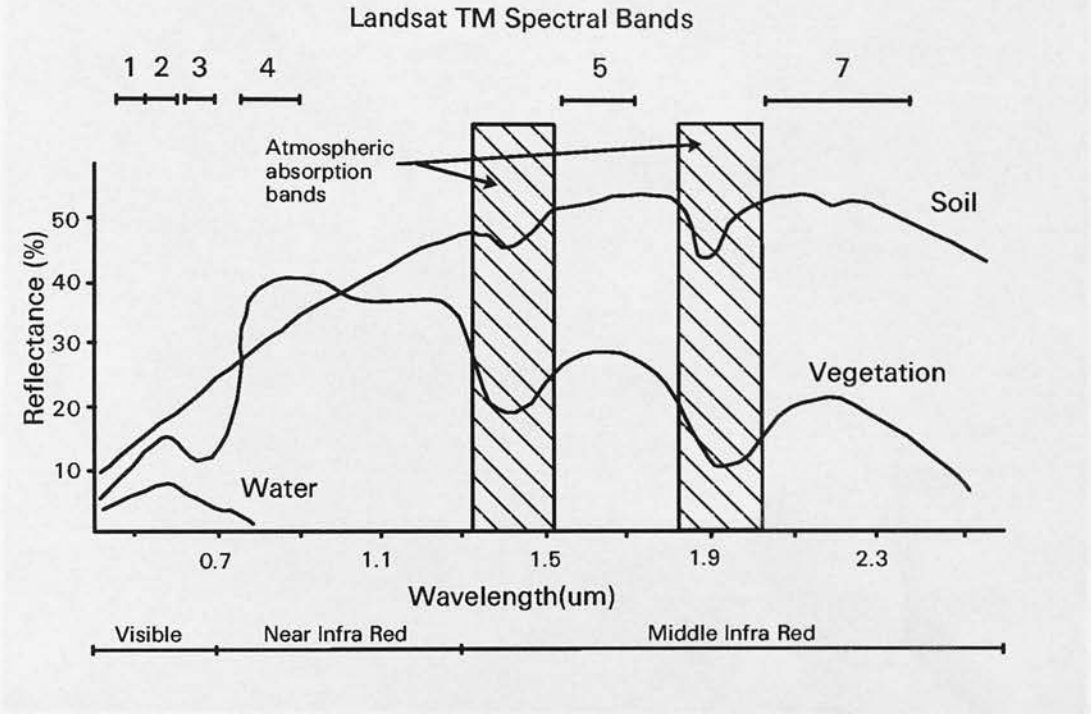

Figure 3.3: Spectral reflectance characteristics of common earth-surface materials in the visible and near-to-middle infra-red range. The positions of Landsat TM spectral bands are shown along the top.

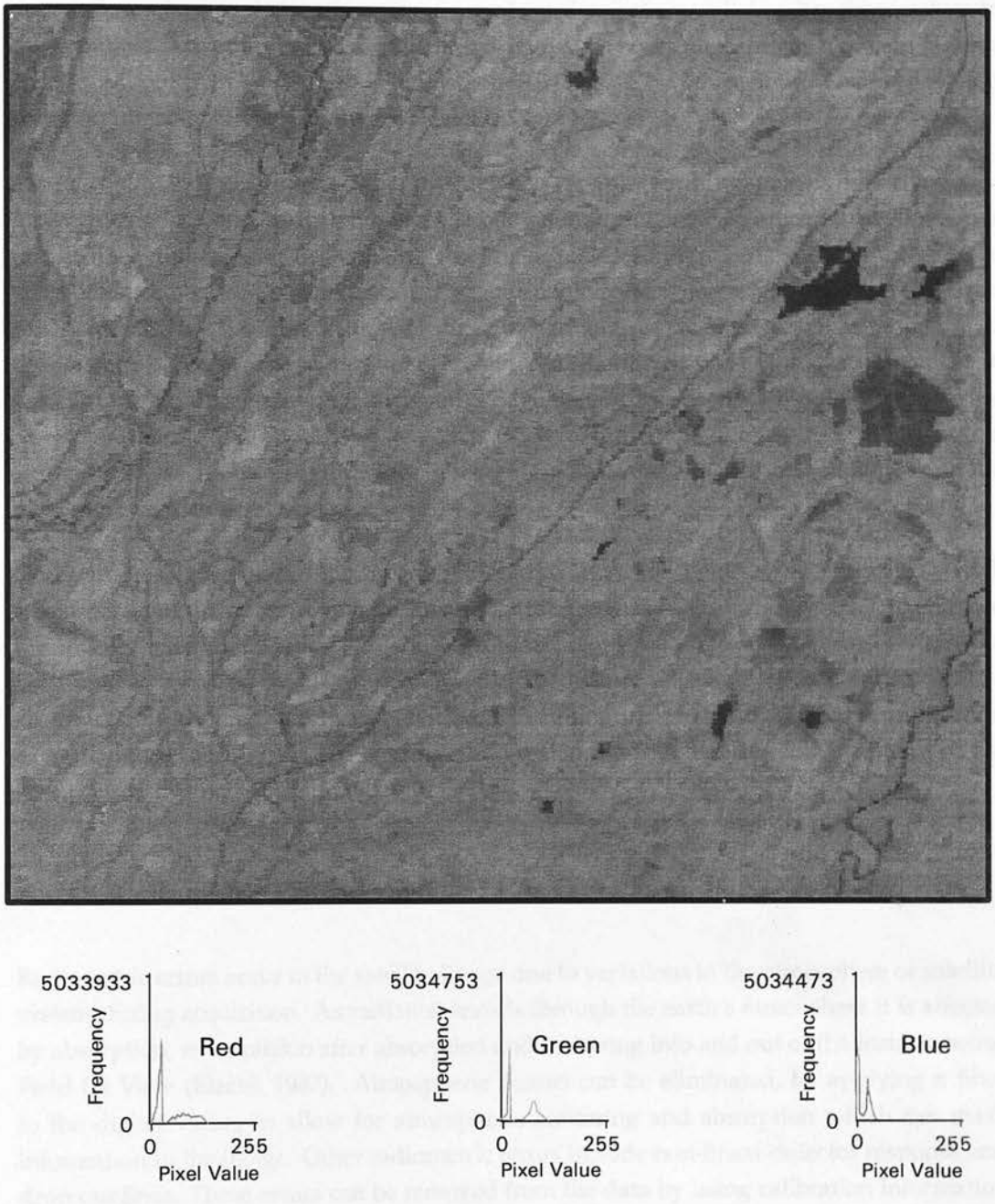

Figure 3.4: Top: Landsat TM false colour composite, bands 4, 5, 7 for red, green and blue respectively: scale 1:100,000; lineations can be seen extending from top right to bottom left of the figure. Bottom: Histogram Intensity profiles used

experience and analysis of an individual image to best highlight the geomorphology. Punkari (1993) used a manual method of altering selected ranges of intensity with a linear contrast stretch. Both of these methods were used along with the method known as a Standard Deviation Contrast Stretch. This method assumes the most important data lies between -1.9 and +1.9 standard deviations from the mean of the data values and stretches those values to the complete range of output screen values. Figure 3.5 shows the same region as in Figures 3.2 and 3.4, but with the histogram intensity profile altered by this method. The original and resultant intensity histograms are displayed in Figure 3.5.

Marsh *et al.* (1995) also used a three by three box convolution filter, passed over the image to enhance edges and further highlight subtle geomorphology. In areas where lineations are distinct, this can further enhance the image making interpretation easier. However, edge enhancement did not enhance the geomorphology with the selected imagery used in this study. Figure 3.6 shows the percentage of agricultural land usage across Finland and the Eastern Baltic region. It can be seen from this figure that there is a steady increase in agricultural land usage towards the south. Edge enhancing sharpens the field boundaries, further obscuring the underlying geomorphology. Throughout the image analysis in this study there was a consistent difficulty in separating the underlying geomorphology from the present day agricultural land usage.

Other processing methods, such as convolution with an inverted point spread function kernel, were not successful in improving the images for interpretation. It was not possible to enhance the images used in this study to show geomorphology as well as those seen within the U.K. images achieved by Marsh *et al.* (1995). The primary difficulty is that winter images are invariably covered with snow. Further difficulties are created by the large proportion of agricultural land within the Eastern Baltic region, and the relative low elevation of the lineations in this region compared with the U.K.

3.5.4 Radiometric Corrections

Radiometric errors occur in the satellite image due to variations in the atmosphere or satellite system during acquisition. As radiation travels through the earth's atmosphere it is affected by absorption, re-emmision after absorption and scattering into and out of the Instantaneous Field Of View (Elachi, 1987). Atmospheric factors can be eliminated, by applying a filter to the digital values to allow for atmospheric scattering and absorption which can mask information in the image. Other radiometric errors include non-linear detector response and drop out lines. These errors can be removed from the data by using calibration information and correction algorithms. Radiometric corrections are particularly useful when comparing images of a single area acquired at different times or using different sensors. Radiometric corrections were not made in this study, because direct spectral comparisons between images was not required and the imagery was sufficiently good to allow visual interpretation of features without correction.

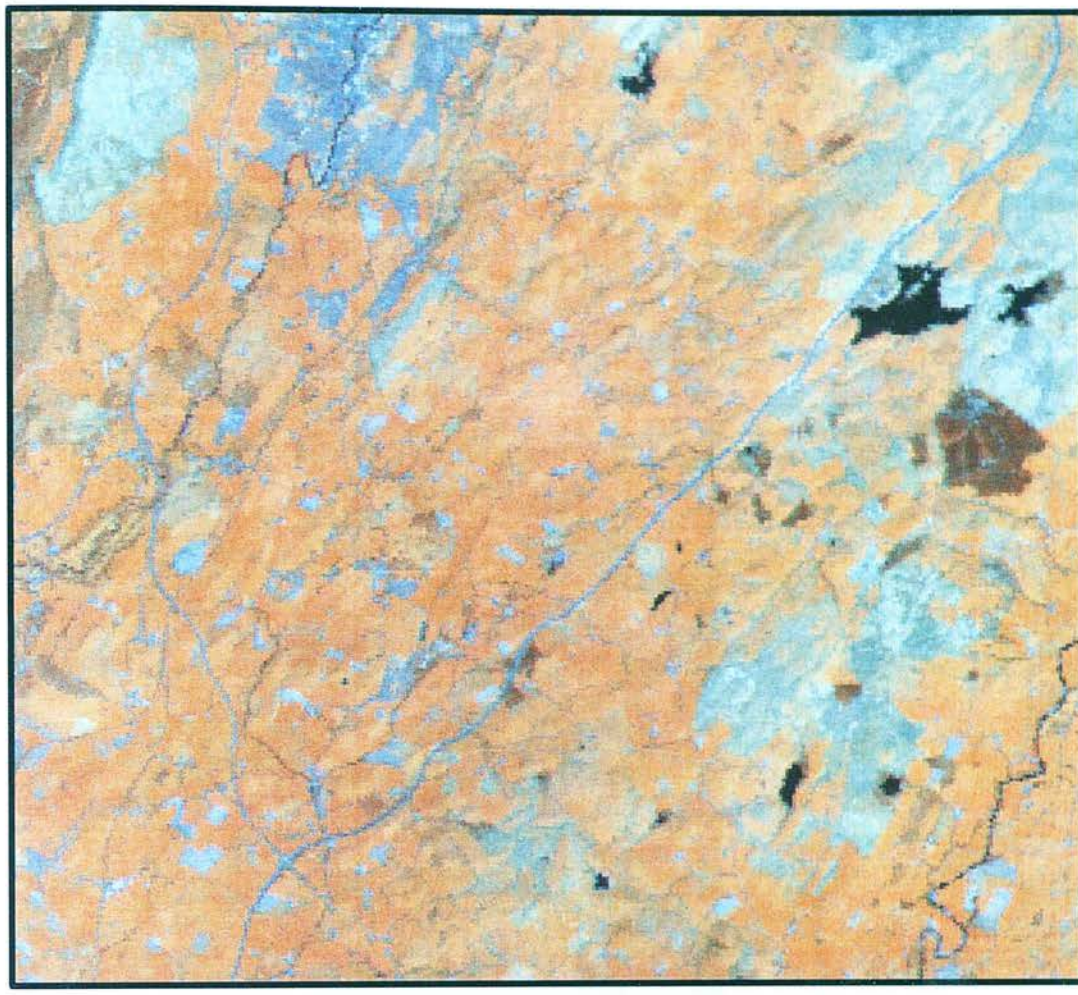

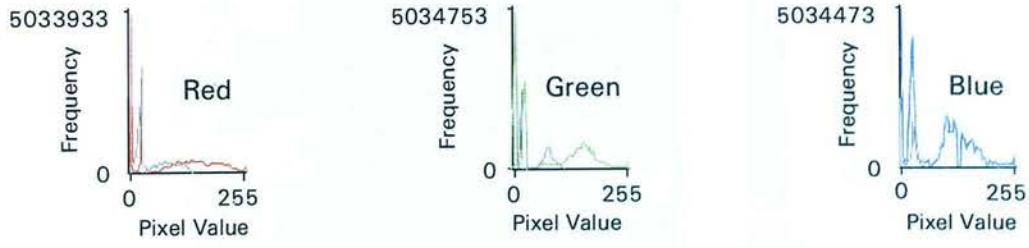

Figure 3.5: Landsat TM false colour composite, bands 4, 5, 7 for red, green and blue respectively: All bands stretched using a standard deviation contrast stretch, standard deviation +/- 1.9; scale 100,000; lineations are better highlighted here than in Figure 3.4 and can be seen extending in the figure from top right to bottom left. Bottom: Histogram Intensity Profile. The grey profiles are the old file values as shown in Figure 3.4, the coloured histograms the new file values.

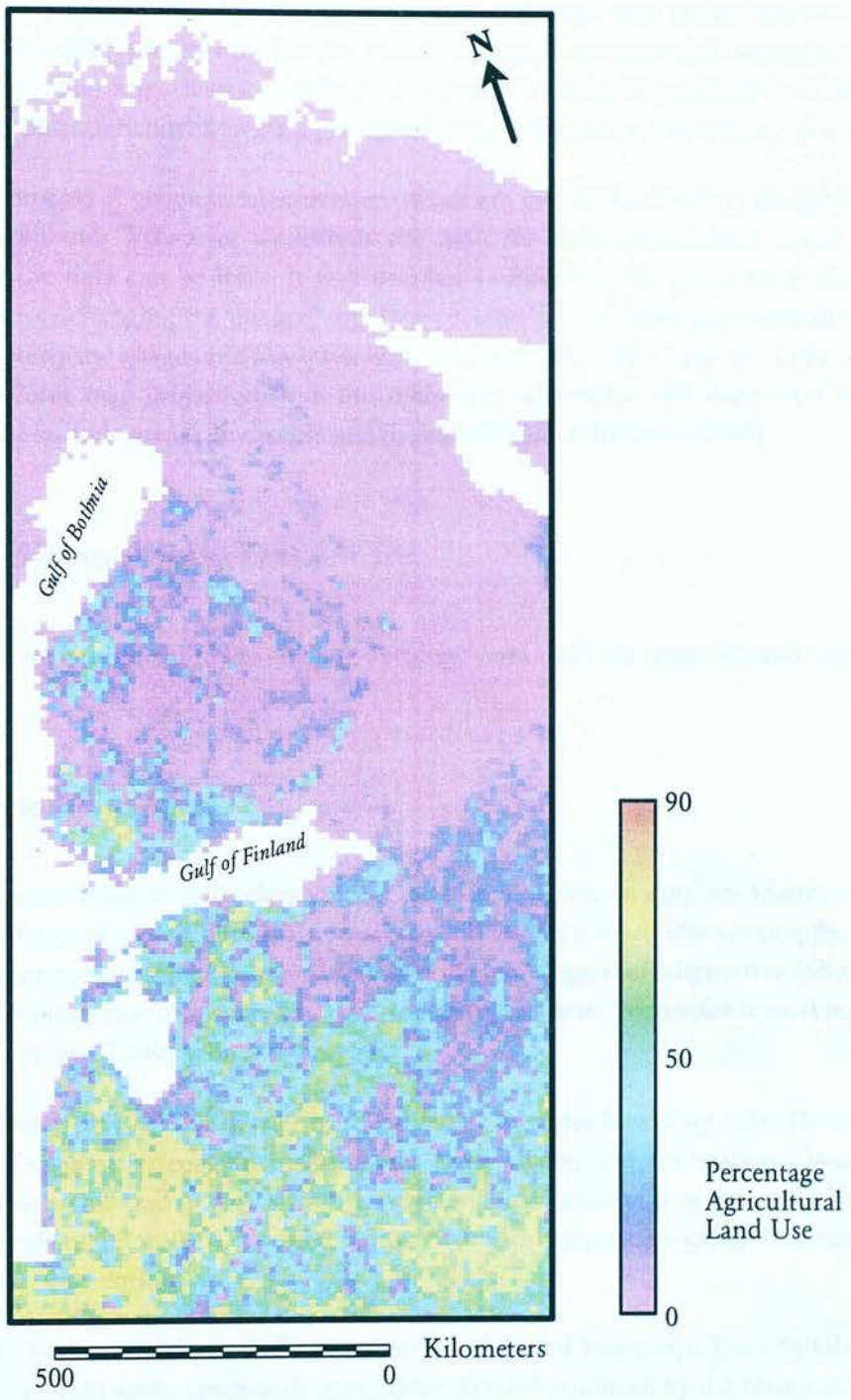

Figure 3.6: Percentage agricultural land use on a 10 x 10 km grid over the Eastern Baltic region and Finland

3.5.5 Geometric Corrections

A Landsat TM image records the Earth's surface in a two-dimensional grid. If this grid can be geometrically corrected to real world co-ordinates (latitude and longitude) then a projection algorithm can convert the image into one of the many different map projections available. A map projection still represents the Earth's surface in two-dimensions and necessarily creates distortions in shape, area, distance or direction. However, a suitable projection can be chosen with known characteristics allowing a greater understanding of the information portrayed.

During the process of geometrical correction, pixels are re-sampled to fit a new grid of pixel rows and columns. Whatever algorithms are used for these calculations, some spectral integrity of the data can be lost. It was decided to interpret the more spectrally correct raw data, before changing the imagery and interpretations to be more geometrically correct. Within this study the images and interpretations were generally transformed into the Lambert Conformal Conic map projection since this maintains orientation and shape and is ideally suited to mid-latitude areas (Environmental Systems Research Institute, 1994).

3.6 Additional Raw Data

Other raw data, additional to the satellite imagery, were used for reference and verification purposes.

3.6.1 Vector Base-Maps

Base-maps were used to geo-reference the satellite imagery, to confirm identification of features on the imagery and provide a visual spatial reference when interpreting the images. Two sources of vector base-maps were used. A vector coverage is an alternative format to the raster format (discussed in Section 3.4.2) for storing spatial data. The vector format represents features as a series of points, lines or polygons.

The World Data Bank II (WDBII) was the initial source of vector base-map data. Three distinct categories of data exist: coastline, islands and lakes; rivers; and international boundaries. While data was collected at scales from 1:1 million to 1:4 million it is generally treated as being at a scale of 1:3 million. Created by the Central Intelligence Agency, it is now freely available over the internet.

The Digital Chart of the World (DCW) became the preferred base-map. The Digital Chart of the World is a world-wide, small-scale geographic data set produced by the National Imagery and Mapping Agency, formerly the Defence Mapping Agency (Raper and Vozenilek, 1993). The DCW data set contains sixteen categories of data including coastline, national borders, roads, railways, rivers, and utilities. The primary sources of information for the data set were

1:1 million scale Operational Navigation Charts and 1:2 million scale Jet Navigation Charts. The data is generally treated as being at a scale of 1:1 million.

3.6.2 Digital Elevation Model

The digital elevation model (DEM) was primarily used to compare interpretations of the satellite imagery with the local topography. The DEM was also used to view the satellite imagery in three dimensions and to calculate the slope and aspect across the region (discussed in Section 7.2). These latter applications, were less successful due to the poor resolution of the elevation model.

The Global 30 Arc-Second elevation data set was used within this study. Created by the U.S. Geological Survey Topographic Data group at the Earth Resources Observation Systems Data Center (Gesch, 1996), the elevation data set provides worldwide coverage at a 30 arc second post spacing (approximately 700 to 1000 meters). The data set is a composite of many data sources. For the region of interest in this study the primary data source is a generalised form of the U.S. National Imagery and Mapping Agency's Digital Terrain Elevation Data (DTED) Level 1. DTED Level 1 is a medium resolution source of raw elevation data with elevation sampling at 3 arc seconds (70 to 100 meters apart). It is produced and distributed by the U.S. National Imagery and Mapping Agency.

3.6.3 Land Cover

Land cover maps (Sweitzer *et al.*, 1996) were used to provide additional information to aid in the identification of features observed on the satellite imagery. The land cover data was derived from the Baltic Sea Region Geographical Information Systems (GIS), map and statistical data set. The data set was a result of the Baltic Drainage Basin Project (BDBP). The BDBP was a multi-disciplinary research project under the EU 1991-1994 Environment Research Programme. The GIS data set, mainly focusing upon land cover/land use and population was developed as a joint effort between the Beijer Institute, Stockholm; Department of Systems Ecology, Stockholm University; and UNEP/GRID-Arendal. It was used for analytical purposes during the BDBP. Following this, the GIS data set was further refined and is now available over the internet (UNEP/GRID - Arendal, 1995).

There are eight categories of data set available (Sweitzer *et al.*, 1996) of which four were used. Arable Lands and Pasture Lands were summed to calculate the percentage of land used for agricultural purposes (Figure 3.6). The resulting file had a pixel resolution of 10 km x 10 km. A further land cover data set categorises the land into six classes: Forest, Open Land, Open Water, Urban Land, Glacier, and Unknown Land, which is either Forest or Open Land. The land cover data set was generated from the Digital Chart of the World and the European Space Agency Remote Sensing Forest Map of Europe with a 1 km resolution. The pixel resolution is

1 km x 1 km. The Wetland Distribution was derived from the association of regional wetland area statistics with locations represented in the DCW Land Cover data layer. Due to the quality of input statistics, the final pixel resolution of the Wetland Distribution was only 50 km x 50 km.

3.6.4 Published Maps and Literature

Geological, geomorphological, tectonic and structural geology maps (Leningrad, 1982) were used to aid in the identification of features observed on the satellite images. Data collected through fieldwork or aerial photograph interpretations is available within published literature. The primary use of this information was to confirm/define the direction of ice flow within an area (discussed later in Section 4.2.2). Papers referred to include: Raukas *et al.* (1995), Rõuk and Raukas (1989), Raukas (1977), Raukas (1986), Mojski (1995), Āboltiņš and Dreimanis (1995), Karukäpp *et al.* (1992), Dreimanis and Zelcs (1995).

3.7 Summary

The primary data used to derive palaeo-ice flows for the study region was Landsat TM satellite imagery. This represents a new data source for the area. Using remote sensing permits a single coherent mapping of glacial landforms which can be interpreted in glacial dynamical form. It was not possible to use winter imagery, as recommended by the Marsh *et al.* (1995), due to snow cover over the region of study. However, imagery from October and May was used and found to be effective at highlighting topographic variations. It was found that TM bands 4, 5 and 7 for red, green and blue respectively best portrayed the glacial geomorphology with simple changes in the histogram intensity profile effectively enhancing the features. Using other data sets in this study, such as a digital elevation model, thematic maps of land cover, and published maps and literature, added new information and gave confidence that the vast majority of features observed from the satellite imagery were accurately interpreted.

Chapter 4

Glacigenic Landforms and the Derivation of Palaeo-Ice Flow Sets

This Chapter is divided into two Sections. In the first, the morphology and formation of glacigenic landforms are discussed. The features thought to have formed parallel to ice flow are the most interesting as these are accurate and widespread indicators of the ice flow direction. The conditions required for the formation of subglacial lineations are reviewed in Subsection 4.1.4 followed by a discussion of the interaction of younger lineations with older ones. The intersection of lineations enables the relative ages between different generations of lineations to be determined.

The second Section describes the process of using raw lineation data to reconstruct flow sets. Flow sets are defined as coherent sets of stream-lined glacigenic features which are thought to relate to one phase of ice flow. Standard criteria permit flow sets to be systematically correlated between neighbouring regions. The resultant regional flow sets provide evidence of large-scale ice movements and their relationships demonstrate temporal changes in ice flow.

4.1 Glacigenic Landforms

In this Section the morphology and formation of glacigenic landforms produced by both glacier ice and glacial meltwater acting on the glacier substratum are discussed. Glacigenic landforms have been subdivided into two categories: (1) landforms created at the ice margin; and (2) landforms created subglacially. A brief description of the landforms in each category and how the features may be related to understanding the glacial dynamics is given below. Particular attention is paid to subglacial lineations which form the majority of observations made using the satellite imagery in this study.

4.1.1 Ice Marginal Landforms

Ice marginal landforms include ice marginal moraines, formed by the action of ice, and glaciofluvial landforms. Ridges which demarcate the ice margin can be grouped into three broad categories. The first category is glaciotectonic moraines which are formed by the tectonic deformation of ice, sediment and rock. The simplest example of a glaciotectonic moraine is the thrust block moraine formed when a glacier advances into proglacial sediment and pushes it up to form a ridge (Benn and Evans, 1998; R., 1992; Hart, 1990). The second category consists of dump moraines formed by the accumulation of ice transported debris along the side or in front of a glacier. A lateral moraine is an example of a dump moraine formed with its elongation direction approximately perpendicular to the ice margin. The final category is hummocky moraine. This is usually the result of high debris cover within or over the glacier margin which insulates the ice from surface heating. If the debris concentration is high and spread over a large area, an irregular assemblage of knolls, mounds or ridges between depressions will result. Where a large amount of meltwater is present the debris may become stratified resulting in the formation of terrain known as kame and kettle topography (Persson, 1991).

It is important to note that while a set of moraines may be referred to as ice marginal moraines, each moraine ridge does not necessarily reflect the position of a former ice margin. For example, a push moraine may reflect the geometry of thrusts within the ice margin. In addition it is often difficult to determine the genesis of individual moraines since they are not always morphologically or sedimentologically distinct, especially after a prolonged period of post glacial modification. In most cases, however, a broad indication of the pattern of ice retreat can be obtained from ice marginal moraines irrespective of their mode of formation (Bennett and Glasser, 1996). They were therefore recorded where observed on the satellite images (Figure 4.1a, b) and used to supplement information gathered from subglacial lineations.

4.1.2 Subglacial Landforms - Eskers

The principal subglacial landform resulting from meltwater flow beneath a glacier is the esker. In general eskers consist of long narrow sinuous or straight ridges comprising of stratified glacial meltwater deposits usually including large amounts of sand and gravel (Flint, 1971). They may form in a variety of different settings which can be summarised as: (1) deposition in subglacial tunnels; (2) deposition in englacial tunnels with subsequent lowering; and (3) deposition in supraglacial channels with subsequent lowering. Their orientation is controlled by glacier slope and the hydraulic gradient within the glacier.

Sedimentation in supraglacial channels has been observed, for example on the margin of Holmstrømbreen in Svalbard (Boulton and der Meer, 1986), and is easily understood in relation to the physical processes. Deposition within englacial or subglacial tunnels is less

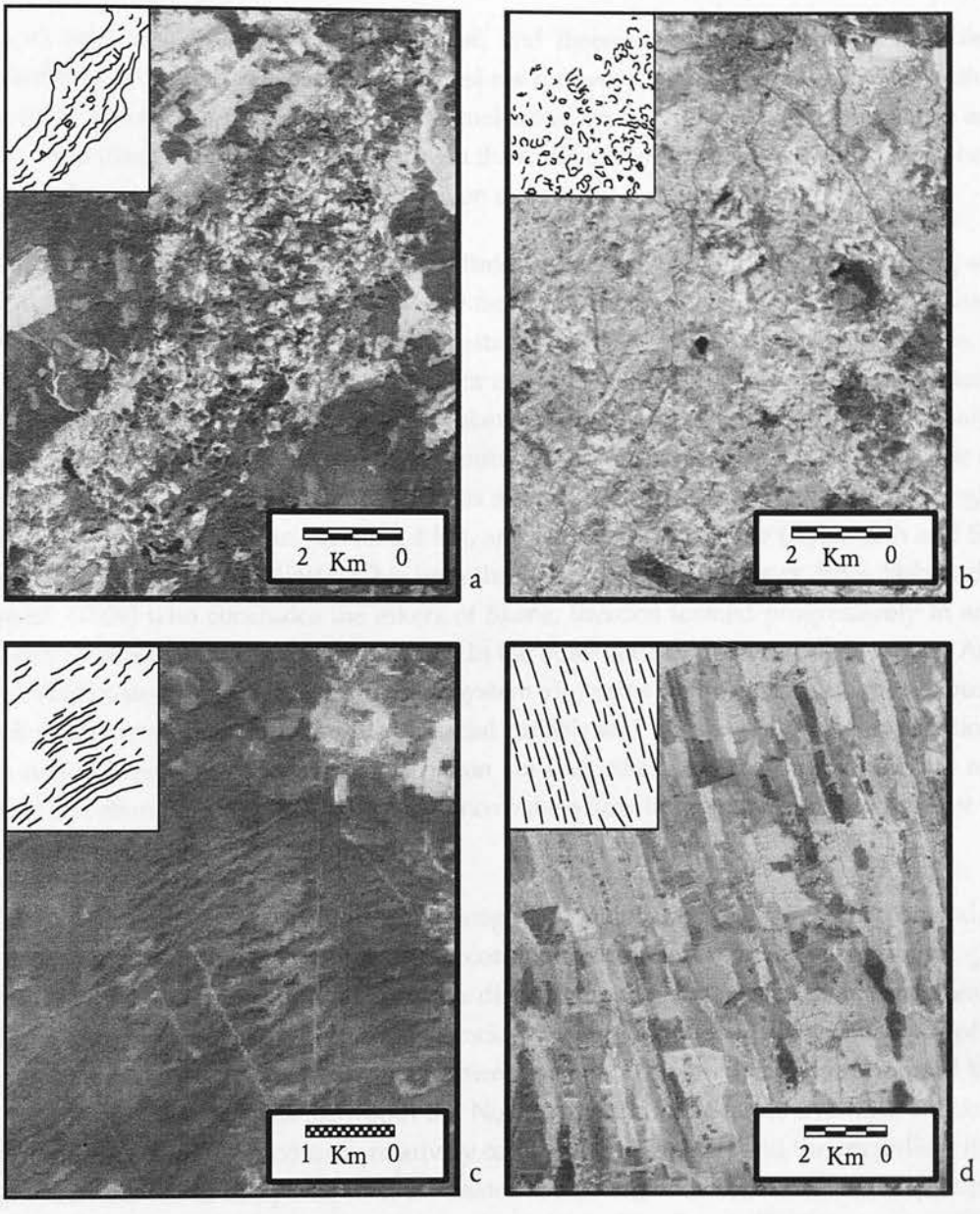

Figure 4.1: Examples of glacigenic landforms observed using satellite imagery. a) Ice Marginal Moraine formed perpendicular to lineations within the area. Note the series of ridges running along the length of the moraine indicating a glaciotectonic origin. b) Hummocky terrain formed in the region of maximum extent of Weichselian ice. c) Transverse features formed on the island of Saaremaa. Narrow ridges regular spaced at 250 m may be indicative of De Geer Moraines. d) Sub-glacial linear features formed parallel to ice flow direction.

well understood. Eskers which result from englacial or subglacial streams discharging into standing water at the glacier margin form a series of small deltas (Geer, 1897; Hebrand and Amark, 1989). Eskers formed in this way are time-transgressive, with older sediments located in the downstream direction.

Eskers have also been recorded on top of, and therefore infilling, channels cut into the underlying sediment indicating that the eskers formed subglacially and that deposition of the esker followed a period of subglacial meltwater erosion (Gray, 1988). Subglacial eskers have been observed melting out of the ice at the south eastern Burroughs Glacier over the past twenty-five years (Mickelson, 1971; Syverson *et al.*, 1994).

Most researchers agree that final esker sedimentation takes place during the waning stages of deglaciation (Syverson *et al.*, 1994). The timing of subglacial and englacial sedimentation remains problematic. One hypothesis suggests that eskers form in a single event (Shreve, 1985; Punkari, 1995; Menzies and Shilts, 1996). For example, Shreve (1985) examining the Katahdin esker system, Maine, cites the increase in esker size downstream, cross cutting of ice marginal positions, and the lack of kame deltas and outwash fans as evidence that all parts of the esker formed simultaneously. Another hypothesis suggest that deposition took place in subglacial tunnels near the ice margin, within 3-4 km, and is time transgressive (Aylsworth and Shilts, 1989; Clark and Walder, 1994). This hypothesis is supported by work from Hebrand and Amark (1989) who concludes the eskers of Skane, Sweden formed progressively in an up-glacier direction, with deposition occuring in the outer zone of the receding ice sheet. Ashley *et al.* (1991), studying the Katahdin esker system also came to the conclusion that deposition took place near the ice margin, in subglacial tunnels and marine fans. The implications of the two theories for ice sheet reconstruction are that esker patterns can be taken to record either direction of ice surface slope and hence palaeo flow lines at an instant in time, or time-dependent marginal retreat patterns.

Mathematical modelling of sub-glacial drainage led Walder and Fowler (1994) to conclude that eskers are formed time-transgressively. According to the Walder-Fowler theory of subglacial drainage eskers are more likely to form on a discontinuous, coarse-grained, high-permeability till derived from underlying crystalline rock than on continuous, fine-grained till of low-permeability derived primarily from sedimentary rock. This prediction is supported by the distribution of eskers formed by both the North America and Scandinavian ice sheets. For example, eskers were found to be relatively common over Finland and the crystalline Fenno-Scandinavian Shield compared with the Eastern Baltic region and the sedimentary sequence of the European Platform. This observation is supported by the satellite imagery used in this study in which no eskers were identified, though Punkari (1992) has demonstrated that similar satellite imagery can be used to map eskers over Finland.

4.1.3 Subglacial Landforms - Transverse Features

Landforms thought to form subglacially and transverse to the direction of ice flow include Rogen moraines, or ribbed moraine, and De Geer moraines. Several models of Rogen moraine formation have been proposed. A large number suggest Rogen moraine form as a result of shearing and stacking of slabs of near-base englacial or subglacial debris, due to localised compressive stresses (Figure 4.2), followed by subglacial melt-out of till ridges (Sollid and Sørbel, 1984; Bouchard, 1989; Shilts and Aylsworth, 1989). Opinions vary to the origin of the compressive flow and the glaciodynamic environment of formation. Shilts and Aylsworth (1989) argue that compression is induced by high concentrations of near-basal debris reducing the plastic behaviour of the ice and causing basal shearing of debris rich ice, while Bouchard (1989) suggest the compressive stresses forming Rogen moraine occur when the ice meets a topographic obstruction at the down-stream end of rock basins, a few kilometers behind the ice margin. A near ice margin environment of formation is also proposed by Punkari (1984), with an inferred frozen outer margin of the ice sheet causing the compressive stresses. If Rogen moraines form close to the margin they may be considered a time transgressive feature. Alternatively, Sollid and Sørbel (1984) put Rogen formation far from the ice margin where patches of water soaked debris are entrained by freezing on to the glacier sole and, subsequently, sheared up into ridges during an expansion of a frozen core area under the ice sheet.

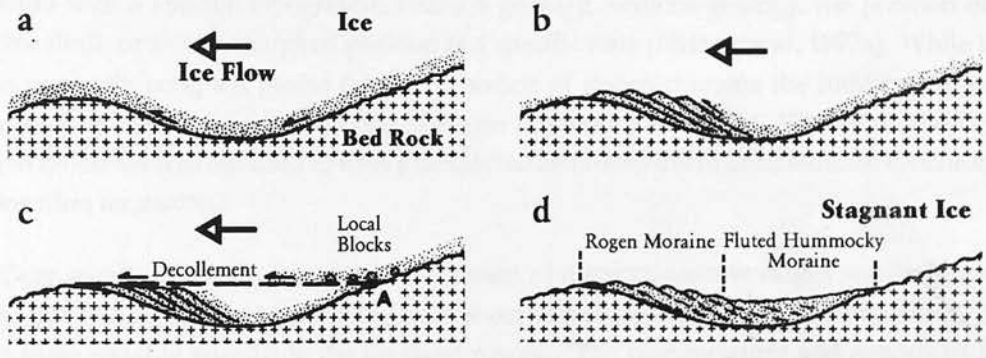

Figure 4.2: Schematic illustration showing the formation of Rogen moraine by processes of shearing and stacking of till slabs under compressive flow, as basal ice flows towards the down-ice end of rock basins. From Bouchard (1989).

Lundqvist (1989) also argues that Rogen moraines form a considerable distance behind the margin and are only preserved within central areas of glaciation where the ice was stagnant during deglaciation. However, he suggests that instead of shearing and stacking, Rogen moraines are formed in two or more steps (Figure 4.3) as proposed by Boulton (1987). Another hypothesis suggests that Rogen moraine occur when a pre-existing till sheet fractures during the transition from cold to warm-based conditions under a deglaciating ice sheet (Hättestrand, 1997b). These conditions are thought to occur within the core areas of former glaciation.

Knight (1996) assumed Rogen moraine formed far from the ice margin and used the presence of Rogen moraines to indicate synchronous ice flow and a synchronous formation time of associated drumlins.

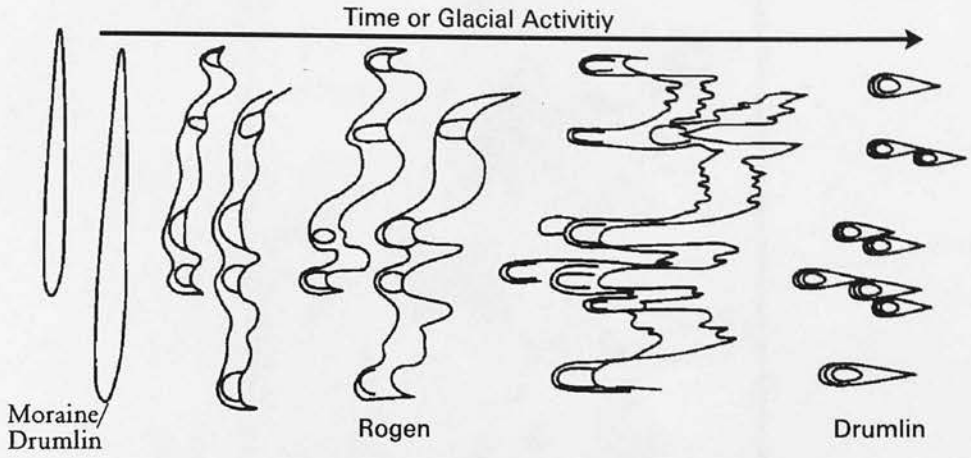

Figure 4.3: Schematic illustration of the way transverse ridges may be progressively transformed to Rogen moraines and drumlins. From Boulton (1987).

The distribution of Rogen moraine in Scandinavia is limited to the central parts of the formerly glaciated region and within this study no Rogen moraines were observed using the satellite imagery (Figure 4.4). The boundary to areas lacking Rogen moraines does not appear to coincide with a specific topography, bedrock geology, surficial geology, the position of the marine limit, or the ice-marginal position at a specific time (Hättestrand, 1997a). While there is no generally accepted model for the formation of Rogen moraine the implication for ice dynamics of the presence or absence of Rogen moraine is uncertain. Therefore, the lack of Rogen moraines was not used to infer glaciodynamic environment or to indicate synchroneity of lineation formation.

De Geer moraines usually occur as a succession of discrete, narrow ridges regularly spaced up to 300 m apart. The ridges range from short and straight to long and undulating. They tend to be roughly parallel to the ice sheet margin. The nomenclature and genesis of these ridges is uncertain. Larsen *et al.* (1991) proposed that the moraines are an ice push feature at the base of the glacier while Beaudry and Prichonnet (1991) proposed an origin within subglacial channels and Laaksonen (1993) suggested laminar basal flow as the cause of the moraines. Several authors have suggested that the moraines form as a consequence of the calving of ice in deep water (Prest, 1968; Zilliacus, 1987) with the moraines possibly being seasonal features. The uncertainty in the genesis of De Geer moraines means that they could either be a subglacial or possibly an ice marginal feature. De Geer moraines could not be identified with certainty from the satellite imagery. For example, Figure 4.1c shows ridges which are transverse to the interpreted direction of ice flow and, while showing some of the characteristics of De Geer moraines, they can not be differentiated from glaciotectonic forms.

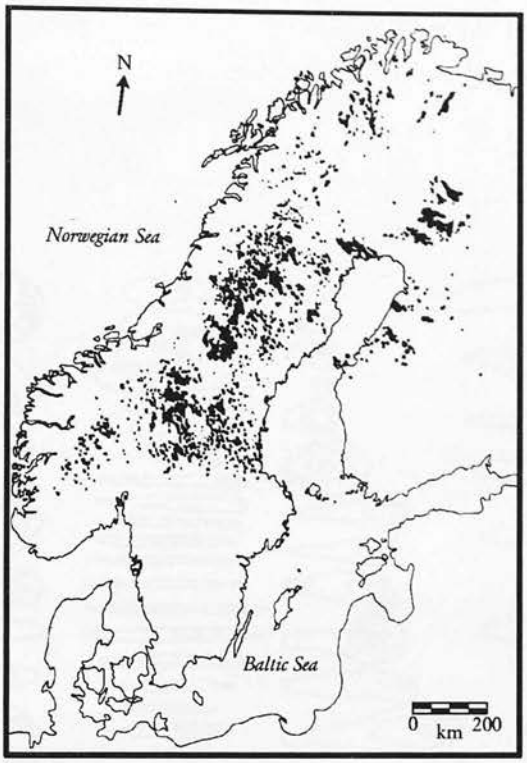

Figure 4.4: Distribution of Rogen moraine in Fennoscandia. From Hättestrand (1997a).

4.1.4 Subglacial Landforms - Longitudinal Features

It was decided to concentrate the present study on longitudinal lineations which are most useful for ice sheet reconstruction. Even a well-defined long axis of a transverse feature may not be parallel with the ice margin, and it is difficult to distinguish between those transverse features formed sub-glacially and those formed at the ice margin. Lineations formed near the margin of a glacier flowing on a flat bed, on the other hand, form perpendicular to the ice margin and accurately reflect the ice-flow. With their smooth and regular ice-moulded appearance they are relatively easy to identify and to distinguish from transverse features. They also provide a spatially continuous data set over large regions.

Subglacial Longitudinal features range in size from small flutes (several metres in length) to megascale lineations which have lengths of 8 to 70 km (Clark, 1993). Even at one scale, the shape of lineations is highly variable (Figure 4.5). They are, however, all elongated in the direction of ice flow. Linear streamlined bedforms are often the result of accumulation, but erosion and scoring of older till surfaces or other unlithified sediments produces similar forms (Lundqvist, 1990). The composition of the bedforms varies from solely till to solely stratified sediments with many lineations containing varying amounts of both till and stratified sediments (Patterson and Hooke, 1995).

There is no single accepted theory for the formation of subglacial linear bedforms. Their

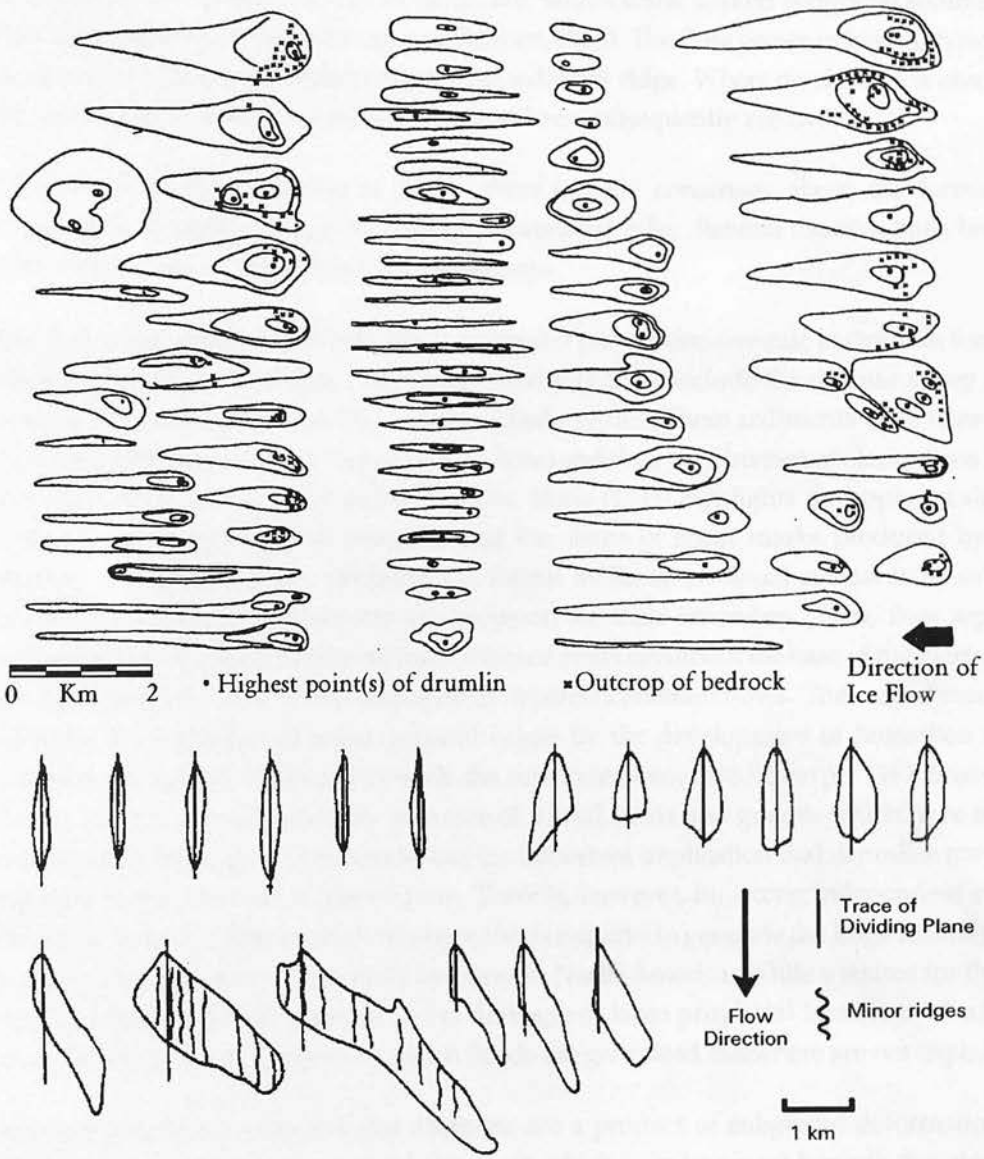

Figure 4.5: Different shapes of drumlin in plan view. Top: From Gluückert (1973), Bottom: From Shaw (1983).

subglacial origin means that the processes of formation have not been observed. Proposed formation mechanisms are derived from theoretical studies and the studies of landform sedimentology from which processes can be inferred.

There is a general consensus about the formation of small-scale flutes. Their presence is caused by a bedrock obstacle at their proximal terminus. As the ice flows around the obstacle, a cavity or an area of low pressure forms in its lee, into which water soaked subglacial sediment may flow forming a linear ridge (Hoppe and Schyatt, 1953). The flute grows in length, down-ice as the low pressure area extends in front of the sediment ridge. Where no obstacle is observed at the up-ice end of a flute it is assumed to have been subsequently removed.

In contrast to the formation of flutes, there is little consensus about the formation of megaflutes, drumlins, megadrumlins or streamlined hills. Several theories have been proposed which can be subdivided into two groups.

The first group assumes that subglacial meltwater plays a decisive role in drumlin formation. Work by Dardis and McCabe (1983) and Hanvey (1989) conclude the drumlins they studied consisted of sediments deposited in water filled cavities. These sediments were later shaped by ice moulding or scouring from sediment flows and thus the direction of elongations is in the direction of ice flow or basal meltwater flow. Shaw (1983) highlights the apparent similarity between the morphology of drumlins and the shape of scour marks produced by fluvial erosion, and proposes that drumlins are fluvial infills or erosional remnants of subglacial floods. Two distinct mechanisms are proposed for their formation. First, flow separation within turbulent subglacial sheet flows erodes or melts cavities in the base of the glacier which are then infilled by sediment transported in hyperconcentrated flows. The second mechanism involves the formation of scour remnant ridges by the development of horseshoe vortices within the subglacial flows which erode the substrate (Shaw, 1983; Sharpe, 1987; Shaw, 1994). The two mechanisms explain the presence of fluvial sands and gravels which have not been deformed by flowing ice. This model has the important implication that drumlins may not be oriented in the direction of glacier flow. There is, however, no strong independent evidence for the widespread floods which this hypothesis requires to generate the huge drumlins fields produced by the former Laurentide Ice Sheet in North America. While a source for the water may be found in North America in the drainage of large proglacial lakes and of subglacial water bodies, the mechanisms by which floods are generated elsewhere are not explained.

Another hypothesis proposes that drumlins are a product of subglacial deformation. This idea is based on the presence of a layer of till which is in transport beneath the glacier and is deformed by the shear stress exerted on it by moving ice. This deforming layer moulds itself around subglacial obstacles such as bedrock bumps, boulder clusters, folded sediment and non-deforming sediment to form drumlins and megaflutes (Smalley and Unwin, 1968; Boulton and Jones, 1979; Aario, 1987; Menzies and Rose, 1987; Boulton, 1987).

The model proposed by Boulton (1987), based on this second hypothesis, suggests that three layers may be identifiable within soft deformable sediment when a glacier flows over it. The

top layer (layer A) is rapidly deforming and contains material in transport. Beneath this there is a slowly deforming layer (layer B_1) and below this the sediment is not deforming but is stable (layer B_2). The layers will vary in thickness spatially due to changing properties of the sediment. For example, if the sediment is not easily deformed the B_1 horizon may be absent. The rheology of the sediment is controlled by a range of variables of which pore water pressure is of particular importance. If the pore-water pressure is high, individual grains of sediment will be pushed further apart and the intergranular friction will reduce, increasing the potential to deform the sediment. Fine grained sediments tend to have a higher pore water content and pressure than coarse sediments and will therefore deform more easily. The boundary between the A and B horizons may be either erosional or depositional, depending on whether the glacier is experiencing extensional or compressional flow respectively.

Boulton (1987) developed a semi-quantitative flow model for the rapidly deforming A horizon on the basis of field observations. Using this model he was able to predict that a zone of reduced sediment flow occurs in the lee of an obstacle with enhanced flow on either side of the obstacle (Figure 4.6). This pattern of sediment flow produces a sheath of soft sediment around a core. The sediment within this sheath is not stationary, although the shape of the sheath is, since sediment is added at the up-glacier side and removed down-glacier. If the glacier decays and/or the stress field beneath it changes then the deforming A horizon will become stationary around the core to form a lineation. Within this model the scale of lineations is simply a function of the glacial flow rate and ease of subglacial deformation, with more rapid rates tending to produce more elongated forms.

The subglacial deformation model successfully accounts for the different types of subglacial landform: streamlined hills, drumlins and megaflutes. Different types of lineation core are commonly found including: bedrock; till; and sands/gravels. These can be related to the type of sediment heterogeneity causing the lineation formation including: bedrock obstacle; folds within the B_1 layer; and undeformed areas of sands/gravels respectively. In addition, the spatial distribution of the distinctive sediment rheology required to create lineations explains the spatial distribution of bedforms. Studies of the microstructures within diamictons which constitute the major portion of drumlins in Chimney Bluffs State Park, New York State support the hypothesis drumlins formed under deformable subglacial bed conditions (Menzies *et al.*, 1997).

There is, however, no direct evidence to suggest that subglacial deformation is pervasive beneath ice sheets (Clayton *et al.*, 1989). Homogeneous till within lineations may indicate no deformation of the till. Alternaively, the homogenous till could be the result of intense sub-glacial deformation which removes layering and forms a diamicton - a homogeneous, unconsolidated sediment (Hart and Boulton, 1991). Direct field observations have been made of subglacial deformation within fast-flowing Antarctic outlet glaciers and some Icelandic glaciers (Blankenship *et al.*, 1986; Alley *et al.*, 1987; Boulton and Hindmarsh, 1987). In addition, sedimentary structures within a large part of east Youkshire, are consistent with the till being a deformation till (Eyles *et al.*, 1994; Evans *et al.*, 1995). The few drumlins within this area, and the lack of drumlins at Wedron, Illinois (Johnson and Hansel, 1989), where there is also good

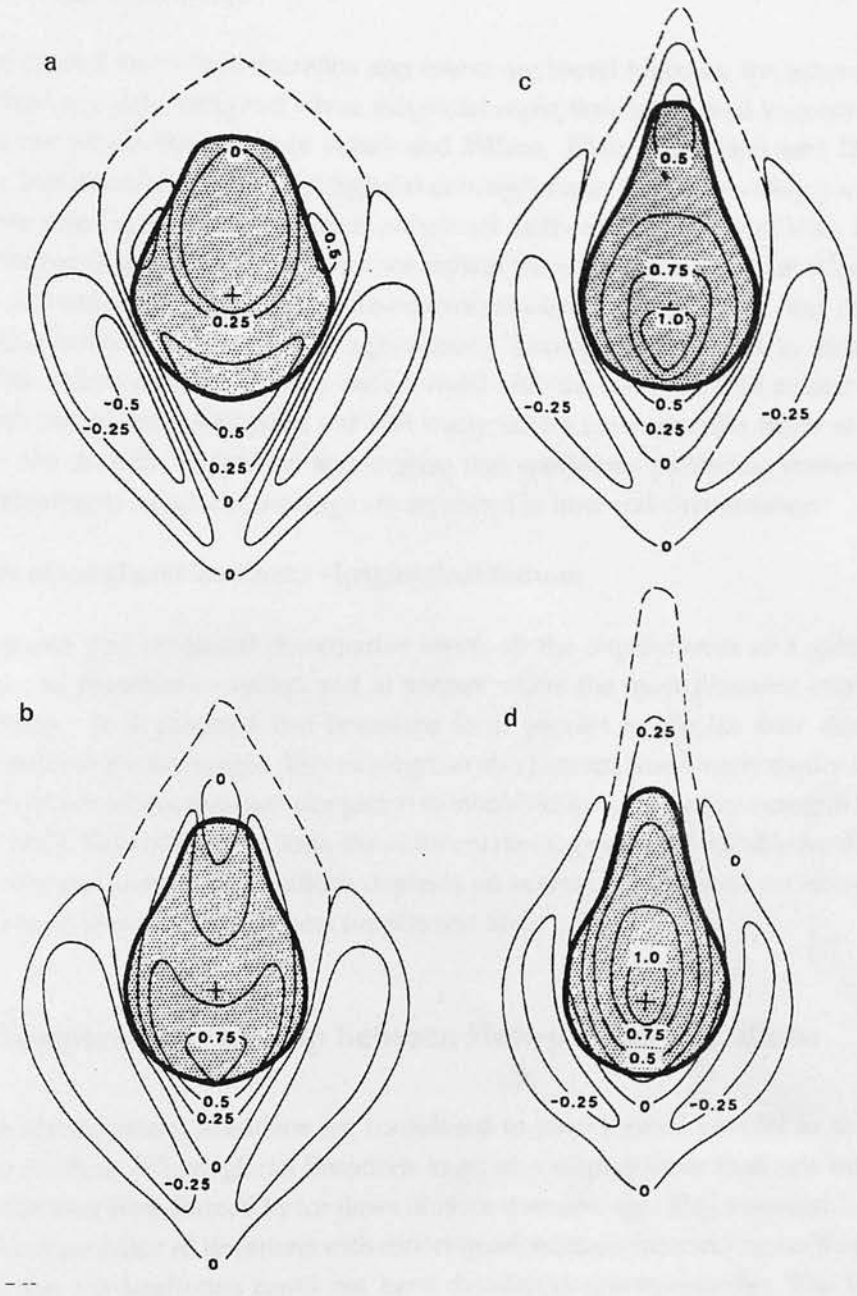

Figure 4.6: Starting from a horizontal plane of relatively soft material intersected by a vertical horizontal plane of relatively soft material intersected by a vertical cylinder of stiffer material. Progressive deformation of the surface and cor (stippled) is shown througha series of time steps from a to d. Contours show elevations with respect to the original surface. From Boulton (1987).

evidence for subglacial deformation, led Hart (1997) to suggest that drumlins only formed during net subglacial deforming bed erosion, when more sediment is removed than enters a given subglacial section. The elongation of the drumlin can still be related to the velocity of the ice sheet and shear strain.

It can be argued that where drumlins and eskers are found together, the eskers could not have formed at a deforming bed where subglacial water flow is believed to occur in shallow channels cut within the sediment (Clark and Wilson, 1994). Brennand and Shaw (1994) proposes that drumlins and mega-subglacial drainage channels (tunnel valleys) were formed during the same catastrophic release of subglacial meltwater. This hypothesis, like that of Shaw (1983) on drumlin formation, does not explain the mechanism by which large quantities of subglacial meltwater are generated. The eskers associated with drumlins may have formed in englacial tunnels and have been subsequently lowered as observed in Iceland (Price, 1982). Alternatively, the eskers may have formed after the sediment had ceased to deform. Aylsworth and Shilts (1989) point out that many eskers cross drumlin fields at near right angles to the drumlin orientation and suggest that conditions producing streamlining and those pertaining to subglacial drainage are separated in time and circumstance.

Summary of subglacial landforms - longitudinal features

It is proposed that subglacial deformation meets all the requirements of a general theory for subglacial lineation formation and at present offers the most plausible explanation of the evidence. It is assumed that lineations form parallel to the ice flow direction and perpendicular to the ice margin. This assumption also remains true for any theory of lineation formation which relates lineation elongation to moulding by ice flow (for example Dardis and McCabe 1983). To produce lineations, the sediment rheology must be suitable for deformation and the size and density of lineations depends on several inter-related variables: effective pressure; basal shear stress; sediment supply; and time.

4.1.5 Temporal Relationship Between Flow-parallel Lineations

From the above, glacial lineations are considered to have formed parallel to the direction of former ice flow. Where glacial lineations in an area display more than one orientation it implies that they were formed by ice flows of more than one age. This assertion is supported further by observation of lineations with differing orientations intersecting each other, which suggests that the landforms could not have developed simultaneously. The intersecting relationship of landforms is expressed in the geomorphological record in two ways (Knight, 1996): (1) Younger lineations have been observed superimposed upon a relatively older set (Rose, 1987, 1989; Dyke and Morris, 1988; Heikkinen and Tikkanen, 1989; Stea and Brown, 1989; Boulton and Clark, 1990); (2) Older lineations have been deformed during the formation of a relatively younger set (Clark, 1990; Punkari, 1982; Dongelmans, 1996).

Heikkinen and Tikkanen (1989) studied the Kuusamo drumlin field in north Finland where older lineations can be recognised underneath younger drumlins and flutes. In general the smaller flutes show more directional variability than drumlins. Heikkinen and Tikkanen (1989) used this as indicating the flutes formed closer to the ice margin and reflected the lobate character of the ice margin more closely than the larger bedforms. Dongelmans (1996) used the intersections of lineations to separate lineations into those formed during the Late Weichselian deglaciation and those formed earlier, possibly during the phase of ice advance.

Summary of the temporal relationship between lineations

The intersection of lineations has been used within this study to assess the temporal relationships of ice flows in an area. Lineation intersection may be the result of lineations formed during relatively older ice advances being preserved and deformed or superimposed by lineations from a younger ice advance. Alternatively the shifts in ice flow can be attributed to changes in ice sheet configuration without any ice advance.

4.1.6 Spatial Distribution of Subglacial Landforms

The pattern of erosion and deposition within an ice sheet at a point in time has been modelled by Boulton (1987) using the mass balance and ice sheet profile (Figure 4.7a-c). This model implies that, in general, deposition occurs within a narrow region at the ice margin. Bennett and Glasser (1996) used this model to examine the shape of the landscape that would result from the growth and decay of a hypothetical ice sheet (Figure 4.7d). From Figure 4.7d several conclusions can be made: the area beneath the ice divide experiences little or no erosion and on deglaciation, a layer of sediment is deposited over the eroded landscape. Field observations support these conclusions: periglacial landscapes often survive under the ice divide (Lagerbäck, 1988) and eroded landscapes occur under a depositional landscape (Kleman, 1994). The layer of sediment deposited over the eroded landscape is not necessarily a continuous layer, but shaped and concentrated into landforms.

There are many assumptions upon which this model is based: the subglacial bed is assumed to be flat and of uniform geology; the ice sheet is warm based throughout; erosion equals deposition within the ice sheet; the ice divide remains in a fixed location. Within Chapter 8 a simple model is used to examine a transect through the Fenno-Scandinavian ice sheet over the last 700 ka. The model used takes into account variations due to the basal topography and basal thermal regime and the length of time that ice occupies a region. The results presented are, in general, in agreement with the model of Boulton (1987) and suggest that lineations form within 100 km of the ice margin and, in general, around 30 km from the ice margin. This is also in agreement with Punkari (1995) who proposes that lineations form 25-100 km from the ice margin.

The spatial distribution of different types of landforms and sediments has been studied by various workers. Several workers have suggested that landforms left by an ice-sheet can be

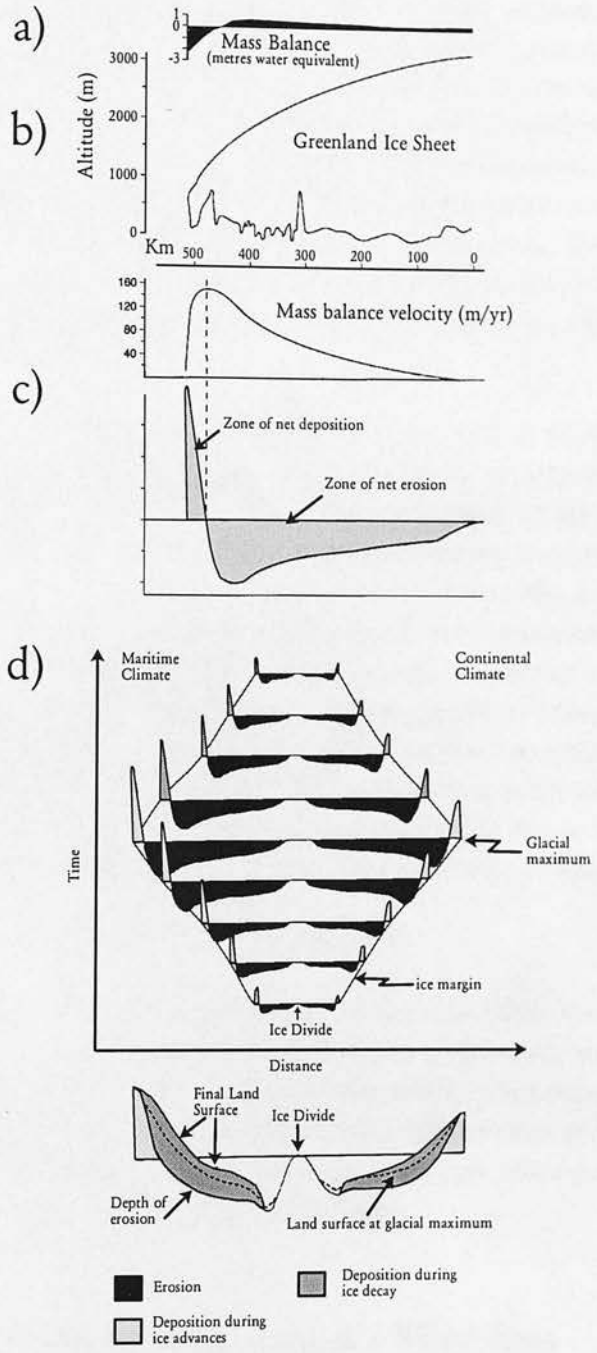

Figure 4.7: a) The approximate surface mass balance of a flow-line transect of the western flank of the Greenland ice sheet at 70° N. b) The surface and bed profile along the same transect. c) Extent of zones of erosion and deposition due to subglacial deformation. a-c from Boulton (1987). d) The expansion and contraction of the ice margin and the pattern of erosion and deposition within it at nine time steps. The shape of the land surface that would result from the growth and decay of this ice sheet is shown below. From Bennett and Glasser (1996).

grouped into zones (Aario, 1987; Sugden and John, 1976; Prest, 1968). For example, using observations from the Northwest Territories in Canada, Prest (1968) describes a gradual transition from a landscape dominated by drumlins at the outer margin, through a landscape of highly elongated drumlinoid forms, into a drumlinized ground moraine, a fluted ground moraine, and finally into an inner zone where the till cover is discontinuous. This highly generalised picture of landscape transition has led to the formulation of depositional models which relate the specific landscape types to specific zones within the ice sheet. In these models, a particular stage during the glaciation (usually the maximum extent) is considered to have produced the majority of landforms (Sugden, 1978; Attig *et al.*, 1989). Rose (1987) proposed that the size of lineations forms a continuum in which the largest forms are created underneath the thickest ice and subsequent smaller forms reflect thinning of the ice sheet as the margin approaches.

It has already been argued, however, that pore-water pressure inside the sediment, sediment supply, time, the magnitude of basal shear and basal velocity are important parameters in determining basal sediment deformation, and the scale of the features produced is not solely dependent on the ice thickness. Pore-water pressure depends, amongst other factors, on subglacial meltwater production and subsurface permeability. Basal velocity can vary laterally as a result of ice streaming and the potential sediment supply is linked to the underlying geology. Small lineations do not necessarily reflect an equilibrium between these variables and may partly be the result of a limited period of formation. It would seem too simplistic to attribute the size of lineations to a specific position within an ice sheet. The model described in Chapter 8 was used to model the distribution of lineation size through a glacial cycle considering additional parameters such as variations due to the basal topography, the basal thermal regime and the length of time that ice occupies a region.

Summary of the spatial distribution of lineations

Models of erosion and deposition within an ice sheet and field studies suggest that: (1) the area beneath the ice divide experiences little or no erosion; (2) on deglaciation, a layer of sediment is deposited over the eroded landscape; and (3), most deposition occurs close to the ice margin (Boulton, 1987). In considering the spatial distribution of different landforms many parameters have to be considered including sediment pore-water pressure, sediment supply, time and the magnitude of basal shear and velocity.

4.2 The Derivation of Palaeo-Ice Flow Sets

4.2.1 Creating the First-Order Interpretation

The first-order interpretation refers to lineations observed directly from the satellite image. Several factors affect the method of first-order interpretation. The scale at which the image is

viewed plays an important part and should be distinguished from spatial resolution. Spatial resolution is the resolution of the satellite sensor on the Earth (Simonett, 1983), in the case of Landsat TM, 30 m^2. In practice, interpretation is limited to an effective spatial resolution of at least five pixels (150 m^2). Scale is the ratio of distance on an image as related to the true distance on the ground (Star and Estes, 1990). In remote sensing, large scale refers to imagery being viewed where each pixel represents a small area on the ground. As soon as an image appears 'blocky' with each individual Instantaneous Field of View being visible, then nothing is gained by increasing the scale.

It was decided to map at a consistent scale, so as to maintain data homogeneity over the region. Interpretations were made on several different scales at first. Figure 4.8 shows two interpretations for the satellite images. Figure 4.8a shows lineations interpreted at a scale of 1:500,000. At this scale the direction of ice flow can be seen, though the temporal relationship between flows remains unknown. On closer inspection it was found that mis-interpretation of non-glacial lineations was more likely at a scale of 1:500,000 than larger scales. Most glacial information was available at a scale of 1:100,000. At this scale lineations, hummocky moraine and transverse ridges are all visible (Figure 4.8b). At larger scales the image becomes blocky and the Instantaneous Working Area becomes too small. At 1:100,000 most computer monitors give an Instantaneous Working Area of at least 20 x 30 km. The software permits two or more simultaneous views of the same image at different scales. This allows the interpretation to be made at one scale, without losing information available from different Instantaneous Working Areas. Regions of ambiguity can be studied with an increased scale, while a broad regional view can be shown by decreasing the scale. In general the imagery was interpreted at a scale of 1:100,000 which ensured a homogeneous interpretation.

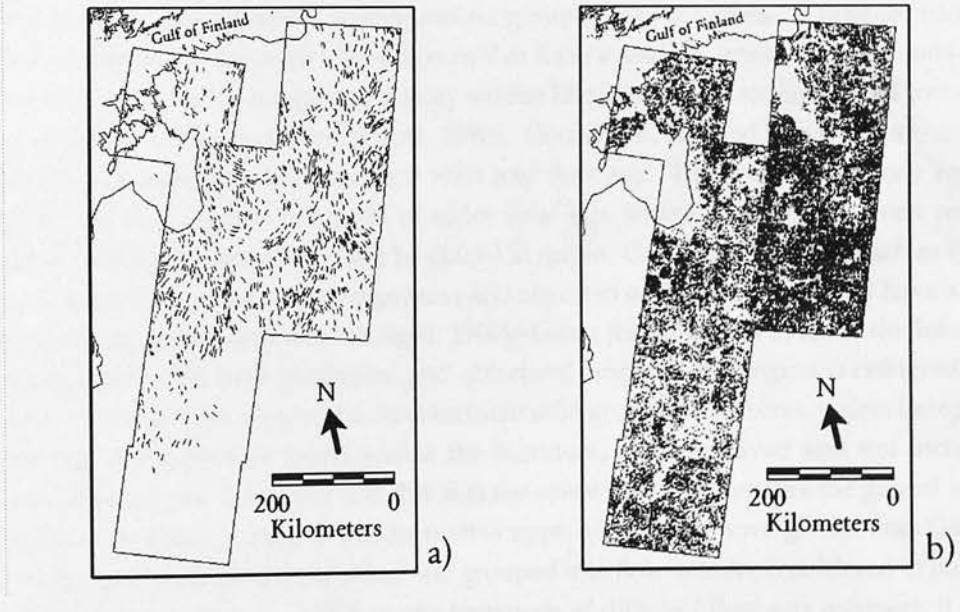

Figure 4.8: First-order interpretation of lineations, mapped at scales of: a) 1:500,000; and b) 1:100,000

Each satellite image was divided into small areas which were interpreted separately. Areas

were not interpreted in a systematic order to avoid biasing from previous areas. Likewise, individual satellite images were not interpreted in a systematic order. To avoid any human bias towards seeing lineations in a particular direction, each area was rotated by different amounts during interpretation. The consistent alignment of lineations from neighbouring areas reaffirms the reliability of the method used.

Different combinations of satellite bands for different areas were used to try to get the most information out of the imagery. TM bands 4, 5 and 7 for red, green and blue was found to be the most successful combination. To further enhance the geomorphic information displayed, the histogram intensity profile of each band was altered for different regions (Section 3.5.3).

The ability to interpret lineations from satellite imagery is a skill acquired with time. Lineations were recorded using an on screen cursor to define their start and end points and so create a vector. The direction of ice movement can be inferred from the morphology of lineations if it is assumed that lineations taper in the down-ice direction. All orientations measured by this method trended southwards. Where the morphological form of the lineations did not indicate an ice flow direction the orientation was taken, as a first approximation, to be southwards. The orientations of the lineations forming the first-order interpretation are compared with published ice flow directions at a later stage (discussed below).

4.2.2 Creating Flow Sets

The number of first-order lineations recorded and the high density of lineations in many regions means that it was difficult to identify the lineation patterns using only the first-order interpretations. The lineations were therefore grouped into flow sets. A flow set consists of lineations that are of the same orientation or that form a smooth, gradual, continuous change of orientation across the image and display similar line lengths, are similarly well formed and have relatively uniform spacing (Clark, 1990). Occasional, isolated lineations are observed which do not appear to be associated with any flow set. These lineations may represent localised ice flow, or the remnants of older flow sets which have mostly been removed. Alternatively the lineations may not be glacial in origin. Geological features such as faults or dyke swarms can extend across large areas and are often of the same scale and have a similar appearance as glacial lineations (Knight, 1996). Using the computer system, the interpreted lineations were lain over geological and structural maps of the region (Leningrad, 1982). Lineations which were observed to be coincident with geological features, unless independent supporting evidence was found within the literature, were removed and not included in subsequent analysis. It was felt that this was the safest method to ensure the glacial origin of lineation even though using this conservative approach may remove glacial lineations from any further analysis. Lineations which are grouped into flow sets are considered to have been formed by the same ice flow. Where the lineations of different flow sets intersect, it may be possible to distinguish the temporal relationships between the flow sets.

Figures 4.9a-h summarises the steps required to interpret ice flow patterns from lineation data.

From the first-order interpretation of lineations shown in Figure 4.9a flow lines can be drawn which depict two flow sets (Figure 4.9b). Flow set 1 is oriented NW-SE while flow set 2 is oriented WNW-ESE. Figure 4.9c shows an enlarged region of Figure 4.9a. It can be seen that lineations from flow set 1 are superimposed upon the lineations of flow set 2. This allows the two flow sets to be separated temporally; flow set 1 is younger than flow set 2 (Figure 4.9d).

Figure 4.9e-f shows how flow set 1 shown in Figures 4.9a-d may form part of a regional flow set in this case in a larger fan shape. The lineations within the fan do not have the same orientation. Instead the orientation gradually changes across the image. Also shown in this image are two WNW-ESE flow sets which form cross-cutting lineations with the fan. From this situation alone, however, it is not clear how to relate these two WNW-ESE flow sets to each other.

Figure 4.9g represents a more realistic picture of lineation data. The two insets show examples of systematic shifts in the direction of the younger lineations. The oldest (and largest) lineations in both insets are trending NW-SE, parallel to the main axis of the fan. The younger lineations show orientations diverging from this axis to NW-SE in the north-east of the region and SE-NW in the south-west. This change from parallel flow to increasingly divergent flow is interpreted as the result of the migration of a fan from SE to NW as shown in Figure 4.9h.

Currently, two interpretations of ice flow have been suggested in the literature. Synchronous ice flow describes the isochronous formation of landforms within a flow set (Clark, 1993; Clark and Wilson, 1994). There are no obvious discontinuities between lineations within the flow set and the lineations display a high degree of parallel alignment and conformity. Time transgressive ice flow is associated with the retreat of the ice margin (Kleman, 1994). Since the ice margin does not retreat evenly and often retreats in a lobate manner, the lineations formed perpendicular to it are less coherent than those formed during synchronous flow. Knight (1996) used eskers to indicate time transgressive sedimentation and assumed that where the eskers were aligned with lineations, the formation of the lineations were also time-transgressive. She additionally used the presence of Rogen moraines to signify synchronous ice flow. The genesis of Rogen moraines and eskers is still debated (Section 4.1.3). Since no eskers or Rogen moraines were identified using the satellite imagery and few are shown on the geomorphological maps (Leningrad, 1982) they could not be used to indicate the synchroneity of lineations. As will be discussed in Section 7.3, the lineations within flow sets observed over the Eastern Baltic region show more variability in their orientations than those observed over Finland. This suggests, along with the close proximity of the margin of the ice at it's maximum extent, that while the synchroneity of lineations is unknown, the majority seem likely to have formed time-transgressively.

The direction of ice movement for each flow set was inferred from the direction of the lineation vectors used to form the flow set. These orientations were compared with data from published literature where the ice flow direction is inferred from the stoss and lee of geomorphological forms (for example drumlins and flutes), from striae and from the clast long axes orientation in tills. Where the flow sets align parallel to the features of known direction they are assumed

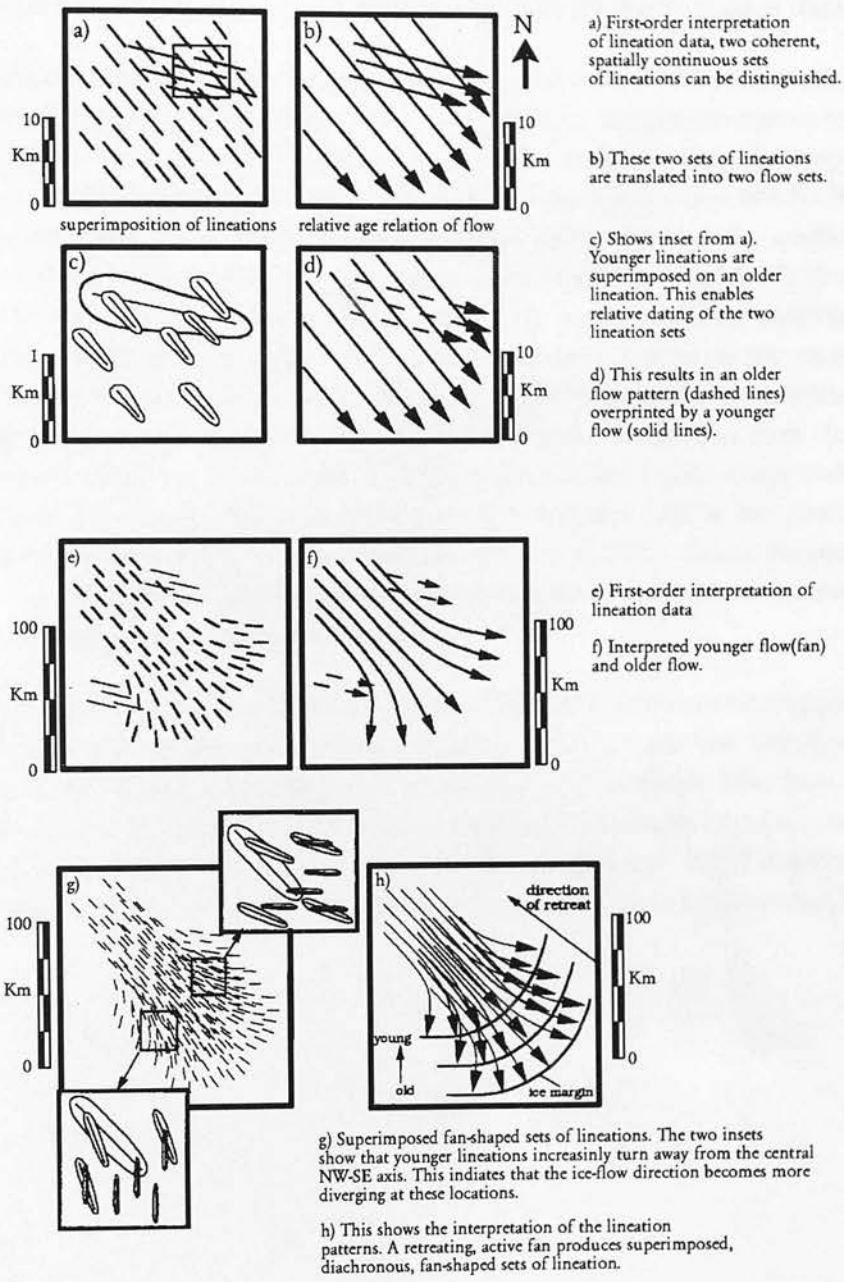

a) First-order interpretation of lineation data, two coherent, spatially continuous sets of lineations can be distinguished.

b) These two sets of lineations are translated into two flow sets.

c) Shows inset from a). Younger lineations are superimposed on an older lineation. This enables relative dating of the two lineation sets

d) This results in an older flow pattern (dashed lines) overprinted by a younger flow (solid lines).

e) First-order interpretation of lineation data

f) Interpreted younger flow(fan) and older flow.

g) Superimposed fan-shaped sets of lineations. The two insets show that younger lineations increasinly turn away from the central NW-SE axis. This indiates that the ice-flow direction becomes more diverging at these locations.

h) This shows the interpretation of the lineation patterns. A retreating, active fan produces superimposed, diachronous, fan-shaped sets of lineation.

Figure 4.9: Method of interpretation of flow sets from lineation data. From Dongelmans (1996).

to represent the same palaeo-ice flow episode. For example, Figure 4.10a shows the first-order interpretation of lineations from the region shown in Figure 4.10d. Figure 4.10b shows four flow sets interpreted from the lineations. These flow sets are compared with the ice direction information published by Raukas and Gaigalas (1993) and given a direction of ice flow accordingly (Figure 4.10c). This is an example of an advantage of using digitised data which, by using a computer, can be overlain and compared directly with other data sets.

The temporal classification of flow sets relative to each other was achieved by considering the intersection of lineations. Dongelmans (1996) used dated ice marginal moraines to correlate spatially separate flow sets and to reconstruct a number of glacio-dynamic 'snap shots' of the ice sheet. While several stadials have been identified during the Late Weichselian glacial retreat, and have been given dated margins (Raukas, 1986), many of the stadials are not marked by end moraines or other glacial marginal landforms (Karukäpp, 1997). As discussed in Section 2.3.4 the dates themselves do not necessarily represent a new readvance of the active glacier (Karukäpp *et al.*, 1992). Perhaps the best dated margin is the margin of the North Lithuanian Stadial as observed south of the Gulf of Riga using the satellite imagery. The margin till overlays deposits of the Raunis interstadial which has been dated using the radiocarbon method at several sites throughout Estonia and Latvia at approximately 13 250 B.P (Table 2.3). It has, however, been proposed that this date is too young, the till being contaminated by recent rootlets (Dreimanis and Zelcs, 1995). Given the uncertainties regarding the dating of the glacial deposits, no attempt was made to date ice margins and associated flow sets relative to the present day.

Initially flow sets were interpreted for local regions. These flow sets were expanded across the images using the same criteria as were used to develop them from the 'raw' lineations: similar orientation of the ice flow lines with no abrupt changes of orientation. That flow sets could be expanded to include lineations from adjacent images demonstrates that the interpretation identified real lineations rather than artifacts of an individual image. A full description of the satellite images and the flow sets interpreted from them is given in the following Chapter.

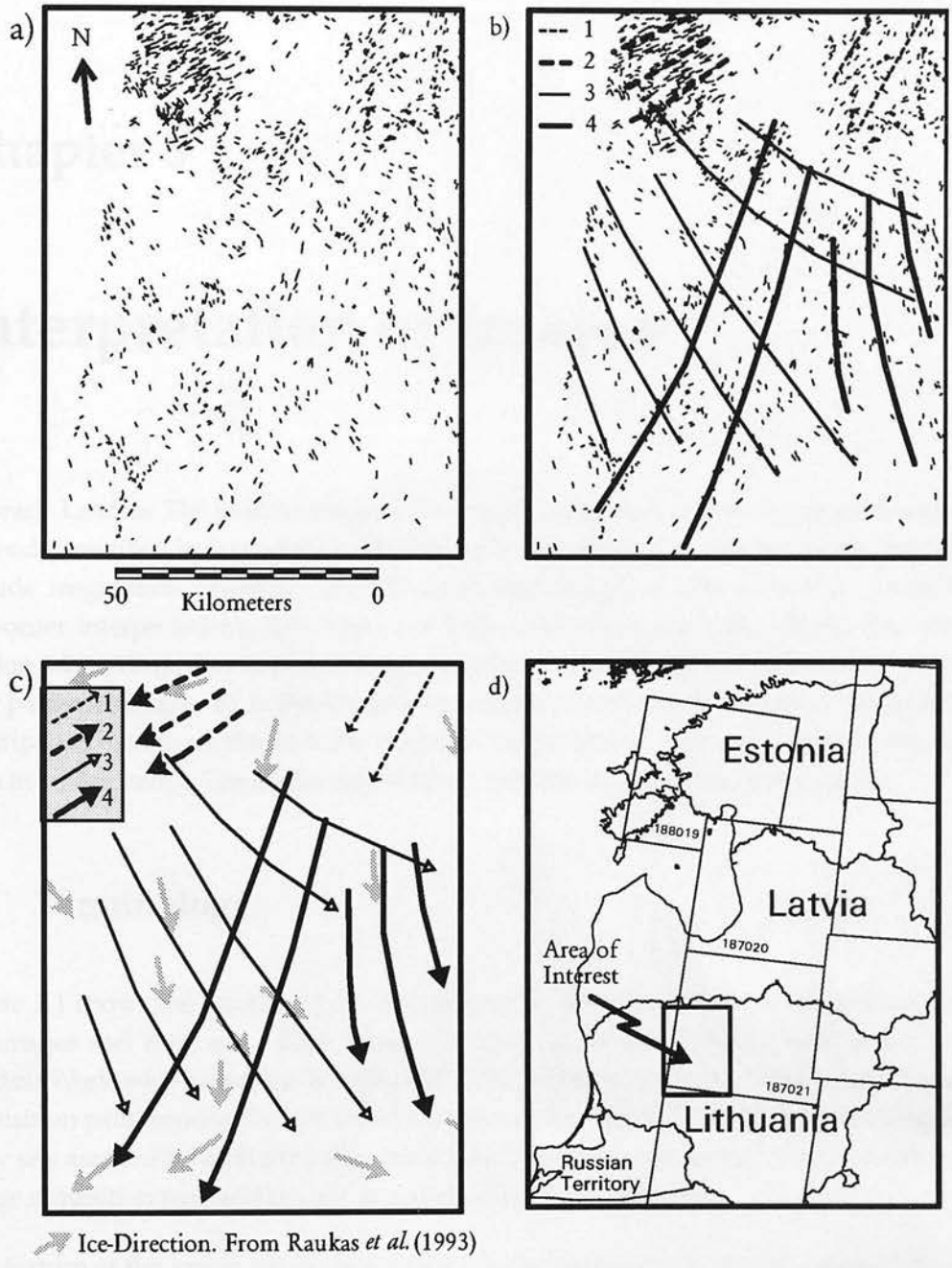

Figure 4.10: An example of interpreting flow sets from lineation data, and of using published data to infer ice direction: a) First order interpretation of area of interest; b) Flow sets interpreted from first order interpretation; c) Ice-direction from the long axis of tills of the Last Weichselian glaciation Raukas and Gaigalas (1993); d) Location of area of interest within Lithuania.

Chapter 5

Interpretation of Images

For each Landsat TM satellite image a first-order interpretation was constructed using the methods described in Section 4.2.1. The first-order interpretations consist of lineations which include megaflutes, drumlins, megadrumlins and elongated hills or basins. From these first-order interpretations, flow sets have been constructed using the criteria described in Section 4.2.2. These flow sets are brought together to form a regional picture of past glacial flow patterns (Chapter 6). In this Chapter each image and flow set is described. These detailed descriptions have been placed in the main text for the sake of logic and completeness, rather than in an Appendix. The reader may prefer to skip the details within this Chapter.

5.1 Terminology

Figure 5.1 shows the location of the images used in this study, and the referencing system for images and flow sets. Each image was given a unique reference code based on the Landsat Worldwide Reference System (WRS, 1981). The image is identified by six digits, the acquisition path forming the first three and the acquisition row forming the remaining digits. Flow sets are labelled alphabetically with a three digit prefix consisting of the last digit of the image acquisition path and the last two digits of the acquisition row.

The texture of the image can be defined by its spatial frequency. A high spatial frequency indicates the intensity of a spectral band varies by a significant amount over a short spatial distance. In this study regions with a large intensity range across distances of about 1000 m and an irregular pattern are referred to as being 'rough' (Figure 4.1b) while regions where the spectral intensity varies smoothly with distance or that contain a regular pattern are considered to be 'smooth'.

All the colour satellite image Figures within this Chapter are false colour composites that use

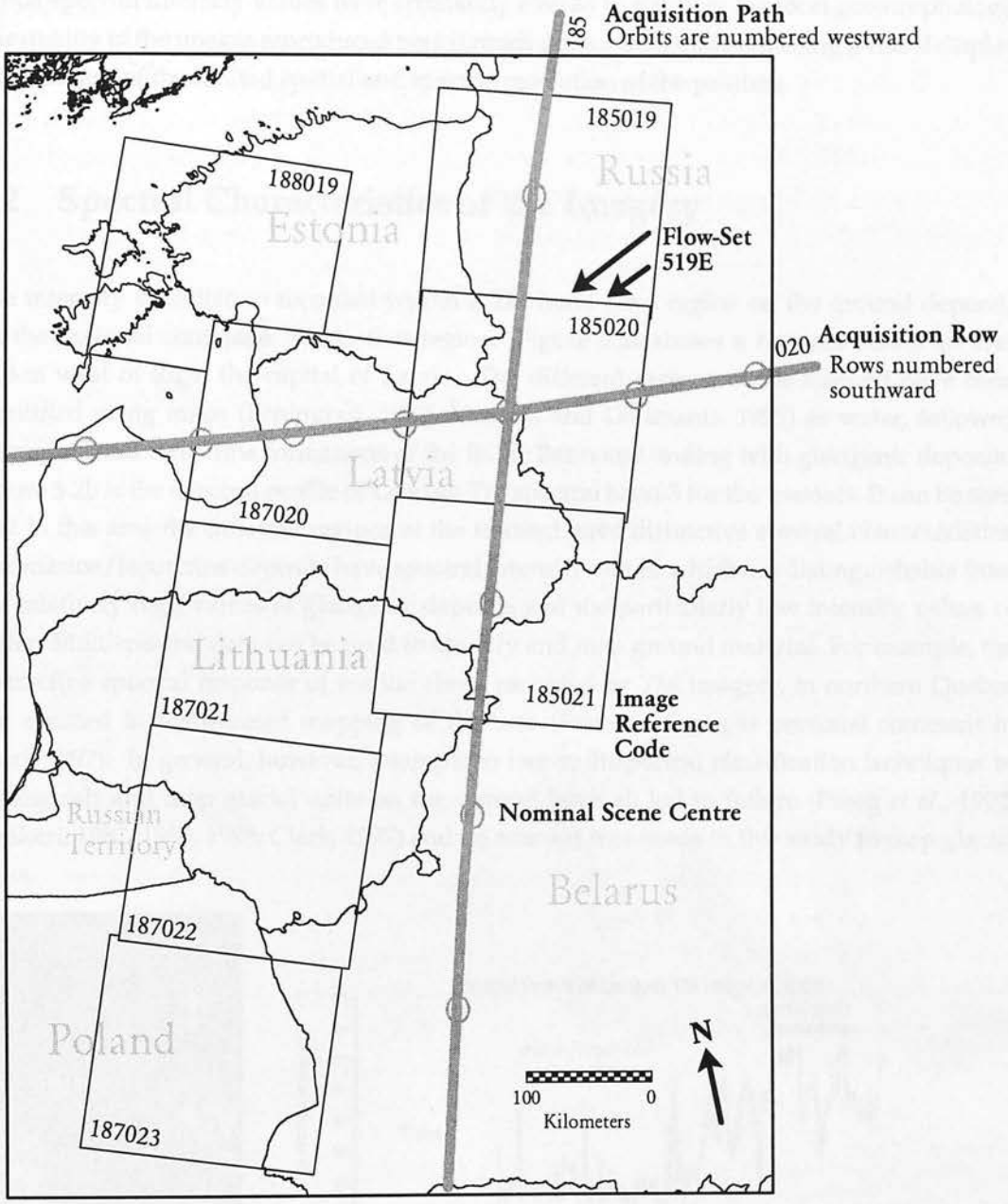

Figure 5.1: Landsat TM images interpreted in this study, and the referencing system used for images and flow sets.

the Landsat TM spectral bands 4, 5 and 7 for the colours red, green and blue respectively. Any colours mentioned within the text refere to these Figures. As described in Chapter 4, several different band combinations were used during interpretation and the histogram profiles of the bands spectral intensity values were constantly altered to enhance the local geomorphology. The quality of the images reproduced here is much poorer than that seen using a visual display unit because of the limited spatial and spectral resolution of the printers.

5.2 Spectral Characteristics of the Imagery

The intensity of radiation recorded within a TM band for a region on the ground depends on the material contained within that region. Figure 5.2a shows a transect across an area 27 km west of Riga, the capital of Latvia. The different regions of the transect have been identified using maps (Leningrad, 1982; Āboltiņš and Dreimanis, 1995) as water, followed by marine and lacustrine formations of the Baltic Basin and ending with glacigenic deposits. Figure 5.2b is the spectral profile of Landsat TM spectral band 5 for the transect. It can be seen that in this area the different regions of the transect have distinctive spectral characteristics. The marine/lacustrine deposits have spectral intensity values which are distinguishable from the relatively high values of glacigenic deposits and the particularly low intensity values of water. Multispectral data can be used to identify and map ground material. For example, the distinctive spectral response of marine clays, recorded by TM imagery, in northern Quebec has assisted in widespread mapping of the unit (Francois Cavayas personal comment in Clark 1997). In general, however, attempts to use multispectral classification techniques to distinguish and map glacial units on the ground have all led to failure (Praeg *et al.*, 1992; Punkari, 1982, 1985, 1993; Clark, 1997) and no attempt was made in this study to map glacial units.

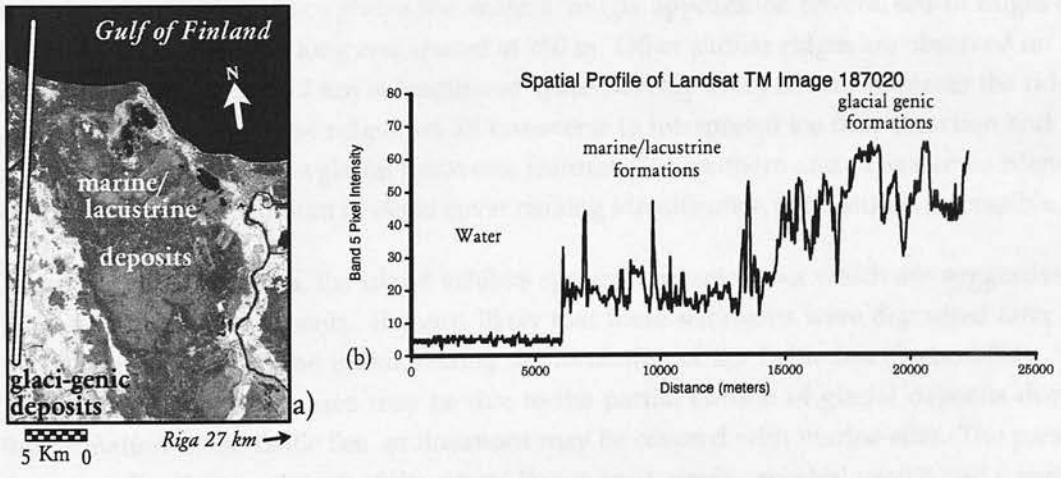

Figure 5.2: Profile of Landsat TM band 5 values along transect shown on left from image 187020

A distinct difference was observed in the spectral character of the images 185019, 185020 and 185021 to their neighbouring images 187020 and 187021, even where the images overlap. This

can be partially explained by the time of acquisition of the images. During the year, vegetation changes in size, shape and colour as it grows or becomes dormant. Spectra of vegetation vary between two end members: wet (green and photosynthetic) and dry (non-photosynthetic). The reflectance spectra of these two end members are shown in Figure 5.3. The near-infrared spectra of green vegetation are dominated by liquid water vibrational absorptions, while the dry vegetation spectrum shows absorptions due to cellulose, lignin and nitrogen (Clark in press). From this diagram the reflectance of vegetation acquired by Landsat TM band 4 during spring is expected to be greater than that gathered during the autumn. This is shown in Figure 5.4. The reflectance of water remains constant between the images while the reflectance intensity of the land cover is greater for image 185020, acquired during May, than for images 187020 and 187021, acquired during October.

5.3 Interpretation of Images

5.3.1 Image 188019

Image 188019 shows northwestern Estonia, including parts of the Saaremaa and Hiiumaa islands, and the northwestern corner of Latvia. Figure 5.5a shows the first order interpretation of lineations. It is proposed that the lineations within image 188019 represent a single flow set, labelled 819A (Figure 5.5b). The TM Image and flow set 819A are described by area in the following Sections.

Flow set 819A: Saaremaa and Hiiumaa Islands

The lineations on the island of Saaremaa trend at 170°. In the east of the island, the TM data has a high spatial frequency giving the image a 'rough' appearance. Several sets of ridges can be observed, up to 4 km long and spaced at 250 m. Other similar ridges are observed on the island of Hiiumaa, up to 7 km in length and spaced evenly every 300 m. In places the ridges appear to bifurcate. These ridges are all transverse to interpreted ice flow direction and are accordingly interpreted as glacial transverse features. The southern area of Saaremaa island is obscured by a small amount of cloud cover making identification of lineations impossible.

In the north of Saaremaa, the island exhibits spectral characteristics which are suggestive of marine/lacustrine sediments. It seems likely that these sediments were deposited after the ice had retreated from the island, during the formation of the Baltic Sea (Section 2.4). The lack of lineations in this area may be due to the partial erosion of glacial deposits during the formation of the Baltic Sea, or lineations may be covered with marine silts. The present day coastal region southwest of the city of Parnu has a similar spectral profile and a similar explanation accounts for the lack of lineations in this region.

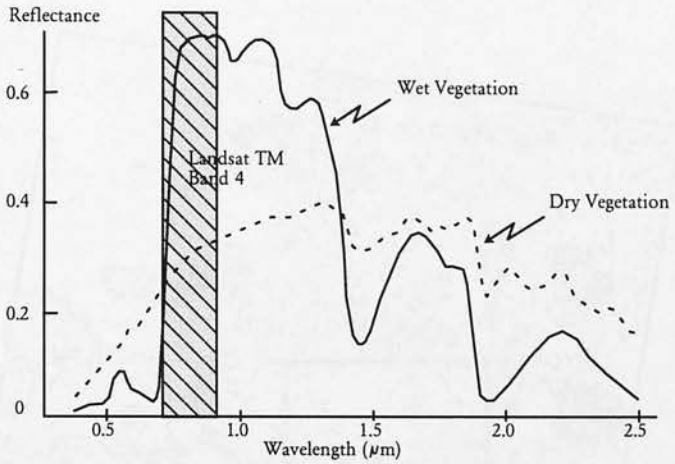

Figure 5.3: Reflectance spectra of photosynthetic (green) vegetation, non-photosynthetic (dry) vegetation. The green vegetation has absorptions short of 1 μm due to chlorophyll. Those at wavelengths greater than 0.9 μm are dominated by liquid water. The dry vegetation shows absorptions dominated by cellulose, but also lignin and nitrogen. These absorptions must also be present in the green vegetation, but can be detected only weakly in the presence of the stronger water bands. The wavelength range of Landsat TM band 4 is also shown.

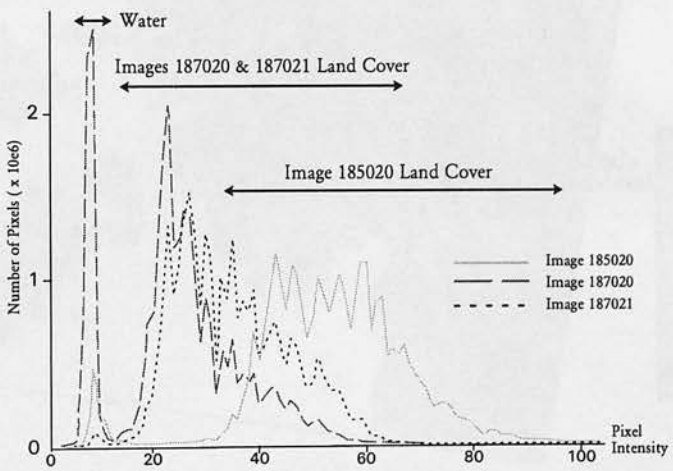

Figure 5.4: Landsat TM band 4 reflectance histograms for images 185020, 187020 and 187021. The reflectance intensity is standardised to the range 1-255. The figure shows 99.7 % of all pixel values within the images

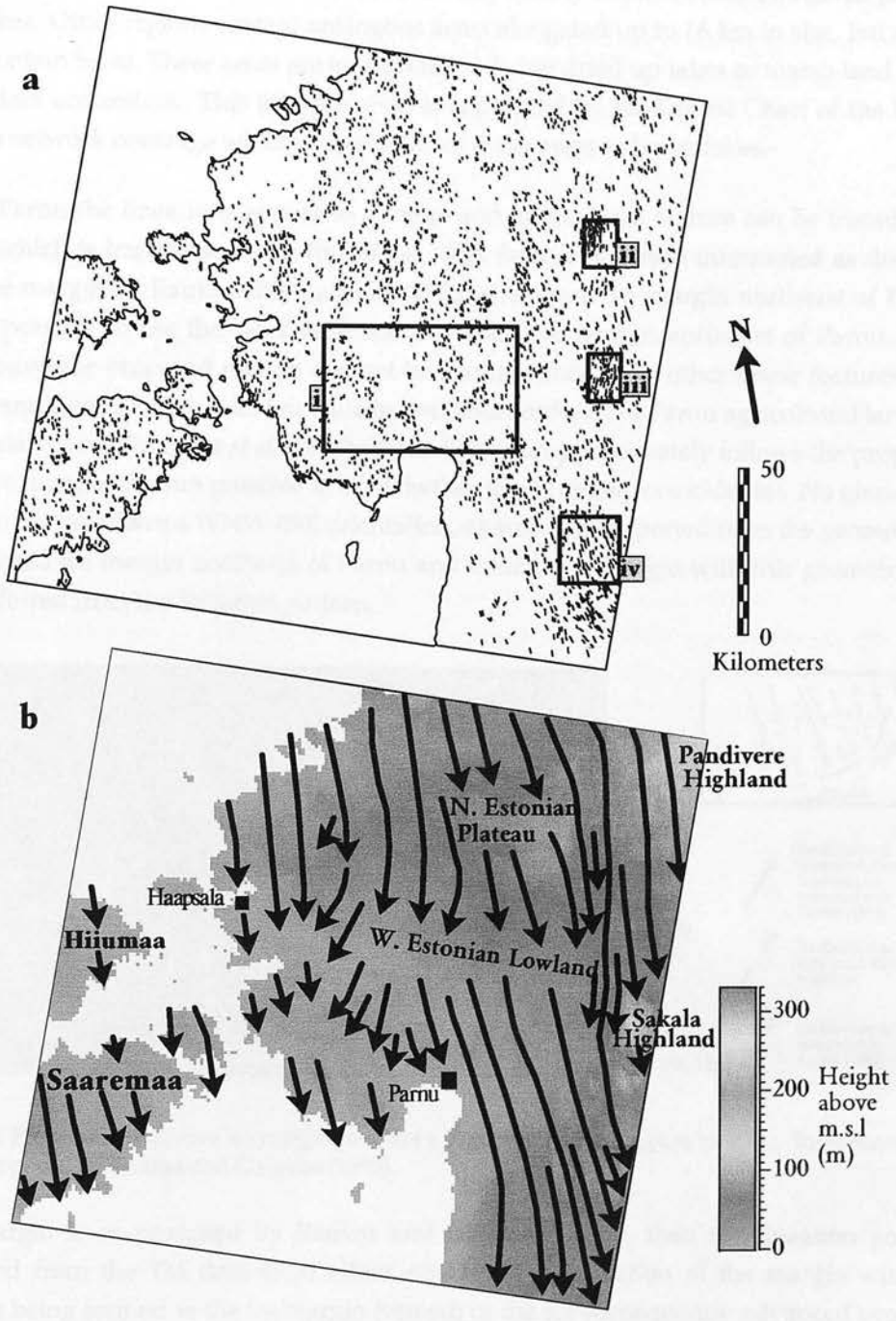

Figure 5.5: a: First order interpretation of Landsat TM Image 188019. Boxes delineate areas shown in further diagrams. b: Flow set 819A superimposed on the present day topography.

Flow set 819A: West Estonian Lowland

The coastal region to the west of Parnu contains lakes elongated at 160°, parallel to the lineations in the area. Some lakes are surrounded by clearly defined areas, elongated parallel to the lakes. Other regions contain analogous areas elongated up to 16 km in size, but which do not contain lakes. These areas are interpreted as being dried up lakes or marsh land at the time of data acquisition. This interpretation is supported by the Digital Chart of the World drainage network coverage which shows some of these areas as being lakes.

West of Parnu the lineations appear to diverge and an elongate feature can be traced (Figure 5.6) which is transverse to the lineations. This feature has been interpreted as the Pandivere ice margin by Raukas and Gaigalas (1993) who trace the margin northeast of Parnu. It is not possible to use the satellite imagery to trace the margin northeast of Parnu, however, because the proposed margin can not be distinguished from other linear features such as roads and rivers. Within a 25 km wide brown area northeast of Parnu agricultural land use is particularly low (Sweitzer *et al.*, 1996). While this area approximately follows the proposed Pandivere margin, it is not possible to say whether this is merely coincidental. No glacial lineations in the area have a WNW-ESE orientation, as would be expected from the geometry of the proposed ice margin northeast of Parnu and therefore a margin with this geometry can not be inferred from the lineation pattern.

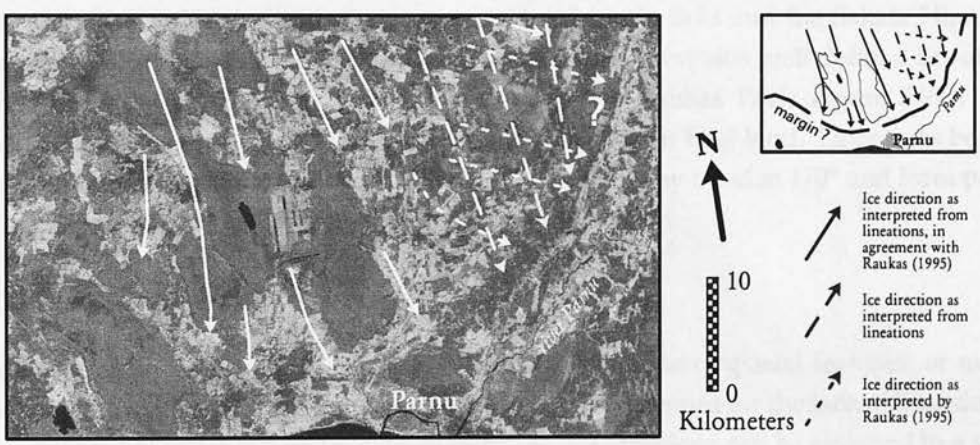

Figure 5.6: Proposed Pandivere ice margin, see box i, Figure 5.5 for the figure location. Inset shows the margin proposed by Raukas and Gaigalas (1993)

If the margin is as proposed by Raukas and Gaigalas (1993), then the lineation pattern interpreted from the TM data must either pre-date the formation of the margin with no lineations being formed as the ice margin formed; or the ice subsequently advanced over the margin removing any WNW-ESE lineations associated with the margin and forming lineations trending at 170° as observed. From the TM data, it is not possible to determine which of these two hypotheses is likely.

South of the river Parnu the West Estonian Lowland is characterised by a series of rivers and areas with small spectral variation interpreted as marsh. In this area lineations are difficult

to discern. Those observed, however, all trend approximately 150°, concordant with flow set 819A. Further south, lineations are more common and have a similar orientation of 150°.

Lineations up to 1.5 km long are observed within the central and northeastern regions of the West Estonian Lowland. East of Haapsalu the density of lineations increases to form a group of parallel lineations. Several areas where lineations are missing are interpreted as basins or marshy ground. These areas become more common towards the north of the West Estonian Lowland.

Flow set 819A: North Estonian Plateau, Pandivere and Sakala Highlands

Across the higher elevation of the North Estonian Plateau the texture of the image becomes slightly more rough. However, the transition from smooth lowland to rough highland is not as marked as that observed further to the southwest, for example between the Vidzeme Highland or Haanja Highland and the lowlands which surround them (Section 5.3.2). Lineations concordant with flow set 819A can be observed over the Pandivere Highland in the east of the image. These lineations are much better defined than the lineations observed over the highlands further south in images 187020, 187021 and 187022.

A group of well-defined, closely spaced, north-south lineations occur between the North Estonian Plateau and Pandivere Highland. These lineations are known as the Türi drumlin field (Rõuk and Raukas 1989; Figure 5.7a). There are less densely packed lineations with a similar trend immediately south, between the Türi drumlin field and the Sakala Highland. The lowland neighbouring the Sakala Highland to the east contains well-defined lineations, referred to as the Suure-Jaani drumlin field (Rõuk and Raukas 1989; Figure 5.7b). Few lineations are observed within the northern part of the Sakala Highland. Lineations become more abundant towards the southwest (Figure 5.7c) where they trend at 170° and form part of the Burtnieks drumlin field discussed in the following Section.

Overview of Image 188019

The density of lineations varies across image 188019. Erosion of glacial features, or marine silt deposition, during the formation of the Baltic Sea may account for the lack of lineations in some regions. Other areas comprise drumlin fields. All lineations can be assigned to a single flow set, 819A, formed by ice flowing with an approximate trend of 170°. North of Parnu the lineation pattern is concordant with that of a diverging fan.

5.3.2 Image 187020

Image 187020 shows the region southeast of image 188019 where the Gulf of Riga occupies the western half of the image. From the first-order interpretation of the image (Figure 5.8a) seven flow sets were identified, (labelled 720A-720G, Figure 5.8b).

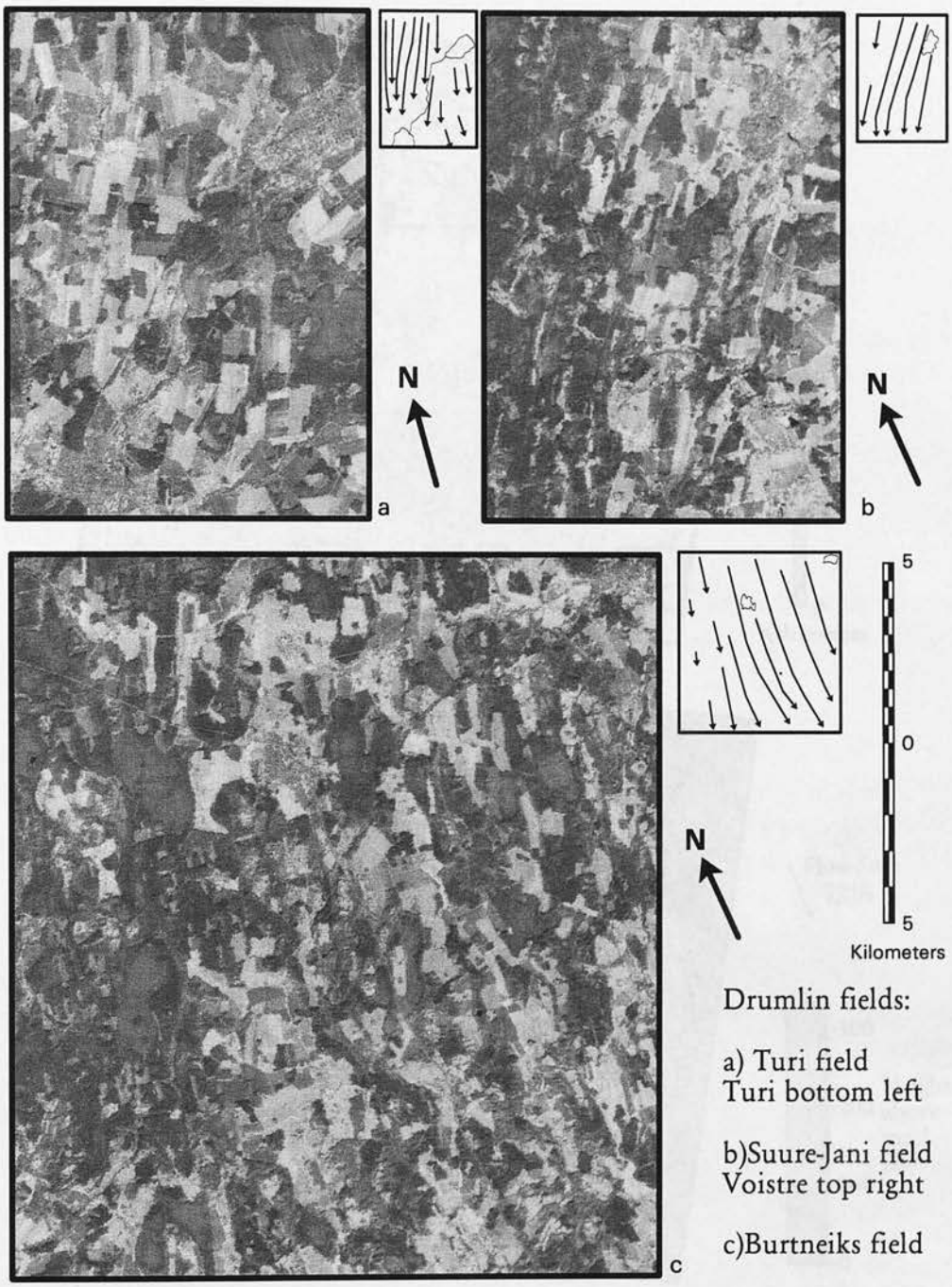

Figure 5.7: Flow set 819A: Well-defined lineations as observed within Landsat TM image 188019, Figures a, b and c correspond with boxes labelled ii, iii and iv in Figure 5.5

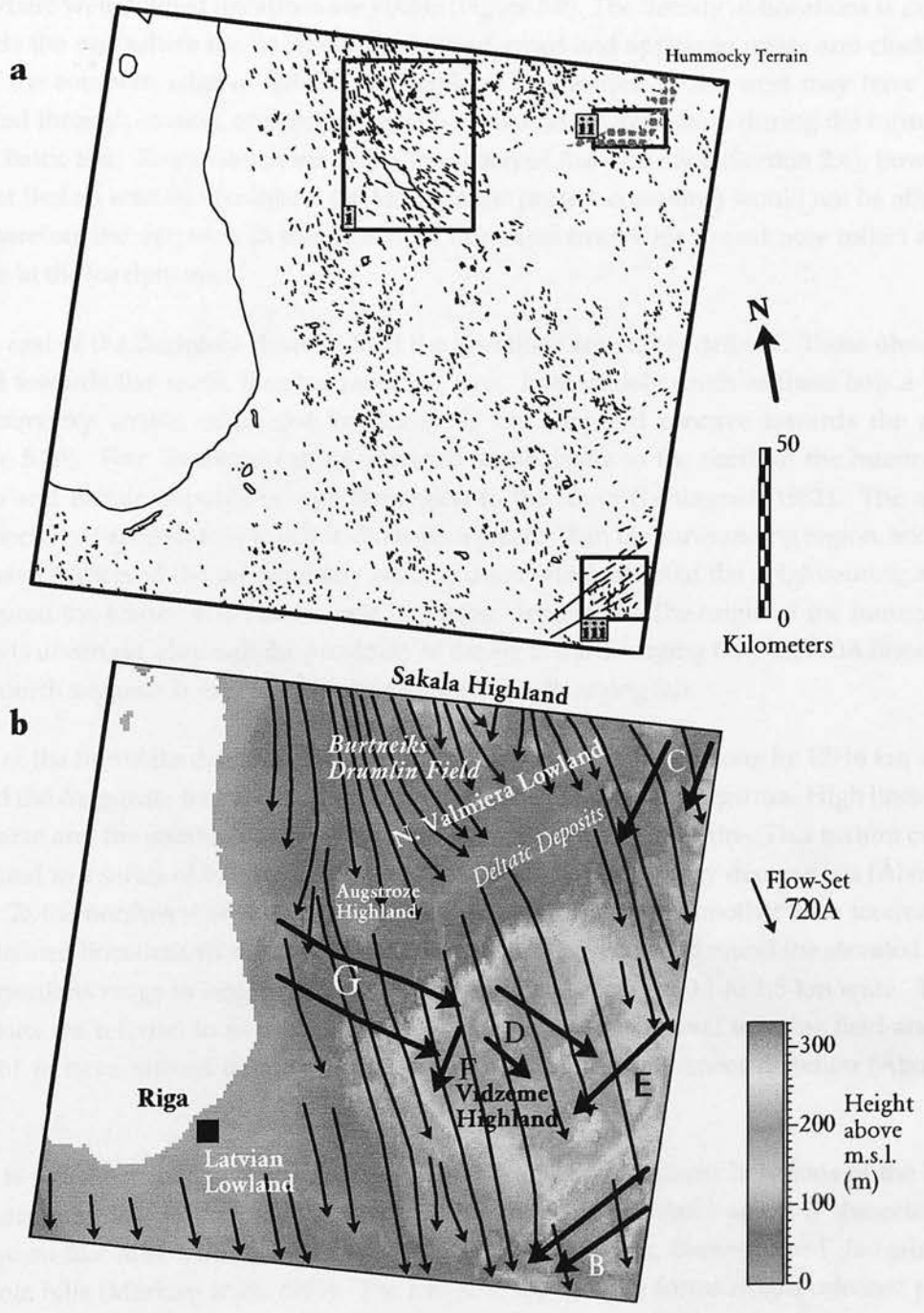

Figure 5.8: a: First order interpretation of Landsat TM Image 187020. Boxes delineate areas shown in further diagrams. b: Flow sets 720A-G superimposed on the present day topography.

Flow set 720A

Flow set 720A covers the whole image at a trend of approximately 170°. Within the North Valmiera Lowland, flow set 720A consists of the southern portion of the Burtnieks drumlin field where well-defined lineations are visible (Figure 5.9). The density of lineations is greater towards the east where the lineations are better formed and appear to rotate anti-clockwise round the southern edge of the Sakala Highland. Lineations in the west may have been removed through erosion, or possibly hidden by marine silt deposition during the formation of the Baltic Sea. Re-constructions of the formation of the Baltic Sea (Section 2.4), however, suggest that an area this far inland (40 km from the present coast-line) would not be affected and therefore the variation in the density of lineations from west to east may reflect a real change in the ice dynamics.

To the east of the Burtnieks drumlin field the lineations are poorly defined. Those observed spread towards the south, forming radiating fans. Immediately south of these fans a band of hummocky terrain exists, 3-4 km wide, 45 km long and concave towards the north (Figure 5.10). Few lineations can be observed immediately to the north of the hummocky terrain and deltaic deposits occupy the region to the south (Leningrad, 1982). The arc of hummocks has an elevation which is about 40 m greater than the surrounding region, and this may have preserved the arc from any water erosion which affected the neighbouring areas, or ensured the feature was not covered by marine deposition. The origin of the hummocky terrain is uncertain, although the proximity of the arc to the diverging flow set 720A lineations to the north suggests it may have formed in front of a diverging fan.

South of the Burtnieks drumlin field lies a small elevated area, 42 km long by 12-16 km wide, termed the Augstroze Interlobate High (Āboltiņš, 1995). Within the Augstroze High lineations are sparse and the southern area is characterised by an irregular texture. This texture can be attributed to a series of hills known as *daugals* surrounded by marshy depressions (Āboltiņš, 1995). To the northwest of the Augstroze High the topography is smoother with moderately well-defined lineations (flow set 720A) which appear to have formed round the elevated area. The lineations range in length between 0.5 to 10 km and are from 0.1 to 1.5 km wide. These lineations are referred to as uval moraines forming the Limbaži uval moraine field and are thought to have formed parallel to the former regional ice movement direction (Āboltiņš, 1995).

There is a distinct change in the geomorphology from the prominent lineations of the Burtnieks drumlin field to the irregular terrain of the Vidzeme Highland which is characterised by plateau-like hills with a cover of glaciolacustrine sediment, dome-shaped daugals and morainic hills (Markots *et al.*, 1995). The irregular topography forms ridges oriented parallel to the north and south margins of the highland.

The region immediately to the west of the Vidzeme Highland displays the characteristic smooth topography of the lowland areas and flow set 720A lineations form a fan which diverges slightly towards the south. Further west, the Latvian Lowland occupies the coastal

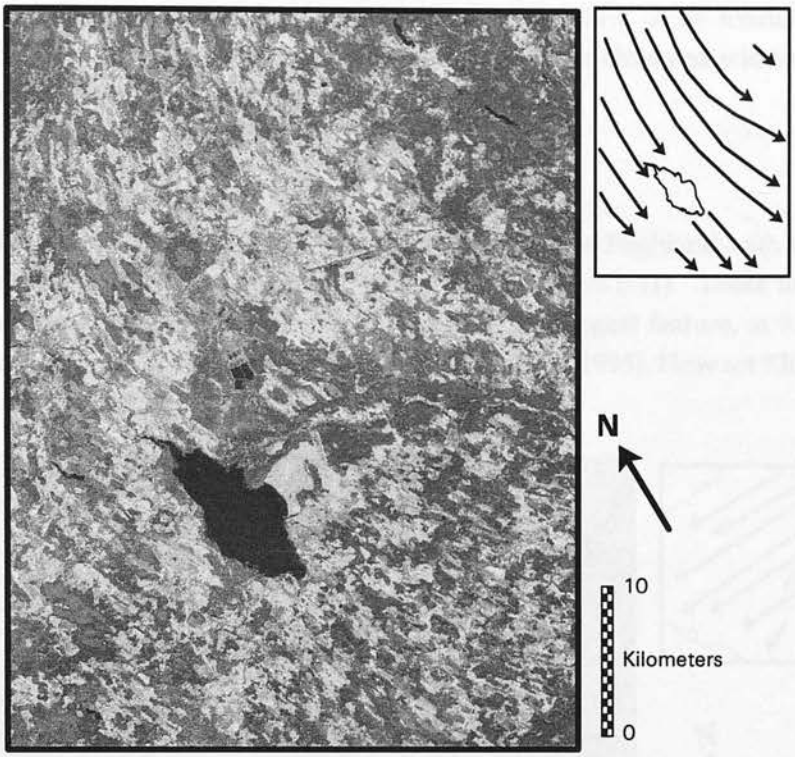

Figure 5.9: The Burtnieks drumlin Field, see box i, Figure 5.8 for location

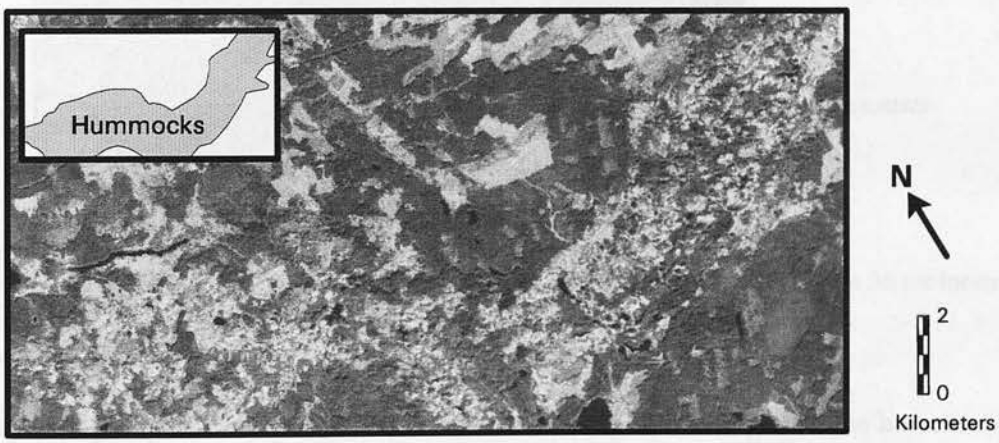

Figure 5.10: Hummocky terrain as seen in image 187020, see box ii, Figure 5.8 for location

regions surrounding the city of Riga and extending along the coast towards the north. The area is characterised by marine and lacustrine sediments of the Baltic Basin (Āboltiņš and Dreimanis, 1995). Few lineations are observed within these coastal regions where Quaternary deposits are thin (Figure 2.4). The lack of lineations may be explained by erosion partially removing glacial deposits during the formation of the Baltic Sea, or by marine deposition obscuring such features. Glacial furrows have, however, been observed within the Gulf of Riga (Sviridov *et al.*, 1977).

Flow set 720B

Flow set 720B is clearly identifiable to the south of the Vidzeme Highland with well-defined lineations trending at 250° and lengths of up to 33 km (Figure 5.11). These lineations are far longer than those seen within flow set 720A, where the longest feature, at 9.6 km, is the Ķoņukalns megadrumlin of the Burtnieks drumlin field (Zelčs, 1995). Flow set 720B continues within image 185021 as flow set 521A.

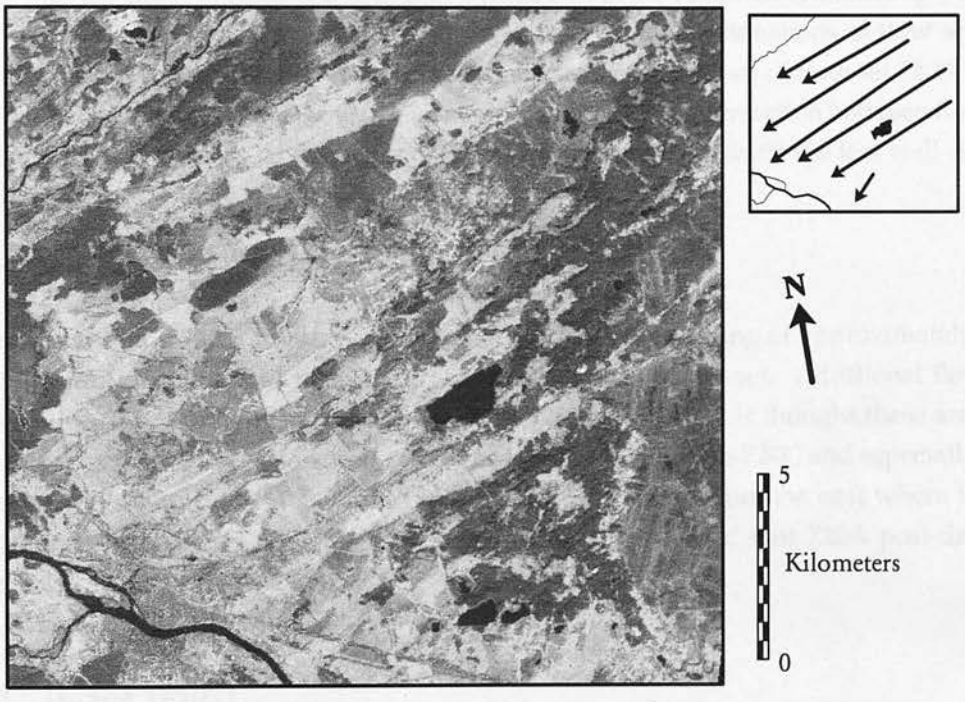

Figure 5.11: Flow set 720B as seen in Landsat TM image 187020. See box iii, Figure 5.8 for location

Flow set 720C

Lineations grouped as flow set 720C can be observed to the southeast of the hummocky arc described above. The flow set 720C lineations trend at 225° and are better defined than the 720A lineations seen in the same region.

Flow sets 720D, 720E, 720F and 720G

In addition to flow set 720A, flow sets 720D, 720E and 720F are also seen over the Vidzeme

Highland (Figure 5.8). Flow sets 720D, 720E and 720F are distinguishable from 720A by their different orientations, 720E and 720F have trends of 210° and 236° respectively, while 720D trends at 140°. Flow set 720D may be a continuation of 720G which lies to the southeast of the Vidzeme Highland at a trend of approximately 125°. The lineations forming these flow sets are poorly defined, generally less than 1 km long and few in number.

The temporal relationships between flow sets

Since flow sets 720D, 720E, 720F and 720G are spatially separate their temporal relationships are unclear. However, 720A is thought to be the most recent flow set because there are no later lineations superimposed upon it and it is much more extensive than the other flow sets. This may imply that it has overridden preceding flow sets and lineations associated with these flow sets were removed.

Flow sets 720D and 720G appear to be part of a single flow set. The similar trends of flow sets 720E and 720F may also suggest they once formed a single flow set. The agricultural land use makes interpretation difficult and prevents clarification of the temporal relationship between flow sets 720B and 720A. It is assumed, however, that the longer lineations of flow set 720B are indicative of a strong ice flow that preceded the smaller lineations of flow set 720A which would otherwise have been removed. Close examination of the intersection between flow sets 720A and 720C suggests that the better defined 720C lineations precede the less well-defined lineations of flow set 720A.

Overview of Image 187020

Lineations forming 720A are pervasive across the image at a bearing of approximately 170°. The Burtnieks drumlin field is considered to be part of this flow set. Additional flow sets are seen over the Vidzeme Highland at trends of 220° and 140°. It is thought these are older flow sets which have been preserved across the highland. Flow sets 720C and especially 720B comprise well-defined lineations. Both of these flow sets trend from the east where images 185020 and 185021 neighbour image 187020. It can be concluded that 720A post-dates all other flow sets within the image.

5.3.3 Image 187021

Image 187021 occupies the region immediately below image 187020 and contains the border between Latvia and Lithuania. Figure 5.12a shows the first-order interpretation of image 187021 from which six flow sets, labelled 721A-F, were identified (Figure 5.12b). Four areas, labelled 1-4, that contain particularly well-defined lineations are shown in Figure 5.12c.

Flow set 721A

The Latvian Lowland occupies the northeast quarter of the image. The topography is smooth

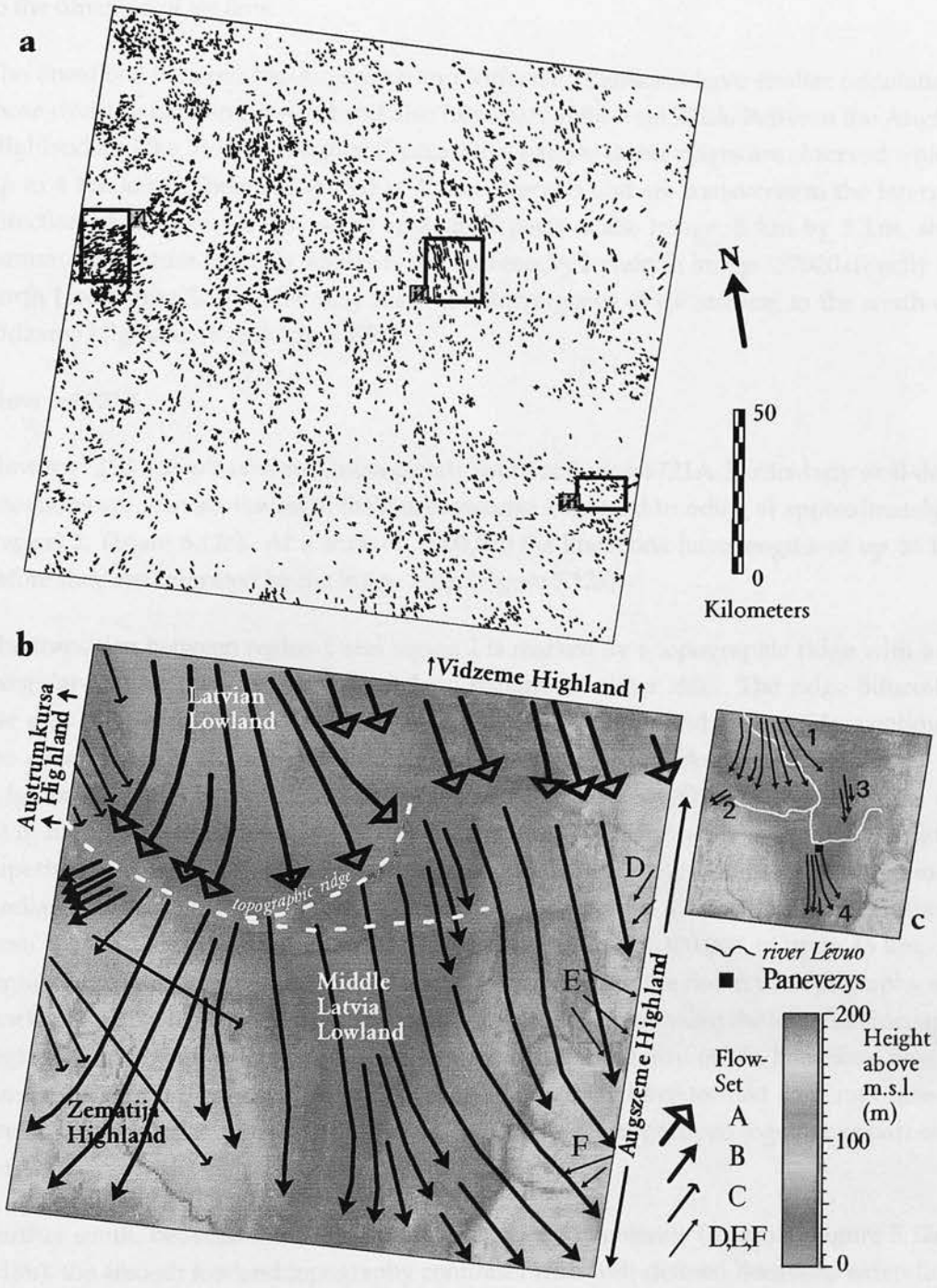

Figure 5.12: a: First order interpretation of Landsat TM Image 187021. Boxes delineate areas shown in further diagrams. b: Flow sets 721A-F superimposed on the present day topography. c: Regions with particularly well-defined lineations are numbered 1-4; the town of Panevezys and the river Lévuo are also shown.

and undulating with well-defined lineations (region 1, Figure 5.12c) radiating out from the Gulf of Riga which lies to the north of the image. Occasional, isolated features occur perpendicular to this trend which have been interpreted as glacial features formed transverse to the direction of ice flow.

The lineations between the Augšzeme and Vidzeme Highlands have similar orientations to those over the Latvian Lowland and also form part of flow set 721A. Between the Augšzeme Highland and the Vidzeme Highland, occasional parallel linear ridges are observed which are up to 4 km long. These are spaced at 400 m intervals and are transverse to the interpreted direction of ice flow. In the same area small parts of the image, 5 km by 5 km, show a hummocky texture which is similar to the hummocky terrain in image 187020 directly to the north (see Figure 5.10). This may mark the convergence of ice streams to the south of the Vidzeme Highland (Karukäpp, 1997).

Flow set 721B

Flow set 721B occupies the area immediately south of flow set 721A. Particularly well-defined lineations are seen southwest of the Austrumkursa Highland trending at approximately 250^o (region 2, Figure 5.12c). At a scale of 1:400,000 the lineations have lengths of up to 15 km before they are truncated by the image edge (Figure 5.12a).

The transition between region 1 and region 2 is marked by a topographic ridge with a more irregular texture than the smooth lowland regions on either side. The ridge bifurcates to the east (Figure 5.12b). A small ridge, less than 10 m high and 4 km wide, continues to the general rise in the topography between the Vidzeme and Augšzeme Highlands. This ridge is elongated perpendicular to the lineations of flow set 721A. A second ridge, up to 20 m high and 8 km wide, extends to the Augšzeme Highland with well-defined lineations superimposed upon it (region 3, Figures 5.12c and 5.13a). The lineations within region 3 are similar in size, shape and density to those of region 2 with a trend changing southwards from 175^o to 186^o. The lineations have lengths, at a scale of 1:400,000, of up to 45 km. As in region 2, the lineations within region 3 do not extend north of the rise in the topography which marks the extent of flow set 721A. The temporal relationship between the lineations occupying regions 2 and 3 is not known, but the morphological similarity of the lineations plus their similar location just south of the ridge, suggest they may have formed contemporaneously under similar glacial dynamic conditions. They are therefore grouped together as part of flow set 721B.

Further south, between the Zemaitija and Augšzeme Highlands (region 4, Figure 5.12c and 5.13b), the smooth lowland topography continues with well-defined lineations extending up to the highlands. The lineations occupying region 4 are not as densely packed, nor as well-defined as the lineations within regions 2 and 3. They can, however, be observed at the small scale (1:400,000) to extend for similar lengths, up to 45 km. The regions labelled 3 and 4 are separated spatially by the town of Panevezys and the river Lévuo (Figure 5.12c). While the lineations cannot be connected spatially, they have a similar trend and the city and/or river

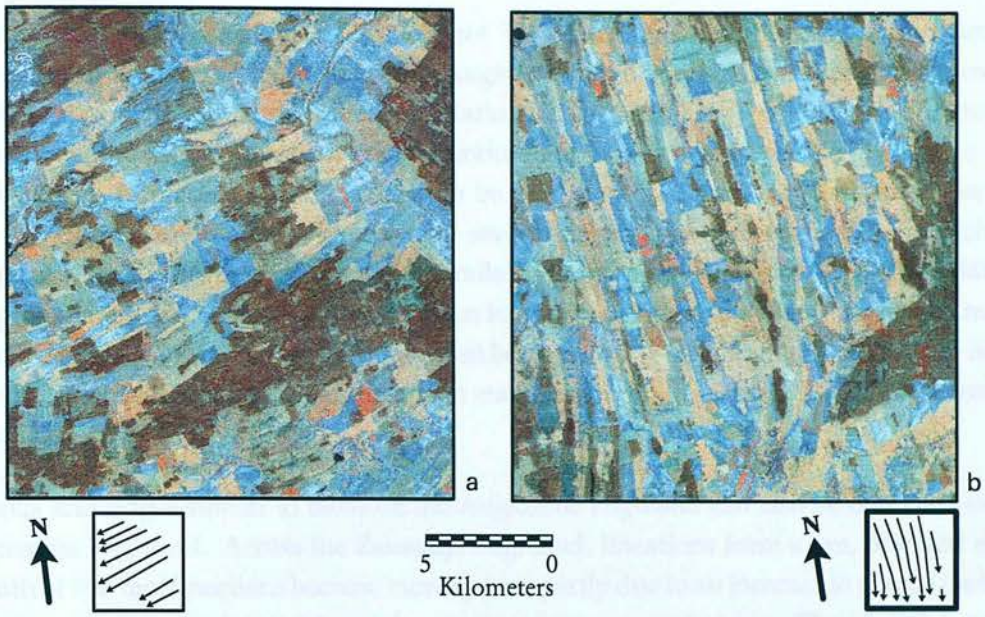

Figure 5.13: Landsat TM Image 187021, spectral bands 4,5,7 for red, green, blue respectively. Figures a and b display parts of regions 2 and 3 respectively. See boxes i and ii, Figure 5.12 for the location of the figures

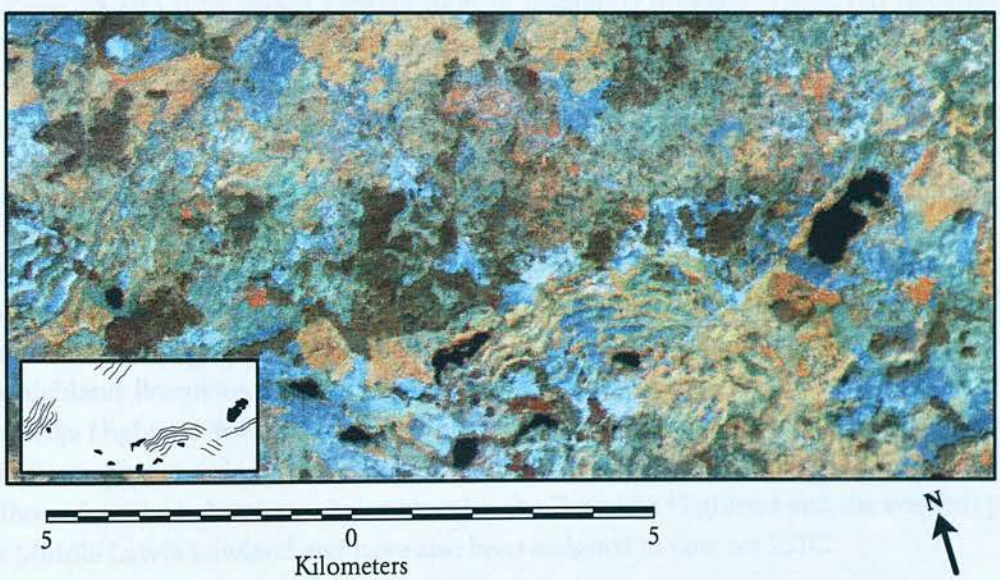

Figure 5.14: Transverse ridges as seen across the Augšzeme Highland, image 187021. The figure location is shown as box iii in Figure 5.12

may obscure, or have removed, lineations between the two flow sets. It appears reasonable to suggest that the two flows are part of a larger flow set, and therefore they have been assigned to flow set 721B.

On the eastern edge of the image flow set 721B lineations have formed perpendicular to the edge of Augšzeme Highland. The Augšzeme Highland is characterised by a complex distribution of features, described by Markots *et al.* (1995) as being kames and terminal moraines. Individual rounded, knolls hundreds of metres across, are clearly visible on the TM image. In places elongate ridges can be seen, up to 10 km long, that are either linear or, more often, undulating. Occasionally several ridges are observed parallel to each other (Figure 5.14). Ridges are also observed parallel to the elongation axes of lakes. These lakes are approximately 500 m wide and up to 4 km long. These ridges may be thrust block moraine and indicate ice movement towards a frozen bed or surging ice margins. Towards the north of the Augšzeme Highland, while the image maintains a rough texture, the knolls become less clear and rounded.

Knolls and ridges similar to those on the Augšzeme Highland can also be observed over the Zemaitija Highland. Across the Zemaitija Highland, lineations form a fan, oriented at 210°. South of this fan, lineations become more sparse, partly due to an increase in glacial transverse features and partly due to rivers dominating the geomorphology. The glacial transverse features include undulating linear features, occasionally in parallel. These features are similar to those observed on the Vidzeme Highland, though they are not as well formed.

Within the Zemaitija and Augšzeme Highlands the rugged topography with numerous depressions and hills makes identification of lineations difficult. Observed lineations are usually less than 1.5 km long and can not be detected at a scale smaller than 1:250,000. The majority of these lineations align with each other and with the well-defined lineations described above. It is therefore proposed that these lineations form part of flow set 721B.

Flow set 721C

Flow set 721C consists of lineations seen in the west of the image with bearings of approximately 160°. Along the edge of the Austrumkursa Highland there is a distinct change in the texture of the topography from smooth lowland, to the rough texture of the highland. Within the highland lineations have a trend of 160° and are less than 1.5 km in length. Over the Zemaitija Highland lineations have a similar length and trend. It is proposed that all these lineations are part of a single flow set, 721C. Further lineations, similar in appearance and trend to those described above are observed across the Zemaitija Highland and the western part of the Middle Latvia Lowland and have also been assigned to flow set 721C.

Flow sets 721D, 721E and 721F

Several small flow sets have been distinguished (721D, 721E and 721F) with trends which differ from 721A and 721B (Figure 5.12). These flow sets are limited in extent to the Augšzeme

Highland and contain lineations generally less than 1 km long.

Temporal relationship between the flow sets

The lineations of flow set 721B are longer and more densely packed than those of 721A. This may be explained by a spatial change in the ice dynamics and basal conditions. For example if the pore-water pressure increased and so reduced inter-granular friction, the underlying sediment would deform more easily. However, the orientation of the lineations between regions 3 (flow set 721B) and region 1 (flow set 721A) are not concordant which suggests they represent two flow sets. In addition, Raukas and Gaigalas (1993) place the margin of the North Lithuanian advance between regions 1 and 2, coincident with the topographic ridge. It is therefore proposed that flow set 721A represents lineations formed during the North Lithuanian Advance, and flow set 721B pre-dates 721A. Evidence of flow set 721B north of the topographic rise may have been eroded by ice forming flow set 721A and the topographic rise may reflect 721A ice marginal deposits.

Raukas and Gaigalas (1993) extend the North Lithuanian margin beyond the topographic rise towards the north, and round the Vidzeme Highland (Figure 2.7). The lineation pattern observed with the TM data does not support a north-south trend of the margin, since no lineations trend east-west, perpendicular to the proposed margin. Instead the ice margin associated with flow set 721A is thought to extend to the east (Figure 5.12).

No lineations concordant with 721C are observed between the Zemaitija and Austrumkursa Highlands in the lowland region occupied by flow set 721B. It therefore appears that 721B is superimposed upon flow set 721C. Since flow set 721A is thought to post-date flow set 721B it follows that 721A also post-dates flow set 721C. In addition flow set 721C lineations do not extend into the lowland regions occupied by flow set 721A lineations. This is what would be expected if flow set 721A followed 721C. The well-defined lineations of flow set 721A within the lowland regions suggest high velocities in these areas with correspondingly greater potential to erode flow set 721C. Across the highlands, flow set 721A is less well-defined and flow set 721C lineations are also seen.

Flow sets 721D, 721E and 721F are spatially separate from flow sets 721A and 721B, and their temporal relationships remain unknown. Since flow set 721B is more extensive, however, it is concluded that these smaller flow sets preceded 721B.

Overview of Image 187021

Flow sets 721C, 721D, 721E and 721F are the oldest flow sets within image 187021 and are confined mostly to the highland regions. A later phase formed flow set 721B which can be seen across the southern half of the image with particularly well-defined lineations in the lowland regions. To the north, flow set 721A is thought to represent the North Lithuanian Advance. No observable evidence was found to support the view that the margin of this phase extended north-south as suggested by Raukas and Gaigalas (1993) and instead it is

thought to have trended east-west.

5.3.4 Image 187022

Image 187022 covers parts of Lithuania, Poland, Belarus and Russia (Figure 5.1). Four flow sets (Figure 5.15b) that were derived from the first-order interpretation (Figure 5.15a) of the image are described below.

Flow set 722A

In the northeast corner of the image, over the Zemaitija Highland, elevations are greater than 100 m. Within this region a series of ridges up to 8 km long, evenly spaced at 400 m and extending over a region 6 km wide can be seen. The ridges are perpendicular to the lineations, are well-defined and taper towards the south. The lineations are oriented at 170° and are less than 1.5 km . Across the highland the image has a rough texture which becomes smoother towards the east where elevations are generally lower.

The terrain is much lower immediately south of the Zemaitija Highland across the Middle Lithuanian Lowland where the image has a smooth appearance and lineations are observed trending at 170°. Lineations are sparse in areas neighbouring the river Nemunas which crosses the Middle Lithuanian Lowland from east to west (Figure 5.15b). This is probably due to water erosion removing glacial geomorphology, or silt deposition obscuring features.

Where the elevation of the terrain decreases to less than 50 m, towards the west of the Middle Lithuanian Lowland (Figure 5.15b), the spectral characteristics of the image suggests the terrain is water-logged. Lineations tend to be less than 2 km long and those forming part of flow set 722A have an orientation of 175°. Trending west from this region to the edge of the image at an angle of approximately 50°, is an area approximately 6 km across with a rough texture (Figure 5.15a). This region has an elevation about 10 m above the surrounding terrain and is covered in small rounded areas, less than 100 m across and dark brown in colour. This hummocky region is elongated perpendicular to the interpreted direction of ice movement and could possibly be a glacial transverse feature.

The image texture changes from the generally smooth appearance of the Middle Lithuanian Lowland, to the rough texture of the Mazury Highland and Baltic Uplands which occupy the southern and eastern portions of the image respectively. Figure 5.16 shows this transition in image texture with change in elevation, from the Middle Lithuanian Lowland to the Mazury Highland. Lineations across both the Mazury Highland and Baltic Upland are generally less than 1 km long, and vary from well-defined to poorly delineated.

The Mazury Highland is characterised by many small knolls, tens of metres to hundreds of metres across which give the image a rough texture. The knolls are sometimes aligned in rows which can be traced for up to 6 km. Ridges also occur, both linear and undulating, single

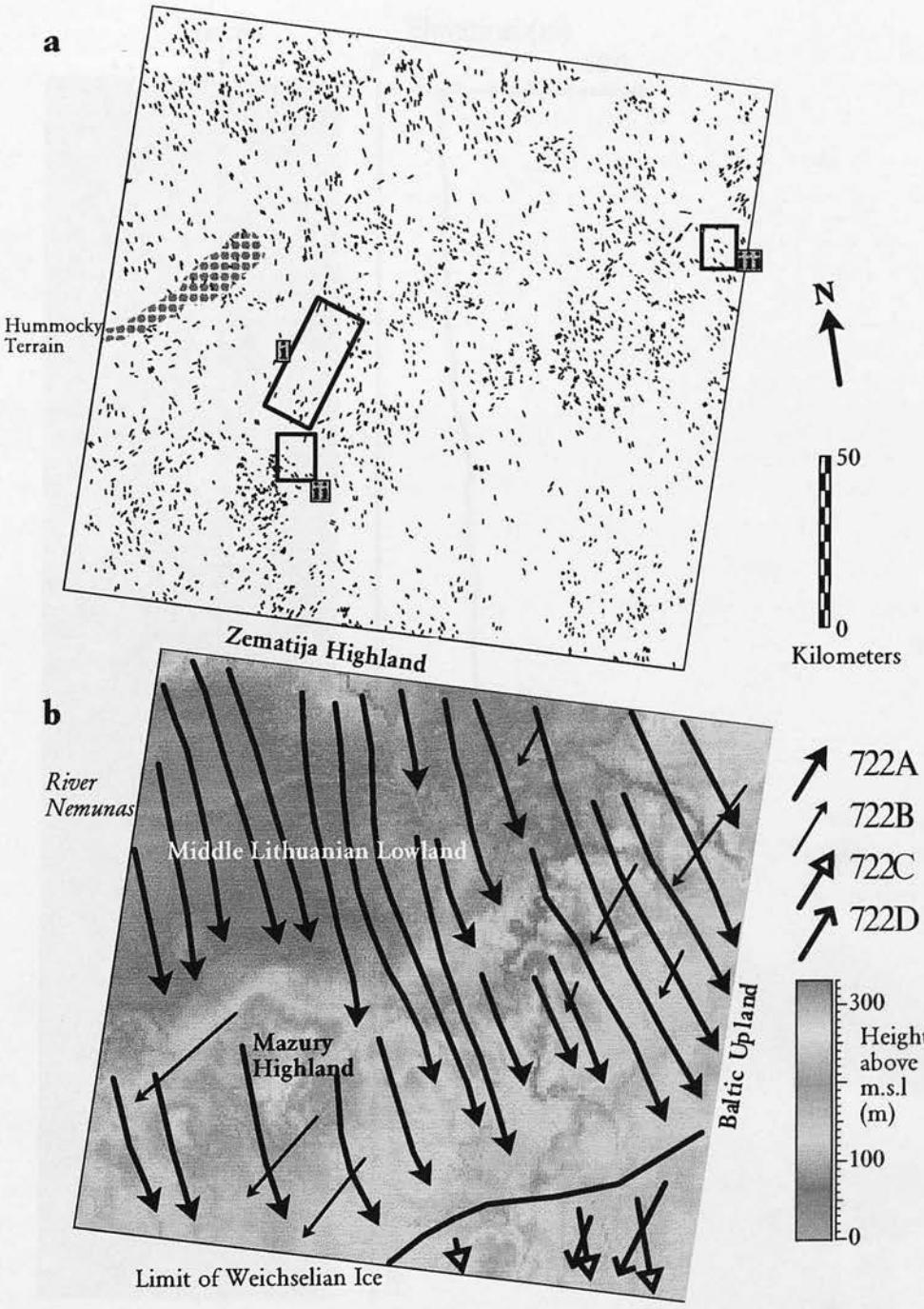

Figure 5.15: a: First order interpretation of Landsat TM Image 187022. Boxes delineate areas shown in further diagrams. b: Flow sets 722A-D superimposed upon the present day topography.

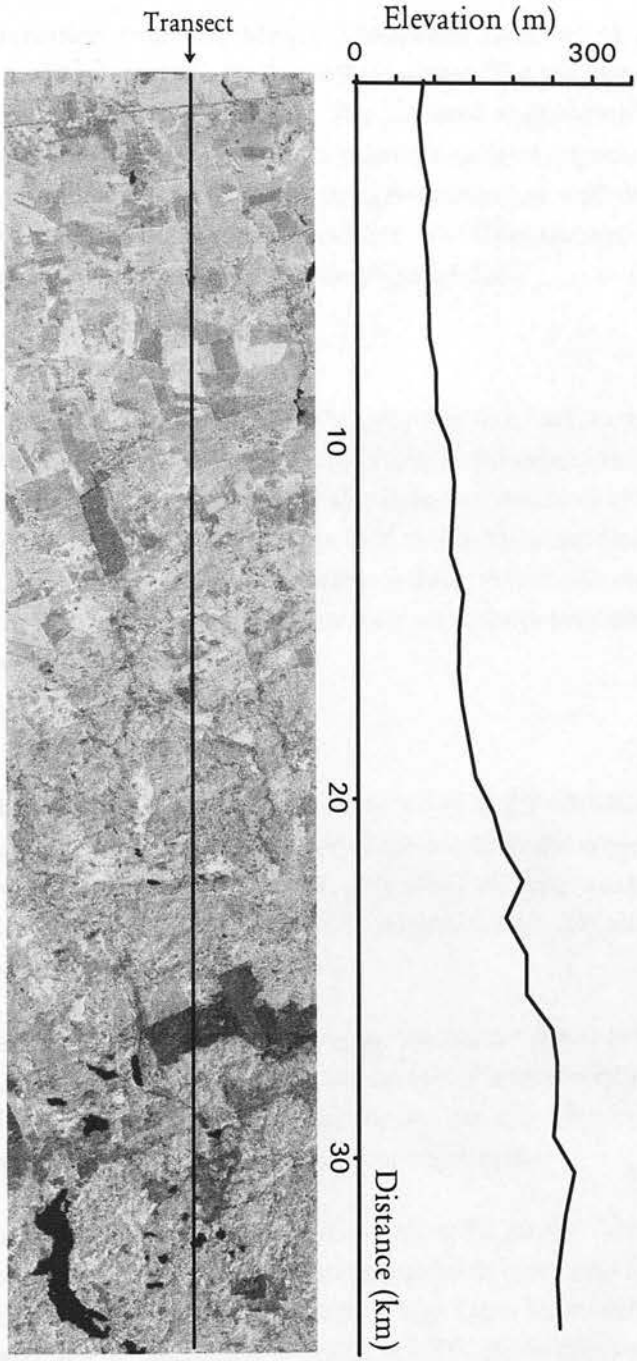

Figure 5.16: Transect from the Middle Lithuanian Lowland to the Mazury Highland. See box i, Figure 5.15, for the figure location

or more often identified in parallel groups (Figure 5.17a). These may have a glaciotectonic origin and represent thrust moraines. The highland also has a large number of lakes, usually elongated into channels between the ridges and undulating in no consistent direction. The lakes range in size with widths from tens of metres to 1.5 km, and lengths up to 7 km long.

The transition from the Middle Lithuanian Lowland to the Baltic Upland is broken by patches of highland alternating with lowland. The patches of highland have a rough texture and are speckled with knolls. The lowland regions are dominated by rivers and areas interpreted as being water-logged land or lacustrine deposits. The Baltic Upland also contains a large number of lakes, mostly elongated east-west, with dimensions generally half of those observed within the Mazury Highland. The lakes can aid the identification of lineations by emphasising the lineation direction (Figure 5.17b).

Flow set 722B

Other lineations, restricted to the Mazury Highland and Baltic Uplands are distinguished from the flow set 722A, oriented at $\approx 170^o$, because they are oriented at $210^o - 215^o$. These lineations are poorly defined and less extensive than the lineations of flow set 722A. They are therefore thought to pre-date the lineations of flow set 722A and have been grouped together as flow set 722B. Within the Highlands other isolated lineations, not concordant with either flow set 722A or 722B exist, which do not have a consistent orientation and are spatially too separated to form into flow sets.

Flow sets 722C and 722D

Viewing the image at a scale of approximately 1:2,000,000 (Figure 5.18) reveals a brown arc extending from the southern edge of the image to the eastern edge Regions shown as brown correspond to regions where the percentage of land used for agricultural purposes is low (Sweitzer *et al.*; c.f. image 188019, Section 5.3.1). These regions have a more mono-tone appearance and lineations are rare.

In this image, the margin marking the maximum extent of the Weichselian ice sheet (Raukas and Gaigalas, 1993) is thought to be coincident with this arc of low agricultural land cover. The Weichselian margin will be more fully discussed in Section 7.1. The lineations to the south of the margin are grouped here as separate flow sets.

Fields are prominent towards the south of the image. The spectral intensity reflected from this region is higher than from the agricultural regions to the north of the arc. Lineations are again observable, usually about 1 km long. These have been grouped into two flow sets, 722C oriented at 170^o and 722D trending at 220^o. If the proposed Weichselian margin is correct, these flow sets are pre-Weichselian, are likely to Saalian and probably pre-date flow sets 722A and 722B.

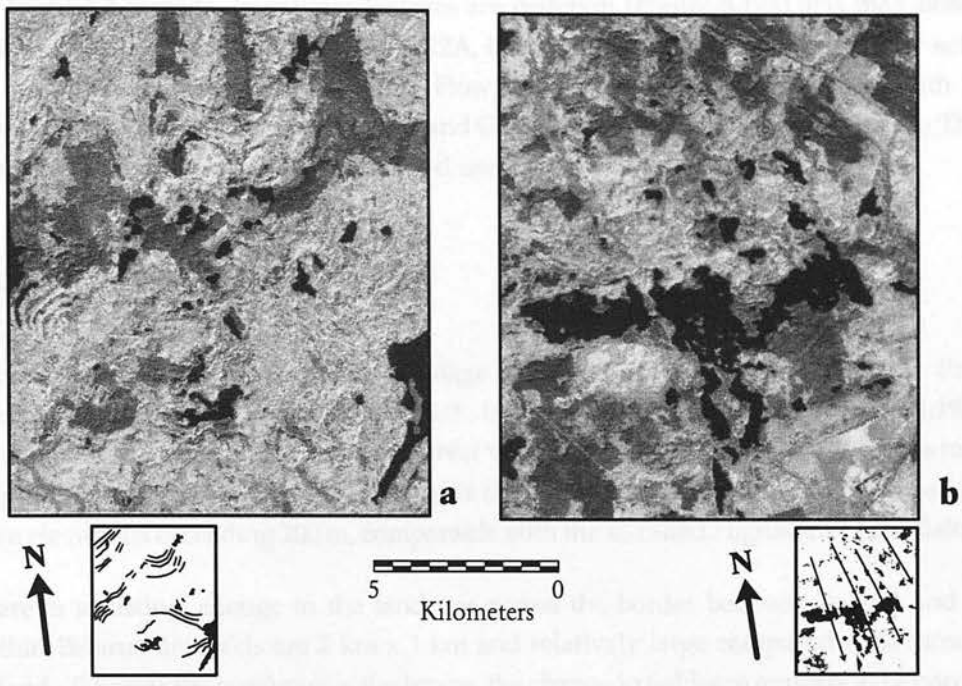

Figure 5.17: a: Ridges as seen over the Mazury Highland. b: Lineations emphasised by lake margins. See boxes i and ii respectively, Figure 5.15 for the figure locations.

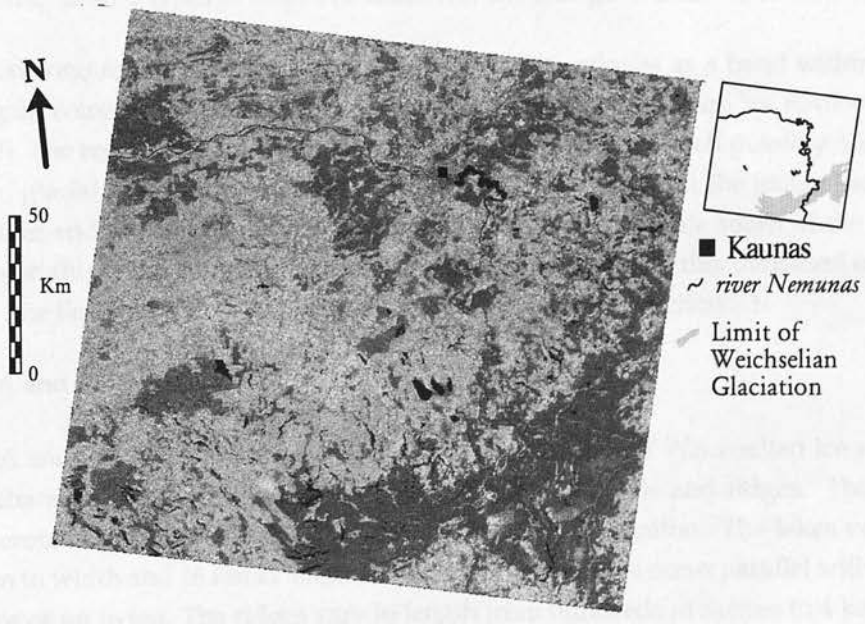

Figure 5.18: Landsat TM Image 187022, false colour composite using the TM bands 4, 5 and 7 for Red, Green and Blue respectively.

Overview of Image 187022

In general, lineations are less well-defined in image 187022 than in previous images. Across the highland regions, transverse features are common (Figure 5.17a) and may obscure lineations. The more extensive flow set 722A, is considered to post-date other flow sets which are restricted to the highland regions. Flow sets 722C and 722D are further south than the proposed Weichselian margin (Raukas and Gaigalas, 1993) which is shown on the TM image as a brown arc with low agricultural land use.

5.3.5 Image 187023

Image 187023 is the most southern image acquired. Figure 5.19a shows the first order interpretation for this image from which flow sets were interpreted (Figure 5.19b). The elevation of the topography, except for river valleys, is generally over 150 m with a maximum height in the northeast of 240 m. Towards the south the Podlasie and Mazowsze Lowlands have elevations exceeding 200 m, comparable with the so called Highlands in the Baltic States.

There is a distinct change in the land use across the border between Poland and Belarus. Within Belarus the fields are 2 km x 1 km and relatively large compared with those seen in Poland. Towards the northeast of the image, the change in field size appears to be correlated to the topography, the larger fields of Belarus being at a lower elevation. In the southeast corner of the image, however, there does not appear to be a significant change in the topography accompanying the change in land use. The colour of the fields across both countries are similar, suggesting similar types of crop. The reason for the change in land use is unknown.

The brown monotone region described from image 187022, continues as a band within this image, and again coincides with the limit of the Weichselian ice proposed by Raukas and Gaigalas (1993). The region contains forested land and several rivers, which possibly obscure or have eroded glacial geomorphic features. North of the proposed limit the image has low reflectance values and an irregular and rough texture with ridges , while south of the limit image appears brighter with a regular texture of stripes. In a few places this transition can be seen directly . The limit of Weichselian ice is discussed more fully in Section 7.1.

Flow sets 723A and 723B

Flow sets 723A and 723B occur to the north of the proposed limit of Weichselian ice where the image is characterised by a rough texture with numerous knolls and ridges. The area contains numerous lakes, often elongated with no consistent orientation. The lakes vary in size up to 5 km in width and 16 km in length. Ridges within this area occur parallel with each other in groups of up to ten. The ridges vary in length from hundreds of metres to 4 km and are aligedn perpendicular to the interpreted direction of ice flow. Lineations are indistinct in character within the region and those seen are often less than 1.5 km long. Two flow sets have been identified, the more extensive flow set 723A is oriented at 170°, while the smaller flow

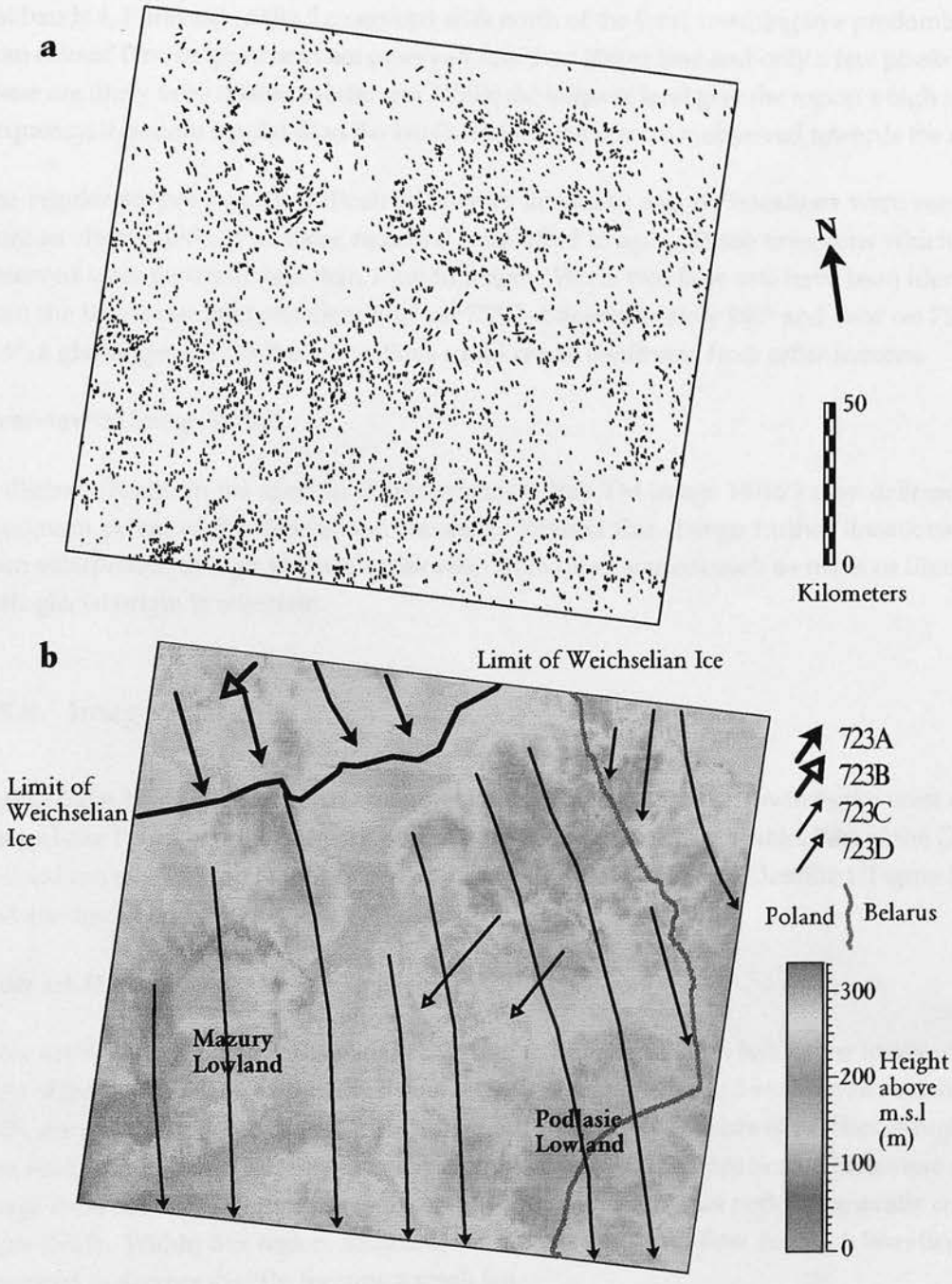

Figure 5.19: a: First order interpretation of Landsat TM Image 187023. Boxes delineate areas shown in further diagrams. b: Flow sets 723A-D superimposed upon the present day topography.

set 723B trends at 228°.

Flow sets 723C and 723D

South of the proposed limit of Weichselian ice, higher reflectance values are recorded in the TM bands 4, 7 and especially 5 compared with north of the limit, resulting in a predominately cyan colour. Fine strips of land are observed, less than 500 m long and only a few pixels wide. These are likely to be related to land use. While the strips of land give the region a high spatial frequency, it is more regular than the knolls and irregular texture observed towards the north.

The regular stripes make it difficult to identify lineations and no lineations were seen that were as clearly defined as those recorded from other images. Those lineations which were observed were generally less than 1 km in length. While two flow sets have been identified from the first-order interpretation, flow set 723C at approximately 180° and flow set 723D at 224°, a glacial genesis for these lineations could not be confirmed from other sources.

Overview of Image 187023

A distinct change in the spectral characteristics within TM image 187023 may delineate the maximum extent of the Weichselian ice sheet. Beyond this change further lineations have been interpreted, though without verification from other sources such as maps or literature, their glacial origin is uncertain.

5.3.6 Image 185019

Figure 5.20a shows the first order interpretation for image 185519. Towards the west of the image Lake Peipsi and the northern part of Lake Pihkva are clearly visible. Part of the Gulf of Finland can also be seen in the north of the image. Six flow sets were identified (Figure 5.20b) and are described below.

Flow set 519A

Flow set 519A trends at approximately 175° and covers the western half of the image. To the west of the Ižora Plateau well-defined flow set 519A lineations, up to 3 km long and oriented at 175°, are observed. South of the Ižora Plateau the topography consists of patches of highland and lowland which vary in elevation between 40 m and 100 m above m.s.l. The texture of the image does not vary significantly with elevation, though the higher regions generally contain more fields. Within this region, southwest of the Ižora Plateau, flow set 519A lineations are observed to diverge slightly, forming a small fan.

To the west of Lake Samro (viewing the image at a scale of 1:400,000) flow set 519A lineations can be identified which are up to 40 km in length and are oriented at approximately 165°. At smaller scales, the lineations are not so easily observable. The lineations do not appear, however, to align with any man-made or geological features and it is proposed that they are

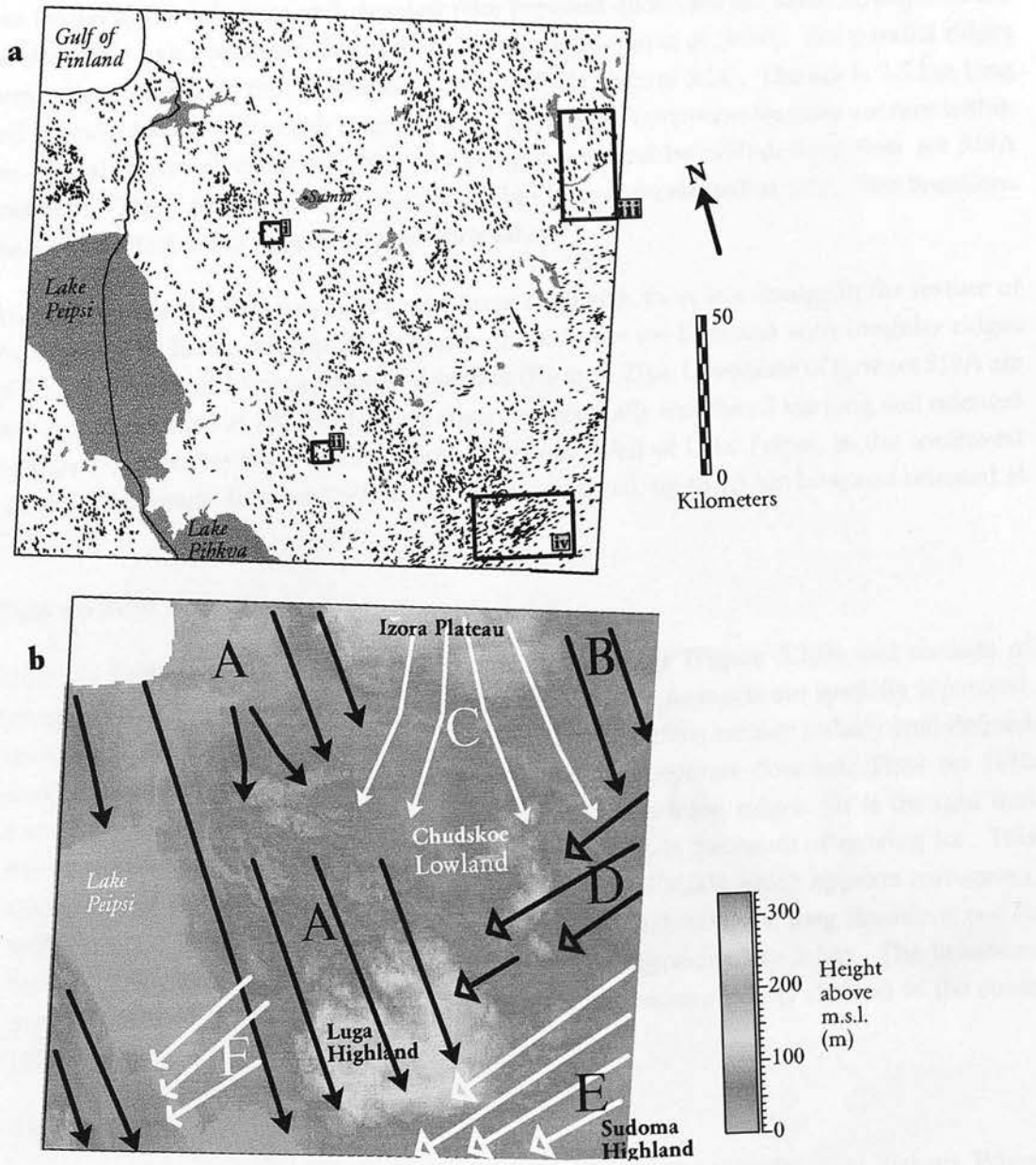

Figure 5.20: a: First order interpretation of Landsat TM Image 185019. Boxes delineate areas shown in further diagrams. b: Flow sets 519A-F superimposed upon the present day topography.

glacial in origin.

Lake Samro and a series of parallel ridges to the south of the Lake may represent glacial thrust blocks and source depression like those observed throughout the prairie region of Canada and the United States where lineations are commonly associated with the ice-thrust topography (Bluemle and Clayton, 1984). The glacial thrust terrain may indicate an area where the glacier was frozen to the substrate and elevated pore pressure decreased the shear strength of the substrate to a value less than that applied by the ice (Moran *et al.*, 1980). The parallel ridges form an arc, similar to that observed in image 187021 (Figure 5.14). The arc is 2.5 km long and concave towards the south (Figure 5.21a). In general, transverse features are rare within the central region of the image, the area being dominated by well-defined flow set 519A lineations. These lineations are generally 2-3 km long and oriented at 175°. The lineations are often clearest in the regions neighbouring lakes.

Towards the south of the image, over the Luga Highland, there is a change in the texture of the image. The image appears more coarse-grained over the highland with irregular ridges and bumps giving the image a rumpled surface (Figure 5.21b). Lineations of flow set 519A are still visible, oriented at 170°. Ridges are observed, generally less than 3 km long and oriented perpendicular to the interpreted ice flow direction. West of Lake Peipsi, in the southwest corner of the image, flow set 519A lineations are observed, up to 1.5 km long and oriented at 170°.

Flow set 519B

Flow set 519B occupies the northeast corner of the image (Figure 5.20b) and consists of lineations with approximately the same trend as 519A. The flow sets are spatially separated, however, by flow set 519C. In addition, flow set 519B lineations are particularly well-defined compared with those of 519A, and is thus treated as a separate flow set. Flow set 519B comprises basin-like regions and lineations on the intervening ridges. It is thought that the elongation of these features in one direction, at 182°, is the result of moving ice. This elongation of features produces a texture at a scale of 1:300,000 which appears corrugated, with lineation lengths of up to 45 km. At a scale of 1:100,000 these long lineations can be broken down into smaller lineations with lengths of approximately 2 km. The lineations are well-defined to the north of the river Oredež, but become poorly defined to the south (Figure 5.21c).

Flow set 519C

To the west of flow set 519B the elevation of the land increases over the Ižora Plateau. Where elevations exceed 100 m and fields form the majority of the image. The texture of the image remains corrugated at a spacing of several hundred metres. Individual lineations, up to 3 km in length, are indistinct in form.

Flow set 519C forms a diverging fan from the Ižora Plateau. Lineations from the fan can be

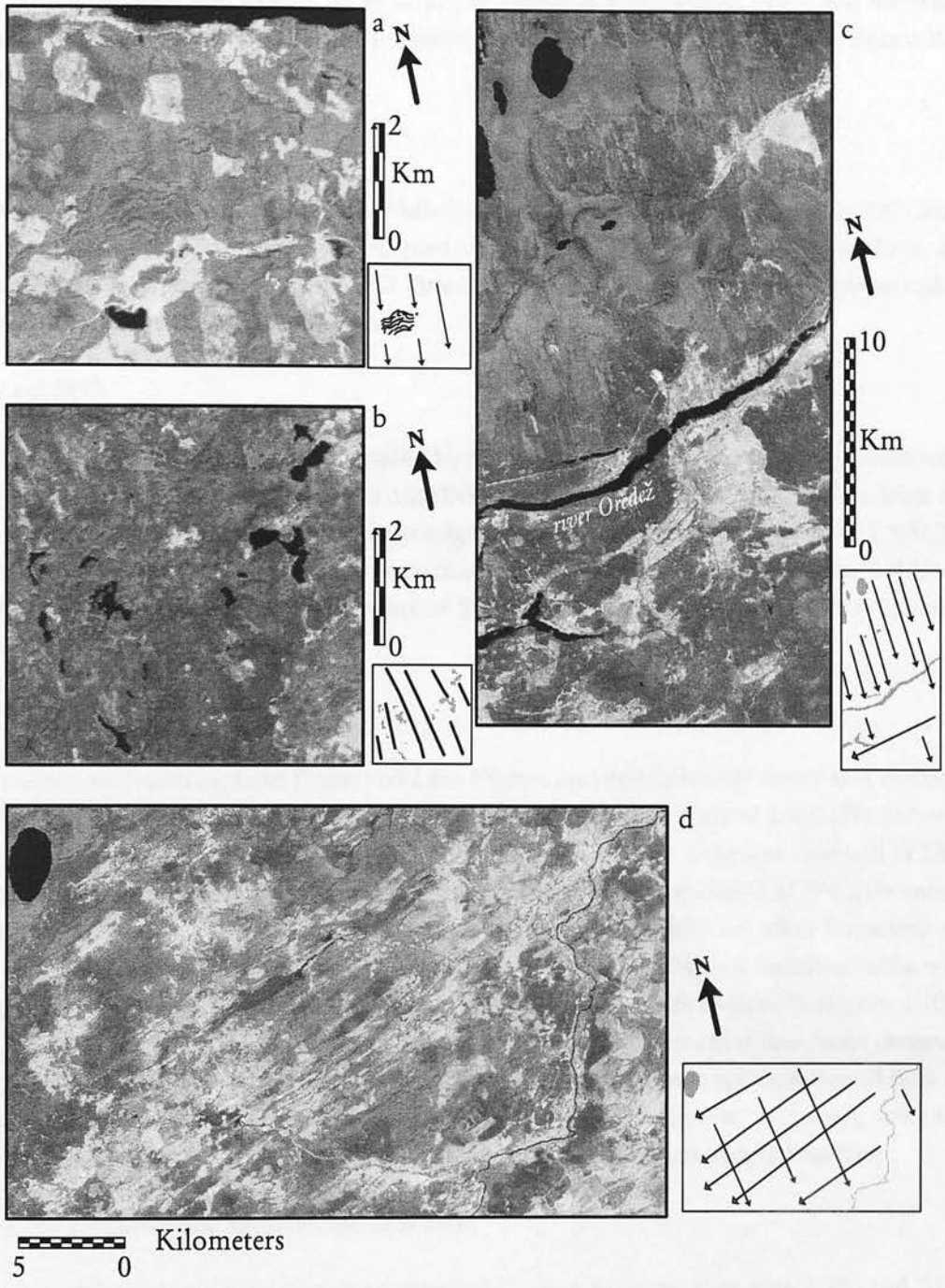

Figure 5.21: a: Flow set 519A and ridges as seen immediately south of Lake Samro b: Flow set 519A and the coarse texture seen across the Luga Highland c: Flow sets 519B and 519D as seen surrounding the River Oredež. d: Flow sets 519D and 519E as seen south of the Luga Highland. Figure a, b, c and d locations are shown as boxes i, ii, iii and iv respectively within Figure 5.20

traced as far south as Lake Samro which lies within the region between flow sets 519C and 519A. Flow set 519C lineations, to the east of Lake Samro, are less distinct than those of flow set 519A to the west and extend up to 12 km in length at a bearing of 215°. The lineations appear to change their trend towards the south, until immediately south of Lake Samro they have a trend of 205°.

Flow set 519D

Flow set 519D lies to the north of 519E. While both flow sets 519D and 519E trend at 250°, there is a clear distinction between the well formed, densely packed lineations of flow set 519E and the indistinct lineations of flow set 519D. Towards the centre of the image the lineations peter out as the elevation of the ground rises.

Flow set 519E

The south corner of the image is dominated by flow set 519E (Figure 5.21d) formed from well-defined lineations which,, at a scale of 1:250000, appear to extend for up to 35 km from the eastern edge of the image to the southern edge at a bearing of 250°. At a scale of 1:100,000, individual lineations can be observed to be made up of aligned, smaller lineations, 3-4 km in length. Compared to the irregular texture of the Luga Highland the texture of the image in this region is relatively smooth.

Flow set 519F

The regions surrounding Lake Peipsi and Lake Pihkva are predominately forest and wetland, except for the northeastern shore where fields are observed. At a scale of 1:400,000, between Lake Peipsi and Lake Pihkva, there appear to be lineations, 20 km long and oriented at 250°. These lineations form flow set 519F and have been interpreted as consisting of elongate basins, containing little or no water. Unlike the lineations of flow set 519B, no other lineations are observed between the basins or aligned with them. The lineations do not continue to the west of the lakes, nor further than 20 km to the east. No reference is made to these lineations within the published literature and they do not appear to be similar to any other lineations observed within the study region. It could be speculated that the features are a continuation of flow set 519D, or alternatively, they may be part of a huge thrust block moraine. However, since it is uncertain as to whether flow set 519F has a glacial origin, it is not considered further.

Temporal relationships between the flow sets

The only observed superimposition of lineations, occur between flow sets 519E and 519A where flow set 519A is seen to be superimposed upon 519E in the region south of the Luga Highland. Further temporal relationships can only be inferred from the spatial relationship of the flow sets.

Three scenarios can be proposed. Scenario 1 (Table 5.1) places flow set 519C after 519A, an order suggested by the spatial arrangement of the flow sets. The sharp transition in the

strength of flow set 519B lineations across the River Oredež suggests that 519D post-dates 519B. Scenario 1, however, separates temporally flow sets 519D and 519E.

Since flow set 519D neighbours flow set 519E and they have a similar trend, it is proposed that they belong to a single flow event. The difference in appearance between the two flow sets may be due to the local topography. Where the ice was impeded by the greater elevations of the Chudskoe Lowland, it formed the poorly defined lineations of flow set 519D. The well-defined lineations of flow set 519E were formed where the ice was unimpeded and confined to the lowland region between the Sudoma and Luga Highlands. Scenario 2 (Table 5.1) places flow sets 519D and 519E together, and maintains the order of flow set 519C after 519A, and flow set 519D after 519B.

Scenario	Sequence Order From Oldest to Youngest
1	519E , 519A, (519C-519B), 519D
2	519B, 519D+519E, 519A, 519C
3	(519D-519E), 519A, (519C-519B)

Table 5.1: Possible scenarios of the temporal sequences of the flow sets within image 185019. Commas indicate flow sets which can be separated temporally. Brackets group flow sets within a single time period, but do not imply flow sets are contemporaneous. Addition signs group separate flow sets as a single event

It could be argued that since flow sets 519C and 519B neighbour each other and have trends which are not dis-similar, they also form a single flow set. The difference in appearance between flow sets 519C and 519B may be due to the ice flowing over highland and lowland regions respectively. Flow sets 519C and 519B can not be grouped together if flow sets 519D and 519E are grouped together as one flow set and flow set 519D is thought to truncate 519B. If it is assumed that both 519B and 519C peter out towards the south, however, and flow set 519E therefore does not truncate 519B, Scenario 3 is also possible (Table 5.1).

It would appear more reasonable to place neighbouring lineations, with similar trends, close together temporally. Therefore, it is thought that Scenario 3 is the most likely to represent the correct temporal ordering of flow sets

Overview of Image 185019

Image 185019 contains two groups of lineations. One group trends at approximately 170° and has been divided into the flow sets 519A, 519B and 519C. The other group trends at approximately 250° and consists of two flow sets (519D and 519E) which are considered to be part of a larger flow-event.

It is argued that flow set 519A followed flow sets 519D and 519E, and the spatial arrangement of lineations between flow sets 519C and 519A suggest 519C followed 519A. It is unclear where flow set 519B fits into the temporal sequence. It may be the youngest flow set along with flow set 519C, or alternatively it may be the oldest. It is thought more reasonable to assume that

the former is correct.

5.3.7 Image 185020

Image 185020 is located immediately south of image 185019 and overlaps to the west with images 187020 and 187021. At a scale of 1:2,000,000 the image comprises areas that are predominately red in colour and other areas that show a mixture of blues and greens. Comparison with land cover maps show these areas correspond to regions of forest and agriculture respectively (Sweitzer *et al.*, 1996). Along with Lake Pihkva to the northeast, the Pskovsko Lowland occupies the central region of the image. Portions of several different highlands can be seen at the image margins. The Haanja Highland is the only highland to be fully within the image (Figure 5.22c). Figure 5.22a shows the lineations of the first-order interpretation of the image. From this interpretation three flow sets were identified as shown in Figure 5.22 b, c and d.

Flow set 520A

Between the Otepää and Haanja Highlands well-defined flow set 520A lineations and elongated lakes occupy a region 20 km wide and 5 km long. These lineations and intervening lakes are up to 600 m wide and 6 km long. The trend of the lineations changes from 200^o in the north to 250^o towards the south. Over the Otepää and Haanja Highlands further lineations of flow set 520A can be seen. These lineations are less distinct than the lineations in the neighbouring lowland regions due to the rugged, irregular texture of the highlands. In addition the lineations are obscured by other flow sets discussed later.

The eastern margin of the Haanja Highland shows well-defined lineations, up to 21 km in length and clearly visible at scales greater than 1:50,000. The lineations extend for 65 km in an arc curving towards the south round the highland. The lineations are 100 m above m.s.l and instead of the irregular texture usually seen at such elevations, the image texture is smooth. The lineations can not be traced to the north of the highland, and their temporal relationship with the lineations between the Haanja and Otepää Highlands is unclear. The similar appearance of the lineations, their similar trends and their similar location at the margins of highlands suggest, however, that they all formed under similar ice dynamic conditions and are part of a single flow set, flow set 520A.

Southeast of the Haanja Highland, flow set 520A can be traced within a red region which curves to the southwest corner of the image (Figure 5.22c). The red region is interpreted as being forested wet-land, with fields bordering it on either side. Within the red-region lineations are generally poorly represented compared with the well-defined lineations on the eastern margin of the Haanja Highland. However, towards the southwest corner the lineations become better defined.

Well-defined lineations, similar in appearance to those described above, are also seen within

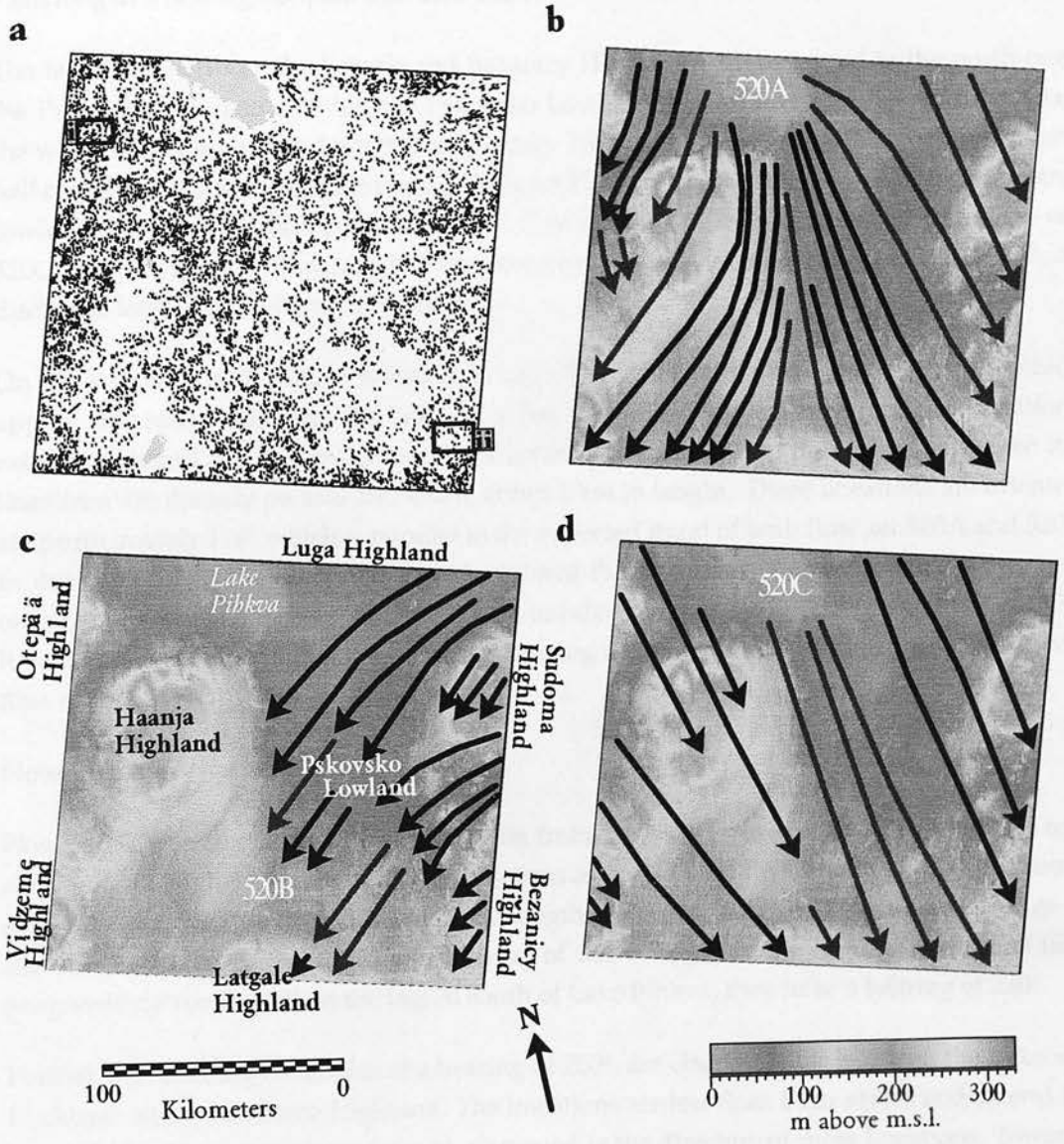

Figure 5.22: a: First order interpretation of Landsat TM Image 185020. Boxes delineate areas shown in further diagrams. b: Flow set 520A. c: Flow set 520B. d: Flow set 520C. b, c and d are superimposed upon the present day topography.

the lowland region between the Latgale and Bežanicy Highlands. The trend of the lineations changes gradually from 180° in the north to 140° in the south. At a scale of 1:300,000 the lineations are observed to be up to 35 km long. At the larger scale of 1:100,000, these lineations are seen to be made up of smaller lineations trending in the same direction with lengths of up to 8 km. The lineations can be traced over the higher ground towards the west, the trend of ice movement being emphasised by elongated lakes which are less than 1 km wide and up to 5 km long at a bearing between 140° and 165°.

The lineations between the Latgale and Bežanicy Highlands can be traced to the north over the Pskovsko Lowland. Within the Pskovsko Lowland the lineations are less distinct than the well-defined lineations described previously. The trend of flow set 520A across the eastern half of the image is similar to the trend of flow set 520C (discussed later) and within the central lowland and the highlands to the southeast, flow set 520A cannot be separated from flow set 520C. It is possible that flow set 520A has been eroded by ice forming flow set 520C which, as discussed later, is thought to post-date it.

On the southern and eastern margins of Lake Pihkva lineations are seen at trends which appear to radiate out from the lake in a fan. It would seem likely that the lineations extending from Lake Pihkva have formed contemporaneously. To the south of the lake the lineations are densely packed and small, about 1 km in length. These lineations are oriented at approximately 178° which is parallel to the expected trend of both flow set 520A and 520C in this region. To the southeast of Lake Pihkva the lineations, similar in appearance and oriented at a bearing of 125°, appear to be truncated by flow set 520C which trends at 175°. It is therefore concluded that the lineations fanning out from Lake Pihkva are associated with flow set 520A.

Flow set 520B

Flow set 520B is characterised by ice flowing from the east (Figure 5.22d). Between the Luga and Sudoma Highlands flow set 520B lineations are particularly well-defined. The lineations are a few hundred metres wide and have lengths of up to 10 km. At the northern edge of the image, the lineations trend at a bearing of 250°. Towards the east the lineations turn progressively south until, in the region south of Lake Pihkva, they have a bearing of 230°.

Further well-defined lineations, at a bearing of 250°, are clearly visible between the Bežanicy Highland and the Sudoma Highland. The lineations are less than 1 km across and extend for up to 15 km. Many lakes have formed, elongated in the direction of these lineations. Towards the south the lineations appear to follow the edge of the Bežanicy Highland, before apparently being truncated by flow set 520A or 520C (these two flow sets being parallel in this area). The temporal relationship between the lineations are discussed later.

Flow set 520B extends up to the region where the well-defined lineations assigned to flow set 520A, curve round the Haanja Highland. The lineations assigned to flow set 520B are distinguished from those of flow set 520A by the large angle between their trends

(approximately 60°). The well-defined lineations of 520B also have smaller widths and are less pervasive than the lineations assigned to flow set 520A.

Flow set 520B is present over the Sudoma and Bežanicy Highlands. The Bežanicy Highland occupies the southern and eastern edges of the image. The elevation of the highland increases from 110 m in the south to 240 m in the north. Across the 35 km of the highland to the southeastern corner the orientation of flow set 520B alters gradually from 215° to 240°. Towards the north, where the elevation of the land is greatest, these lineations are very strongly delineated by lakes which are scoured out in the direction of ice movement.

Lineations at a bearing of 230° are observed over the eastern half of the Latgale Highland. While these lineations are spatially separate from the lineations over the Bežanicy Highland, the similarity in their direction and strength suggests that they were formed at the same time. Both sets of lineations are therefore assigned to flow set 520B.

Flow set 520C

Flow set 520C is pervasive across both highlands and lowlands trending between 165° and 175° (Figure 5.22e). Over the Sudoma Highland the flow set 520C lineations appear to fan out from approximately 180° in the west to 165° in the east. Flow set 520C lineations are also found over the northern part of the Latgale Highland and the Vidzeme Highland at a bearing of 175°. The Vidzeme Highland is characterised by an irregular surface of lakes, ridges and knolls which obscure the lineations. Flow set 520C lineations tend to be small, less than 1.5 km in length and less distinct than the well-defined lineations associated with flow sets 520A and 520B.

Additional lineations

Further isolated lineations are recorded which do not co-align with flow sets 520A, 520B or 520C. The majority of these lineations are seen over the highland regions where their restricted spatial distribution and differing orientations prevents them from being assigned to any flow set. For example, indistinct lineations are preserved across the Haanja Highland with orientations varying between 130° and 230°. Most lineations can be best distinguished at a scale of approximately 1:300,000. While the trend of some lineations are parallel with identified flow sets described above, lineations at differing orientations suggest that traces of other, possibly older, ice flows have been preserved across the highland. Similarly, poorly defined lineations which do not align with flow sets 520A, 520B or 520C are seen over the Vidzeme Highland.

There is a sharp transition between the Haanja Highland and the surrounding lowland, the margin to the northeast being particularly abrupt. Over the highland, the texture of the image becomes more uneven in shape, with a surface of ridges and knolls forms a coarse image texture while the lowland is generally smooth. Anomalous lineations within the lowland regions of the image are scarce, only occurring in an area approximately 2 km southwest

of Lake Pihkva within the Pskovsko Lowland. Two elongate lakes appear to have had their shapes altered by flow set 520B, so that their shorelines are corrugated. The lakes are elongated at 126°. This trend, if it is a flow direction, does not appear to be reflected in any of the surrounding lineations.

Temporal relationship between the flow sets

Flow set 520C lineations are observed superimposed upon 520A to the northwest of Lake Pihkva. The long lineations of flow set 520A are clearest at a scale of 1:300,000. At a larger scale (1:100,000) the long lineations are less distinct and more amorphous in character while the smaller lineations of flow set 520C (up to 1.5 km long) can be seen with a bearing varying between 150° and 170°. In places, these lineations are superimposed upon the longer lineations of flow set 520A, or appear to have altered the edges of the longer lineations so that they undulate (Figure 5.23). Flow set 520C can also be seen to be superimposed upon 520A over the Otepää Highland.

Further flow set 520C lineations are observed superimposed on flow set 520A in the region south of the Haanja Highland, between the Otepää and Haanja Highlands and to the southeast of Lake Pihkva. South of the Haanja Highland the lineations of flow set 520A become less distinct. The ground has a slightly higher elevation and as a consequence is drier. The texture of the image becomes more coarse with a semi-blocky character, and is interpreted as agricultural land. Over this region lineations of flow set 520C are observed at a bearing of 180°, superimposed upon the lineations of flow set 520A. To the southeast of Lake Pihkva lineations assigned above to flow set 520A are truncated by flow set 520C at a bearing of 175°. The temporal relationship in this area can only be inferred since no cross-cutting lineations can be seen.

The available evidence suggests that flow set 520C post-dates 520A and is superimposed upon 520B in the lowland regions along the eastern edge of the image and also over the Bežanicy Highland in the southeastern corner. Between the Sudoma and Bežanicy Highlands, and westwards across the Pskovsko Lowland, the lineations of flow set 520B are also superimposed by lineations of flow set 520C

The temporal relationship between flow sets 520B and 520A is more difficult to ascertain. No lineations of flow set 520B are seen further west than the well-defined flow set 520A lineations by the Haanja Highland, and it is possible that flow set 520A truncated flow set 520B. In addition, no flow set 520B lineations are observed within the lowland between the Latgale and Bežanicy Highlands, suggesting that flow set 520A obliterated flow set 520B in that region.

However, while the spatial arrangement of the flow sets may suggest that the flow set 520A post dates flow set 520B, the arrangement of individual lineations suggest otherwise. Within the southwestern portion of the Bežanicy Highland displayed within the image, lineations from three local flow sets are seen. One flow set appears to come from the northeast and veer southeastwards across the highland. This flow set appears to be a continuation of the

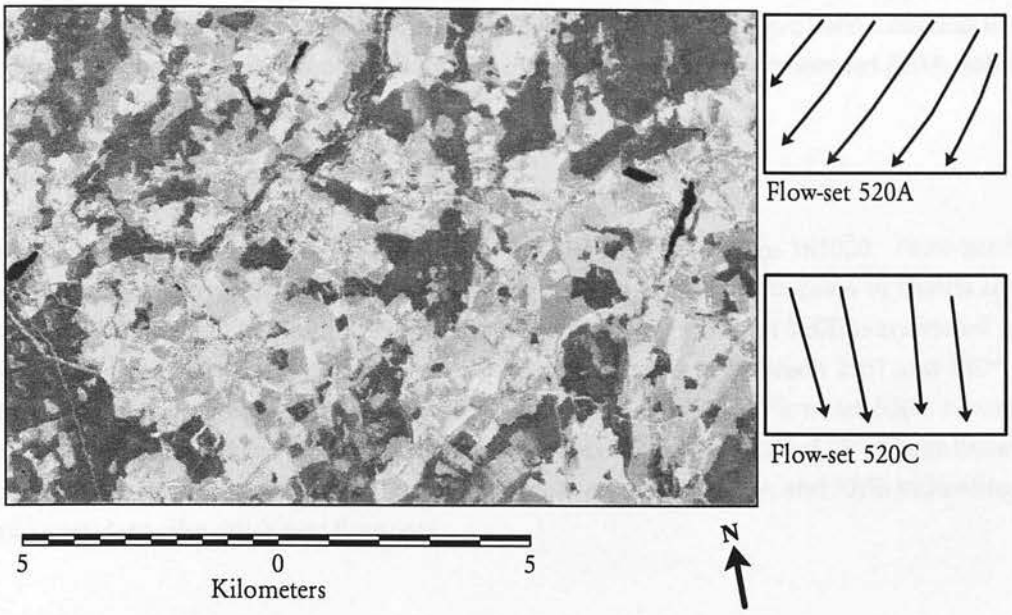

Figure 5.23: Cross-lineations in the north of image 185020. Box i within Figure 5.22 shows the figure location

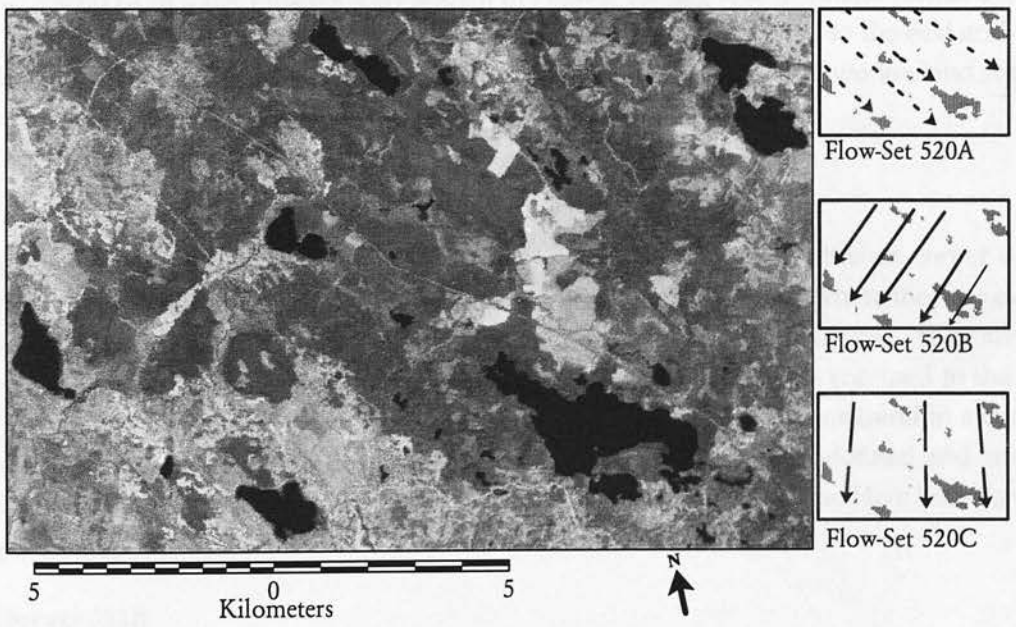

Figure 5.24: Cross-lineations in the south of image 185020. Box ii within Figure 5.22 shows the figure location

lineations forming flow set 520A. The lakes in this area are elongated parallel to the flow set 520A lineations. Corrugation of the lake shores parallel to an axis trending at approximately 215° indicates the presence of a later flow set, ascribed as flow set 520B (Figure 5.24). Both of these flow sets are best observed at a scale of 1:250,000. The third flow set appears to cross both the previous lineations at a bearing of 180°. These lineations have been assigned to flow set 520C. The temporal order of the flow sets therefore, appears to be flow set 520A, followed by 520B and then flow set 520C.

Overview of Image 185020

Three flow sets have been interpreted from the lineations of image 185020. Flow set 520A is characterised by well-defined lineations neighbouring highland regions at trends of 160° to 130°. This flow set is thought to precede the other two. Flow set 520B is restricted to the southeast of the image where flow set 520B lineations trend at between 215° and 240°. The arrangement of lineations suggest flow set 520B post-dates 520A. Flow set 520C consists of pervasive small lineations, up to 1.5 km long at a trend of approximately 175°. These lineations are seen to be superimposed upon lineations from both flow set 520A and 520B indicating that 520C post-dates the other two flow sets.

5.3.8 Image 185021

Figure 5.25a shows the first-order interpretation for the image 185021 and the flow sets interpreted from these lineations are shown in Figures 5.25b, c and d. Image 185021 consists of two lowland regions extending from the northern edge of the image to the east and west edges respectively (Figure 5.25). The Latgale Highland separates these two lowland regions and widens towards the south.

Flow set 521A

Flow set 521A is clearly visible within the lowland region in the northwest corner of the image (Figure 5.25b). The lineations are best defined towards the north where they are clearly identifiable with widths 500-900 m and lengths of up to 45 km (Figure 5.26a). They are also visible using the digital elevation model (Figure 5.25). Flow set 521A is confined to the west of the Latgale Highland. From the north edge of the image the lineations trend in a curving arc to the western edge. To the south the lineations become less well-defined and are best preserved in the elevated region bordering the western edge of the image. Here lineations are up to 6 km long.

Flow set 521B

Flow set 521B is located within the lowland region to the east of the Latgale Highland (Figure 5.25a). It has a similar appearance to flow set 521A, though the lineations are less well-defined (Figure 5.26b) and become more poorly defined towards the south. The orientation

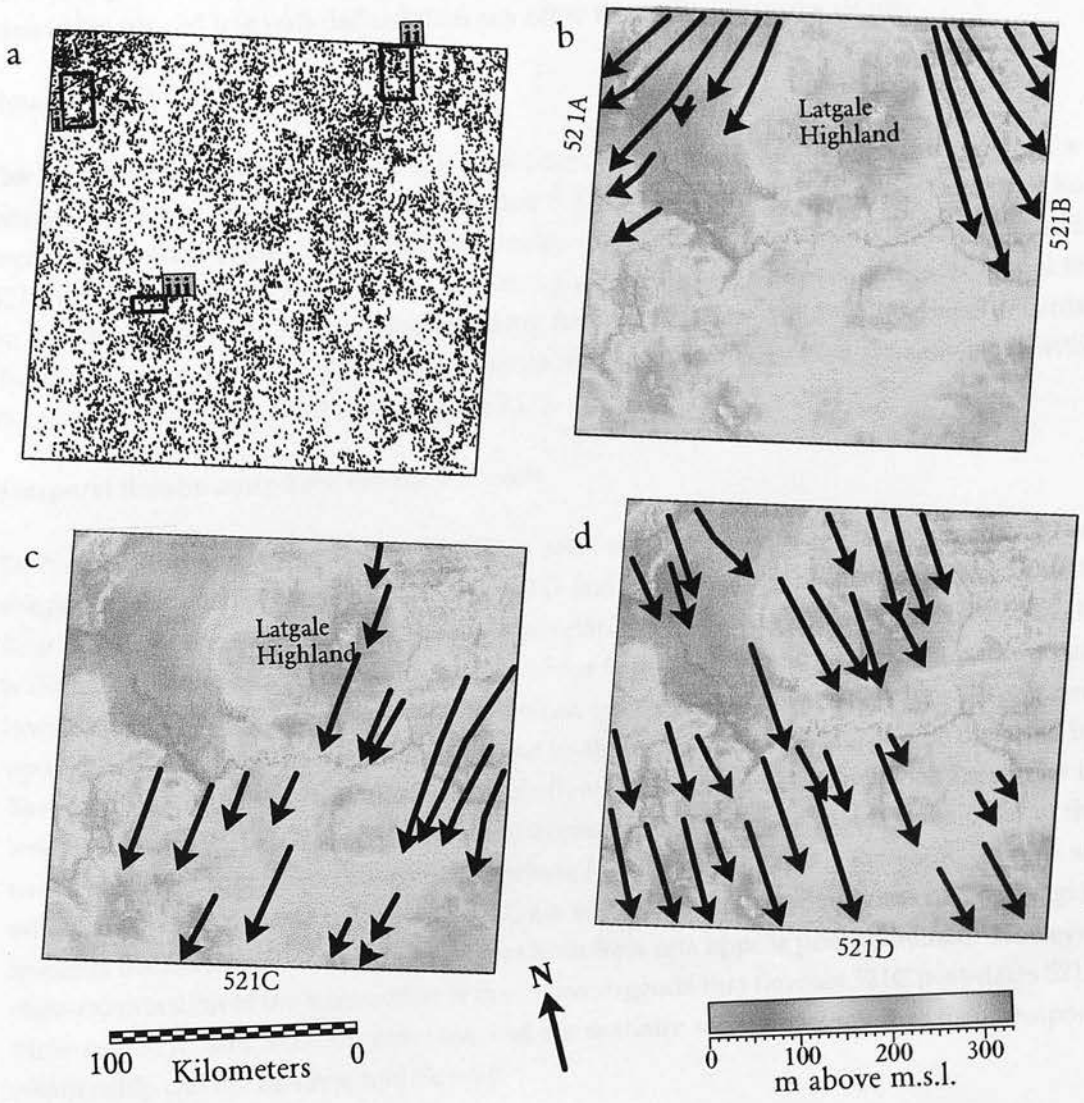

Figure 5.25: a: First order interpretation of Landsat TM Image 185021. Boxes delineate areas shown in further diagrams. b: Flow sets 521A and 521B. c: Flow set 521C. d: Flow set 521D. b, c and d are superimposed upon the present day topography.

of the lineations forming flow set 521B are approximately 160° along the northern edge of the image gradually becoming more easterly towards the south.

Flow set 521C

Flow set 521C consists of lineations located within the highland regions with similar orientations of approximately 210° (Figure 5.25c). The lineations are similar in appearance, less than 4 km in length and less well-defined than any other flow sets within the image.

Flow set 521D

The lineations of flow set 521D are less than 4 km in length and can be seen throughout the image trending at approximately 175° (Figure 5.25d). Flow sets 521B and 521D can not be separated by their orientations which are similar. It could be argued that flow sets 521B and 521D are part of a larger flow set. By considering all the images, however, this is found not to be the case (Section 6). The lineations forming flow set 521D are quite well-defined towards the north, becoming less well-defined towards the south. In places they are associated with the corrugation of lake shore-lines (Figure 5.27).

Temporal Relationship between the flow sets

To the north of the image flow set 521D is seen superimposed upon flow set 521A. The temporal relationship between flow sets 521D and 521B can not be distinguished as both flow sets have the same trend. The temporal relationship between flow set 521D and 521C is difficult to determine. The rough surface of the Latgale Highland prevents superimposed lineations from being clearly identified. Instead interpretations of the relationship is based upon the distortion of the lakes which appear to align with flow set 521C and be distorted by flow set 521D (Figure 5.27). In addition, while flow set 521C and 521D lineations are similar in length, flow set 521C is less well-defined in appearance, suggesting that it is the older of the two. From the above observations it is concluded that flow set 521D is the youngest flow set within the image. Flow sets 521B and 521C are only observed together within a small region towards the northwest of the image, where both flow sets appear poorly defined. However, close examination of the intersection of lineations suggests that flow set 521C post-dates 521B. Flow sets 521C and 521A do not cross and are spatially separated such that their temporal relationship can not be discerned directly.

Overview of Image 185021

Flow set 521A contains well-defined lineations extending from the northern edge of the image to the west. These lineations are easily identified within the image and the digital elevation model. Slightly less well-defined lineations form flow set 521B which curves from the northern edge to the east. The relationship between flow sets 521A and 521B is unclear from this image. They are, however, the oldest flow sets within the image. Flow set 521C is confined to the highland regions of the image. It is thought to have followed flow set 521B and trends at 210°. The final flow set, 521D is pervasive across the majority of the image with a trend of 175° and

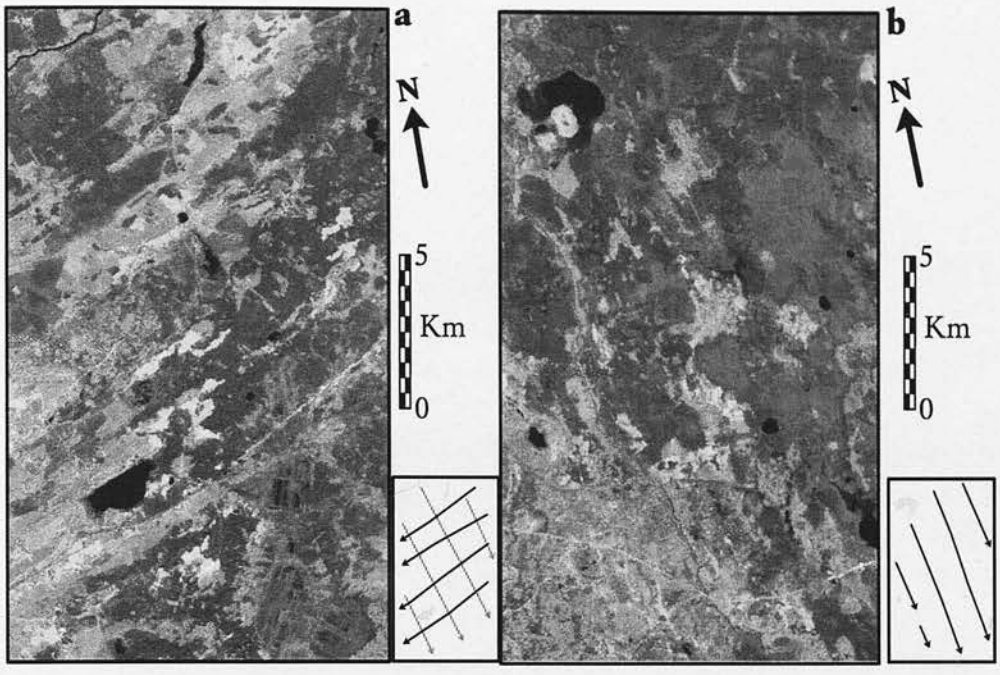

Figure 5.26: a: Flow set 521D superimposed upon flow set 521A b: Flow set 521B. The location of Figures a and b is shown by boxes i and ii respectively within Figure 5.25

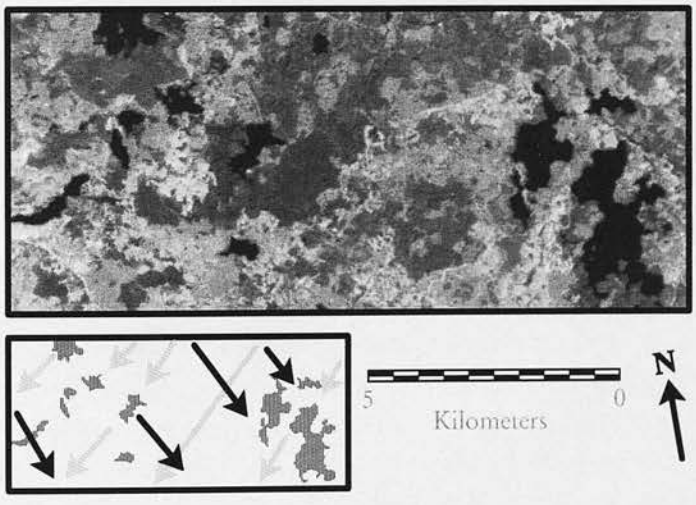

Figure 5.27: Flow set 521C eroded basins trending at 215°, with margins which were later altered by flow set 521D, trending at 160°. Figure location shown by box iii within Figure 5.25

is superimposed upon flow sets 521A and 521C.

Chapter 6

Synthesis of Image Interpretations

This Chapter is divided into three Sections. In the first Section a brief review is made of current models of the North European glaciations. This is followed by a description of present day ice sheets where fast ice flow is recorded. The observations made from present-day ice sheets are used within the final Section to relate the regional flow sets, which are formed from the flow sets described in the previous Chapter, to ice dynamics.

6.1 Models of Glaciation

Models of the typical course of a North European glaciation generally use the Late Weichselian as an example (Lundqvist, 1986; Ehlers, 1990), since the record of previous glaciations are less complete. In Scandinavia, the glaciation model presented by Ljunger (1949) is still generally accepted with a few alterations (Lundqvist, 1986). In this model, the Late Weichselian ice sheet was initiated in the Scandinavian mountains. As the ice sheet grew towards the east and south, the ice divide gradually moved eastward to a position east of the Gulf of Bothnia. Upon deglaciation the ice divide migrated back to the mountains eventually breaking up into several domes. This model is supported by indicator boulders within tills across the Baltic States which show an initial ice flow direction of northwest-southeast, followed by a dominant north-south orientation as the ice divide moved eastwards, only to return to northwest-southeast during deglaciation (Raukas and Gaigalas, 1993). Whilst this model, with the ice sheet growing from the Scandinavian mountains, seems plausible, in North America there is no mountainous area associated with ice sheet initiation (Ehlers, 1990), and it has been suggested that the ice sheet developed from large scale, approximately simultaneous accumulation of snow which formed ice sheets within a few centuries. It has been proposed that this latter 'instantaneous glacierization' model could explain the rapid build up of Weichselian ice in Scandinavia (Mangerud *et al.*, 1981; Ehlers, 1990). Till fabric measurements and lithological studies show that during the Weichselian maximum the ice flowed radially

from the ice divide to the margins (Ehlers, 1990; Houmark-Nielsen, 1990; Ringberg, 1988).

Work in south Sweden (Lagerlund, 1987; Ringberg, 1988), Denmark (Houmark-Nielsen, 1990) and Germany (Ehlers, 1992) shows that the ice sheet glacio-dynamics were more complex during deglaciation than previously thought, with the orientation of ice flow along the southern margin of the ice sheet fluctuating through time. The simple radial model of ice flowing from the ice divide during deglaciation can no longer be maintained. To explain the complicated changes in the direction of ice flow in the southern Baltic, Lagerlund (1987) proposed the existence of Late Weichselian ice domes within the southern Baltic, formed on surged ice masses. Ice would also radiate out from these domes, as well as from the ice divide. Ringberg (1988) disagrees with this hypothesis claiming that there is no geological evidence to support the existence of these separate ice domes. Instead he proposes that the pattern of ice flow can be explained by differences in the ice flow over the mainly crystalline bedrock of the Baltic Shield and the fine-grained sediments of the Baltic. Where the ice is underlain by crystalline bedrock we would expect coarse-grained, permeable sediments, a high effective pressure and no sediment deformation (Boulton, 1996). In contrast, water-saturated, fine-grained sediments have a strongly reduced shear strength which will cause them to deform rapidly, even under very low driving stresses (Clarke, 1987). Deforming till can contribute towards rapid ice velocities and as discussed in the next Section, has been used to account for the fast motion of ice stream B, Antarctica (Alley *et al.*, 1987). Over the unlithified sediments in the Baltic, rapid ice movement may have been caused by basal deformation of water soaked sediments at the glacier sole (Ehlers, 1992). A model which includes deforming basal sediments also permits a much reduced estimate of ice thickness (Boulton *et al.*, 1985) which may partly explain the rapid Weichselian deglaciation (Ehlers, 1990). It is not known why the glacier dynamics might have switched from radial ice flow during the glacial maximum to streaming ice during deglaciation. However, Ehlers (1990) proposes that the ice may initially have advanced over deep permafrost, which has the same rheological characteristics as undeformable lithified rock. As a new thermal equilibrium was established between geothermal heat flux and insolation from atmospheric cooling by the overlying ice, the sediments may have become water-saturated and therefore easily deformed. This would produce relatively slow ice flow over the crystalline bedrock of the Baltic Shield and ice streaming within the Baltic.

6.2 Modern Ice Streams

In modern ice sheets, a strong contrast exists between sluggish areas of sheet flow and relatively fast ice streams (Clarke, 1987). In regions of sheet flow, internal deformation of the ice is responsible for relatively slow ice movement (Dongelmans, 1996). An ice stream may be defined as a region in a grounded ice sheet in which the ice flows much faster than in the regions on either side (Paterson, 1994). While ice streams comprise only 13 per cent of the Antarctic coastline, they may drain as much as 90 per cent of the accumulation in the interior (Morgan *et al.*, 1982). Similarly, much of the discharge from Greenland is concentrated

in twenty large outlet glaciers. The state of these ice sheets is therefore controlled largely by flow in ice streams (Paterson, 1994).

Many of the ice streams of Antarctica and the Jakobshavns Isbræ ice stream, Greenland occupy deep subglacial valleys (Figure 6.1a). The high velocities of these ice streams are usually attributed to basal ice sliding over the underlying material, (Paterson, 1994). In contrast, the ice streams on the Siple coast of west Antarctica tend to follow relatively shallow bedrock troughs approximately 300 m deep (Figure 6.1b), but do not always fully occupy these or are situated on the trough edges (Shabtaie *et al.*, 1987).

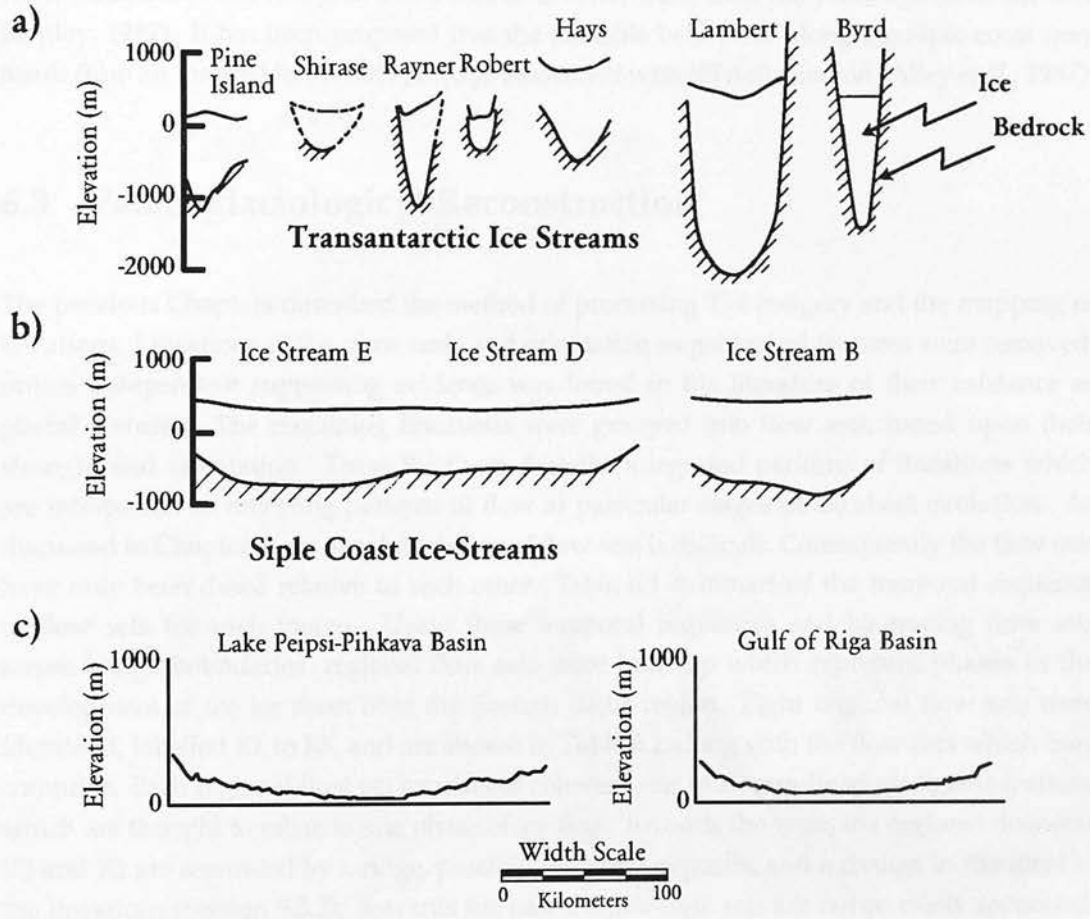

Figure 6.1: Transverse profiles across present day ice streams from Antarctica (a and b) and the present day topography across two basins occupied by ice streams in the Eastern Baltic region (c).

Five major ice streams have been identified on the Siple coast, Antarctica. Ice Stream B is the most studied and is 300 km long, 30-80 km wide (Figure 6.1b). The lateral boundaries of the ice streams are sharply delineated by 5 km wide crevasse systems that denote zones of very strong shear (Clarke, 1987). In many areas the ice streams are separated by ridges which can be up to 300 m higher than the ice stream surfaces (Shabtaie *et al.*, 1987). Ice stream velocities vary between 50 to 825 m/a compared with less than 10 m/a in the ice ridges on either side (Shabtaie *et al.*, 1987). Basal temperatures estimated by Rose (1979) suggest that the base of the ice stream is at melting point whereas the bases of the intervening ridges are

frozen. While there is no direct evidence from the base of the intervening ridges, bore-hole evidence shows melting point temperatures at the base of the ice stream (Blankenship *et al.*, 1986). The high driving stress within Ice Stream B (20 kPa) suggests that ice deformation is an insignificant component of ice flow (Alley and Whillans, 1991). Alley *et al.* (1987) and Blankenship *et al.* (1987) believe till deformation accounts for most, if not all, of the ice motion. Seismic observations indicate that the till has a porosity of 40 per cent (Blankenship *et al.*, 1987), a value characteristic of a till that is deforming (Paterson, 1994), and deformation of till has been measured directly in at least two areas (Blankenship *et al.*, 1986; Engelhardt *et al.*, 1990). The west Antarctica ice streams are not in steady state. Ice Stream C is virtually stagnant, while buried crevasses suggest that it was once active more than 100 years ago (Shabtaie and Bentley, 1987). It has been proposed that the unstable behaviour along the Siple coast may result from an internal instability, perhaps associated with till deformation (Alley *et al.*, 1987).

6.3 Palaeoglaciological Reconstruction

The previous Chapters described the method of processing TM imagery and the mapping of lineations. Lineations of the same scale and orientation as geological features were removed, unless independent supporting evidence was found in the literature of their existence as glacial features. The remaining lineations were grouped into flow sets, based upon their strength and orientation. These flow sets describe integrated patterns of lineations which are interpreted as reflecting patterns of flow at particular stages of ice sheet evolution. As discussed in Chapter 4, the absolute dating of flow sets is difficult. Consequently the flow sets have only been dated relative to each other. Table 6.1 summarises the temporal sequence of flow sets for each image. Using these temporal sequences and by tracing flow sets across image boundaries, regional flow sets were built up which represent phases in the development of the ice sheet over the Eastern Baltic region. Eight regional flow sets were identified, labelled R1 to R8, and are shown in Table 6.2 along with the flow sets which they comprise. Each regional flow set consists of coherent sets of stream-lined glacigenic features which are thought to relate to one phase of ice flow. Towards the west, the regional flow sets R3 and R2 are separated by a ridge, possibly marginal deposits, and a change in the form of the lineations (Section 5.3.3). Towards the east the two flow sets are not so easily separated, and the margin has been traced to the east using techniques described later. As a consequence of tracing the margin eastward, flow set 521D has been separated into two flow sets, indicating that it formed time-transgressively.

Flow set R8 (Figure 6.2a) consists of lineations which are south of the Late Weichselian margin, as proposed by Raukas and Gaigalas (1993) and are discussed in the following Chapter. Assuming the glacial genesis of these lineations is confirmed, they are thought to represent Saalian or older glacial flow directions. Flow set R7 (Figure 6.2a) contains lineations which occur north and south of the Late Weichselian margin. The lineations are not, however, perpendicular to the Weichselian margin and their orientation at 225° suggests that a margin existed further to the south and that it had a northwest-southeast trend. The proposed Late

Image	Flow sets Youngest to Oldest
188019	819A
187020	720A, (720B, 720C, 720D, 720E, 720F, 720G)
187021	721A, 721B, 721C, (721D, 721E, 721F)
187022	722A, 722B, 722C, 722D
187023	723A, 723B, 723C, 723D
185019	(519B+519C), 519A, (519D+519E)
185020	520C, 520B, 520A,
185021	521D, 521C, (521A, 521B)

Table 6.1: Temporal Sequence of the flow sets within each image. Brackets group flow sets within a single time period, but do not imply flow sets are contemporaneous. Addition signs group separate flow sets as a single flow event.

	Regional flow set	Flow sets
Young	R1	519B, 519C
	R2	819A, 720A, 721A, 519A, 520C, $\frac{1}{2}$521D
	R3	721B, 722A, 723A, $\frac{1}{2}$521D
	R4	519D, 519E, 520B, 521C
	R5	720B, 720C, 720E, 520A, 521A, 521B
	R6	720D, 720G, 721C,
	R7	722B, 722D, 723B, 723D
Old	R8	722C, 723C

Table 6.2: Individual flow sets forming the regional flow sets.

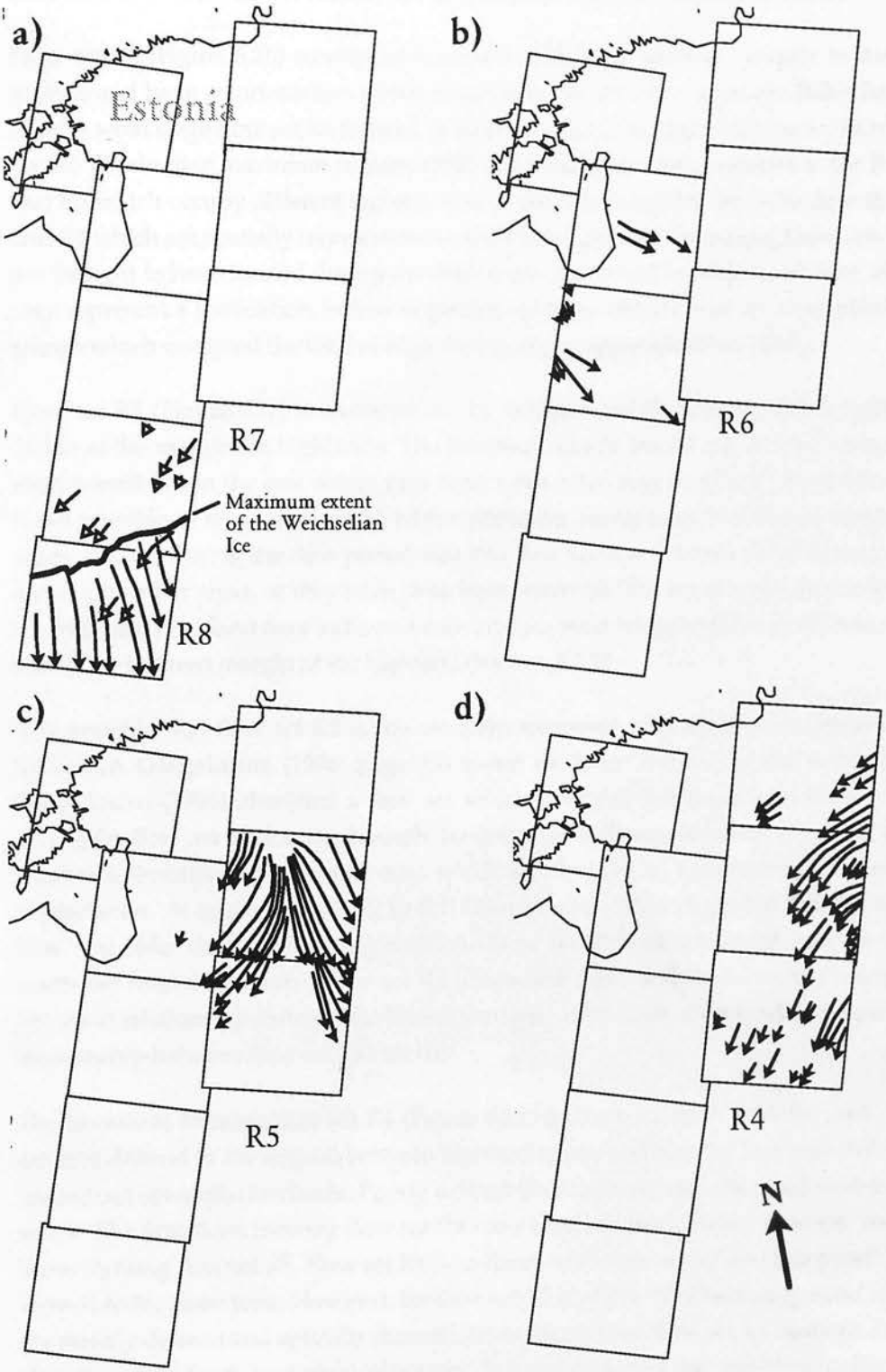

Figure 6.2: Regional flow sets: Pre-final deglaciation.

Weichselian margin represents the maximum limit of Weichselian ice so flow set R7 must predate the Weichselian and would have been formed during the Saalian or earlier.

Flow set R6 (Figure 6.2b) consists of lineations which are restricted mainly to the highland regions and have an orientation which suggests an ice direction from the Baltic Sea. It is not clear at what stage flow set R6 formed. It does not appear to align with the ice flow proposed for the Weichselian maximum (Ehlers, 1990) and it cannot be dated relative to the flow sets R4 and R5 which occupy different regions. It is, however, thought to be older than flow sets R1 and R2 which are spatially more extensive with better defined lineations. Flow sets R1 and R2 are thought to have formed during the final deglaciation and are discussed later. Flow set R6 may represent a fluctuation, before deglaciation, in the direction of an antecedent of the ice stream which occupied the Gulf of Riga during deglaciation (flow set 720A).

Flow set R5 (Figure 6.2c) is characterised by well-defined lineations, with lengths of up to 21 km at the margins of highlands. The lineations can be traced across four images, and are most prominent in the east where they form a fan extending from the Lake Pihkva basin. It is not possible to relate flow set R5 with a particular configuration of the ice sheet across the study region. During the time period that this flow set was formed, either lineations did not develop in other areas, or they have since been removed. The hummocky area to the south of the Vidzeme Highland may indicate a convergence zone between flow set R5 and ice flowing round the western margin of the highland (Section 5.3.3).

It is possible that flow set R5 is the southern extremity of a zone of ice stream formation for which Dongelmans (1996, page 83) found evidence 360 km to the north in Finland. Dongelmans (1996) identified a flow set which diverged southwards to form a lobe. The diverging flow set had a north-south central axis and was separate from the northwest-southeast lineations in the same area which are thought to have formed during the final deglaciation. At approximately 12 ka B.P. Dongelmans (1996) suggested that the north-south flow was older than the final deglaciation. Flow set R5 is clearly older than the northwest-southeast final deglaciation flow set R2 (discussed later) and therefore the orientation and temporal relationship between the lineations north of the Gulf of Finland is comparable to the relationship between flow set R5 and R2.

The lineations forming flow set R4 (Figure 6.2d) indicate ice flow from the east. Lineations are best defined in the regions between highland areas, and become less well-defined as they spread out across the lowlands. Poorly defined lineations are also observed over the highland areas. The lineations forming flow set R4 have been relatively dated as being younger than those forming flow set R5. Flow set R4 is co-linear with flow set R7 and it is possible that they formed at the same time. However, the flow set R7 is of pre-Weichselian age and its lineations are weakly defined and spatially discontinuous. In contrast flow set R4 contains well-defined lineations which are spatially continuous. It is not expected that pre-Weichselian lineations would have been preserved in this way, so it is proposed that flow set R4 is of Weichselian age. Flow set R4 may represent a northeast-southwest flow. Punkari (1993) identifies a northeast-southwest ice flow to the east of the images, referred to as the Novgorod ice stream

(Figure 6.3), which formed during the deglaciation of the Weichselian ice. However, only the southern part of flow set R4 is aligned with the Novgorod ice flow and it is not thought that flow set R4 is part of this deglaciation ice stream. The spatial distribution of flow set R4, with well-defined lineations flowing round highlands and poorly defined lineations across highlands, is similar to the western part of flow set R5 and suggests that flow set R4 may be the western part of a diverging north-south ice flow with a central axis in the lowland regions to the east of the images.

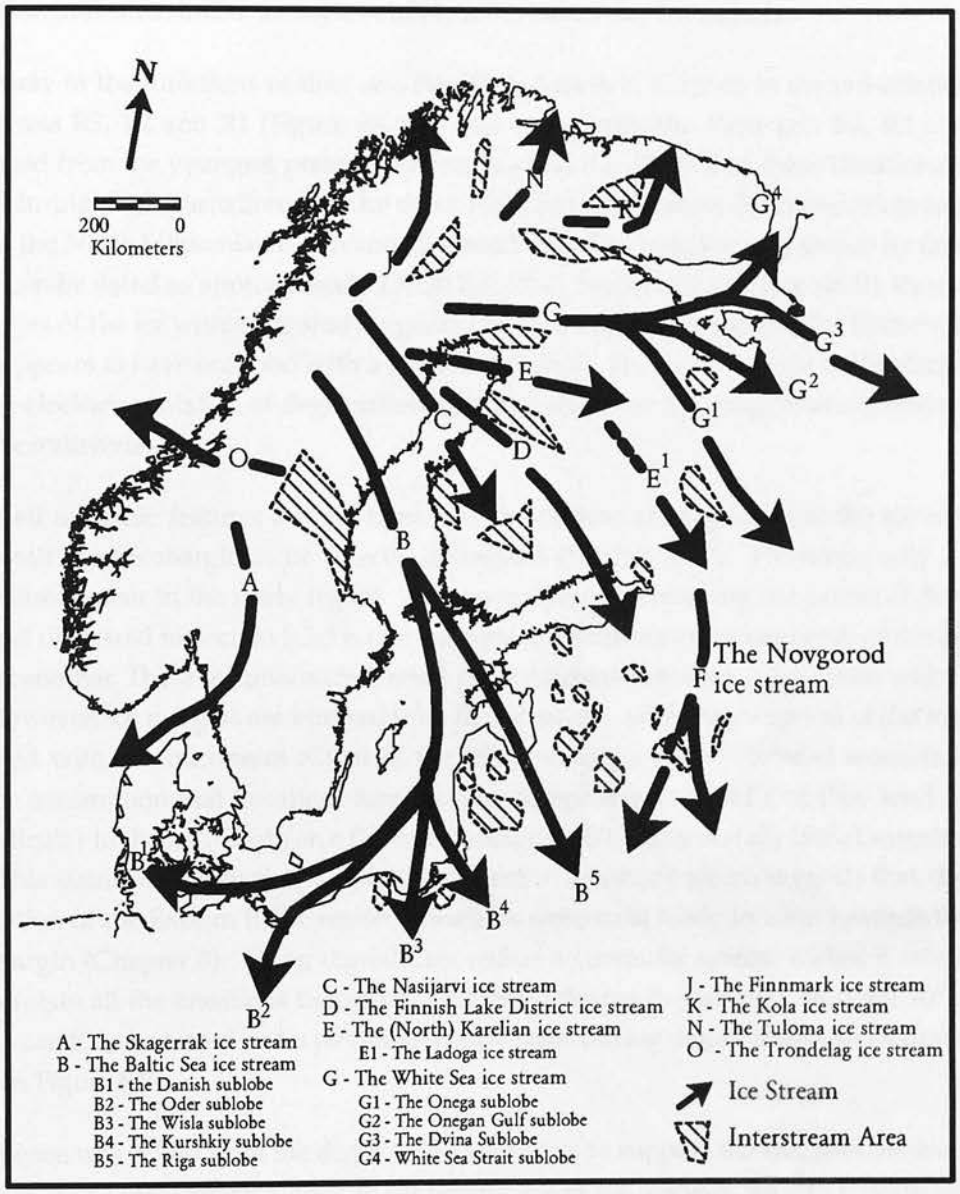

Figure 6.3: Ice streams and interstream regions of the Fenno-Scandinavian ice, after Punkari (1997).

While flow set R4 is dated younger relative to flow set R5, the similar appearance of flow set R5 and flow set R4 suggests that they formed during a similar phase of glaciation. Punkari and Forsström (1995) propose that ice flowed north-south immediately north of the Gulf of

Finland during the advance phase of the Late Weichselian, but flowed northwest-southeast during the deglaciation. Indicator boulders within till suggest similar orientations of ice flow across the Baltic States (Raukas and Gaigalas, 1993). It is proposed that the flow sets R4 and R5 were formed during the glacial maximum, when the ice divide was close to the Gulf of Bothnia. Flow sets R4 and R5 would therefore show that the activity of the two adjacent lobes varied through time. Thus R5 was initially dominant, with R4 encroaching on the same area during a later period. Similar temporal changes in the activity of adjacent ice lobes have been identified within Fenno-Scandinavia (Punkari, 1997) and the slowing of Ice Stream C, west Antarctica, indicates similar unstable behaviour in present day ice streams.

The variety in the directions of flow sets R6, R5 and R4 is in contrast to the uni-orientation of flow sets R3, R2 and R1 (Figure 6.4 a, b and c respectively). Flow sets R3, R2 and R1 are formed from the youngest preserved lineations and it is likely that these lineations were formed during the deglaciation of the ice sheet. Flow set R3 represents the lineations preserved south of the North Lithuanian re-advance (Section 5.3.3). The re-advance is shown by flow set R2 and can be dated as approximately 13,250 B.P. (^{14} C, Section 2.3.4). Flow set R1 shows the final stages of the ice within the study region. The final deglaciation across the Eastern Baltic region appears to have occurred with a single orientation. This is in contrast to the clockwise and anti-clockwise rotation of deglaciation flowlines observed by Dongelmans (1996) across Fenno-Scandinavia.

Almost all morainic features formed transverse to ice flow are deposited at the ice margin and permit the ice margin to be directly delineated (Section 4.1.1). However, only a few such features occur in the study region. The topographic rise marking the extent of flow set 721A and discussed in Section 5.3.3 is one example, the transverse feature north of the city of Parnu is another. These features were formed perpendicular to the latest lineations within the area. However, ice margins are inferred from the lineations, with the exception of the margin associated with the maximum extent of the Weichselian ice sheet. Several workers have used the assumption that lineations form in near-marginal zones, and that they tend, to lie perpendicular to the ice margin on a flat bed (Punkari, 1980; Boulton *et al.*, 1985; Dongelmans, 1996). This assumption is further supported by work in this study which suggests that, during deglaciation of the Eastern Baltic region, lineations were most likely to form towards the ice sheet margin (Chapter 8). Using digital data within a computer system makes it relatively easy to rotate all the lineations thought to be formed during deglaciation through 90°. The margins can then be traced and a picture of the ice sheet during deglaciation can be drawn as shown in Figure 6.5.

No evidence was found from the deglaciation lineations to support the sharp lobate margins of Raukas *et al.* (1995) which appear to confine the ice to the lowland regions (Figure 6.5). It is suggested that these ice marginal lines are drawn on the basis of a valley glacier model of ice flow in which ice streams are strongly controlled by the topography. Such a model may be appropriate for the tongues of ice which flowed between the highlands during the formation of flow set R5. It may be that the southward flowing ice was confined by highland regions to the east and west such that no lineations formed perpendicular to the highland margins.

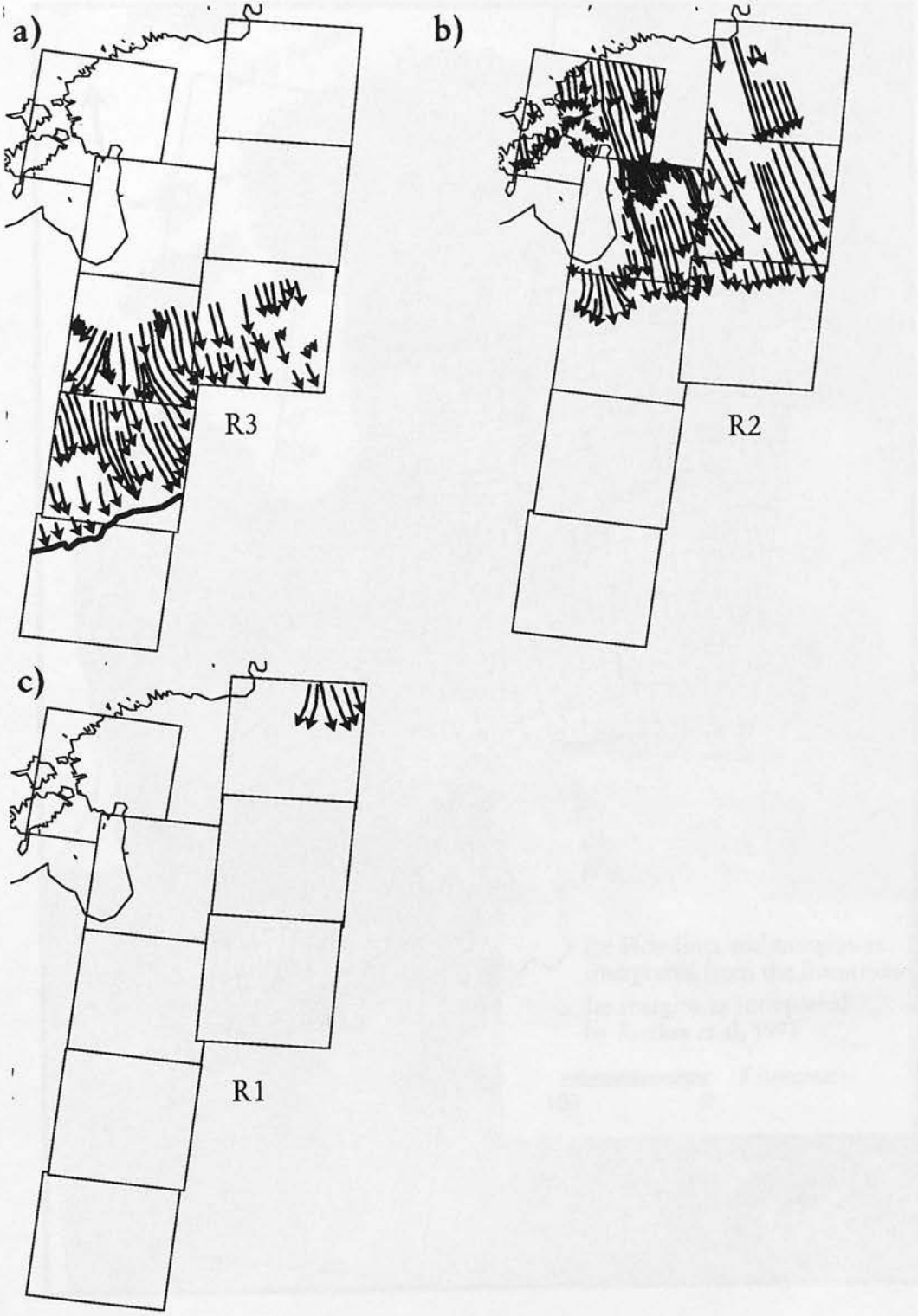

Figure 6.4: Final deglaciation regional flow sets.

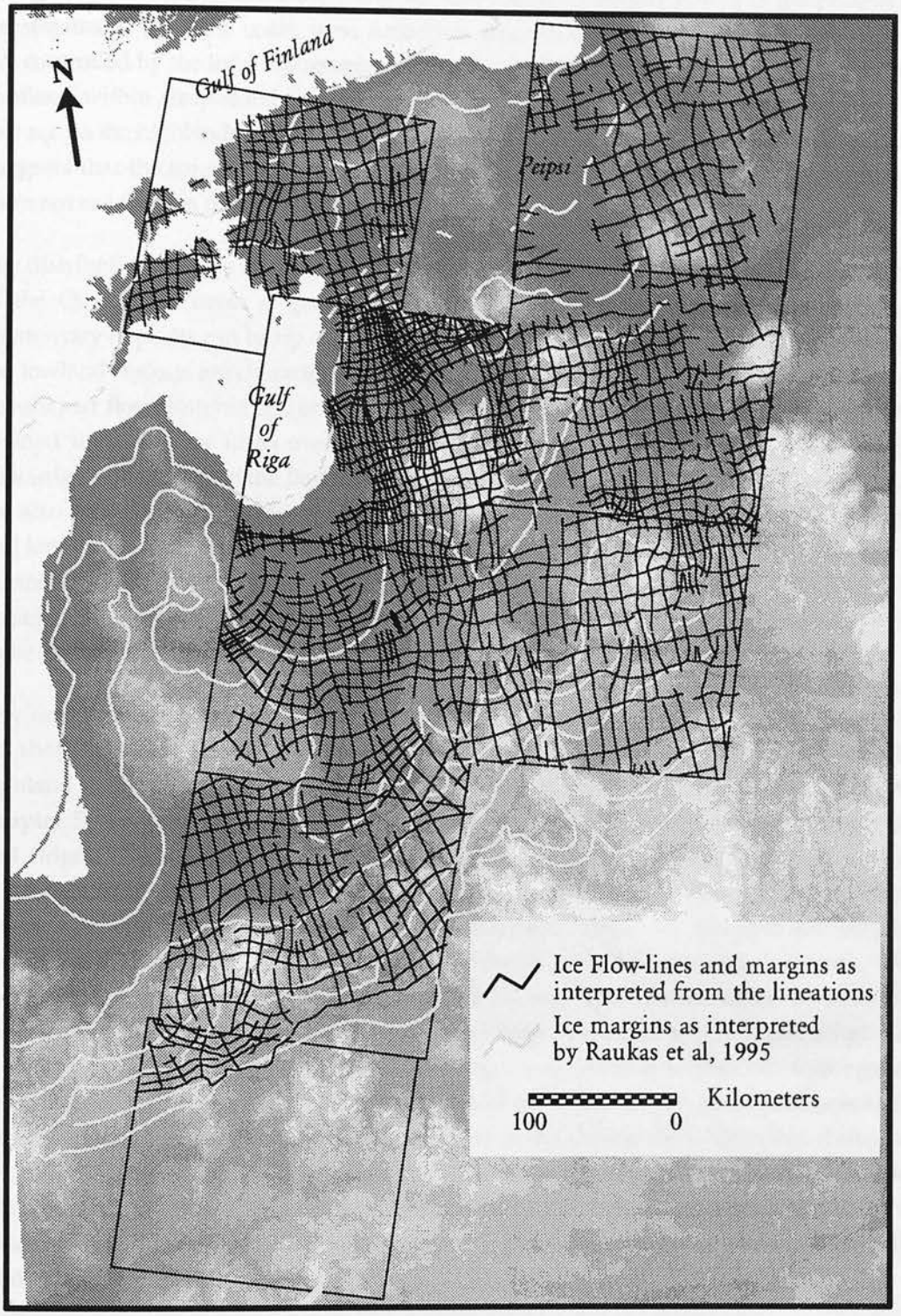

Figure 6.5: Temporally composite ice flow lines and margins during the Weichselian deglaciation as interpreted within this study and by Raukas *et al.* (1995).

However, the transverse profile across the ice stream flowing from the Gulf of Riga (flow set 720A) and the Lake Pihkva basin (flow set 520A) shows a similar profile to the present day ice streams of the Siple coast, west Antarctica (Figures 6.1b and c). These ice streams are not controlled by the local topography, unlike many other present-day ice streams which are confined within steep-sided basins (Figure 6.1a). While the lineations of the regional flow sets across the highlands are less well-defined than those in the lowland areas, their existence suggests that the ice was not strongly confined by the topography and that the ice margins were not as lobate as previously thought.

The distribution of till is uneven across the study region. In the lowland regions the thickness of the Quaternary cover is generally less than 50 m while in the highland regions the Quaternary deposits can be up to 300 m thick (Section 2.2). Throughout the images studied, the lowland regions are characterised by an abundance of flow-parallel features which form fan-shaped flow patterns within lowland plains. To the east of the study region, the well-defined lineations are often over 15 km long and are formed between highland regions. Towards the west, within the Burtnieks drumlin field and south of the Gulf of Riga, lineations are also well-defined, but shorter, up to 10 km in length. Lineations are often best defined and longest close to the margins of the neighbouring highlands. Particular examples are: the Burtnieks drumlin field (flow set 720A) and the Sakala Highland; flow set 520A beside the Haanja Highland; and flow set 521A adjacent to the Vidzeme Highland. The lineations within these lowlands are considered to have been formed by glacial ice streams.

Few lineations are observed within the highlands themselves and those which are recorded are short, generally less than 1 km. Great thicknesses of Quaternary deposits contribute to highland areas which have altitudes well above the surrounding terrain. As described in Chapter 5, the highland regions are characterised by a rough texture of hummocky knolls and ridges. Field work in these highlands show that the landforms consist of mixtures of till, glaciofluvial and glaciolacustrine material (Raukas *et al.*, 1995). These landforms are thought to have a polygenetic origin with subglacial, englacial, marginal accumulation and stagnant ice processes all contributing (Karukäpp, 1996; Āboltiņš and Dreimanis, 1995). Some of the ridges observed (Figures 5.14 and 5.17) may be thrust moraines. Bitinas (1994) suggests that the formation of the interstream highlands within Lithuania, began subglacially as basal debris which was lifted into ice flowing across bedrock elevations. Subsequently deposition occurred in a marginal environment of crevassed and stagnant ice masses. It is generally agreed that these highland areas accumulated during the Weichselian (Lukashov, 1982; Āboltiņš and Dreimanis, 1995), though some sediment may have originated from older strata (Gaigalas, 1995). This supports a Weichselian age for the flow sets R5 and R6 which appear to have formed simultaneously with the highland regions, flowing round them rather than being truncated by them.

The highland areas can be compared with the interstream regions observed between present day ice streams along the Siple coast, west Antarctica, where ice velocities are of the order of a few metres a year. The low velocities over interstream highlands may in part explain the small size of the lineations observed. A comparative lack of erosion across the interstream highlands

may also be expected compared with the bases of the ice streams, which may lead to greater preservation of any older lineations. If the highlands become cold-based, as some of the interstream regions within Antarctica appear to be, this would further protect the subsurface from remolding. Evidence for cold-based ice under the highlands may come from the ridges observed over the highlands (Figures 5.14 and 5.17). If these ridges are thrust moraines, they may be caused by the ice flow being compressed towards areas of ice frozen to the substrate. Studies of landforms from the Fennoscandia and Laurentide ice sheets, such as lineations, suggest that some features have escaped destruction, despite complete ice overriding during several tens of millenia (Dyke, 1993; Kleman, 1994). The general opinion appears to be that preservation potential is greatest where the ice-sheet base is frozen to its bed. The flow sets 721D, 721E and 721F could not be assigned to any of the regional flow sets identified and may be evidence of older lineations which have been preserved over the Augšzeme Highland. In general, most lineations which could not be assigned to a flow set occurred over the highland regions, suggesting that they are relics preserved because they have underlain interstream zones.

On a large scale the interstream highland regions generally coincide with elevated bedrock (Figure 2.4). Local topography would have been expected to play an initial role in concentrating ice into valleys. The higher shear stresses produced by thick ice in the valleys would result in an increase in ice velocity in those areas (Paterson, 1994). Conditions may be similar to those observed within the ice streams strongly controlled by the present day topography (Figure 6.1a). With time, the ice expanded to become independent of local conditions. Two positive feedback loops could, however, help maintain high ice velocities within regions of ice streaming. Faster flow produces more frictional heat, which raises the temperature of the basal ice, which in turn, deforms more easily. Once the basal ice reaches the pressure melting point, meltwater can be produced and sliding or till deformation may develop.

Similar ice stream and interstream regions have been observed across Fenno-Scandinavia (Punkari, 1993; Dongelmans, 1996). There are, however, important differences. The glacial stream regions across Finland contain an abundance of eskers (Punkari, 1997) while few eskers are observed across the East European Platform. Walder and Fowler (1994) relates this spatial distribution with the different underlying geology of the two regions. According to the Walder-Fowler theory of subglacial drainage, eskers are more likely to form on a discontinuous, coarse-grained, high-permeability till derived from underlying crystalline rock than on continuous, fine-grained till of low-permeability derived primarily from sedimentary rock. Deglaciation across the Baltic Shield appears to have been more stable with the formation of more regular morainic arcs, such as the Sapausselka moraines (Punkari, 1997). Several re-advances have been proposed during the deglaciation (Chapter 2), with perhaps the best dated being the North Lithuanian Advance which followed the Raunis Stadial. After this advance the ice rapidly retreated back to a position immediately north of the Gulf of Finland where the rate of retreat appears to have decreased. Clark and Wilson (1994) noted a similar pattern at the southern edge of the Laurentide ice sheet where rapid fluctuations of the large ice lobes were limited to areas underlain by deformable sediments while the retreat of the ice

sheet over areas with a rigid bed was more stable. The differences in the size and shape of the ice stream and interstream areas of Fennoscandinavia and the East European Platform may also reflect differences in the stability of deglaciation. The interstream regions within Finland tend to be triangular in plan view, while those further south are more rounded (Figure 6.3). Within Finland the southeastern ice stream lobes are generally over 250 km wide during the final deglaciation while those within the Eastern Baltic region are usually less than 100 km. The underlying geology therefore appears to be a controlling factor on ice sheet dynamics. As discussed earlier (Section 6.1), fine-grained sediments are more likely to deform and this will allow rapid flow of ice. A slow permeable substrate, such as fine-grained sediments, have been proposed as the cause of surge events within the Laurentide ice sheet (L. Clayton, 1985). The slow escape of water would result in a build up of subglacial water decoupling the ice sheet from its base. This may also explain the less stable flow thought to have occured over the Eastern Baltic region.

6.4 Summary

Eight regional flow sets have been identified across the study region. Two regional flow sets are thought to pre-date the Weichselian, while the remainder are thought to be Weichselian in age. Three regional flow sets are shown to pre-date the final deglaciation. The activity of these flow sets appears to have varied with time suggesting an internal instability, possibly related to till deformation. Three regional flow sets relate to final deglaciation during which a more consistent flow orientation was maintained. The highland areas are thought to be interstream areas, where ice velocities were low and net sediment accumulation could occur. Thickening by marginal stacking of sediment and glaciotectonism over areas of ice frozen to the substrate may also help explain the large thicknesses of Quaternary deposits observed. Old lineations may be preserved within these regions, where the cold-base helped to preserve the sub-ice surface. In contrast the lowland regions are characterised by many flow-parallel features and a thin cover of Quaternary till. These regions are thought to have been occupied by ice streams with high ice velocities and high basal temperatures resulting in water saturated till and possibly subglacial till deformation. The underlying geology may also explain the instability of the ice streams across the East European Platform compared with the more stable ice streams formed within Finland where the ice moved over crystalline bedrock with a cover of sandy deposits.

Chapter 7

Spatial Analysis

The shape and pattern of glacial geomorphological features are widely thought to be a reflection of the glaciological conditions at the time of formation and the processes that formed them (Clark and Wilson, 1994). There is already a large literature on spatial and morphometric analysis of glacial lineations and in particular drumlins (e.g. Vernon 1966; Smalley and Unwin 1968; Trenhaile 1971; Rose and Letzer 1977; Menzies 1979; Boots and Burns 1984; Stea and Brown 1989; Rõuk and Raukas 1989; Clark 1993). A large proportion of the papers were written in the pre-computer era and consequently sample sizes are often small, usually from individual drumlin fields. It is not possible to compare results between studies where the raw data is not published and the techniques differ. This prohibits the use of results from different areas to produce an overview of lineation formation. Clark and Wilson (1994) recognised this problem and proposed a single set of techniques to be applied to a large number of drumlins from many different drumlin fields. However, the techniques they propose are not generally suitable. The reasons for this are discussed below; and alternative methods of analysis are proposed here.

Throughout this study extensive use has been made of computers using techniques developed within Geographical Information Science to visualise, manipulate, and analyse geographically referenced information. Such computer systems are referred to as Geographical Information Systems (GIS). GIS has been used to visualise large volumes of complex glaciological data gathered at many scales Punkari (1989); Knight (1996); Broadgate (1997). Using a GIS, a glaciotectonic data set for the whole of North America was compiled, leading to the production of a glaciotectonic map (Aber *et al.*, 1995). Computer Aided Design (CAD) software has also been used in palaeo-glaciological reconstructions to manipulate data with the object of revealing hitherto unknown associations (Punkari, 1989; Clark, 1990). C. Wilson custom-developed a GIS software package for Knight (1996) to ease the data input and manipulation of ice flow information, while Broadgate (1997) developed a GIS to visualise lineation data using angular histograms and combined lineation data with esker, moraine and relative sea-level (isostatic) data sets. No single software package was found to be

suitable for the needs of this study. Consequently many computer packages were utilised to visualise and manipulate the data, including ERDAS IMAGINE, ARC/INFO and Generic Mapping Tools, as well as supporting FORTRAN programs and UNIX scripts. Visualisation and manipulation of data has been used continuously throughout this study to compare interpreted glacial features with topography (e.g., Sections 6.3 and 7.2), land cover (e.g., Section 3.5.3), underlying geology (Section 6.3), field measurements (Section 4.2.2) and satellite imagery (e.g., Section 5.2), as well as to manipulate flow sets which permitted numerous alternative scenarios to be explored and lead to a single reconstruction which best explains the lineation data and published field evidence (Chapter 6). Further use of computers to manipulate and visualise data sets to study the limit of Weichselian ice will be shown in Section 7.1.

Current GIS software packages tend to focus their spatial analysis on area-based or point-based manipulation with lineation analysis being neglected (Clark and Wilson, 1994). (Punkari, 1993; Dongelmans, 1996; Broadgate, 1997) all developed their own computer systems to measure the density of lineations, while Clark and Wilson (1994) also describe methods to measure lineation spacing and apply a nearest neighbour analysis. The proposed analysis of lineation spacing, however, is only valid for lineations which are parallel. Nearest neighbour analysis is not suitable for the analysis of glacial lineations, since the lineations are reduced to points with no account being taken of their spatial nature, and lineations are assumed to be free to locate anywhere in an infinite area. Within this Chapter, several approaches are taken to analyse the lineation data collected. In Section 7.2 the relations between lineations and topography are examined. Section 7.3 looks at the variance in the orientation of lineations while Section 7.4 analyses the spatial distribution of lineation lengths. Several models are used to examine the sample length distribution to try and characterise the underlying distribution and provide information on the process of lineation formation.

The lineations are stored as two sets of co-ordinates marking the end-points of the lineations. The data-analysis programs use these co-ordinates to calculate the size and orientation of the lineations. The co-ordinate values depend on the location of the lineations and the map-projection in which they are portrayed. To maintain orientation and shape the Lambert Conformal Conic (LCC) map projection was generally used. A comparison of the calculated lengths using the LCC map projection, and those calculated assuming a spherical earth show a maximum difference of 2.85 m. Similar differences were observed between the LCC map projection and other suitable map projections, such as the Mercator projection. When reprojecting the lineation data to other map projections the lineations were still recorded by only two points. It was concluded that the recorded lineations are so small relative to the curvature of the earth's surface that distortions related to the map-projection were negligible.

In addition to the data gathered across the Eastern Baltic region, lineation data collected from Landsat MSS and Landsat TM imagery across Finland has been used to complete a transect from the Scandinavian ice sheet divide to the ice margin during the period of maximum extent. This additional data was gathered by Punkari (1996) and Dongelmans (1996), and integrated into a single, accurately georeferenced, data set by Broadgate (1997). The lineations were also

stored in an LCC map projection using the same projection to ensure that the combined data set could be viewed seamlessly.

7.1 The Maximum Extent of the Weichselian Ice

The maximum extent of the Weichselian ice can be seen using several different forms of data. By highlighting only water bodies the imagery can also be used to show that lakes are abundant in the region extending to the proposed margin and not beyond. The margin is also delineated by changes in land use which, to a lesser degree, also mark the extent of other proposed margins. The texture of the Landsat TM image is also useful for delineating the margin and, in combination with the variation in spectral reflectance properties of the tills on either side of the margin, offers a possibility of mapping the margin automatically using TM imagery. A similar marginal position is shown by these different data sets, as discussed below.

The lake channels which occur between the numerous ridges at the Weichselian margin (Section 5.3.4) were first used to distinguish the Weichselian landscapes from those of older glaciations by Majdanowski (1949). Figure 7.1 shows only those TM band 5 values for images 187022 and 187023 which correlate with water. It can be clearly seen from Figure 7.1 that the margin is preceded by an abundant number of lakes. The inset shows that the dense region of lakes continues to the north and south, following the Weichselian Margin as proposed by Raukas *et al.* (1995).

The margin is also marked by a change in land use of the region. Figure 7.2 shows that the Weichselian margin is concordant with a band of forested land. The area may not be suitable for farming because of the large number of ridges and lake channels which exist there. Interestingly, it appears that several other margins drawn from the deglaciation map (Figure 6.5) are also marked by areas of forested land. This differentiation between forested and non-forested land at the ice margins becomes more obscure to the north where the land is mostly forested. To the south, land use is dominated by field boundaries.

The Weichselian margin can be delineated best using the TM data because of the change in the textural and spectral characteristics of the TM imagery across it (Section 7.1). Immediately north of the proposed margin, over the region thought to be covered by Weichselian till, the image is characterised by a rough texture with numerous knolls and ridges. The ridges are parallel with each other, grouped in sets of up to ten, and have lengths that vary from hundreds of metres to 4 km. The ridges are aligned perpendicular to the direction of ice flow. The observed lineations have indistinct margins and are less than 1.5 km in length.

Immediately south of the proposed margin the imagery has a texture not present in any of the regions towards the north. The area consists of fine strips of land, less than 500 m long and 100 m wide. These strips are thought to be related to land use. While the strips give the image

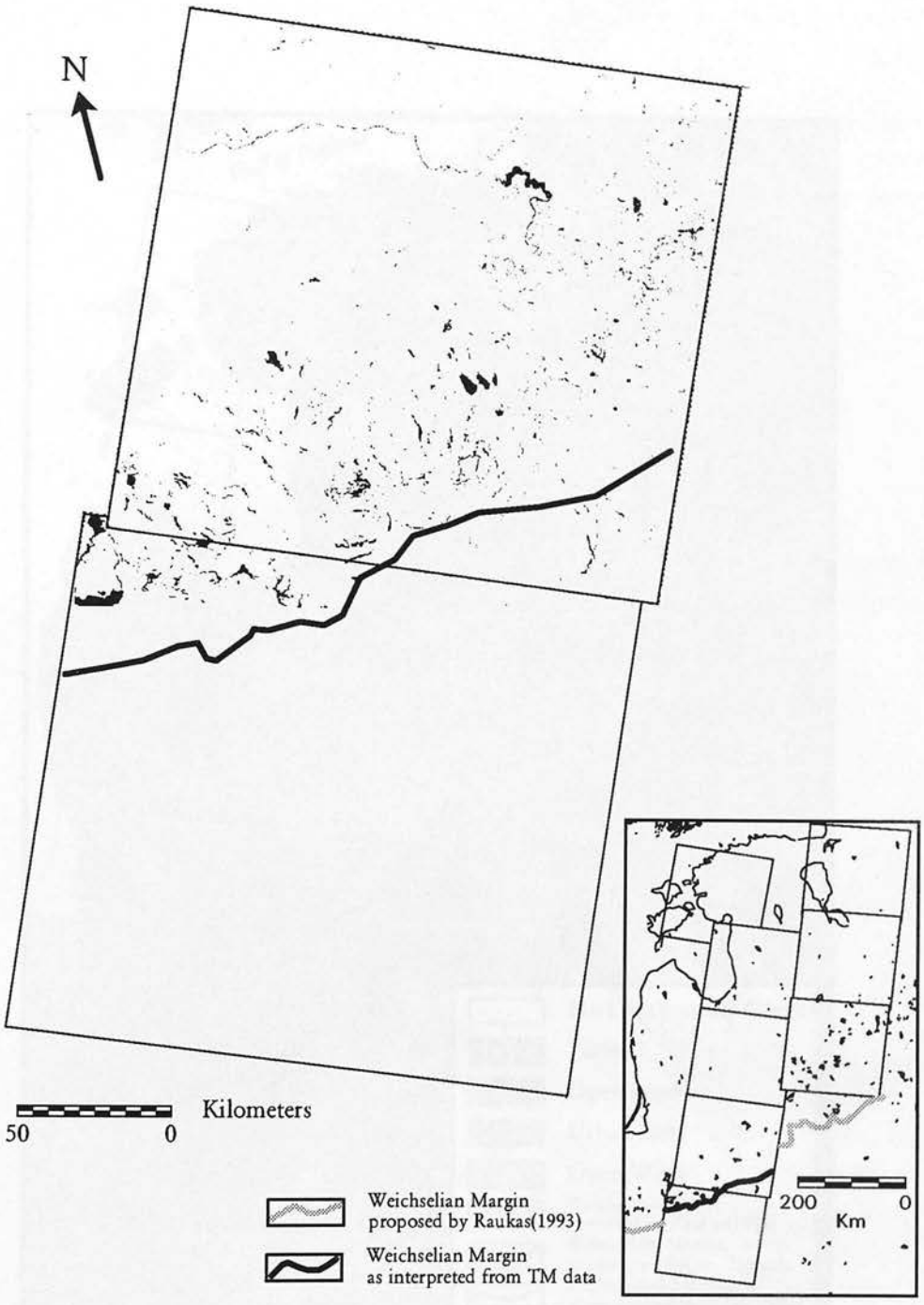

Figure 7.1: Regions of open water for Images 187022 and 187023. The Figure was constructed by showing only the TM band 5 values which correlate with open water. The inset shows all images, with Lakes taken from WDBII. In both the figure and inset, it can be seen that there is a greater number of lakes to the north of the Weichselian margin than to the south. The Weichselian margin shown is formed after considering all methods described in Section 7.1.

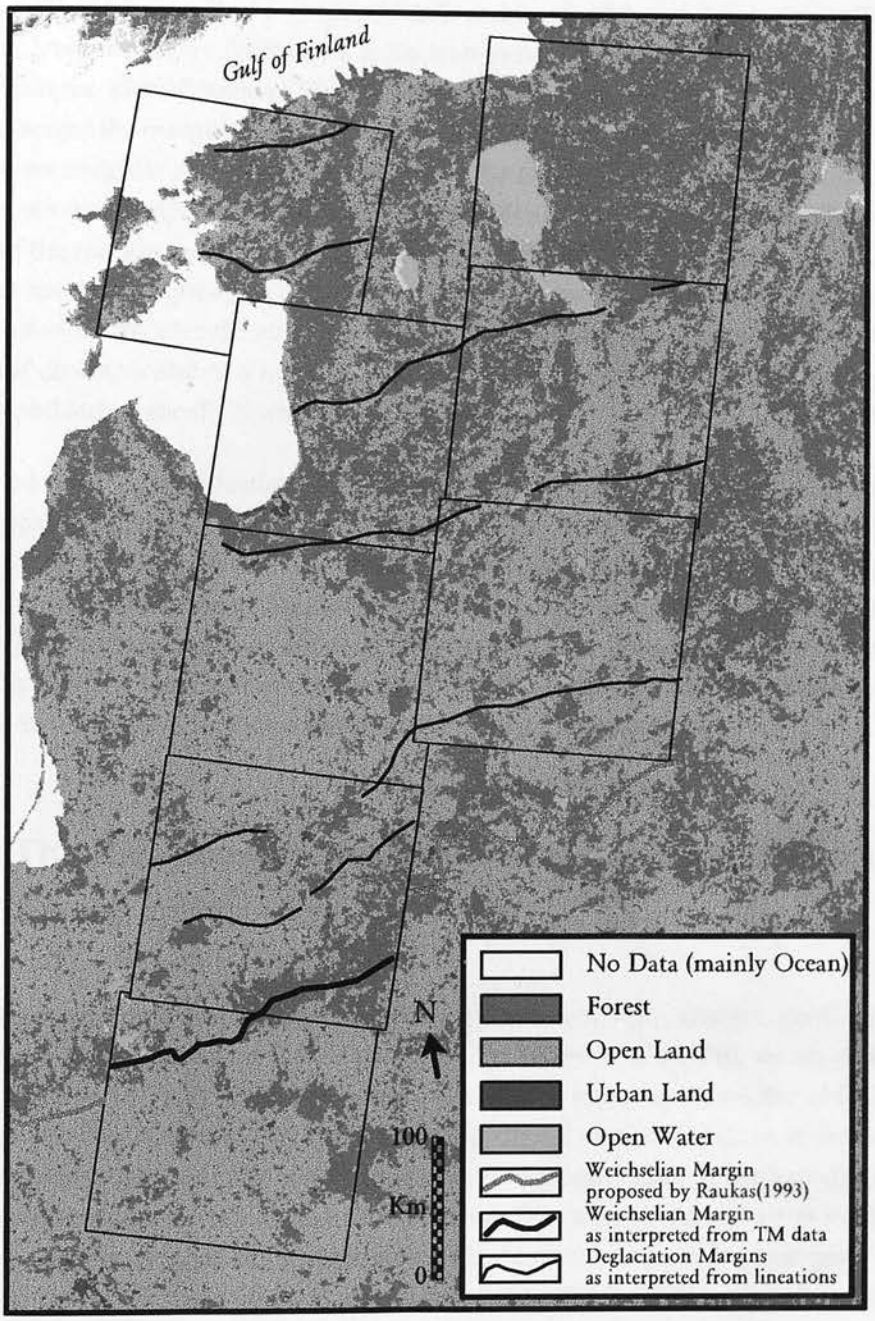

Figure 7.2: Land-use within the regions studied, using data from Sweitzer *et al.* (1996).

a high spatial frequency, they are regularly spaced and the region appears smoother than the area to the north. Lineations are difficult to distinguish across the regular pattern of strips and their glacial origin could not be confirmed. Since the region's texture is not present elsewhere, comparisons with other similar regions could not be made.

The transition between the two regions north and south of the margin is generally marked by forested land and rivers. Within the forested regions, the image has a monotone appearance, preventing the identification of lineations or other features. In a few places a direct change can be seen across the margin. Figure 7.3 shows this transition. The region to the north can be seen to have an irregular and rough texture, while the region to the south is smoother. Figure 7.3 also shows the change in the spectral characteristics of the imagery across the margin. To the north of the margin the intensity of the imagery is duller than that seen to the south, which is characterised by bright cyan. This is possibly due to the change in lithology of the soil from Weichselian till to older till material. Without acquiring further data it is unclear whether this is a local characteristic or a more general one which would allow the Weichselian margin to be mapped automatically from Landsat TM data.

While the origin of the lineations south of the proposed margin are uncertain, if they are glacial they appear to continue with the same trend as the lineations to the north of the proposed margin. They could represent older features which have a similar trend to the later lineations further north. Alternatively, the changes in lake frequency, spectral reflectance values, image texture and land use may not delineate the margin, but a change within the margin of the ice sheet. In this case the lineations to the south of the margin may be Weichselian in age and the Weichselian margin is further south than it is thought to be at present.

7.2 The Relationship Between Lineations and the Underlying Topography

It has been proposed that drumlins form on approximately flat ground, gently rising terrain (Aartolahti, 1968; Gluückert, 1973; Haavisto-Hyvärinen *et al.*, 1989), or on convex shaped ground (Aario, 1977a,b). However, assessment of such topographic relationships has usually been qualitative (Menzies, 1979). By analysing digital elevation data, a comparison can be made between the slope and aspect (direction of steepest slope) of the topography, and the lineations interpreted from the satellite imagery. The only digital elevation model available to date is for the present day topography. This, however, reflects the basement topography (Figure 2.4) and while the absolute values may differ, the direction and relative magnitude of the slope is considered to be applicable to the time period of lineation formation.

The digital elevation model consists of a grid of cells, each cell containing a topographic height. Using standard calculations (discussed fully in ERDAS 1995) two further grids were calculated showing slope (the maximum gradient from the cell to a neighbouring cell

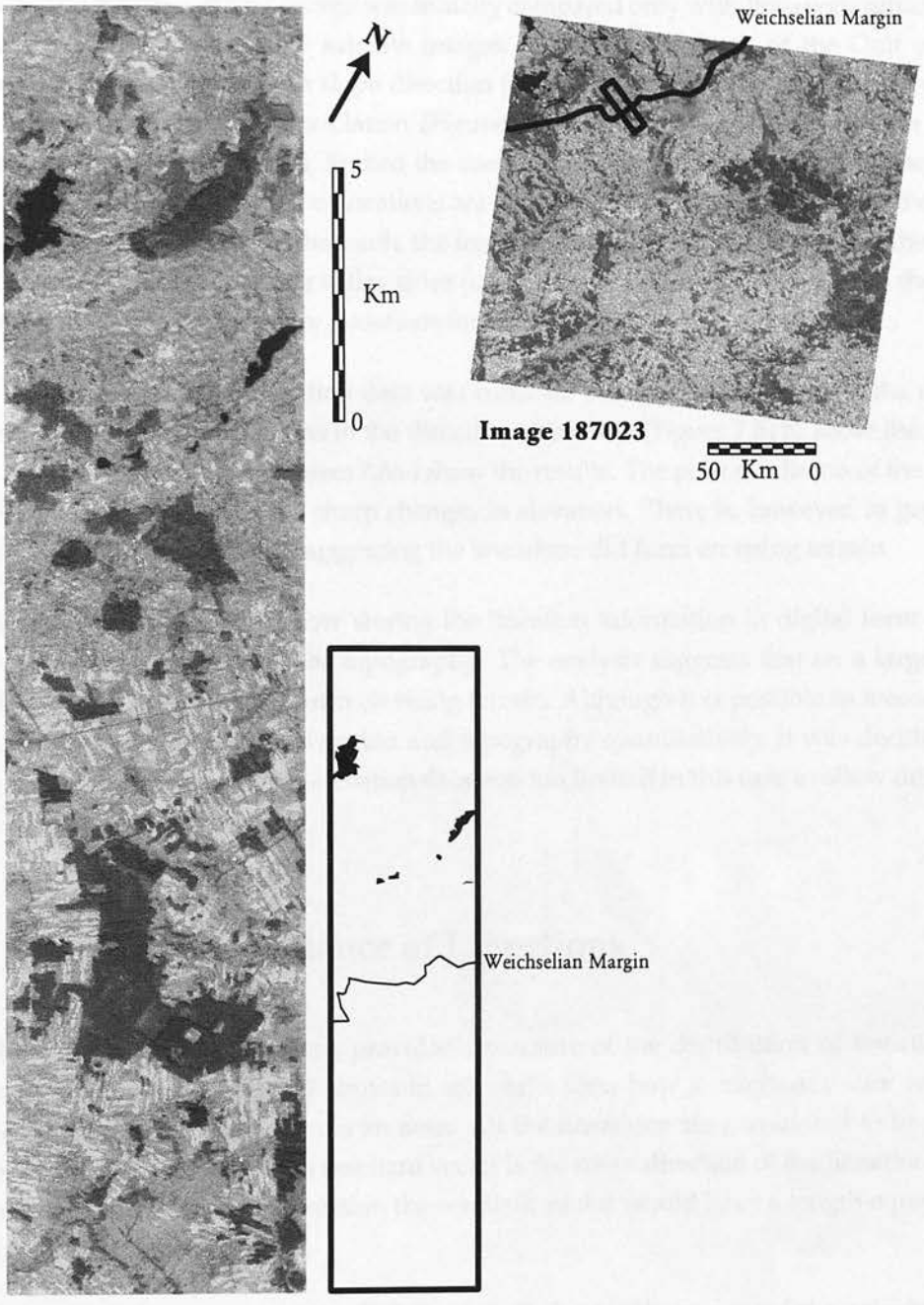

Figure 7.3: Transect across a change in image texture and brightness which, it is proposed, marks the maximum extent of the Weichselian ice.

Figure 7.4c) and aspect (downslope direction of this gradient Figure 7.4b) for each cell. For ease of comparison with the lineation data the two grids were merged into a single vector coverage where each grid point is represented by an arrow, scaled so that it is proportional to the slope, and pointing in the aspect direction (Figure 7.4a).

The slope and aspect vector coverage was initially compared only with lineations which were particularly well-defined on the satellite images. Towards the south of the Gulf of Riga the lineations were aligned with slope direction (Figure 7.5f); however, in general over the whole region there was little correlation (Figures 7.5a-e,g-i). The coarse resolution of the digital elevation model, however, limited the usefulness of the slope and aspect method. For example, in Figure 7.5g, where the lineations are between the Vidzeme Highland to the north and the Augšzeme Highland to the south, the frequency of data points is so low that the slope-aspect analysis is based upon the valley sides rather than providing information on the slope and aspect along the valley where lineations formed.

As an alternative method, elevation data was collected along transects through the regions containing well-defined lineations in the direction of ice flow (Figure 7.5) to show the topography along these flow lines. Figures 7.6a-i show the results. The poor resolution of the digital elevation data is reflected in the sharp changes in elevation. There is, however, in general a positive trend through the data suggesting the lineations did form on rising terrain.

The above analysis highlights how storing the lineation information in digital form allows it to be analysed in relation to the topography. The analysis suggests that on a large scale, the well-defined lineations did form on rising terrain. Although it is possible to measure the association between lineation formation and topography quantitatively, it was decided that the poor resolution of the digital elevation data was too limited in this case to allow definitive conclusions to be drawn.

7.3 The Circular Variance of Lineations

The circular variance of lineations provides a measure of the distribution of lineation orientations in a region. Figure 7.7 shows in schematic form how a resultant vector could be calculated from all the lineations in an area. All the lineations are considered to be of unit length, and the orientation of the resultant vector is the mean direction of the lineations. If all the lineations had the same orientation the resultant vector would have a length equal to the number of lineations measured.

The data gathered by Dongelmans (1996) across Finland only measured the orientation of lineations between 0^o and 180^o. To calculate the circular variance over these regions the

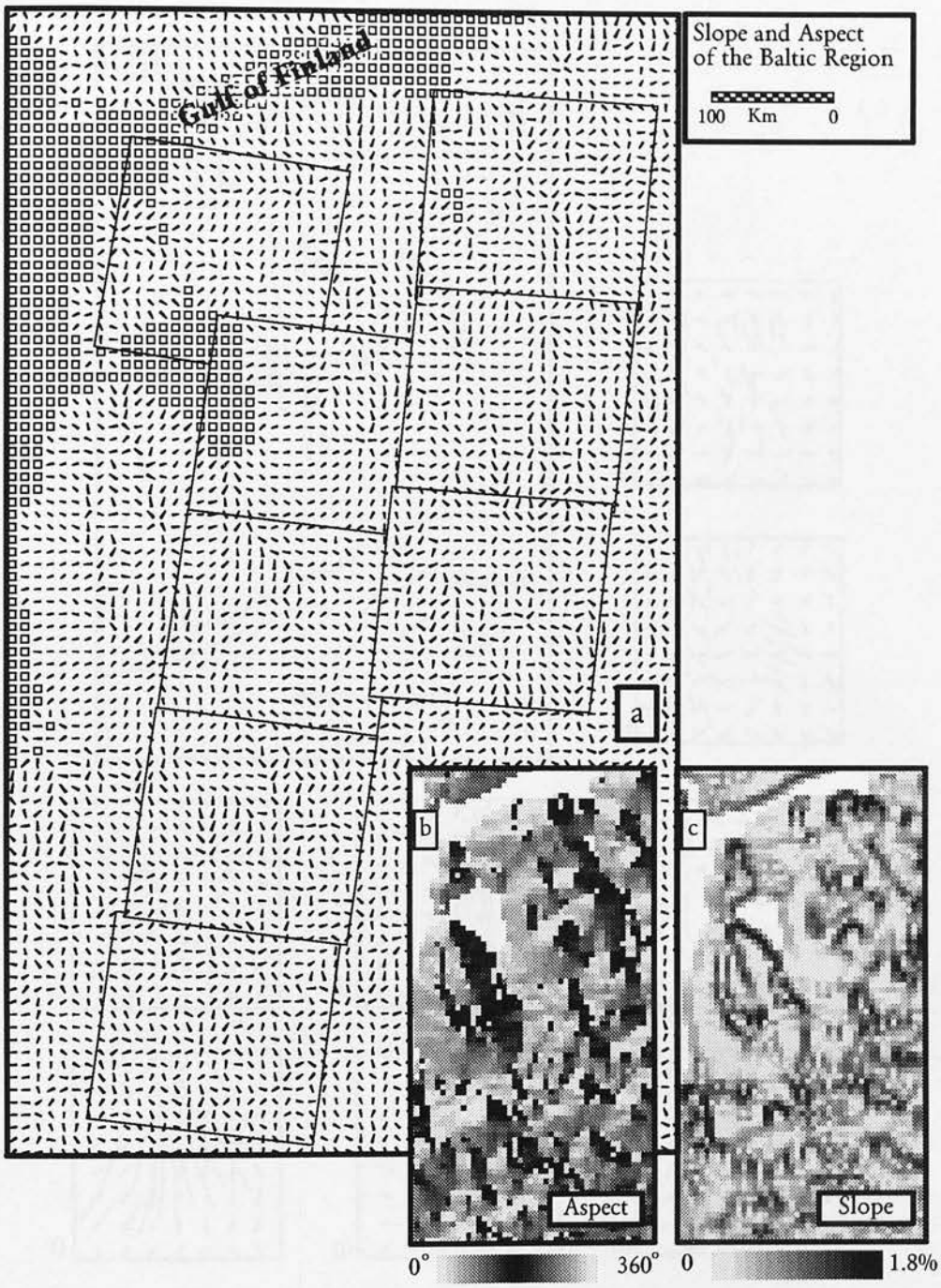

Figure 7.4: a) Slope and Aspect of the Eastern Baltic region. Each arrow points down slope and is drawn at a scale proportional to the slope gradient. b) Aspect of the Eastern Baltic region. c) Slope of the Eastern Baltic region.

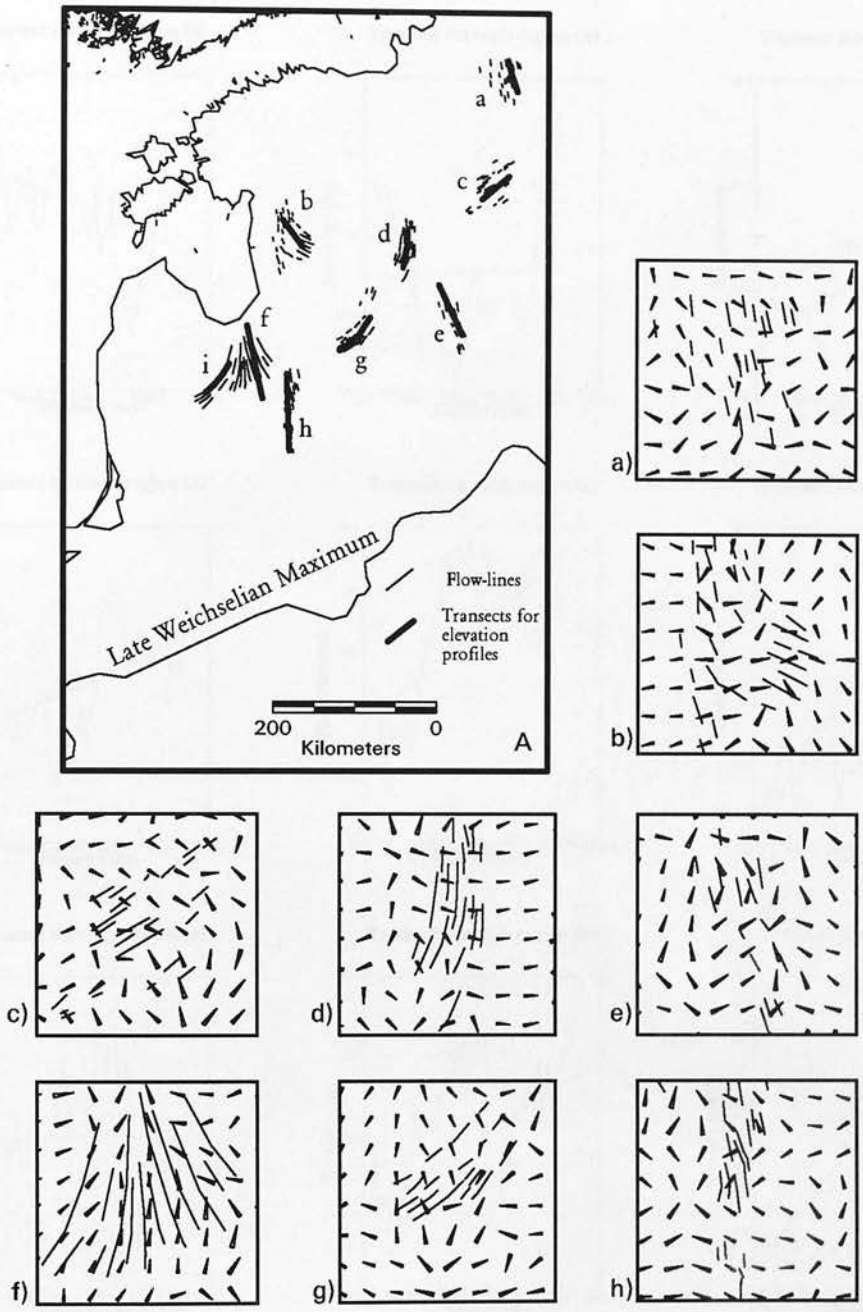

Figure 7.5: A. Areas with well-defined lineations shown by flow lines and labelled a-i. Thick lines mark transects shown in Figure 7.6

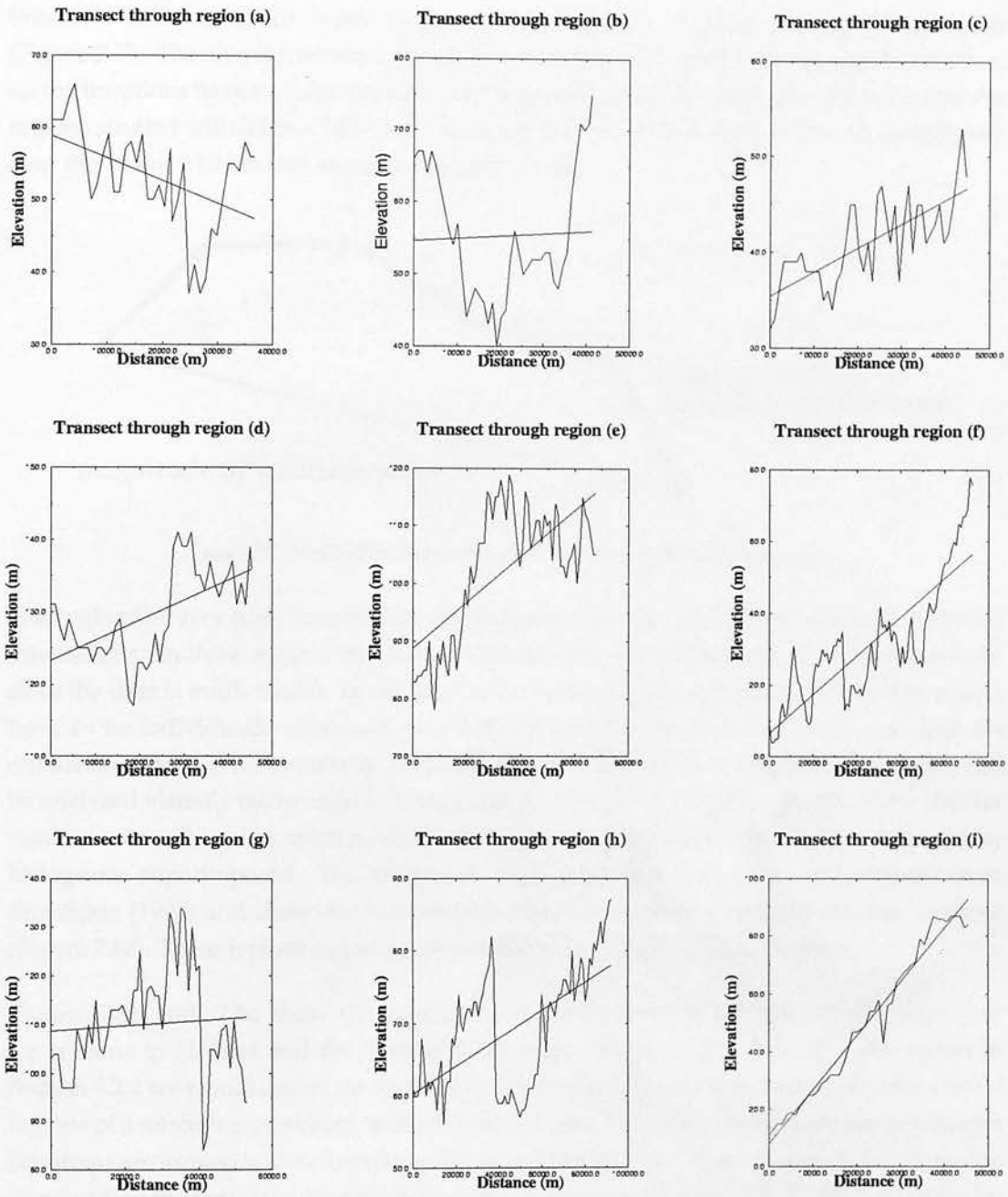

Figure 7.6. Elevation transects through the regions shown in Figure 7.5. Direction of ice flow is from left to right for each plot. For each transect, a linear line of regression is plotted to show the overall trend in elevation.

circular variance is calculated using equation (7.1) (Mardia,1972; page 26).

$$\text{Circular Variance} = 1 - \left(\frac{r}{n}\right)^{\frac{1}{4}} \tag{7.1}$$

Where, r is the resultant vector length of lineations and n is the number of lineations (Figure 7.7). The circular variance therefore varies between 0 and 1, being equal to 0 when all the lineations have the same orientation. Using equation (7.1) a grid was created across the regions studied with 5 km x 5 km cells. Each cell was given the value of the circular variance over the 10 km x 10 km region centred upon that cell.

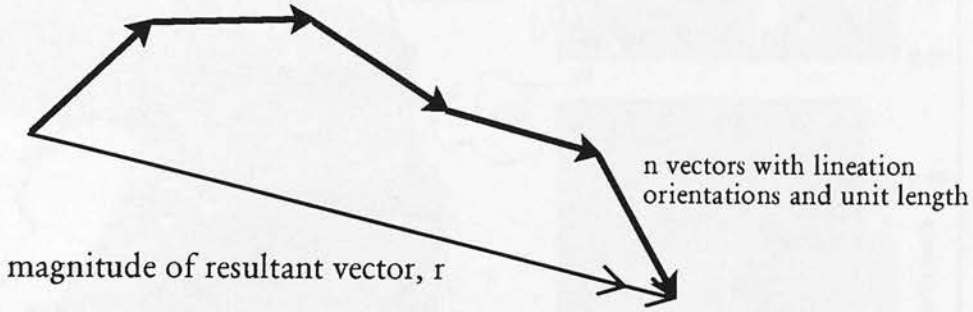

Figure 7.7: Method of calculating the resultant vector magnitude (r).

The regions of very high variance usually indicate areas containing flow sets with differing orientations. In these regions the circular variance should not be applied in the above form since the data is multi-modal. To calculate the variance in these regions each lineation would have to be individually attributed to a flow set and the mean direction of each flow set calculated, which is an intractable problem. The distribution of orientations in a region can be analysed visually using angular histograms (Fischer, 1995). Figure 7.8 shows the circular variance of the lineation orientations for Finland and the Eastern Baltic region with angular histograms superimposed. The histograms were calculated using programs adapted from Broadgate (1997) and show the multi-modal nature of regions with high circular variance (Figure 7.8c). These regions can occur over both lowland and highland regions.

Figures 7.8b and 7.8d show the values of circular variance of lineation orientations over ice streams in Finland and the Eastern Baltic region respectively. From the discussion in Section 4.2.2 we would expect the variance in the lineation orientations to be low in the central regions of a retreating ice stream, while the outer edges will have a higher variance as younger lineations are formed with orientations diverging from the central axis (Figure 4.9). The region surrounding the Burtnieks drumlin field shows this pattern (Figure 7.8d), as do three of the ice streams interpreted from the lineation data by Dongelmans (1996) and depicted in Figure 7.8a.

It can also be seen from Figure 7.8a that the variance of lineation orientations are generally higher in the Eastern Baltic region than in Finland. This is also shown by the angular histograms in Figures 7.8b and 7.8d. It is thought that the majority of lineations formed during the final deglaciation (Chapter 6, Dongelmans, 1996) and it is shown in Chapter 8 that these

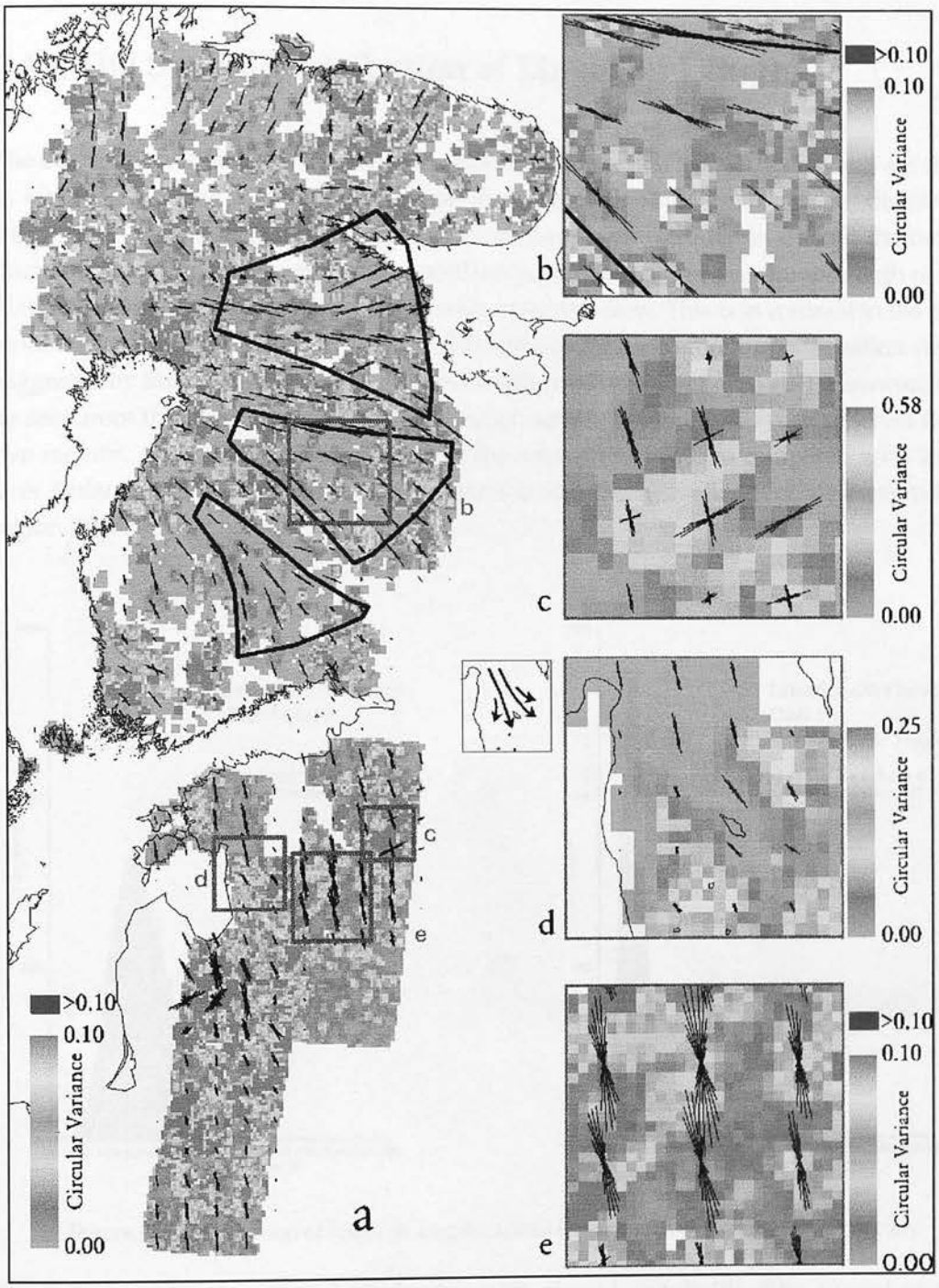

Figure 7.8: Spatial distribution of lineation orientations shown by angular histograms and circular variance values.

lineations are most likely to have formed near the retreating margin. The higher variance of lineation orientations over the Eastern Baltic region may therefore indicate a retreating margin which was more irregular in its retreat here than over Finland.

7.4 The Spatial Distribution of Lineation Length

The distribution of lineation lengths in the Eastern Baltic region and across Finland are shown in Figure 7.9. Using a bin width of 20 m, the histograms show a very 'clean' distribution suggesting that a sufficient number of lineations have been recorded to smooth the random fluctuations which have been superimposed upon the background distribution. Both of these diagrams show a uni-modal distribution with a positive skew. This is in contrast to the multi-modal distribution proposed by Clark (1993) and supports a continuum of lineation sizes as suggested by Rose (1987), Boulton and Hindmarsh (1987) and Boulton (1987). However, it can be seen from the two diagrams that the lineation length distribution is very different for the two regions. Over the Eastern Baltic region the mean value is 655 m compared with 1654 m over Finland. The variance of the distributions is also much smaller over the Eastern Baltic region than across Finland.

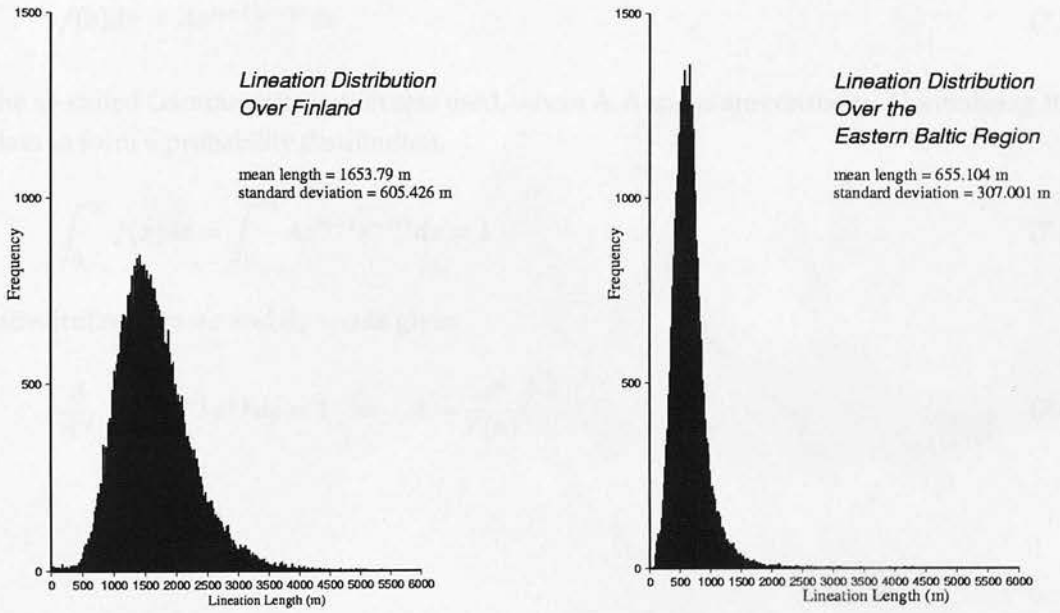

Figure 7.9: Distribution of lineation lengths across Finland and the Eastern Baltic region.

The information gathered across Finland was interpreted and digitised by several workers. Ideally, we should ensure that the different distributions were not solely the result of different operators interpreting the imagery. This may have been achieved by re-interpreting part of the imagery of Finland used by Dongelmans (1996) and comparing the new results with his earlier interpretations. Unfortunately the imagery was no longer available. However, the

difference between interpretations made using Landsat TM imagery from Finland (d7, d8, c7 Figure 7.10) and those from the Eastern Baltic region is thought to be too great to be explained as sampling bias of different operators.

Figure 7.10 shows how the length distribution varies spatially. It can be seen from this figure that the sharp difference between Finland and the Eastern Baltic region is superimposed upon a general north-south trend in the distribution shape. In the north the lineation length distribution is very broad with a high mean value. Towards the south the mean length decreases, and the distribution narrows. This north-south trend can be seen more clearly in the inset to Figure 7.10 which shows the frequency length distribution for the regions b7, b5, b3 and b1. The spatial distribution of the mean lineation length was investigated further using glaciological models and is discussed in Section 7.4.

An attempt was made to characterise the data using a known distribution. Achieving this has several benefits for studying glacial lineations: (1) the length distribution can be characterised by a few parameters allowing easy comparison of the distribution between different regions; (2) knowledge of the length distribution can be used by workers trying to model the formation of lineations; (3) fitting the data to a known distribution may provide an insight into the processes which form lineations. Considering the positive skewness of the data and the long tail, a distribution of the form

$$f(x)dx = Ax^{n-1}e^{-\alpha x}dx \tag{7.2}$$

the so-called Gamma distribution was used, where A, n and α are constants. Normalising the data to form a probability distribution,

$$\int_0^\infty f(x)dx = \int_0^\infty Ax^{n-1}e^{-\alpha x}dx = 1 \tag{7.3}$$

substituting $y = \alpha x$ and $dy = \alpha dx$ gives

$$\frac{A}{\alpha^n}\int_0^\infty y^{n-1}e^{-y}dy = 1 \quad \Rightarrow \quad A = \frac{\alpha^n}{\Gamma(n)} \tag{7.4}$$

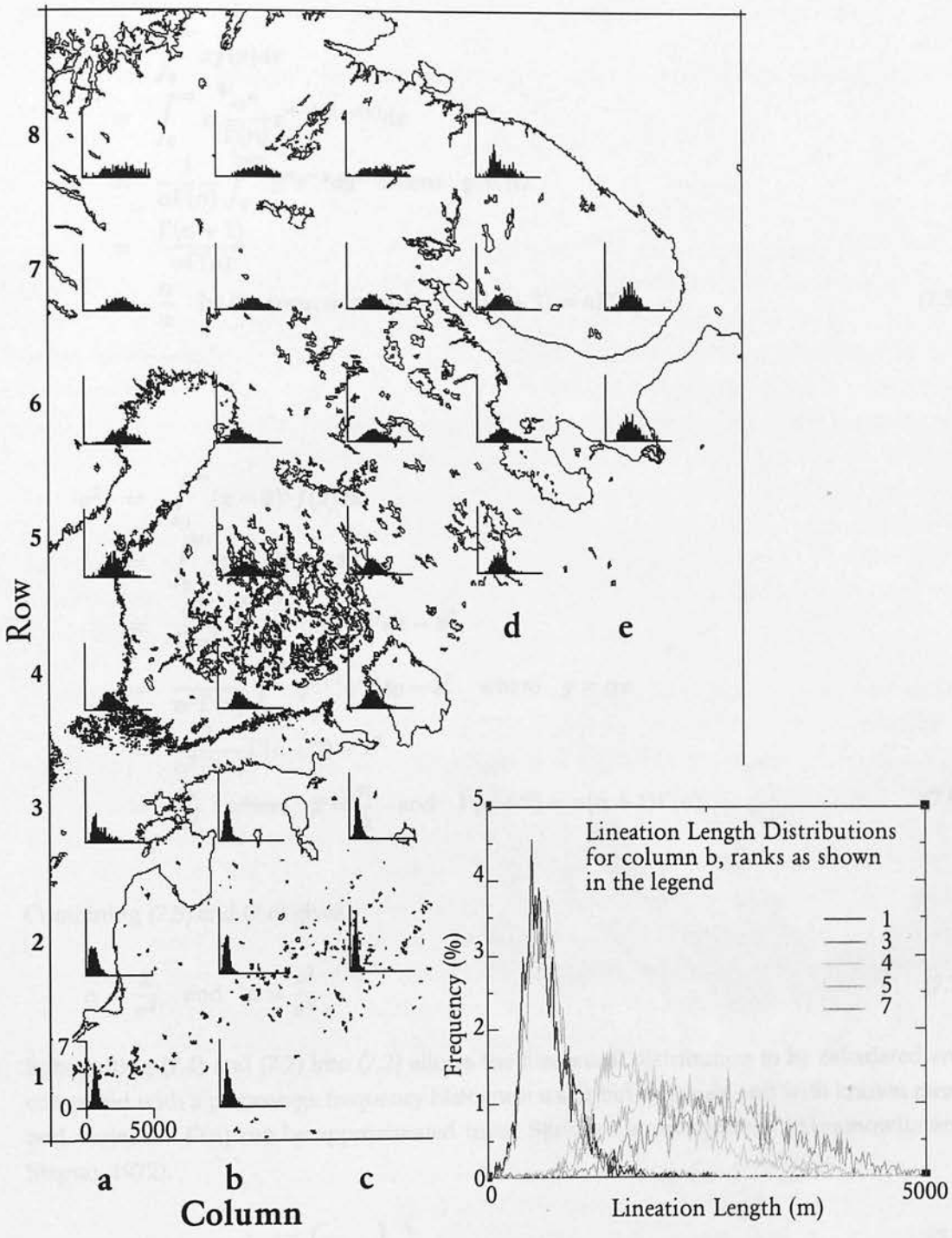

Figure 7.10: Distributions of Lineation lengths, plotted using 20 m bins, for 300 km x 300 km regions across Finland and the Eastern Baltic region. Inset shows the plots for the regions b1, b3, b4, b5 and b7.

where the integral is the Gamma function $\Gamma(n)$ (Abramowitz and Stegun, 1972). The coefficients n and α are defined by the mean ($\bar{x}$) and variance (σ^2) of $f(x)$.

$$\begin{aligned}
\bar{x} &= \int_0^\infty x f(x) dx \\
&= \int_0^\infty x . \frac{\alpha^n}{\Gamma(n)} x^{n-1} e^{(-\alpha x)} dx \\
&= \frac{1}{\alpha \Gamma(n)} \int_0^\infty y^n e^{-y} dy \quad \text{where} \quad y = \alpha x \\
&= \frac{\Gamma(n+1)}{\alpha \Gamma(n)} \\
&= \frac{n}{\alpha} \quad \text{by the recursion relation} \quad \Gamma(n+1) = n\Gamma(n)
\end{aligned} \tag{7.5}$$

$$\begin{aligned}
\sigma^2 &= \int_0^\infty (x - \bar{x})^2 f(x) dx \\
&= \int_0^\infty x^2 f(x) dx - \bar{x}^2 \\
&= \frac{\alpha^n}{\Gamma(n)} \int_0^\infty x^{n+1} e^{(-\alpha x)} dx - \bar{x}^2 \\
&= \frac{1}{\alpha^2 \Gamma(n)} \int_0^\infty y^{n+1} e^{-y} dy - \bar{x}^2 \quad \text{where} \quad y = \alpha x \\
&= \frac{1}{\alpha^2 \Gamma(n)} \Gamma(n+2) - \bar{x}^2 \\
&= \frac{n}{\alpha^2} \quad \text{where} \quad \bar{x} = \frac{n}{\alpha} \quad \text{and} \quad \Gamma(n+2) = n(n+1)\Gamma(n)
\end{aligned} \tag{7.6}$$

Combining (7.5) and (7.6) gives

$$\alpha = \frac{\bar{x}}{\sigma^2} \quad \text{and} \quad n = \frac{\bar{x}^2}{\sigma^2} \tag{7.7}$$

Substituting (7.4) and (7.7) into (7.2) allows the theoretical distribution to be calculated and compared with a percentage frequency histogram using bin-width dx and with known mean and variance. $\Gamma(n)$ can be approximated using Stirling's approximation (Abramowitz and Stegun, 1972).

$$\Gamma(n) \approx e^{-n} n^{n-\frac{1}{2}} \sqrt{2\pi} \left(1 + \frac{1}{12n}\right) \tag{7.8}$$

Figure 7.11 shows histograms of the raw data compared with the theoretical distributions. It can be seen from this Figure that the theoretical distribution fits the data values best towards

the north. Across the Eastern Baltic region, and in some of the lower regions in Finland, the fit is less good, the data peak being under-represented and the tail being too shallow. This lack of fit towards the south is shown more clearly in Figure 7.12. Closer examination of the tail, suggests that towards the south the data may be better represented by a power-law.

The power-law distribution may be defined using the cumulative distribution function (Pickering *et al.*, 1995).

$$N = cl^{-D} \quad \Rightarrow \quad \log(N) = \log(c) - D\log(l) \tag{7.9}$$

where l is the lineation length and N is the cumulative number of values $\geq l$, c is a normalising constant and D is the exponent. The definition can describe the distribution at all scales, is independent of interval choice and embodies the hierarchal nature of power-law distributions (Pickering *et al.*, 1995). The shape of the power law distribution is not, however, representative of the lineation length distributions observed. This is as expected since a power-law distribution for the exponents observed must be physically truncated, or an infinite amount of material would be required to form the smaller lineations. In addition the data sample may be biased. All data sets represent samples from a population of values. If this sample excludes certain types of values the sample is biased, and is not representative of the population. By analogy with rock fracture studies (for example Einstein and Baecher 1983), we may expect two common biases in measuring the size of glacial lineations: truncation and censoring.

If the size of lineations which may be measured is limited by either the resolution of the method or the Instantaneous Working Area (IWA), then the sample will be truncated. Using Landsat TM imagery there is a lower theoretical limit of 60 m on the size of lineations which can be measured, although practically the limit is about 150 m (Section 4.2.1). As this limit is approached there will be a loss of information. Data within this region is not representative of the distribution and should be excluded from the analysis. By using digital data, the IWA can be increased to include the whole image, approximately 186 x 186 km, and this can be further increased by adding congruent images. The spatial resolution at which an IWA can be viewed is limited, however, by the scale of the computer screen. It may be that very large lineations are not observed because they are not resolved at the scale required to view the IWA which contains the lineations. The lineations recorded in this study were measured at a scale of 1:100,000 with an IWA of 400-900 km^2.

Censoring occurs when some, or all of the values within a sample are systematically under- or over-estimated. In fracture length statistics (Pickering *et al.*, 1995) three types of censoring can be defined. They are also applicable to the measurement of glacial lineations using satellite imagery: (1) lineations longer than the IWA will be underestimated; (2) lineations which extend beyond the image coverage area will be underestimated; and (3) with limited resolution the tips of lineations cannot be observed and the length of lineations will be underestimated. In the study of rock fractures, corrections have been made for censoring using assumptions based on the relationship between parameters such as displacement,

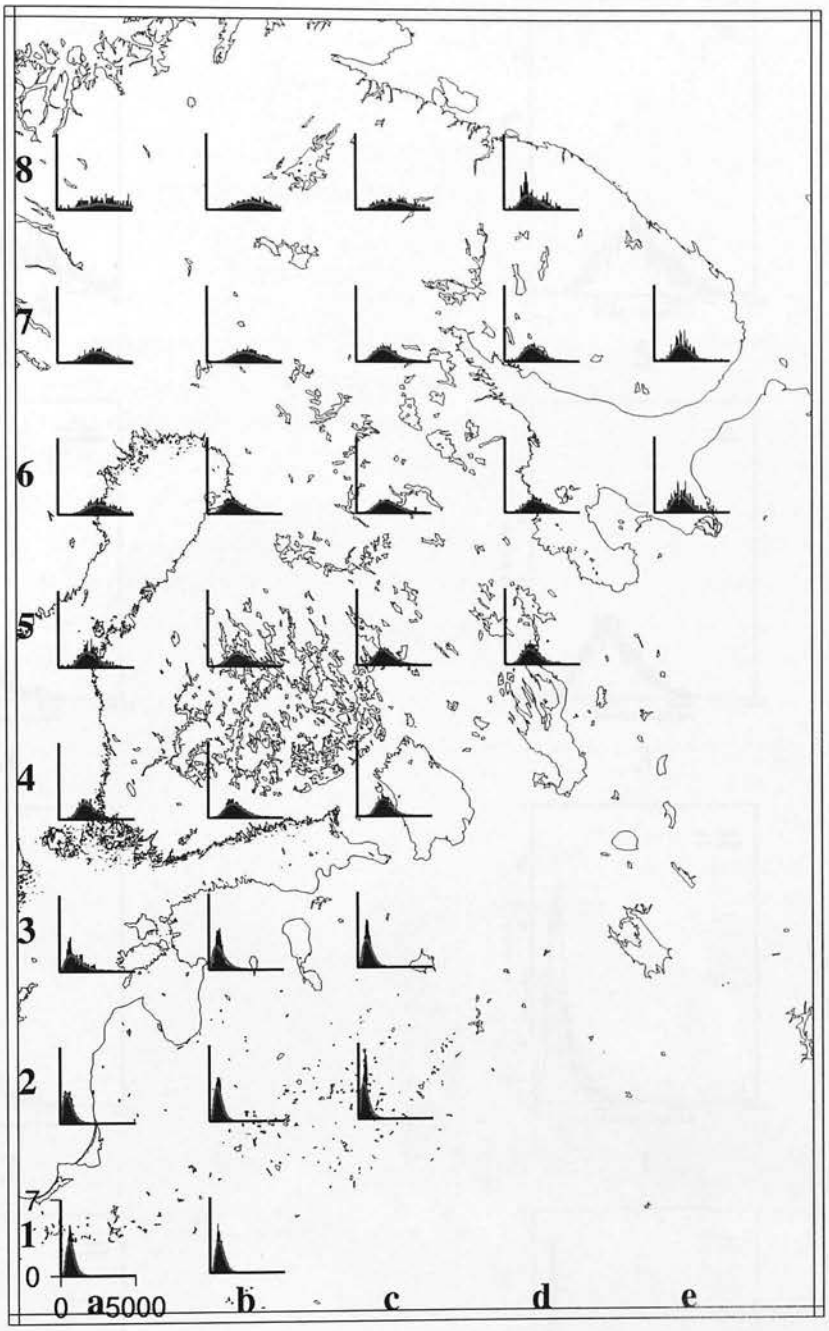

Figure 7.11: Lineation length distributions compared with theoretical distributions within 300 km x 300 km regions across Finland and the Eastern Baltic region.

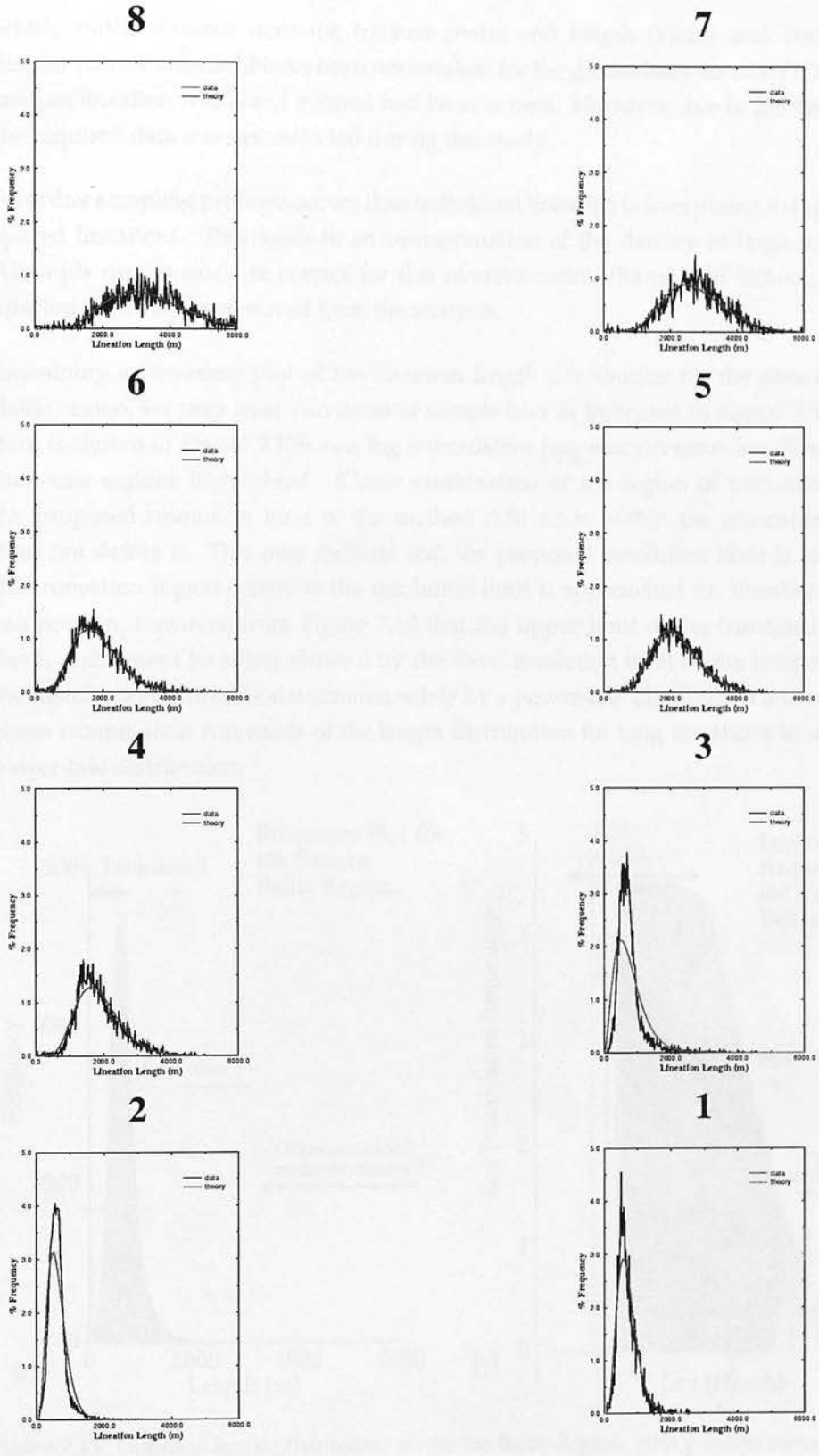

Figure 7.12: Plots of measured (black) and theoretical (red) distributions of lineation length. The plots are numbered 8-1 and are equivalent of the eight north-south plots in column b of Figure 7.11.

width, radial distance from the fracture centre and length (Walsh and Watterson, 1988). Similar corrections could have been undertaken for the glacial lineation data if measurements such as lineation width and volume had been known. However, due to the time limitations, the required data was not collected during this study.

A further sampling problem occurs if an individual lineation is interpreted to represent closely spaced lineations. This leads to an overestimation of the density of large-scale lineations. Attempts can be made to correct for this overestimation (Baron and Zoback, 1992), or the affected data may be removed from the analysis.

Examining a frequency plot of the lineation length distribution for the data in the Eastern Baltic region, we may infer two areas of sample bias as indicated in Figure 7.13a. The same data is shown in Figure 7.13b as a log (cumulative frequency) versus log (length) plot with the same regions highlighted. Closer examination of the region of truncation shows that the proposed resolution limit of the method (150 m) is within the truncation region, and does not define it. This may indicate that the proposed resolution limit is too low or that the truncation region occurs as the resolution limit is approached for lineations < 500 m. It can be seen, however, from Figure 7.10 that the upper limit of the truncated region is not fixed, and cannot be solely defined by the fixed resolution limit of the imagery. Therefore, the distribution cannot be determined solely by a power-law distribution and sample bias. A closer examination was made of the length distribution for long lineations to see if this fits a power-law distribution.

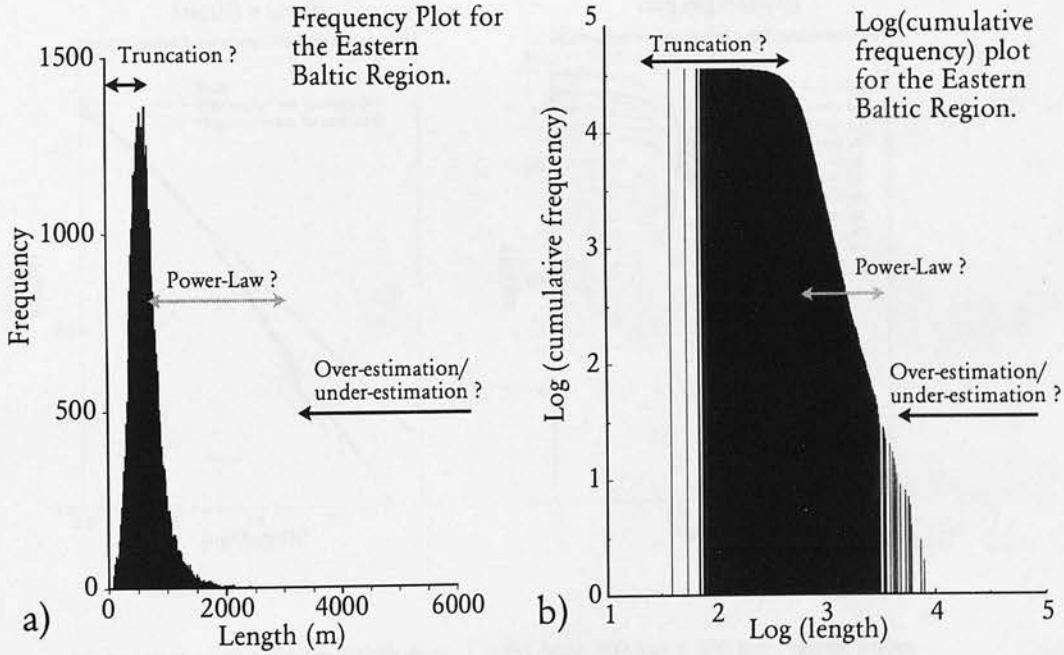

Figure 7.13: Lineation length distribution across the Baltic Region, with possible areas of sample bias indicated if the distribution is assumed to be modelled by a power-law.

Figure 7.14a shows a log-log graph of the lineation length distribution across the Eastern Baltic

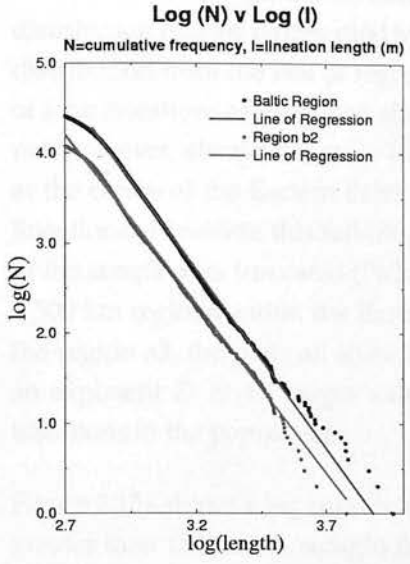

(a) Two distributions with linear regressions: (1) All lineations across the Eastern Baltic region; (2) the central region of the Eastern Baltic region, b2 (shown in Figure 7.11)

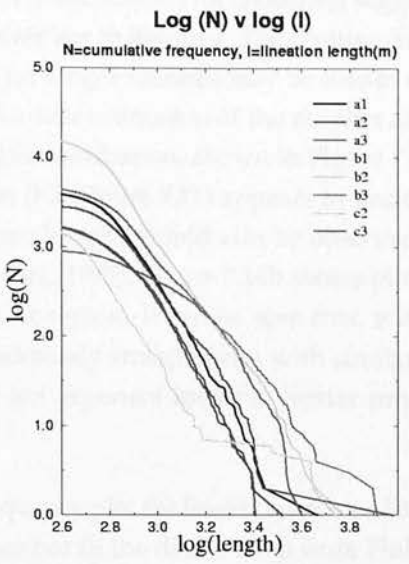

(b) Eight 300 km x 300 km regions across the Eastern Baltic region, labelled with the row number and column letter as shown in Figure 7.11

Figure 7.14: Cumulative frequency distributions of lineation length across the Eastern Baltic region

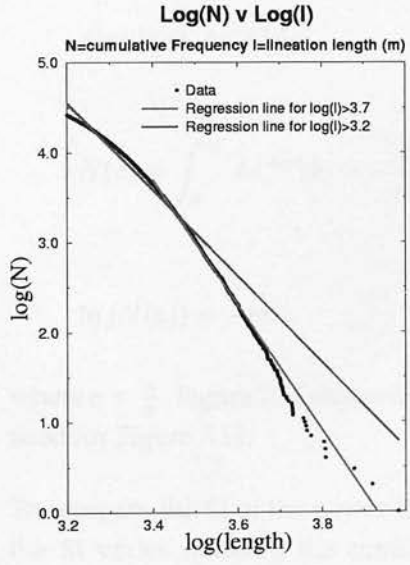

(a) All lineations across Finland with two lines of linear regression: (1) for lengths $> 10^{3.7} m \approx 5010\ m$ and (2) lengths $> 10^{3.2} m \approx 1580\ m$

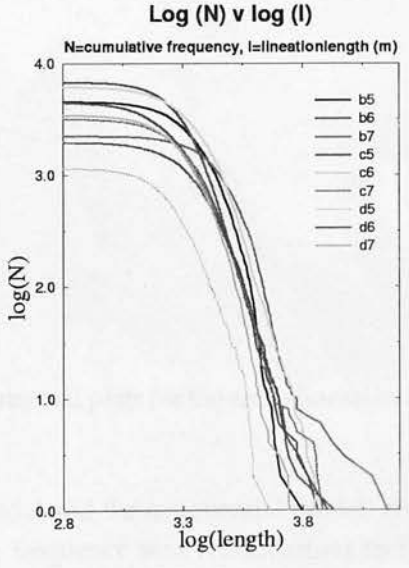

(b) Nine 300 km x 300 km regions across Central Finland, labelled with the row number and column letter as shown in Figure 7.11

Figure 7.15: Cumulative frequency distributions of lineation length across Finland

region for lineation lengths greater than 500 m. It can be seen that the plot provides a good fit to a straight line. A good fit of data which is uncorrected for censoring suggests that the length distribution may be represented by a power law in this area. The positive deviation of the data distribution from the line of regression for longer features may be due to an over-estimation of long lineations as discussed above. An over-estimation of the number of large lineations is not, however, always the case. The length distribution, shown in Figure 7.14a, for the region at the centre of the Eastern Baltic region (b2, Figure 7.11) appears to under-represent longer lineations. However, this fall-off at longer lengths would also be observed if the scale range of the sample was truncated (Pickering *et al.*, 1995). Figure 7.14b shows plots for eight 300 km x 300 km regions within the Eastern Baltic region. It can be seen that, with the exception of the region a3, the plots all show approximately straight lines with similar gradients, giving an exponent $D \approx 4$. Larger values of the exponent imply a greater proportion of smaller lineations in the population.

Figure 7.15a shows a log cumulative frequency plot for lineations across Finland with lengths greater than 1500 m. A straight line does not fit the distribution from Finland as well as the distribution from the Eastern Baltic region. Close examination shows a systematic difference between the data values and the straight line, with the data values initially over-estimated, then under-estimated and finally over-estimated. A similar pattern is observed across Finland (Figure 7.15b).

For comparison the same data shown in Figure 7.15b was modelled by an exponential function of the form

$$f(x)dx = Ae^{-\alpha x}dx \tag{7.10}$$

$$N(x) = \int_x^\infty Ae^{-\alpha x}dx = -\frac{A}{\alpha}e^{-\alpha x} \tag{7.11}$$

$$ln\,(N(x)) = -cx \tag{7.12}$$

where $c = \frac{A}{\alpha}$. Figure 7.16 shows the log-normal plots for the same lineation length distribution used for Figure 7.15.

To compare the fit of the power-law model and the exponential model, and to examine how the fit varies spatially, the cumulative frequency was renormalised to form a probability distribution $p(x)$.

For regions from column b (Figure 7.11) with >200 lineations, the values where $0.01 < p(x) < 0.1$ were plotted as log(p(x)) against log (length) and log(p(x)) against length. For these plots the linear regression was calculated. Table 7.1 shows the calculated regression correlation coefficients. Over areas of the East European Platform the distribution appears to be better

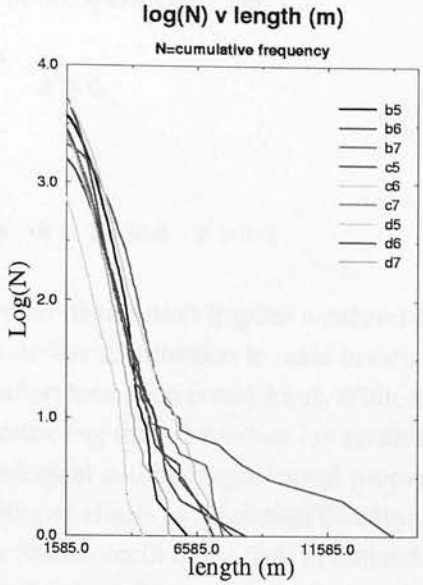

Figure 7.16: Log-normal plot of the same data used for Figure 7.15

expressed as a power-law than as an exponential function, while over the Baltic Shield a better fit is found by using an exponential function. There does not appear to be a gradual transition between these two regions, suggesting that the data consists of two separate data sets, supporting the initial observation that there is a distinct change in the distributions north and south of the Gulf of Finland.

Geology	Region (Figure 7.11)	No. Lineations	1 - |Correlation Coefficient|	
			log-log	log-normal
East European Platform	b2	1573	0.0005871	0.0019415
	b3	415	0.0006903	0.007345
Baltic Shield	b4	401	0.0061024	0.0025848
	b5	411	0.0062828	0.0040696
	b6	407	0.0045974	0.0020979

Table 7.1: Linear regression correlation coefficients of the plots log(N) v log(length) and log(N) v length for 300 x 300 km regions along column b (Figure 7.11).

The poor fit of the power-law distribution to the lineation data across Finland suggests that either the power-law distribution is a poor model of the distribution, or that sample biases are significant. As mentioned earlier, further corrections were not possible with the data set used within this study, and more detailed analysis would be required to verify possible effects of sample bias. It is perhaps significant that other workers using different lineation data sets across Sweden have also been unable to model length distributions using the Pareto cumulative distribution (Patrik Vidstand, personal communication), shown below, which for

$x >> 1$ is similar to equation(7.9) (Turcotte, 1997).

$$f(x) = \left(\frac{k}{(k+x)}\right)^{a} \quad x \geq 0 \tag{7.13}$$

$$f(x) \approx x^{-a} \quad \text{where} \quad k = 1 \quad \text{and} \quad x >> 1 \tag{7.14}$$

A better fit to an exponential distribution implies a natural length scale for the formation of lineations, while the power-law distribution is scale invariant. A natural length scale may exist if the process of lineation formation is restricted. While the genesis of lineations is poorly understood the factors restricting their formation are an area of speculation only. However, it is thought that the rheological and hydrogeological properties of bed sediments influence the erosional and depositional effects of glaciation (Boulton, 1996). The change in geology from the crystalline Baltic Shield, north of the Gulf of Finland, to the sedimentary rocks of the Eastern Baltic region have been used to explain variations in the glaciofluvial activity of the ice sheet (Clark and Walder, 1994; Boulton, 1987). Considering the better fit of the exponential distribution over the Baltic Shield suggests that local geology may be restricting lineation formation, either by limiting sediment supply or by having physical properties unsuitable to lineation formation. The better fit of the power-law distribution across the East European Platform suggests that here the lineations are not as restricted by physical properties in their formation. It would also suggest an interconnected system where subglacial deformation in one area, influences deformation in other areas.

Summary

There appears to be a general southwardly decreasing trend in mean lineation length and in the spread of values about the mean. Superimposed upon this general trend, the Gulf of Finland appears to delineate a distinct change in the form of the distribution. An attempt was made to model the sample distribution using the function defined in equation (7.2). The exponential tail of this function appears to fit the data values well towards the north, but less well towards the south. It is possible that the shape of the distribution could be explained partly by sampling biases. However, the resolution limit of the imagery can not account entirely for left-hand truncation of the sample distributions. This implies that either other sampling biases exist which have not been accounted for, or that the data values really do represent the underlying distribution. In either case, closer inspection of the tail of the sample distribution can provide useful information about the underlying distribution form. Over areas of the East European Platform the sample distribution appears to be better expressed as a power-law than an exponential function, while over the Baltic Shield a better fit is found using an exponential function. There does not appear to be a gradual transition between these two regions, suggesting that the data consists of two separate data sets supporting the initial observation that there is a distinct change in the distributions north and south of the Gulf of Finland. It is speculated that this distinct change is related to the variation in underlying geology (Chapter 2) limiting the formation of lineations across the Baltic Shield.

Chapter 8

Comparison of Lineation data with a Glaciological Model

Section 7.4 described analysis of the spatial distribution of lineation lengths and compared various mathematical models of the distribution from the ice divide to the maximum limit of ice. Boulton (1996) suggests that the length of drumlins within a region is a function of the deforming rate and the occupancy time of ice in that area. A glaciological model was used to explore whether the predictions of this theory agreed with the observed distribution. The model was originally developed by Boulton and Payne (1992) and the results used in this analysis were derived from an application of the model by Boulton *et al.* (1995). A summary of the mathematics and techniques behind the ice physics are summarised in Boulton and Payne (1992). A brief explanation of the basis of the model is given below.

8.1 Model Description

The model is driven by specifying time-dependent changes to the Equilibrium Line Altitude (ELA) and the sea-level temperatures. The ELA is the notional altitude for any given sector of the glacier where the surface mass balance is zero. Below this altitude there is more melting than snowfall over a period of a year. Above the ELA snow accumulation is greater than the total melt. For a given ELA the model mass-balance field can be raised or lowered. The sea-level temperature is used to calculate the temperature boundary condition at the surface of the ice sheet using a lapse rate of 10°C/km. Other input parameters include basal topography and the constants relating to the physical behaviour of the ice and bedrock adjustment (caused by the overlying weight of ice).

The output parameters are calculated for points spread throughout the ice sheet. In the horizontal, points are regularly spaced every 20 km. In the vertical the ice sheet is represented

by ten ice layers whose thickness varies while remaining a constant proportion of the total ice thickness at a particular point. The spacing of the points decreases with depth to improve the resolution of the larger strain rates and temperature gradients towards the base of the ice sheet. The model is restricted to two dimensions to increase the model return speed. A flow line model is appropriate where the ice flow direction does not change much through time, which is the case for the transect used in this study.

Using the input parameters the evolution of the ice sheet is simulated by estimating for each point the amount of snowfall or melt and also the amount of ice flowing to other areas. The model time increments are in twenty year intervals. For each increment the internal flow, external mass exchange and surface elevations are updated. The model also produces values of internal temperature, basal temperature, basal melt rate and ice balance velocity. The two parameters used in this application are the ice balance velocity (m/a) (referred to as the ice velocity) and the basal melting rate (mm/a). These parameters have been calculated for each point along a transect through Sweden for each 1000 year period from 700 ka until the present day. A transect through Finland and the Eastern Baltic region, where the satellite imagery was gathered would have been preferred, but model output was only available for Sweden. The model has thus been used as a general description of a transect through the Fenno-Scandinavian ice sheet from the ice divide to the ice margin for the last 700,000 years.

8.2 Location of Lineation Formation

Figure 8.1a shows the ice balance velocity profile along a transect and how this profile changes with time. The influence this velocity will have on the formation of lineations depends on the basal thermal regime. The basal thermal regime of glaciers has two end-members. Cold-based glaciers, where the heat generated at the base is less than the heat conducted away, are frozen to their beds and no meltwater is present at the ice bed interface. These glaciers do not erode their bed or deposit sediment at the bed and therefore do not produce lineations. In contrast, the bed of a warm-based glacier has an ice bed interface lubricated by melt-water. The bed is eroded and till is deposited on it. Increasingly, it has been suggested that the processes of erosion and deposition beneath a warm bed are determined by deformation of sediment on the bed (Menzies and Rose, 1987; Hart and Boulton, 1991). The presence of this deforming layer is dependent on several factors of which pore water pressure is of particular importance (Section 4.1.4). It is therefore thought that subglacial deformation occurs only under warm based ice sheets where the glacier is not frozen to its bed (Menzies and Rose, 1987). At present there is no consensus on formulating sliding and soft sediment deformation laws and the model used considers only internal ice shear deformation. To take account of the basal thermal regime in this analysis, however, only ice velocities for points where basal ice melting occurs, and therefore where the glacier is warm-based, were included in further calculations. These velocities are shown in Figure 8.1b.

The velocity profiles along the model transect were first considered for each 1000 year time

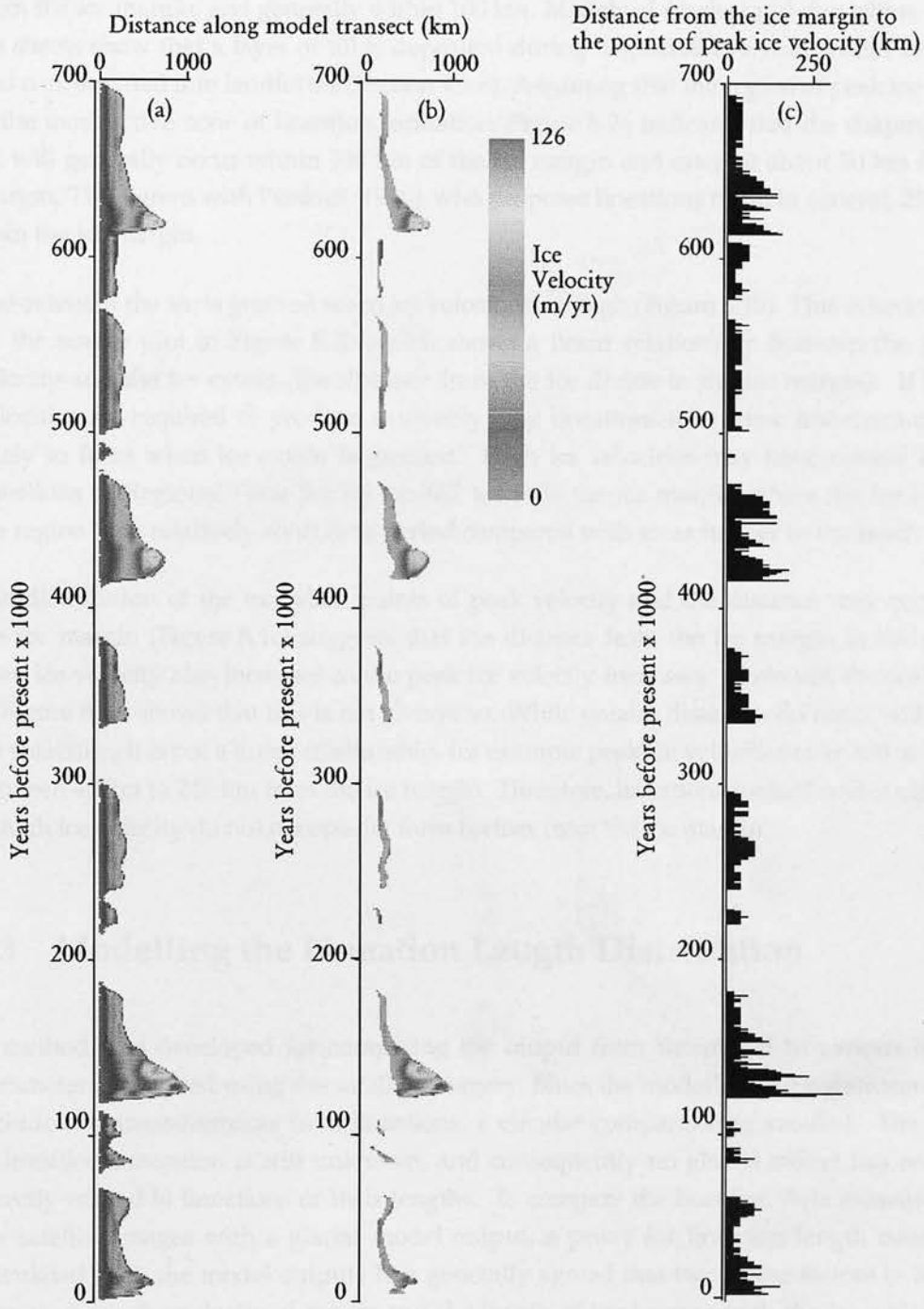

Figure 8.1: a) Balance ice velocity along a transect from the ice divide to the ice margin. b) Balance ice velocity along the same transect with only ice velocities shown where basal melting occurs. c) Distance from the ice margin to the point of maximum ice velocity for each 1000 year period for places where basal melting occurs. Data derived from an application of the model by Boulton *et al.* (1985).

interval. Figure 8.1c shows the distance from the point of peak velocity to the ice margin for each 1000 year period. Figure 8.2a summarises this information as a frequency histogram. It can be seen from this histogram that the peak velocities occur most often at a distance of 50 km from the ice margin, and generally within 100 km. Models of erosion and deposition beneath ice sheets show that a layer of till is deposited during deglaciation which would be shaped and concentrated into landforms (Section 4.1.6). Assuming that the region of peak ice velocity is the most active zone of lineation formation, Figure 8.2a indicates that the shaping of this till will generally occur within 100 km of the ice margin and often at about 50 km from the margin. This agrees with Punkari (1996), who proposes lineations form, in general, 25-100 km from the ice margin.

The extent of the ice is greatest when ice velocities are high (Figure 8.1b). This is better shown by the scatter plot in Figure 8.2b which shows a linear relationship between the peak ice velocity and the ice extent (the distance from the ice divide to the ice margin). If high ice velocities are required to produce extremely long lineations then these lineations are most likely to form when ice extent is greatest. High ice velocities may have caused the long lineations of Regional Flow Set R5 located towards the ice margin where the ice occupied the region for a relatively short time period compared with areas further to the north.

The distribution of the modelled points of peak velocity and the distance they occur from the ice margin (Figure 8.1c) suggests that the distance from the ice margin to the point of peak ice velocity also increases as the peak ice velocity increases. However, the scatter plot in Figure 8.2c, shows that this is not always so. While greater distances do occur with higher ice velocities, it is not a linear relationship, for example peak ice velocities over 100 m/a occur between 40 km to 240 km from the ice margin. Therefore, lineations formed under conditions of high ice velocity do not necessarily form further from the ice margin.

8.3 Modelling the Lineation Length Distribution

A method was developed for comparing the output from the model to various lineation parameters measured using the satellite imagery. Since the model's input parameters do not include any measurements from lineations, a circular comparison is avoided. The process of lineation formation is still unknown, and consequently no glacial model has an output directly related to lineations or their lengths. To compare the lineation data measured from the satellite images with a glacial model output, a proxy for lineation length needs to be calculated from the model output. It is generally agreed that two major factors in lineation formation are the velocity of the ice and the length of time over which the ice occupied the region. Work by Boyce and Eyles (1991) on drumlins formed beneath the Laurentide ice sheet correlates the length and length/width ratio of drumlins with the time available for subglacial deformation. The duration of the deforming bed conditions was greatest up-glacier, where the drumlins are elongated while towards the limit of the ice lobe where subglacial deformation will have only occurred for a short period of time, the drumlins are more oval in shape. The

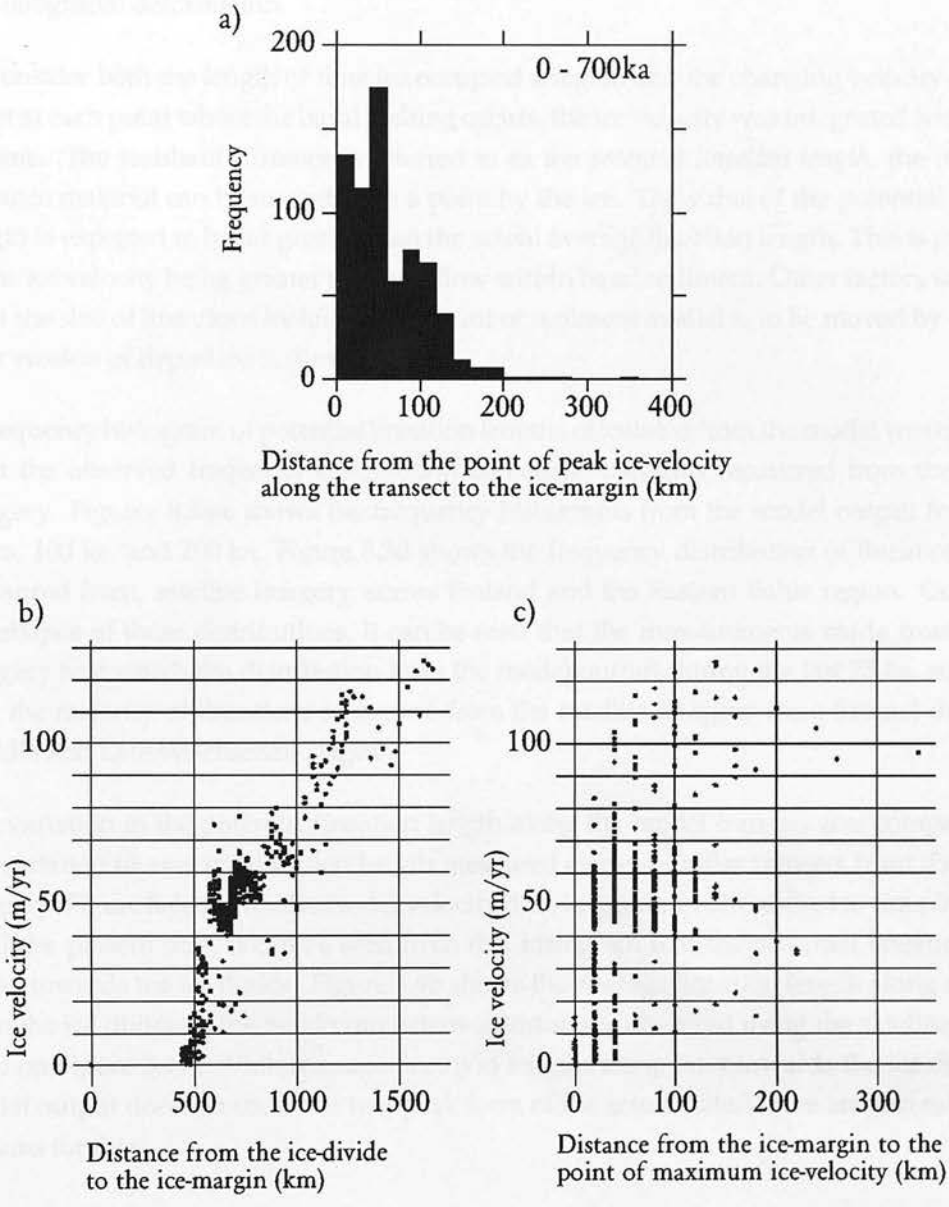

Figure 8.2: a) Frequency histogram of the distance from the point of peak ice velocity along the transect to the ice margin. b) Scatter plot of ice velocity versus ice extent c) Scatter plot of the ice velocity versus distance from the point of peak velocity along the transect to the ice margin.

velocity of the ice will influence the supply of deforming sediment. According to Boulton and Hindmarsh (1987), a large supply of deforming sediment will result in longer tails of accumulated sediment around obstacles (more rigid regions within the basal layer). In this model megaflutes are simply a subtype of drumlin produced by rapid rates of glacier flow and subglacial deformation.

To consider both the length of time ice occupied a region and the changing velocity of the ice sheet at each point where the basal melting occurs, the ice velocity was integrated with respect to time. The resultant distance is referred to as the *potential lineation length*, the maximum distance material can be moved from a point by the ice. The value of the potential lineation length is expected to be far greater than the actual average lineation length. This is partly due to the ice velocity being greater than any flow within basal sediment. Other factors which will limit the size of lineations include the amount of sediment available to be moved by the ice or later erosion of deposited sediment.

A frequency histogram of potential lineation lengths calculated from the model was compared with the observed frequency distribution of lineation lengths measured from the satellite imagery. Figures 8.3a-c shows the frequency histograms from the model output for the last 75 ka, 100 ka, and 200 ka. Figure 8.3d shows the frequency distribution of lineation lengths measured from, satellite imagery, across Finland and the Eastern Baltic region. Comparing the shapes of these distributions, it can be seen that the measurements made from satellite imagery best match the distribution from the model output during the last 75 ka, suggesting that the majority of lineations measured from the satellite imagery were formed during the Middle and Late Weichselian stages.

The variation in the potential lineation length along the model transect was compared with the variation in average lineation length measured along a similar transect from the satellite imagery. Figure 8.4c shows the model velocity data integrated with respect to time from 75 ka until the present day. It can be seen from this histogram that the potential lineation length peaks towards the ice divide. Figure 8.4b shows the average lineation length along a transect from the ice divide to the maximum extent of lineations observed using the satellite imagery (A-B on Figure 8.4a). While average lineation lengths are greater towards the ice divide, the model output does not show the two-peak form of the actual data. There are several possible reasons for this.

a) The model assumes that all flow is along the transect. Shifts in the ice divide in particular can produce large shifts in flow direction (e.g., Boulton and Clark 1990) which may then remove previously formed lineations. Available evidence, however, suggests that this was only likely to have been a significant problem during the phase of ice retreat in northern Finland (Dongelmans, 1996; Broadgate, 1997).

b) A second reason relates to the velocity values themselves. The large peak within the model output at the ice divide is achieved by summing many low velocities over a long period of time. It is more realistic to assume that there will be a threshold velocity above which

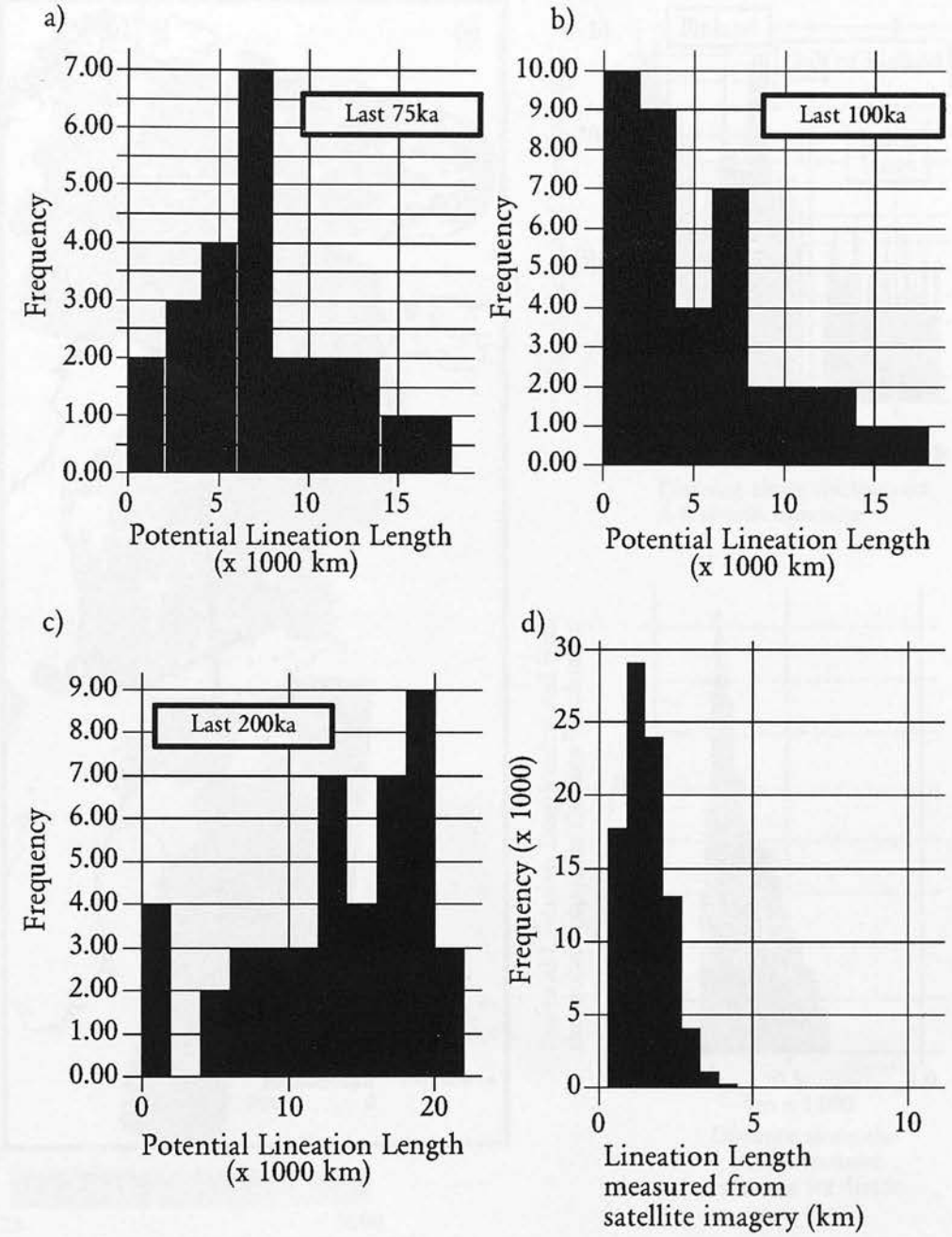

Figure 8.3: a) Frequency histogram of the potential lineation length for the last 75 ka b) Frequency histogram of the potential lineation length for the last 100 ka c) Frequency histogram of the potential lineation length for the last 200 ka d) Observed frequency distribution of lineation length as measured from satellite imagery.

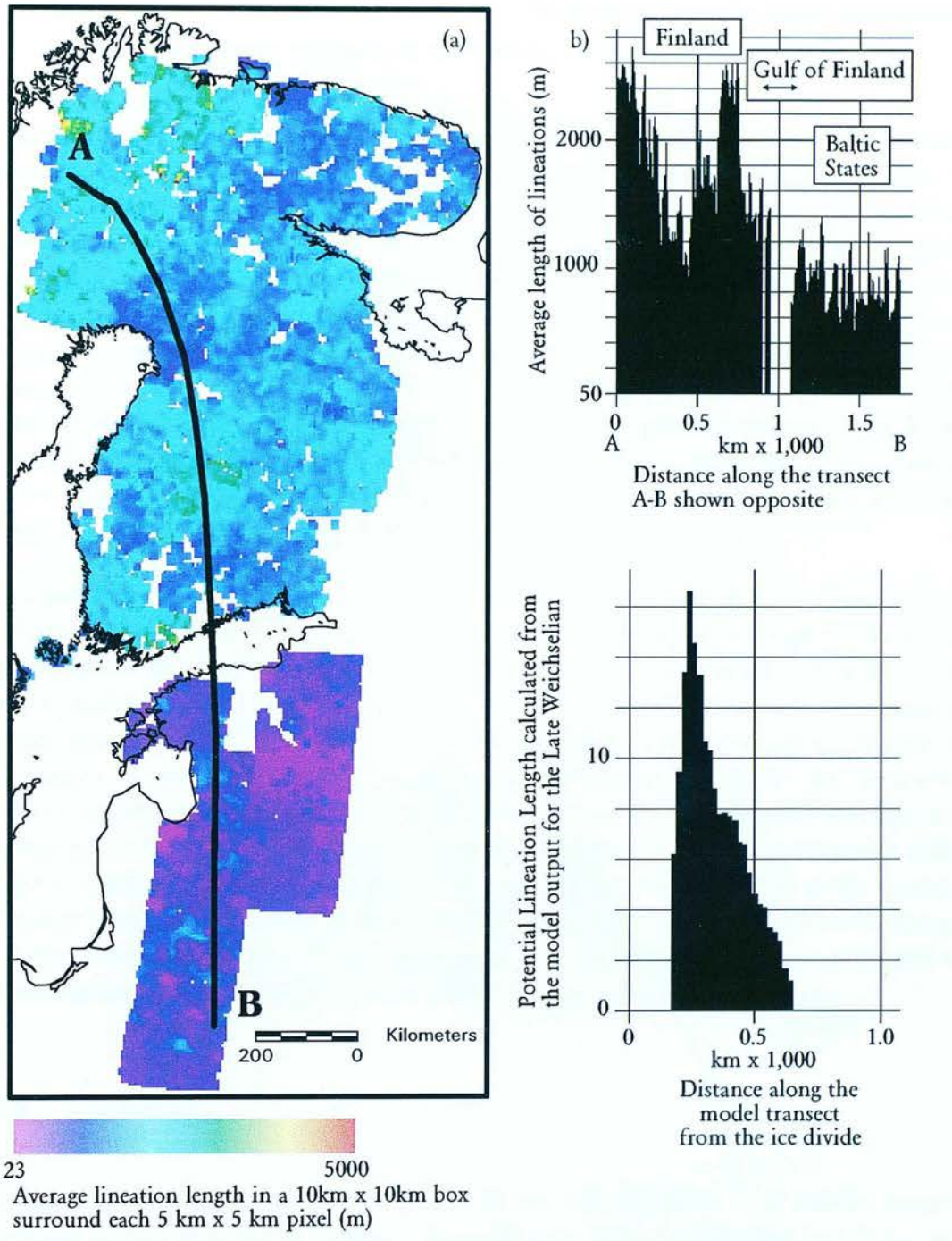

Figure 8.4: a) Spatial distribution of average lineation length calculated for a 10 km x 10 km box surrounding each 5 km x 5 km pixel. Transect A-B from the ice divide to the ice margin is also shown. b) Spatial profile of average lineation length along the transect A-B. c) Spatial profile of Proxy Distance, calculated using the model output from the ice divide to the ice margin during the last 75 ka.

till deformation and lineation formation will become significant, when the yield stress of the sub-stratum is exceeded. Few field measurements exist for the yield-stress of till (e.g., Boulton *et al.*, 1974; Kamb, 1992; Humphrey *et al.*, 1993; Fischer and Clarke, 1994) and these values vary from 2 kPa to 57 kPa. The potential lineation length was therefore calculated for a range of threshold velocities as shown in Figure 8.5.

The Figures show that with a threshold velocity of 55 m/a the distribution of the potential lineation length resembles, in shape, the observed average length of lineations from the satellite imagery. With this threshold the model output shows a peak near the ice divide, followed by a trough and another peak of approximately the same height, before rapidly decreasing towards the ice margin. From Figure 8.4a we can see that the average lineation length is high towards the ice divide in north-west Finland, low across the middle of Finland and then increases again before decreasing through the Eastern Baltic region towards the maximum extent of the Late Weichselian ice. Figure 8.6 shows how the potential lineation length along the transect changes with time. It shows that the peak towards the ice divide had formed by 25 ka with the second peak towards the ice margin forming later. This stresses the time transgressional nature of lineations and implies that in ice divide areas in particular, old lineations which may pre-date the final deglaciation may survive.

Figures 8.2a and 8.3a-c were recalculated to include the effect of imposing a threshold velocity of 55 m/a. The results are shown in Figure 8.7. Figure 8.7a shows the frequency histogram of the distance between the point of peak ice velocity and the ice margin for the last 75 ka, only considering velocities greater than 55 m/a. It can be seen that the majority of peak ice velocities occurred within 100 km of the ice margin, with a peak value at 30 km from the ice margin. As before the region of peak velocities and therefore probably the most active zone of lineation formation occurs towards the ice margin. This supports the assumption in Section 6.3 that lineations may be used as a good indicator of the shape of the margin within approximately the same region during retreat. Comparing Figures 8.7b-d to the observed lineation length frequency distribution shown in Figure 8.3d, it can be seen that imposing a velocity threshold of 55 m/a did not significantly alter the shape of the histograms and the model results from the last 75 ka are still the best fit to the observed lineations.

8.4 Summary

Comparing the glaciological model output with the interpretations from satellite imagery indicates that the majority of lineations recorded were formed during the last 75 ka, with the lineations across the Eastern Baltic Region forming during the last 25 ka (Figure 8.6). It is thought that the zone of most active lineation formation occurs within 100 km of the ice margin and often approximately 30 km from the glacier terminus. The period of most active lineation formation would occur when the ice was at its maximum extent. It was inferred that a yield strength of bed sediments may play a key role in determining lineation formation.

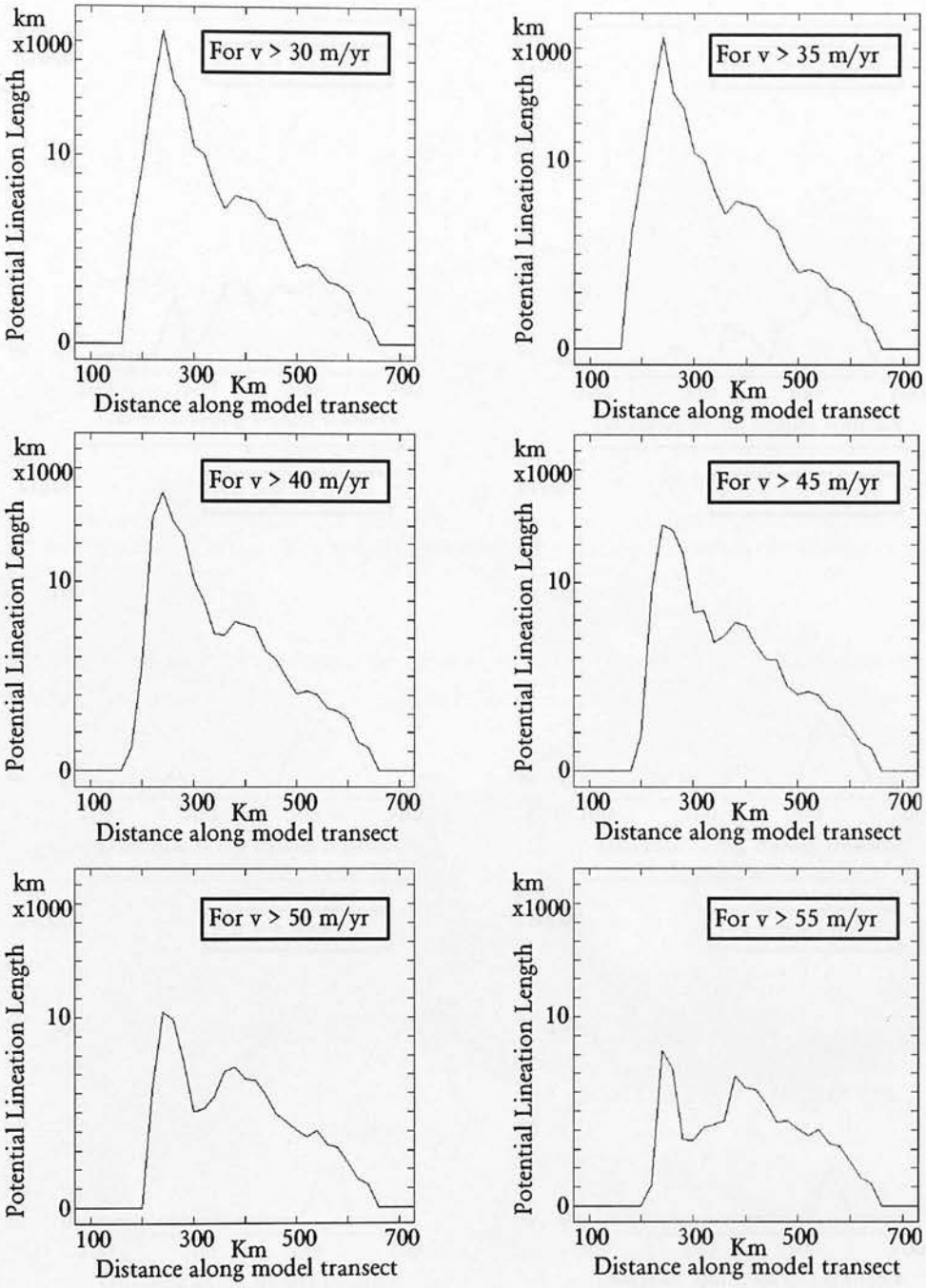

Figure 8.5: Potential lineation length along the model transect calculated by integrating velocities above a threshold velocity (v) during the last 75 ka, continued over leaf.

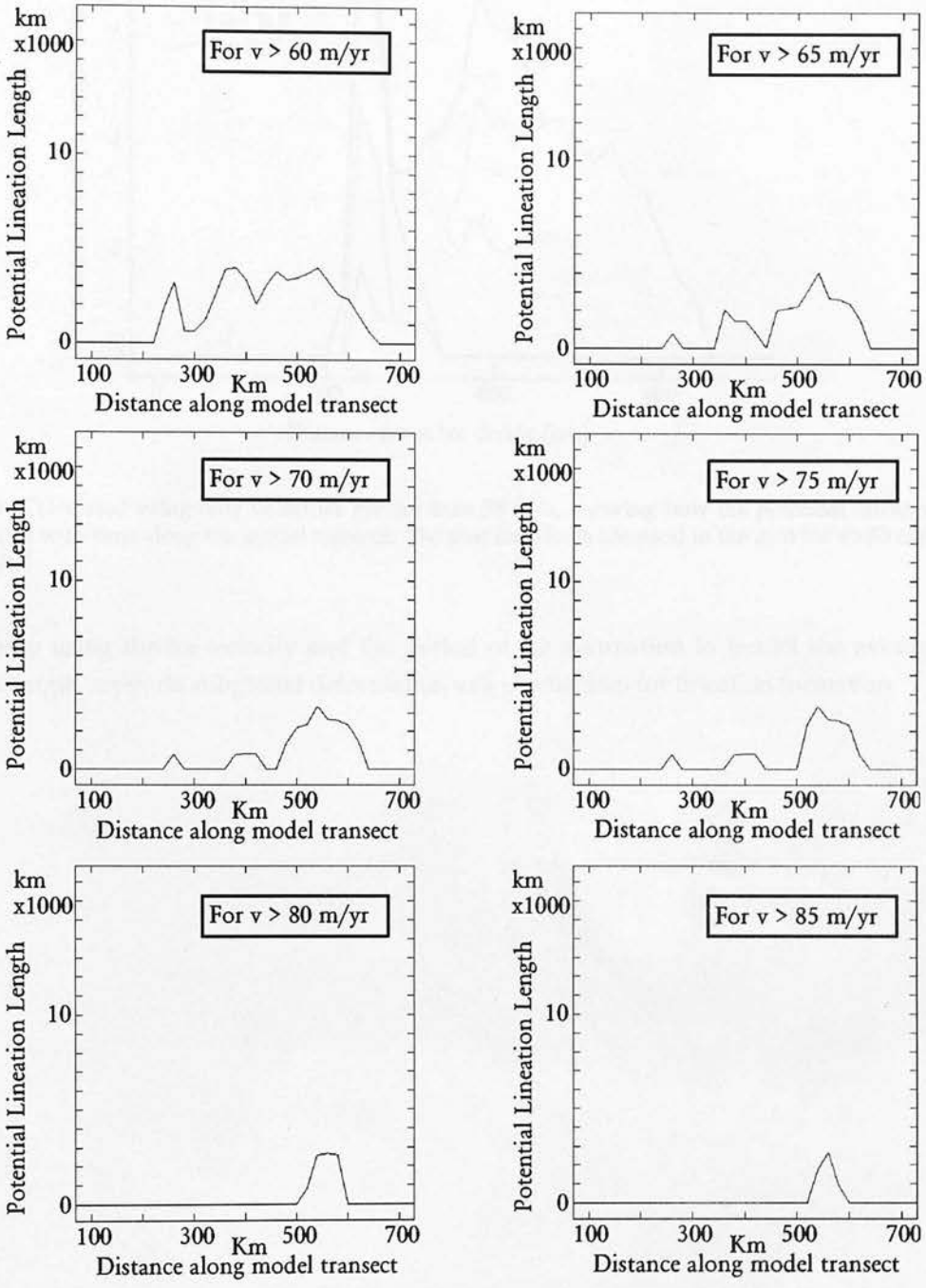

Potential lineation length along the model transect calculated by integrating velocities above a threshold velocity (v) during the last 75 ka, continued from the previous page.

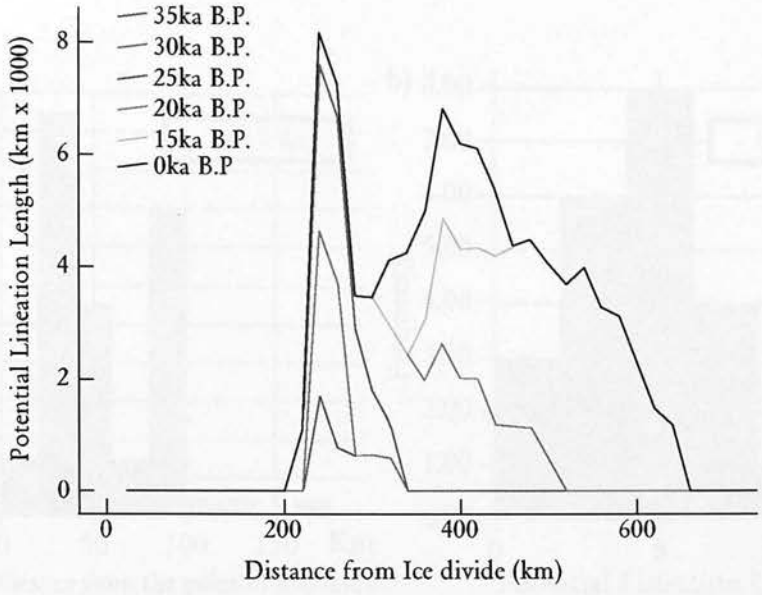

Figure 8.6: Calculated using only velocities greater than 55 m/a, showing how the potential lineation length varies with time along the model transect. The plot for 0 ka is identical to the plot for v>55 m/a in Figure 8.5

Successfully using the ice velocity and the period of ice occupation to model the average lineation length supports subglacial deformation as a mechanism for lineation formation.

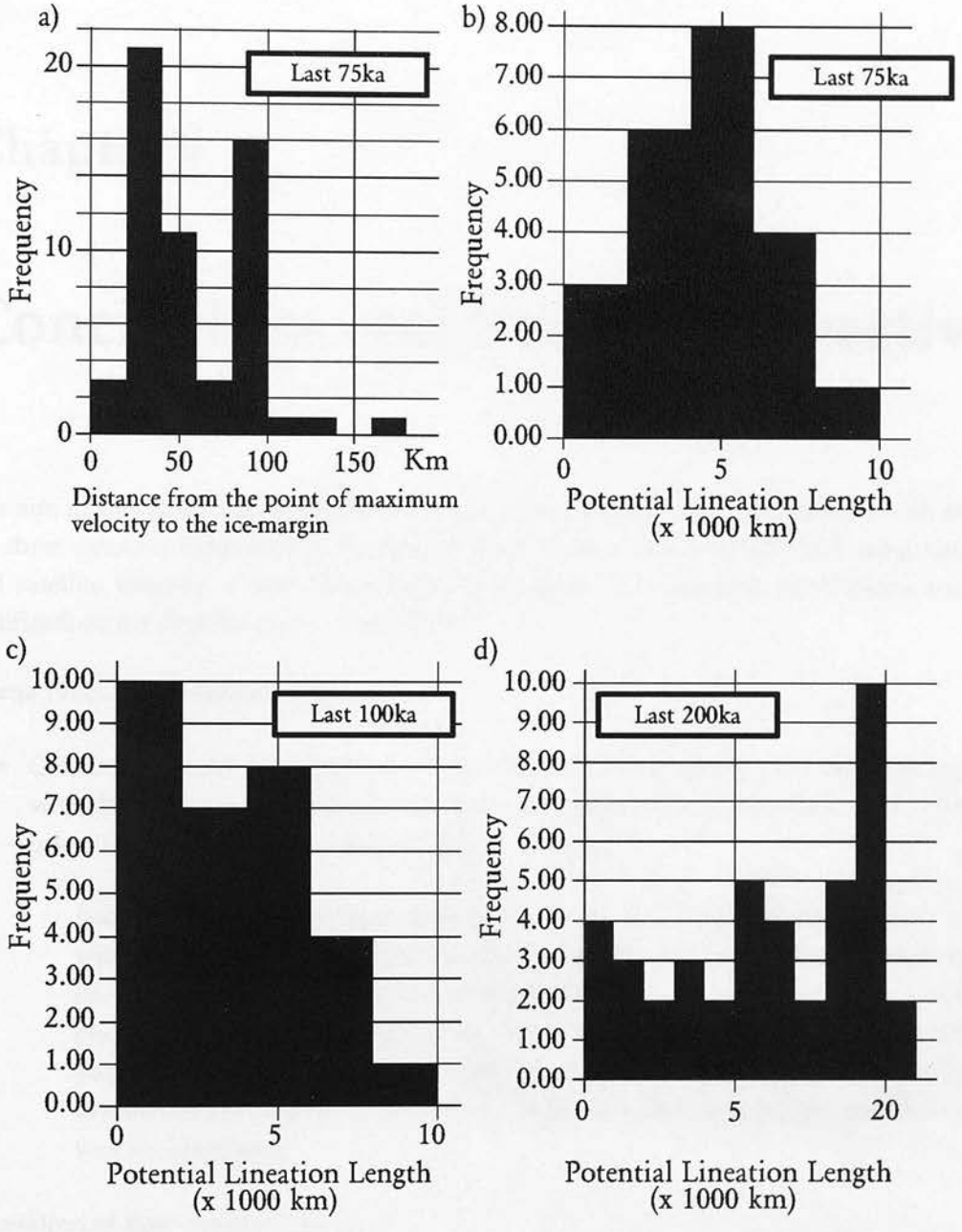

Figure 8.7: Figures a-d show the calculated potential lineation length using only velocities above 55 m/a and where basal melting rate was occurring. a) Frequency histogram of the distance from the point of peak ice velocity along the model transect to the ice margin. b) Frequency histogram of the potential lineation length for the last 75 ka c) Frequency histogram of the potential lineation length for the last 100 ka d) Frequency histogram of the potential lineation length for the last 200 ka

Chapter 9

Conclusions and Future Perspective

The aim of this study was to produce a single coherent mapping of landforms which reflect ice sheet dynamic behaviour in the Eastern Baltic region. This was achieved using Landsat TM satellite imagery, a new data source for the area. The principle conclusions and the justifications for them are summarised below.

Image Processing Methodology

- *Conclusion:* Geomorphology is best expressed in images acquired in early spring and with simple contrast stretching of the intensity values of the TM bands 4, 5 and 7 for the colours red, green and blue respectively.

  Justification: In contrast to studies within the United Kingdom (Marsh *et al.*, 1995), winter was not found to be the best time of year to acquire images, mainly because the Eastern Baltic region is covered in snow throughout the winter season. Geomorphology was found to be highlighted better in images taken during May than those acquired during October. Edge enhancing, as used by Marsh *et al.* (1995), was found to enhance the underlying agricultural land use rather than the geomorphology, so was not employed.

Formation of flow-parallel lineations

- Flow-parallel lineations are probably formed by a single mechanism

  The frequency distribution of lineation lengths in Finland and also in the Eastern Baltic region are continuous and uni-modal, in contrast to the multi-modal distributions suggested by Clark (1993). The continuum in lineation length suggests a single mechanism of formation.

- The most likely mechanism for flow-parallel lineation formation is that of subglacial deformation

  The successful application of a glaciological model (Boulton *et al.*, 1995) to represent average lineation length along a transect of the Fenno-Scandinavian ice sheet, using the assumption that the length of lineations within a region is a function of the ice velocity and the occupancy time of ice in that area (Boulton, 1996), supports the model of subglacial deformation as the most plausible mechanism for lineation formation. The yield strength of bed sediments was also inferred to play a key role in the formation of lineations.

- The most active zone of lineation formation is within 100 km of the ice sheet margin, often at 30 km

  Evaluation of glaciological model output (Boulton *et al.*, 1995) using Boulton's model (Boulton, 1987) of ice sheet erosion and deposition suggests that the most active zone of lineation formation is generally within 100 km of the ice sheet margin, and often at 30 km. This supports the assumption that deglaciation flow-parallel lineations tend, on flat terrain, to form near and perpendicular to the ice sheet margin.

- The majority of lineations within the Eastern Baltic region formed during the Late Weichselian

  The limit of the Weichselian ice was reached during the Late Weichselian (Raukas and Gaigalas, 1993). Lineations with the form and appearance seen north of this limit of Weichselian ice, are not observed south of the limit and it is concluded that the majority of the lineations north of the limit were formed during the Late Weichselian. This conclusion is supported by analysis of the output from the glaciological model (Boulton *et al.*, 1995)and suggests that the frequency distribution of lineation lengths is best explained by the formation of the majority of lineations within the Eastern Baltic region during the Late Weichselian. The analysis also suggests that, towards the ice divide in Finland, lineation growth was initiated during the Middle Weichselian and lineations were further extended during later glacial periods.

- There were different controls on lineation formation over the regions of Finland and the Eastern Baltic

  The frequency distributions of lineation lengths show two distinct sample data sets. The mean lengths and spread of values in the Eastern Baltic are much less than those from Finland.

  Mathematical modelling of these frequency distributions show that the larger sample data values within Finland are better modelled using an exponential function than by a power-law, while similar data values in the Eastern Baltic region were

better modelled by a power-law than by an exponential function.

A better fit to an exponential distribution implies a natural length scale for the formation of lineations, while the power-law distribution is scale invariant. By analogy with rock fracture studies, a natural length scale may exist if the process of lineation formation is restricted by boundary conditions. These boundary conditions may relate to sediment supply or the rheological and hydrogeological properties of bed sediments.

- A gradual change in the frequency distribution of lineation lengths is observed over the regions of Finland and the Eastern Baltic

  The frequency distribution of lineation lengths in Finland and the Eastern Baltic region are distinct. However, superimposed upon these two data sets, a general trend of decreasing mean lineation length and a narrowing in the spread of length values is observed from north to south, indicating a gradual north-south change in one or some of the parameters controlling lineation formation.

Spatial and temporal relationship of glacial landforms in the Eastern Baltic

Criteria were developed which permitted the lineations to be grouped into flow sets. Eight regional flow sets were identified in the Eastern Baltic region.

- Two pre-Weichselian Flow Sets were identified

  Flow sets R8 and R7 occur towards the south of the study region. They are thought to pre-date the Weichselian and are likely to be Saalian in age.

- Three Pre-final deglaciation Flow Sets were identified, two of which formed during the Late Weichselian maximum

  Three Flow Sets (R6, R5 and R4) are thought to have formed during the Weichselian before deglaciation.

  The lineations of Flow Set R6, oriented at 140° are mainly restricted to highland areas to the west of the study region and may represent a fluctuation of an antecedent ice stream which occupied the Gulf of Riga during deglaciation.

  Flow Set R5 comprises lineations from both highland and lowland regions. It has a north-south trend and may represent the southern extremity of an ice stream for which evidence is found 360 km further north, in Finland. Flow Set R4 may also represent a north-south ice stream. Both of these Flow Sets contain well-defined lineations with lengths of up to 21 km.

  Reconstructions of the Fenno-Scandinavian ice sheet suggest a north-south radial flow may have occurred within the Eastern Baltic region during the Late Weichselian maximum when the ice divide was located towards the Gulf of Bothnia (Lundqvist,

1986). Further analysis of the output from the glaciological model (Boulton *et al.*, 1995) suggested that ice velocities are greatest, and hence the ability to form lineations is greatest, when the ice sheet reaches its maximum extent. This may explain the long lineations of Flow Sets R4 and R5 in regions where the period of ice occupancy was small.

The Flow Sets R5 and R4 are therefore thought to have formed during the Late Weichselian maximum.

- Three deglaciation Flow Sets were identified. No evidence was found for the extremely lobate deglaciation margins previously proposed

  The Flow Sets (R3, R2 and R1) formed during the final deglaciation of the region and consist of lineations with lengths generally smaller than those observed in Flow Sets R4 and R5. Towards the east of the region studied, lineations contained in these Flow Sets are shown to post-date the lineations forming Flow Sets R5 and R4. Towards the west, the margin of Flow Set R2 is delineated by a topographic ridge and marginal deposits correlated with the North Lithuanian re-advance (Raukas and Gaigalas, 1993). The North Lithuanian re-advance occurred after the Raunis interstadial which has been dated at 13,250 B.P. (Punning *et al.*, 1968).

  Rotating the lineations by 90° allowed the margin of the ice sheet during deglaciation to be traced. No evidence was found to support the extremely lobate deglaciation margins previously proposed by (Raukas and Gaigalas, 1993).

- The limit of Weichselian ice could be delineated by several different methods

  It was possible to delineate the limit of Weichselian ice by four methods: 1) the number of lakes increases towards the limit of Weichselian ice and then falls sharply; 2) the limit is marked by land which has distinctly lower agricultural usage than on either side; 3) there is a significant change in the texture of the imagery across the limit, from the rough surface of lakes and knolls in the north, to the smooth texture in the south; 4) a distinct change in the spectral intensity occurs across the limit. These variations across the limit of Weichselian ice are probably due to the large number of ridges and lakes that exist at the Weichselian margin, which form an area unsuitable for farming.

- The highland and lowland areas of the Eastern Baltic region were once glacial interstream and streaming regions respectively.

  Using the TM imagery and digital elevation data the Eastern Baltic region can be divided into highland and lowland regions.

  The highland regions are characterised by large thicknesses of Quaternary deposits (Raukas and Gaigalas, 1993), a rough texture of knolls and ridges and few lineations, usually of short length are observed on the TM images. By comparison with modern

ice streams, the highland areas are thought to represent interstream areas where ice velocities were low restricting the growth of lineations, and little glacial erosion occurred allowing the accumulation of glacial till. These areas may also have been cold based which would enhance their potential to preserve older lineations. The significant numbers of lineations observed over highland regions which could not be grouped into regional flow sets may therefore represent older ice flow directions.

The lowland areas are covered by thin layers of till which have been sculptured into a smooth surface, usually with elongated landforms. The lowland regions are thought to represent areas occupied by glacial streams, with high ice velocities and possible basal sediment deformation causing the formation of the well-defined lineations observed.

- The interstream regions generally coincide with areas of elevated bedrock.

  The highland areas, and therefore the interstream regions, appear to coincide with regions of elevated bedrock suggesting that, initially at least, the ice sheet dynamics were controlled by the topography. The topography is, however, low lying and unlikely to directly control the dynamics of the later, larger ice sheet. A positive feedback loop may help maintain high ice velocities within regions of ice streaming. Faster flow produces more frictional heat, which raises the temperature of the basal ice, which in turn, deforms more easily causing faster flow. Once the basal ice reaches the pressure melting point, meltwater can be produced and sliding or till deformation may develop, further increasing the flow of ice.

Differences between the deglaciation in the Eastern Baltic region and Finland

- The ice streams over Finland are greater in size, with more regular morainic arcs, and therefore are concluded to have been more stable than those observed in the Eastern Baltic region.
- During deglaciation there was a greater variance in the orientation of lineations in the Eastern Baltic than in Finland.
- In plan view, the interstream regions are more rounded in the Eastern Baltic region than in Finland.
- The frequency distribution of lineation lengths is distinctly different between Finland and the Eastern Baltic region, with a greater spread of values and a larger mean measured over Finland.
- In Finland the glacial stream areas contain an abundance of eskers, while few eskers are observed in the Eastern Baltic region.

  Many of these differences can be explained by the differences in the underlying geology of Finland and the Eastern Baltic region. The crystalline sediments of the

Baltic Shield, underlying the ice in Finland were less susceptible to deformation than the fine-grained sediments of the East European Platform which underlies the Eastern Baltic region. Hence more stable ice lobes could form in Finland, producing more stable morainic arcs and lineations with a smaller spread of orientations.

Mathematical modelling of subglacial drainage led Walder and Fowler (1994) to propose that the distribution of eskers between the two regions was also explained by the difference in the underlying geology between the areas.

9.1 Future Perspective

In this study a distinct difference was observed between the lineations formed over the Baltic Shield and the East European Platform. The transition zone between these two regions could not be studied directly, however, since it lies beneath the Gulf of Finland. Further to the east of the present study area the change could be observed directly. Interpretations from these regions would also provide important information on the extent and form of the glacial dynamics which produced Flow Set R4 which appears to have been formed by ice flowing from this area.

The North American Laurentide ice sheet occupied an area similar to that of the Eurasian ice sheet, with an inner zone of crystalline basement rock being surrounded by a zone of deformable sediment. Studies of the areas formerly glaciated by the American ice sheet using the same analysis techniques employed in this study would provide a useful comparison to the conclusions drawn here and allow more general conclusions to be made concerning the spatial pattern of glaciation and the influence of the underlying geology on ice dynamics.

The recent loss in August of the LEWIS spacecraft, the first spaceborne hyperspectral sensor providing 384 bands of data between 0.4 and 2.5μm, is a major blow to the prospect of using enhanced satellite sensors for mapping of glacial landforms. However, further satellites are due to be launched in the coming years which will have sensors with greater spatial and spectral resolutions than were available for use in this project (Table 9.1). The data they will produce, combined with the flexibility of viewing the data in 3-dimensions (Figure 9.1) will greatly increase the ability to interpret areas accurately and quickly and sample the frequency distribution of lineation lengths for smaller features than those possible in this study.

Attempts were made during this study to try to automate the process of image interpretation, removing the possibility of operator bias and reducing the time to gather data. However, problems were encountered due to the coarse spatial and spectral resolution of the data. The use of digital elevation models with finer spatial resolution than used here, combined with the data from new satellite platforms may provide sufficient information on the land surface to facilitate automatic interpretation. The distinctive change in spectral intensity values across the limit of Weichselian ice may permit the automatic mapping of this margin. With finer spectral resolutions, future hyperspectral satellites may allow other margins to be identified

spacecraft	Launch Date	Spatial Resolution	Number of Bands
LEWIS	22 August 1997 Failed 26 August 1997	30 m	384
NMP/EO-1	Late Autumn 1998	10 m	315
OrbView 3	Summer 1999	4 m	Unknown
Aries-1	Operational 2000	30 m	64
Clark	Unknown, if at all	3 m	Unknown

Table 9.1: Hyperspectral satellites due to be launched over the next few years. Spatial resolution shown is that of the multi-spectral sensors. Source Denniss (1997) and Bussel (1998)

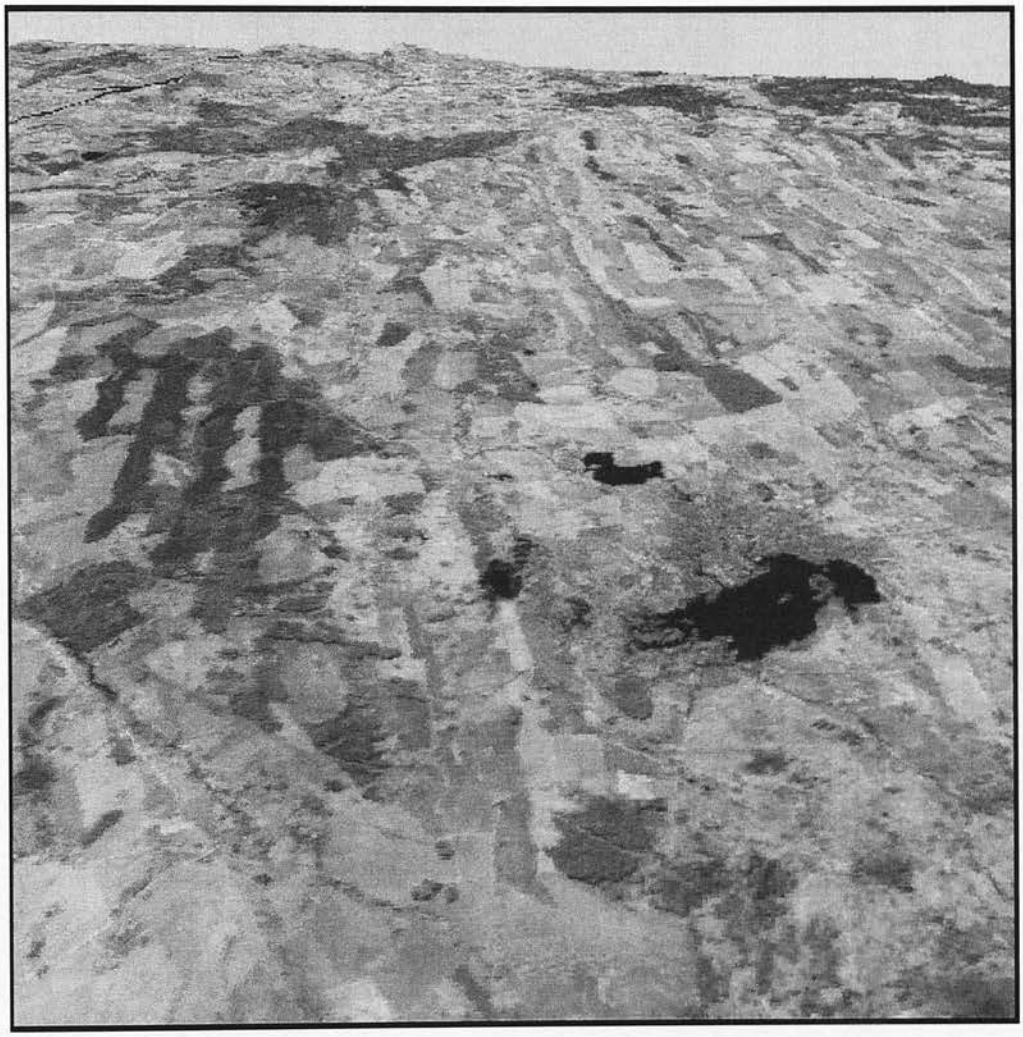

Figure 9.1: Example of how satellite data may be viewed in 3-dimensions. Lineations can be seen extending from the observer towards the horizon. The picture is created by overlaying image 187021 on to the GTOPO30 elevation model (Gesch, 1996) which has been vertically exaggerated by ten times. It is seen as if viewed from 24.81E 56.32N with a pitch of -31.2°, at an elevation of 8000 m above m.s.l. and oriented to face 173° (south across Latvia). The range of view is 46.3 km.

and mapped in a similar manner.

Bibliography

Aario, R. (1977a). Associations of flutings, drumlins, hummocks and transverse ridges. *Geological Journal*, **1**, 65–72.

Aario, R. (1977b). Classification and terminology of morainic landforms in Finland. *Boreas*, **6**, 67–100.

Aario, R. (1987). Drumlins of Kuusamo and rogen-ridges of Ranua, northeast Finland. In *Drumlin Symposium*, pages 87–102. Balkema.

Aartolahti, T. (1968). Die geomorphologie des gebietes von Tammela (the geomorphology of the areas of Tammela). *Fennia*, **97**, 1–97.

Aber, J. S., Spellman, E. E., and Webster, M. P. (1993). Landsat remote sensing of glacial terrain. *Canadian Plains Proceedings*, **25**(1), 215–225.

Aber, J. S., Bluemie, J. P., Brigham-Grette, J., Dredge, L., Sauchyn, D. J., and Acerman, D. L. (1995). Glaciotectonic map of North America. *Geological Society of America Map and Chart Series MCH 079*.

Āboltiņš, O. (1995). Quaternary Field Trips in Central Europe, Baltic Traverse, Site 26. Technical report, International Union for Quaternary Research XIV Congress, Berlin.

Āboltiņš, O. and Dreimanis, A. (1995). Glacigenic deposits in Latvia. In J. Ehlers, S. Kozarski, and P. Gibbard, editors, *Glacial deposits in North-East Europe*, pages 115–124. A. A. Balkema.

Abramowitz, M. and Stegun, I. A., editors (1972). *Handbook of Mathematical Functions with Formulas, Graphs and Mathematical Tables*, pages 253–295. Dover Publications.

Ager, D. V. (1980). *The Geology of Europe*. McGraw-Hill Book Company Ltd.

Alley, R. B. and Whillans, I. M. (1991). Response of East Antarctica Ice Sheet. *Journal of Geophysical Research*, **89**, 6487–6493.

Alley, R. B., Blankenship, D. D., Bentley, C. R., and Rooney, S. T. (1987). Till beneath ice stream B. Till deformation: evidence and implications. *Journal of Geophysical Research*, **92**(B9), 8921–8929.

Andersen, B. G. and Mangerud, J. (1990). The last interglacial - glacial cycle in Fennoscandia. *Quaternary International*, **34**, 21–29.

Andrews, J. T. (1989). Quaternary geology of the northeastern Canadian Shield. In R. J. Fulton, editor, *Quaternary Geology of Canada and Greenland*, pages 276–317. Geological Survey of Canada.

Andrews, J. T. and Tedescoo, K. (1992). Detrital carbonate-rich sediments northwestern Labrador sea: Implications for ice-sheet dynamics and iceberg rafting (Heinrich) events in the North Atlantic. *Geology*, **20**, 1087–1090.

Arslanov, K. A. and Stelle, V. J. (1975). Opit i metodi izotopno-geokhimicheskikh issledovaniy v Pribaltike i Belorussii. In *Raodiouglerodniye datirovki mezhmorennikh otlozheniy u st.* Riga.

Ashley, G. M., Boothroyd, J. C., and Borns, H. W. J. (1991). Sedimentology of late Pleistocene (Laurentide) deglacial-phase deposits, eastern Maine: An example of a temperate marine grounded ice-sheet margin. In J. B. Anderson and G. M. Ashley, editors, *Glacial marine sedimentation: Paleoclimatic significance.* Geological Society of America Special Paper 261.

Attig, J. W., Mickelson, D. M., and Clayton, L. (1989). Late Wisconsin landform distribution and glacer bed conditions in Wisconsin. *Sedimentary Geology*, **62**, 399–405.

Aylsworth, J. M. and Shilts, W. W. (1989). Glacial features around the Keewatin ice divide: Districts of Mackenzie and Keewatin. *Geological Survey of Canada*, pages 88–24.

Baron, C. A. and Zoback, M. D. (1992). Self similar distribution and properties of macroscopic fractures at depth in crystalline rock in the Cajon Pass scientific borehole. *Journal of Geophysical Research*, **97**, 5181–5200.

Beaudry, L. M. and Prichonnet, G. (1991). Late glacial De Geer moraines with glaciofluvial sediment in the Chapais area, Quebec (Canada). *Boreas*, **20**(4), 377–394.

Benn, D. I. and Evans, D. J. A. (1998). *Glaciers and Glaciation.* Arnold. 733 pp.

Bennett, M. R. and Glasser, N. F. (1996). *Glacial Geology, Ice Sheets and Landforms.* John Wiley and Sons, New York. 364 pp.

Bitinas, A. (1994). Peculiarities of formation of flat glaciolacustrine hills. In *Proceedings of the 29th International Geological Congress Part B.*

Blankenship, D. D., Bentley, C. R., Rooney, S. T., and Alley, R. B. (1986). Seismic measurements reveal a saturated porous layer beneath an active Antarctic ice stream. *Nature*, **322**, 54–57.

Blankenship, D. D., Bentley, C. R., Rooney, S. T., and Alley, R. B. (1987). Till beneath ice stream b: 1. Properties derived from seismic travel times. *Journal of Geophysical Research*, **92**(B9), 8903–8911.

Bluemle, J. P. and Clayton, L. (1984). Large-scale glacial thrusting and related processes in North Dakota. *Boreas*, **13**(3), 279–299.

Boots, B. N. and Burns, R. K. (1984). Analyzing the spatial distribution of drumlins: A two-phase mosaic approach. *Journal of Glaciology*, **30**(106), 302–307.

Bouchard, M. A. (1989). Subglacial landforms and deposits in central and northern Québec, Canada, with emphasis on Rogen moraines. *Sedimentary Geology*, **62**, 293–308.

Boulton, G. S. (1987). A theory of drumlin formation by subglacial sediment deformation. In *Drumlin Symposium*, pages 25–79. Balkema.

Boulton, G. S. (1996). Theory of glacial erosion, transport and deposition as a consequence of subglacial sediment deformation. *Journal of Glaciology*, **42**, 43–61.

Boulton, G. S. and Clark, C. D. (1990). The Laurentide ice sheet through the last glacial cycle: The topology of drift lineations as a key to the dynamic behaviour of former ice sheets. *Transactions of the Royal Society of Edinburgh Earth Sciences*, **81**, 327–347.

Boulton, G. S. and der Meer, J. J. M. V. (1986). Renewed interest in research of ice-pushed ridges. First results of the Glacitecs'84 expedition to Spitsbergen. *Geografisch Tijdschrift KNAG*, **20**(3), 236–244.

Boulton, G. S. and Hindmarsh, R. C. A. (1987). Sediment deformation beneath glaciers: Rheology and geological consequences. *Journal of Geophysical Research*, **92**(B9), 9059–82.

Boulton, G. S. and Jones, A. S. (1979). Stability of temperate ice caps and ice sheets resting on beds of deformable sediment. *Journal of Glaciology*, **24**(90), 29–.

Boulton, G. S. and Payne, A. (1992). Simulation of the European ice sheet through the last glacial cycle and prediction of future glaciation. Svensk kärnbränslehantering ab (skb) - Swedish Nuclear Fuel and Waste Management Co., Edinburgh University.

Boulton, G. S., Dent, D. L., and Morris, E. M. (1974). Subglacial shearing and crushing, and the role of water pressures in tills from south-east Iceland. *Geografiska Annaler. Series A: Physical Geography*, **56A**, 135–145.

Boulton, G. S., Smith, G. D., Jones, A. S., and Newsome, J. (1985). Glacial geology and glaciology of the last mid-latitude ice sheets. *Journal of the Geological Society (London)*, **42**, 447–474.

Boulton, G. S., Hulton, N., and Vautravers, M. (1995). Ice-sheet models as tools for palaeoclimatic analysis: The example of the European ice sheet through the last glacial cycle. *Annals of Glaciology*, **21**, 103–110.

Bowen, D. Q., Rose, J., McCabe, A. M., and Sutherland, D. G. (1986). Correlation of Quaternary glaciations in England and Ireland and Scotland and Wales. *Quaternary Science Reviews*, **5**, 299–340.

Boyce, J. I. and Eyles, N. (1991). Drumlins carved by deforming till streams below the laurentide ice sheet. *Geology*, **19**, 787–790.

Brennand, T. A. and Shaw, J. (1994). Tunnel channels and associated landforms, south-central Ontario: Their implications for ice-sheet hydrology. *Canadian Journal of Earth Sciences*, **31**(3), 505–522.

Broadgate, M. (1997). *An Integrated Approach to Palaeoenvironmental Reconstruction using GIS*. Ph.D. thesis, University of Edinburgh.

Bussel, A. (1998). Sensor news. *Geological Remote Sensing Group Newsletter*, **22**, 11–13.

Cepek, A. G. (1962). Zur grundmoränenstratigraphie in Brandenburg. *Berichte der Geologischen Gesellschaft der DDR*, **7**, 275–278.

Clark, C. D. (1990). *Reconstruction of the Behaviour of the Laurentide Ice Sheet using Satellite Imagery*. Ph.D. thesis, University of Edinburgh.

Clark, C. D. (1993). Mega-scale glacial lineations and cross-cutting ice flow landforms. *Earth Surface Processes and Landforms*, **18**, 1–29.

Clark, C. D. (1997). Reconstructing the evolutionary dynamics of former ice sheets using multi-temporal evidence, remote sensing and GIS. *Quaternary Science Reviews*, **16**, 1067–1092.

Clark, C. D. and Wilson, C. (1994). Spatial analysis of lineaments. *Computers and Geosciences*, **20**(78), 1237–1258.

Clark, P. U. and Walder, J. S. (1994). Subglacial drainage, eskers and deforming beds beneath the Laurentide and Eurasian ice sheets. *Geological Society of America Bulletin*, **106**, 304–314.

Clark, R. N. (1999). *Manual of Remote Sensing*. John Wiley and Sons, New York. In Press. Expected Publication date January 1999.

Clarke, K. C. (1987). Fast glacier flow: Ice streams, surging and tidewater glaciers. *Journal of Geophysical Research*, **92**(B9), 8835–8841.

Clayton, L., Mickelson, D. M., and Attig, J. W. (1989). Evidence against pervasively deformed bed material beneath rapidly moving lobes of the southern Laurentide ice sheet. *Sedimentary Geology*, **62**, 203–221.

Crimes, T. P., Chester, D. K., and Thomas, G. S. P. (1992). Exploration of sand and gravel resources by geomorphological analysis in the glacial sediments of the Eastern Llyn Peninsula, Gwynedd, North Wales. *Engineering Geology*, **32**, 137–156.

Danilāns, I. (1973). *Chetvertichnykh otlozheniy Latvii*. Zinātne, Riga. 312 pp.

Dardis, G. F. and McCabe, A. M. (1983). Facies of subglacial channel sedimentation in late Pleistocene drumlins, Northern Ireland. *Boreas*, **12**, 263–278.

Denniss, A. (1997). New sensor news. *Geological Remote Sensing Group Newsletter*, (20), 9–14.

Dongelmans, P. (1996). *Glacial Dynamics of the Fennoscandian Ice-Sheet: A Remote Sensing Study*. Ph.D. thesis, University of Edinburgh.

Donner, J. and Raukas, A. (1989). On the geological history of the Baltic Ice Lake. *Proceedings of the Academy of Sciences of the Estonian SSR, Geology*, **38**(4), 128–137.

Donner, J. J. (1995). *The Quaternary history of Scandinavia*, volume 7 of *World and regional geology*. Cambridge University Press.

Dreimanis, A. and Zelcs, V. (1995). Pleistocene stratigraphy of Latvia. In J. Ehlers, S. Kozarski, and P. Gibbard, editors, *Glacial deposits in North-East Europe*, pages 105–113. A.A.Balkema.

Drozdowski, E. (1986). Stratigraphy and origin of the Vistuian glaciation in the northern part of lower Powiś. In *Prace Geograficzne Instytutu Geografii i Przestrzennego Zagospodarowania Polskiej Akademii Nauk*, volume 146, page 90.

Drury, S. A. (1986a). Geological structures on landsat tm images of southern britain. In *Mapping from Modern Imagery. Proc. symposium of ISPRS Commission IV and RSS, Edinburgh, 1986*. ISPRS and Remote Sensing Society, Nottingham; International Archives of Photogrammetry and Remote Sensing, 26 part 4), pp 710-718.

Drury, S. A. (1986b). Remote sensing of geological structure in temperate agricultural terrains. *Geological Magazine*, **123**, 1130121.

Dyke, A. S. (1993). Landscapes of cold-centred late Wisconsinan ice caps, Artic Canada. *Progress in Physical Geography*, **17**(2), 223–247.

Dyke, A. S. and Morris, T. F. (1988). Drmlin fields, dispersal trains, and ice stream in Artic Canada. *Canadian Geographer*, **32**(1), 86–90.

Ehlers, J. (1990). Reconstruction of the dynamics of the north-west European Pleistocene ice sheets. *Quaternary Science Reviews*, **9**, 71–83.

Ehlers, J. (1992). Origin and distribution of red tills in North Germany. *Sveriges Geologiska Undersökning*, **Ser. Ca 81**, 97–105.

Ehlers, J. (1996). *Quaternary and glacial geology*. Chichester New York: Wiley. translated from Allgemeine und historische Quartargeologie by Philip L. Gibbard.

Ehlers, J. and Stephan, H.-J. (1983). Till fabric and ice movement. In J. Ehlers, editor, *Glacial deposits in North-West Europe*, pages 267–274. A. A. Balkema.

Ehlers, J., Kozarski, S., and Gibbard, P. (1995). General overview. In J. Ehlers, S. Kozarski, and P. Gibbard, editors, *Glacial deposits of North-East Europe*, pages 547–561. A.A.Balkema.

Einstein, H. H. and Baecher, G. B. (1983). Probabilistic and statistical methods in engineering geology, specific methods and examples Part i: Exploration. *Rock Mechanics and Rock Engineering*, **16**, 39–72.

Elachi, C. (1987). *Introduction to the Physics and Techniques of Remote Sensing*. John Wiley and Sons, New York.

Engelhardt, H. F., Humphrey, N., Kamb, B., and Fahnestock, M. (1990). Physical conditions at the base of a fast moving Antarctic ice stream. *Science*, **248**, 57–59.

Environmental Systems Research Institute (1994). *Map Projections. Georeferencing Spatial Data*. ESRI.

ERDAS (May 1995). *Graphical Models Reference Guide: Erdas Imagine Version 8.2*. ERDAS Inc, 2801 Buford Highway, Suite 300, Atlanta, GA 30329, USA.

Evans, D. J. A., Owen, L. A., and Roberts, D. (1995). Stratigraphy and sedimentology of Devensian (Dimington Stadial) glacial deposits, east Yorkshire, England. *Journal of Quaternary Science*, **10**(3), 241–265.

Eyles, N., McCabe, A. M., and Bowen, D. Q. (1994). The stratigraphic and sedimentological significance of Late Devensian ice sheet surging in Holderness, Yorkshire, UK. *Quaternary Science Reviews*, **13**, 727–759.

Eyton, J. R. (1989). Low-relief topographic enhancement in a Landsat snow-cover scene. *Remote Sensing Environment*, **27**, 105–118.

Fischer, N. I. (1995). *Statiscal analysis of circular data*. Cambridge University Press. 277 pp.

Fischer, U. H. and Clarke, G. K. C. (1994). Ploughing of subglacial sediment. *Journal of Glaciology*, **40**, 168–170.

Flint, R. F. (1971). *Glacial and Quaternary Geology*. John Wiley and Sons, New York.

Gaigalas, A. (1995). Glacial history of Lithuania. In J. Ehlers, S. Kozarski, and P. Gibbard, editors, *Glacial Deposits in North East Europe*, pages 127–135. A.A.Balkema.

Geer, G. D. (1897). Om rullstensåsarnas bildnignssätt. *Geologiska Föreningens i Sockholm Förhandlinagar*, **19**, 366–388.

Geer, G. D. (1940). Geochronologia suecica. Principles. *Kungliga Svenska Vetenskapsakademiens Handlingar*, **18**(6). Series 3.

Geer, J. D., Hyyppä, J., Panova, P., and Persson, G. (1985). Brief sketch of the physical geography of the region E4. In L. Ivanova, editor, *Explanatory Notes for the International Hydrogeological Map of Europe 1:1,500,000, Sheet E4 KIEV*, volume E4. Hannover Paris.

Gesch, D. (1996). GTOPO30 documentation. Internet WWW: http://edcwww.cr.usgs.gov/, EROS Data Center, U.S. Geological Survey, EROS Data Center, Sioux Falls, SD 57198.

Gluückert, G. (1973). Two large drumlin fields in central Finland. *Fennia*, **120**, 37.

Goodchild, M. F. (1988). Stepping over the line: Technological constraints and the new cartography. *American Cartographer*, **15**(3), 311–319.

Gray, J. M. (1988). Glaciofluvial channels below the Blakeney esker, Norfolk. *Quaternary Newsletter*, **55**, 8–12.

Gripp, K. (1924). Über die äußerste Grenze der letzen Vereisung in Nordwest-Deutschland. *Mitteilungen der Geographischen Gesellschaft in Hamburg*, **36**, 159–245.

Gripp, K. (1964). *Erdgeschichte von Schleswig-Holstein*. Wachholtz. 411 Pages.

Guobyte, R. (1995). Saalian and Weichselian relief in aerial photographs, south-eastern Lithuania. Abstracts of International Union For Quaternary Research XIV International Congress. Lithuania.

Guobyte, R. and Pavlovskaya, I. (1998). The stadial limits and maximum extent of the Weichselian glaciation in north-eastern Lithuania and north-western Belarus. Abstracts of Field Symposium on Glacial Processes and Quaternary Environment in Latvia.

Haavisto-Hyvärinen, M., Kielosto, S., and Niemelä, J. (1989). Pre-crags and drumlin fields in Finland. *Sedimentary Geology*, **62**, 337–348.

Hanvey, P. M. (1989). Stratified flow deposits in a late Pleistocene drumlin in northwestern Ireland. *Sedimentary Geology*, **62**, 211–221.

Hart, J. K. (1990). Proglacial glaciotectonic deformation and the origin of the Cromer Ridge push moraine complex, North Norfolk, England. *Boreas*, **19**(2), 165–180.

Hart, J. K. (1997). The relationship between drumlins and other forms of subglacial glaciotectonic deformation. *Quaternary Science Reviews*, **16**, 93–107.

Hart, J. K. and Boulton, G. S. (1991). The interrelation of glaciotectonic and glaciodepositional processes within the glacial environment. *Quaternary Science Reviews*, **10**, 335–350.

Hättestrand, C. (1997a). *Ribbed Moraines and Fennoscandian Palaeoglaciology*. Ph.D. thesis, The Department of Physical Geolgraphy, Stockholm University.

Hättestrand, C. (1997b). Ribbed moraines in Sweden - distribution pattern and paleoglaciological implications. *Sedimentary Geology*, **111**, 41–56.

Hebrand, M. and Amark, M. (1989). Esker formation and glacier dynamics in eastern Skåne and adjacent areas, southern Sweden. *Boreas*, **18**, 67–81.

Heerdt, S. (1965). Zur stratigraphie des jungpleistozäns im mittleren N-Mecklenburg. *Geologie*, **14**, 589–609.

Heikkinen, O. and Tikkanen, M. (1989). Drumlins and flutings in Finland: Their relationships to ice movement and to each other. *Sedimentary Geology*, **62**, 349–356.

Holmlund, P. and Fastook, J. (1995). A time dependent glaciological model of the Weichselian ice sheet. *Quaternary International*, **27**, 53–58.

Hoppe, G. and Schyatt, V. (1953). Some observations on fluted moraine surfaces. *Geografiska Annaler*, **35**, 105–115.

Houmark-Nielsen, M. (1990). The last interglacial-glacial cycle in Denmark. *Quaternary International*, **34**, 31–9.

Hughes, T. J., Denton, G. H., Andersen, B. G., Schilling, D. H., Fastook, J. L., and Lingle, C. S., editors (1981). *The last great ice sheets*, pages 263–317. John Wiley and Sons, New York.

Humphrey, N., Kamb, B., Fahnestock, M., and Engelhardt, H. (1993). Characteristics of the bed of the lower Columbia Glacier, Alaska. *Journal of Geophysical Research*, **98**, 837–846.

International Hydrogeological Map of Europe (1985). International Hydrogeological Map of Europe, scale 1: 1,500,000. Bundesanstalt für Geowissenschaften und Rohstoffe, Hannover, and the United Nations Educational Scientific and Cultural Organization (Unesco), Paris.

Johnson, W. H. and Hansel, A. K. (1989). Multiple Wisconsin glacigenic sequences at Wedeon, Illnois. *Journal of Sedimentary Petrology*, **60**, 20–91.

Johnston, A. C. (1987). *The Identification of Ancient Glacier Marks using Advanced Very High Resolution Radiometer Imagery*. Master's thesis, University of Dundee.

Kamb, B. (1991). Rheological nonlinearity and flow instability in the deforming bed mechanism of ice stream motion. *Journal of Geophysical Research*, **96**, 16585–16595.

Karukäpp, R. (1996). Stagnant ice features in the eastern Baltic. *Proceedings of the Academy of Sciences of the Estonian SSR, Geology*, **45**(4), 216–224.

Karukäpp, R. (1997). Gotiglacial morphogenesis in the southeastern sector of the Scandinavian continental glacier. Technical report, Geologicae Universitatis Tartuensis.

Karukäpp, R., Raukas, A., and Hyvärinen, H. (1992). Geology of the Gulf of Finland. In *The deglaciation of the territory*. Tallinn.

Kleman, J. (1994). Preservation of landforms under ice sheets and ice caps. *Geomorphology*, **9**(1), 19–32.

Knight, J. (1996). *A Geographical Information Systems Based Synthesis of the Labrador Sector of the Laurentide Ice-Sheet*. Ph.D. thesis, University of Sheffield.

Knoshin, G. I. (1965). *Petrograficheskiy sostav i orientirovka galechnograviynogo materiala moren Latviiskoi SSR. Avtoreferat dissertasii kandidata geologicheskikh i mineralogicheskikh nauk*. Vilnius. 25 pp.

Kolago, C. (1985). Geography of the region D4. In L. Ivanova, editor, *Explanatory Notes for the International Hydrogeological Map of Europe 1:1,500,000, Sheet D4*, volume D4 of *International Hydrogeological Map of Europe, 1:1,500,000*. Hannover Paris.

L. Clayton, J. T. Teller, J. W. A. (1985). Surging of the southwestern part of the Laurentide ice sheet. *Boreas*, **14**(3), 235–241.

Laaksonen, K. (1993). De Geer moraines and basal flow of ice. *Terra*, **101**(4), 302–328.

Lagerbäck, R. (1988). The Veiki moraines in northern Sweden - widespread evidence of Early Weichselian deglaciation. *Boreas*, **17**, 469–486.

Lagerlund, E. (1987). An alternative Weichselian glaciation model, with special reference to the glacial history of Skâne, south Sweden. *Boreas*, **16**, 443–459.

Larsen, E., Longva, O., and Follestad, B. A. (1991). Formation of De Geer moraines and implications for deglaciation dynamics. *Journal of Quaternary Science*, **6**(4), 263–277.

Lehmann, R. (1992). Artic push moraines, a case study of the Thompson Glacier moraine, Axel Heiberg Island, NWT, Canada. *Zeitschrift fur Geomorphologie, Supplementband*, **86**, 161–171.

Leningrad (1982). Geological, tectonic, geomorphological, hydrogeological, neotectonic and structural maps of the Soviet Baltic Republics. Technical report, Ministry of Geology of the USSR Board of Geology of the Lithuanian SSR.

Liivrand, E. (1991). Biostratigraphy of the Pleistocene deposits in Estonia and correlations in the Baltic region. Technical Report 19, University of Stockholm, Department of Quaternary Geology.

Liivrand, E. (1992). Problems of reconstructing Pleistocene stratigraphy in Estonia. *Sveriges Geologiska Undersökning*, **Ser. Ca 81**, 171–176.

Lillesand, T. M. and Kiefer, R. M. (1987). *Remote Sensing and Image Interpretation*. John Wiley and Sons, New York.

Ljunger, E. (1949). East-west balance of the Quaternary ice caps in Patagonia and Scandinavia. *Bulletin of the Geological Institution of the University of Upsala*, **33**, 95.

Lukashov, A. D. (1982). Guidebook for excursions A-4 and C-4 Karelia. Technical report, International Union for Quaternary Research XI Congress, Moscow.

Lundqvist, J. (1986). Stratigraphy of the central area of the Scandinavian glaciation. *Quaternary Science Reviews*, **5**, 269–292.

Lundqvist, J. (1989). Rogen (ribbed) moraine - identification and possible origin. *Sedimentary Geology*, **62**, 281–292.

Lundqvist, J. (1990). Glacial morphology as an indicator of the direction of glacial transport. In R. Kujansuu and M. Saarnisto, editors, *Glacial Indicator Tracing*. Balkema, Rotterdam.

Majdanowski, S. (1949). The southern limit of the Baltic glaciation in the European Plain in the light of the extent of lake-channels. *Bulletin de las Société des Amis des Sciences et des Lettres de Poznan*, **+ map**, 185–208. preésente à la séance du 5 Février.

Mangerud, J. (1983). *The glacial history of Norway*. Balkema. pages 3-9.

Mangerud, J., Guillikesen, S., Larsen, E., Longva, O., Miller, G., Sejrup, H.-P., and Sønstegaard, E. (1981). A Middle Weichselian ice-free period in western Norway: The Ålesund interstadial. *Boreas*, **10**, 447–462.

Mardia, K. V. (1972). *Statistics of Directional Data*, chapter 2. Academic Press.

Markots, A., Zelcs, V., and Strautnieks, I. (1995). Quaternary field trips in Central Europe, Baltic Traverse, site 22. Technical report, International Union for Quaternary Research XIV Congress, Berlin.

Marsh, S. H., Boulton, G. S., Perry, J., and Punkari, M. (1995). Operational geological surveying in temperate regions using Landsat TM. Technical Report WC/95/61, British Geological Survey, Keyworth and Nottingham and British Geological Survey.

Meirons, Z. (1986). Stratigrafiya pleistotsenovykh otlozheniy Latvii. In O. Kondratienė and A. P. Mikalauskas, editors, *Issledovaniya lednikovykh obrazovaniy Pribaltiki*. Vilnius.

Meirons, Z., Punning, J. M., and Hütt, G. (1981). Results obtained through the TL dating of southeast Latvian Pleistocene deposits. *Eesti NSV Teaduste Akademia Toimetised and Geologia*, **82-84**.

Meirons, Z. V. and Yushkevichs, V. V. (1984). Chetvertichnye otlozheniya. In J. P. Misans and A. P. Brangulis, editors, *Geologiya Latviyskoi SSR*, pages 89–122. Rīga: Zinātne.

Menzies, J. (1979). A reveiew of the literature on the formation and location of drumlins. *Earth Science Reviews*, **14**, 315–359.

Menzies, J. and Rose, J., editors (1987). *Drumlin Symposium*. Balkema, Rotterdam.

Menzies, J. and Shilts, W. W. (1996). *Past Glacial Environments: Sediment Forms and Techniques*. Butterworth Heinneman, Oxford.

Menzies, J., Zaniewski, K., and Dreger, D. (1997). Evidence, from microstructures, of deformable bed conditions within drumlins, Chimney Bluffs, New York State. *Sedimentary Geology*, **111**, 161–175.

Mickelson, D. M. (1971). Glacial geology of the Burroughs glacier area, southeastern Alaska. *Ohio State University Institute of Polar Sudies Report*, **40**, 149pp.

Mojski, J. E. (1995). Pleistocene glacial events in Poland. In J. Ehlers, S. Kozarski, and P. Gibbard, editors, *Glacial Deposits in North-East Europe*, pages 287–292. A. A. Balkema.

Moran, S. R., andR. LeB. Hooke, L. C., Fenton, M. M., and Andriashek, L. D. (1980). Glacier-bed landforms of the prairie region of north america. *Journal of Glaciology*, **25**(93), 457–476.

Morgan, V. I., Jacka, T. H., Akerman, G. J., and Clarke, A. L. (1982). Outlet glacer and mass-budget studies in Enderby, Kemp, and Mac. Roberson Lands, Antarctica. *Annals of Glaciology*, **3**, 204–210.

Orelemans, J. and Van der Veen, C. J. (1984). *Ice Sheets and climate*. D. Reidel, Dordrecht, Holland.

Paterson, W. S. B. (1994). *The Physics of Glaciers*. Pergamon. 480 pp.

Patterson, C. J. and Hooke, R. L. (1995). Physical environment of drumlin formation. *Journal of Glaciology*, **41**(137), 30–38.

Persson, K. M. (1991). Internal structures and depositional environment of a kame. *Geologiska Foreningens i Stockholm Forhandlingar*, **113**(2-3), 163–170.

Pickering, G., Bull, J. M., and Sanderson, D. J. (1995). Sampling power-law distributions. *Tectonophysics*, **248**, 1–20.

Praeg, D. B., Stravers, J. A., and Luman, D. (1992). Quantitative geological discrimination using AVHRR imagery across southern Baffin Island. *Photo-interpretation*, **5**, 169–181.

Prest, V. K. (1968). Nomenclature of moraines and ice flow features as applies to the glacial map of Canada. *Geological Survey Papers Canada*, pages 67–57.

Price, R. J. (1982). Changes in the proglacial area of Breidamerkurjokull, southeastern Iceland, 1890-1980. *Jokull*, **32**, 29–35.

Punkari, M. (1978). *Suomen glasifluviaalisten ja muiden glasigeenisten suurouotojen tulinta Landsat-satelliittikuvista*. Ph.D. thesis, University of Helsinki.

Punkari, M. (1980). The ice lobes of the Scandinavian ice sheet during the deglaciaton in Finland. *Boreas*, **9**, 307–310.

Punkari, M. (1982). Glacial geomorphology and dynamics in the eastern parts of the Baltic Shield interpreted using Landsat imagery. *Photogrammetric Journal of Finland*, **9**(1), 77–93.

Punkari, M. (1984). The relations between glacial dynamics and tills in the eastern part of the Baltic shield. *Striae*, **20**, 49–54.

Punkari, M. (1985). Glacial geomorphology and dynamics in soviet Karelia interpreted by means of satellite imagery. *Fennia*, **163**(1), 113–153.

Punkari, M. (1989). Glacial dynamics and related erosion-deposition processes in the Scandinavian ice sheet in south-western Finland: A remote sensing, fieldwork and computer modelling study. Technical Report 01/663, Research Council for the Natural Sciences, Academy of Finland.

Punkari, M. (1992). Glacial geology in eastern Fennoscandia and western Russia interpreted by means of satellite imagery. In A. P. Cracknell and R. A. Vaughan, editors, *Remote Sensing From Research To Operation*. The Remote Sensing Society.

Punkari, M. (1993). Modelling of the dynamics of Scandinavian ice sheet using remote sensing and GIS methods. *Canadian Plains Proceedings*, **25**(1), 232–250.

Punkari, M. (1995). Function of the ice streams in the Scandinavian ice sheet: Analyses of glacial geological data from southwestern Finland. *Transactions of the Royal Society of Edinburgh: Earth Sciences*, **85**, 283–302.

Punkari, M. (1996). Glacial dynamics of the northern European ice sheets. Academic Dissertation, Department of Geology, University of Helsinki.

Punkari, M. (1997). Glacial and glaciofluvial deposits in the interlobate areas of the Scandinavian ice sheet. *Quaternary Science Reviews*, **16**, 741–753.

Punkari, M. and Forsström, L. (1995). Glacial flow systems in the zone of confluence between the Scandinavian and Novaya Zemlya ice sheets. *Quaternary Science Reviews*, **14**, 589–603.

Punning, J. M. K., Raukas, A. V., Serebryanny, L. R., and Stelle, V. J. (1968). Paleogeograficheskiye osobennosti i absolyutniy vozrast luzhskoy stadii valdaiskogo oldeneniya na Russkoi ravnine. *Dokladi Akademii Nauk SSSR*, **178**, 916–918. Seriya geograficheskayan.

Raper, J. and Vozenilek, V. (1993). The Digital Chart of the World: controversial but invaluable. *GIS Europe*, **2**(2), 57–60.

Raukas, A. (1977). Ice-marginal formations and the main regularties of the deglaciaton in Estonia. *Z. Geomorph. N.F.*, **Suppl.-Bd.27**, 68–78.

Raukas, A. (1986). Deglaciation of the Gulf of Finland and adjoining areas. *Bull. Geol. Soc. Finland*, **58**(Part 2), 21–33.

Raukas, A. (1992). Ice marginal formations of the Palivere zone in the eastern Baltic. *Sveriges Geologiska Undersökning*, **Ser. Ca 81**, 277–284.

Raukas, A. (1996). *Estonian Environment: Past, Present and Future*, pages 7–18. Tallina Raamatutrükikoda, Ministry of the Environment of Estonia Environment Information Centre.

Raukas, A. and Gaigalas, A. (1993). Pleistocene glacial deposits along the eastern periphery of the Scandinavian ice sheets - an overview. *Boreas*, **22**, 214–222.

Raukas, A., Aboltins, O., and Gaigalas, A. (1995). Current state and new trends in the quaternary geology of the Baltic States. In *Proceedings of the Estonian Academy of Sciences Geology*, volume 44(1), pages 1–14. Eesti TA Toimetised. Geoloogia.

Reeh, N. (1989). Dynamic and climatic history of the Greenland ice sheet. In R. J. Fulton, editor, *Quaternary Geology of Canada and Greenland*, chapter 14. Geological Survey of Canada.

Ringberg, B. (1988). Late Weichselian geology in southern most Sweden. *Boreas*, **17**, 243–263.

Rose, J. (1987). Drumlins a part of a glacier bedform continuum. In *Drumlin Symposium*, pages 103–118. Balkema.

Rose, J. (1989). Glacier stress pattern and sediment transfer associated with the formation of superimposed flutes. *Sedimentary Geology*, **62**, 151–176.

Rose, J. and Letzer, J. M. (1977). Superimposed drumlins. *Journal of Glaciology*, **18**, 471–480.

Rose, K. E. (1979). Characteristics of ice flow in Marie Byrd Land, Antarctica. *Journal of Glaciology*, **24**, 63–75.

Rõuk, A.-M. and Raukas, A. (1989). Drumlins of Estonia. *Sedimentary Geology*, **62**, 371–384.

Rühberg, N. (1987). Die grundmoräne des jüngsten Weichselvorstoßes im Gebiet der DDR. *Zeitschrift für Geologische Wissenschaften*, **15**, 759–767.

Sakson, M. A. and Seglinsh, V. E. (1990). Razrez dolinkuvskikh interstadialnikh ootlozheniy savaini vozle g. Dobele. In A. M. Miidel and A. N. Molodtsov, editors, *Chetvertichnyi period: metody issledovaniya, stratigrafiya i ekologiya, VII Vsesoyuznoye sovesschaniye*, volume 3(88-89) of *Tezis*. Tallinni.

Sauramo, M. (1923). Studies on the Quaternary varve sediments in southern Finland. *Bulletin de la Commission géologique de Finlande*, **60**.

Shabtaie, S. and Bentley, C. H. (1987). West Antarctic ice streams draining into the Ross ice shelf: Configuration and mass balance. *Journal of Geophysical Research*, **92**, 1311–1336.

Shabtaie, S., Whillans, I. M., and Bentley, C. H. (1987). The morphology of ice streams A, B and C, west Antarctica, and their environs. *Journal of Geophysical Research*, **92**(B9), 8865–8883.

Sharpe, D. R. (1987). The stratified nature of drumlins from Victoria Island in southern Ontario. In *Drumlin Symposium*, pages 185–214. Balkema.

Shaw, J. (1983). Drumlin formation related to inverted melt-water erosional marks. *Journal of Glaciology*, **29**(103), 461–479.

Shaw, J. (1994). Hairpin erosional marks, horseshoe vortices and subglacial erosion. *Sedimentary Geology*, **91**, 269–283.

Shilts, W. W. and Aylsworth, J. M. (1989). *Glacial features around the Keewatin ice divide: Districts of Mackenzie and Keewatin*. Geological Survey of Canada.

Short, N. M. and Blair, R. W. J., editors (1976). *Geomorphology from space: A global overview of regional landforms*. NASA sp-360.

Shreve, R. L. (1985). Esker characteristics in terms of glacier physics, Katahdin esker system, Maine. *Geological Society of America Bulletin*, **96**, 639–646.

Simonett, D. S. (1983). *The Devolpment and Principles of Remote Sensing*. American Society of Photogrammetry.

Skoye, K. R. and Eyton, J. R. (1992). Digital analysis of low-relief topography in a Landsat snow-cover scene in south-central Alberta. *Canadian Journal of Remote Sensing*, **18**, 143–150.

Smalley, I. J. and Unwin, D. J. (1968). The formation and shape of drumlins and their distribution and orientation in drumlin fields. *Journal of Glaciology*, **7**(51), 377–390.

Sollid, J. L. and Sørbel, L. (1984). *Distribution and genesis of moraines in central Norway*, volume Straie 20 of *Ten Years of Nordic Till Research*, pages 63–67.

Star, J. and Estes, J. (1990). *Geographic Information Systems: An Introduction*. Englewood Cliffs, New Jersey: Prentice Hall.

Stea, R. R. and Brown, Y. (1989). Variation in drumlin orientation, form and stratigraphy relating to successive ice flows in southern and central Nova Scotia. *Sedimentary Geology*, **62**, 223–240.

Stephan, H.-J. (1983). XI. INQUA congress, Moscow, Report of the excursion C5 from 11-17.8.1982. *Eiszeitalter und Gegenwart*, **33**, 177–180.

Strömberg, B. (1990). A connection between the clay varve chronologies in Sweden and Finland. *Annales Academiae Scientiarum Fennicae A III*, **154**.

Sugden, D. E. (1978). Reconstruction of the morphology, dynamics and thermal characteristics of the Laurentide ice-sheet at its maximum. *Arctic and Alpine Research*, **9**, 21–47.

Sugden, D. E. and John, B. S. (1976). *Glaciers and Landscape*. Edward Arnold, London. 376 pp.

Sviridov, N. I., Litvin, V. M., Gaygalas, A. I., and Repechka, M. A. (1977). Relief of the pre-Quaternary surface of the Baltic region. *Internatial Geology Reveiw*, **19**(5).

Sweitzer, J., Langaas, S., and Folke, C. (1996). Land use and population density in the Baltic sea drainage basin: a GIS database. *Ambio*, **25**(3).

Syverson, K. M., Gaffield, S. J., and Mickelson, D. M. (1994). Comparison of esker morphology and sedimentology with former ice-surface topography, Burroughs glacier, Alaska. *Geological Society of America Bulletin*, **106**, 1130–1142.

Thwaites, F. T. (1947). Use of aerial photographs in glacial geology. *Photgrammetric Engineering*, **13**(4), 584–586.

Trenhaile, A. S. (1971). Drumlins: Their distribution, orientation and morphology. *Canadian Geographer*, **15**(2), 113–126.

Turcotte, D. L. (1997). *Fractals and Chaos in Geology and Geophysics*. Cambridge University Press. 398 pp.

UNEP/GRID - Arendal (August 1995). *Baltic Sea Region GIS, Maps and Statistical Database*. Baltic Drainage Basin Project, EU 1991-1994 Environment Research Programme, Department of Systems Ecology, University of Stockholm, Sweden. Uniform Resource Locator: http://www.grida.no/baltic/.

V. Ya. Stelle, A. S. S. and Veksler, V. S. (1975). Absolute age of chronostratigraphic stages and boundaries of the late glacial and post glacial periods in the middle Baltic region. In G. D. Afanasyev, editor, *Status of methodological studies in the fields of absolute Geohronology*, pages 187–191. Moscow: Nauka.

Velichko, A. A. (1984). *Late Quaternary Environments of the Soviet Union*. Unknown.

Vernon, P. (1966). Drumlins and Pleistocene ice flow over the Ards Peninsula/Srangford Lough area, County Down, Ireland. *Journal of Glaciology*, **6**(45), 401–409.

Vinogradov, A. P., Devirts, A. L., Dobkina, E. I., and Markova, N. G. (1966). Verkhniy pleistotsen. Stratigrafiya i absolyutnaya khronologiya. In *Spiski radiougleodnikh datirovok, poluchennikh v laboratoriyakh SSSR za period s I yanvarya 1962 goda do l yanvarya 1966 goda*. Moscow.

Walder, J. S. and Fowler, A. (1994). Channelized subglacial drainage over a deformable bed. *Journal of Glaciology*, **40**(134), 3–15.

Walsh, J. J. and Watterson, J. (1988). Analysis of the relationship between displacements and dimensions of faults. *Structural Geology*, **10**, 239–247.

Williams, R. S. J. (1986). Glaciers and glacial landforms. In N. M. and R. W. J. Blair, editors, *Geomorphology from space: A global overview of regional landforms*, volume 360 of *NASA-sp*, page 459.

Wintle, A. G. (1990). A review of current research on TL dating of loess. *Quaternary Science Reviews 9*, **9**, 385–397.

Woldstedt, P. (1925). Die großen endmoränenzüge norddeutschlands. *Zeitschrift der Deutschen Geologischen Gesellschaft*, 77, 172–184.

WRS (1981). *Landsat-D worldwide reference system (WRS) users guide: [Greenbelt, Md.]*. National Aeronautics and Space Administration.

Zelčs, V. (1995). Quaternary field trips in Central Europe, Baltic Traverse, site 28. Technical report, International Union for Quaternary Research XIV Congress, Berlin.

Zilliacus, H. (1987). The De Geer moraines in Finland. In V. Gardiner, editor, *International Geomorphology 1986. Proc. 1st conference*, volume 2, pages 711–724. Wiley.